

Project no. NMP2-CT-2003-505485

Project acronym ELISHA

Project title Electronic Immuno-Interfaces and Surface

Nanobiotechnology: A Heterodoxical Approach.

Instrument Specific Targeted Research Project

Thematic Priority Nano-technologies and nano-sciences, knowledge-based

multifunctional materials, and new production processes and

devices - 'NMP'

Final Project Report

Period covered: from 1st January 2004 to 30th June 2007 Date of preparation: July-Aug 2007

Start date of project: 1st January 2004 Duration: 36 Months (+ 6 months)

Project coordinator name Dr Paul Millner

Project coordinator organisation name University of Leeds Revision [1.1]

ELISHA Final Report INDEX	Page
Publishable Executive Summary	2
Section 1: Project Objectives and Major Achievements	5
Section 2: Workpackage Progress.	8
Overview:	8
Deliverables Progress Table	10
Workpackage 1 Affinity Reagent Production and Testing.	14
Workpackage 2 Electrochemical Transducer Production.	37
Workpackage 3 Production of Matrix Precursors.	42
Workpackage 4 Fabrication of Nanostructured Immunosensors	58
Workpackage 5 Investigations into Immobilisation Strategies and Matrix Construction	74
Workpackage 6 Sensor Address Systems and Interrogation Electronics	102
Workpackage 7 Signal Generation and Non-Specific Binding Optimisation	115
Workpackage 8 Evaluation of Affinity Sensor Systems including Signal Processing	130
Workpackage 9 Laboratory Prototype Instrument	156
Exploitation and Market Activities that Underpin the Technical Workpackages.	165
Section 3. Consortium Management.	167
Project Bar Chart and Status	170
Short comments on: Coordination activities, communication between partners, project meetings, cooperation with other projects.	171
Annex: Exploitation and Dissemination	172
Appendix 1: Background Characterisation of Existing Antibodies	179
Appendix 2: Existing Immunosensor Formats Potential Competitors	185
Appendix 3: Biomarkers. New Press Release for Prostate Cancer Diagnosis. CJD Diagnosis using Prionbiomarkers	188
Appendix 4: Patents, Publications and Abstracts	192
Appendix 5: Interim eTIP	202

Publishable Executive Summary – Final Project Report.

Background

The ELISHA project was designed to improve knowledge in molecular interfaces and enable manufacture of new affinity sensors, by understanding the rules for controlled manufacture at the nanoscale. Interrogating antibodies on nanostructured surfaces will help us to produce practical immunosensor formats that work as simply the most successful commercial biosensors and which can be manufactured at high quality and low cost. These were the main aims of ELISHA, which stands for: Electronic Immuno-Interfaces and Surface Nanobiotechnology: A Heterodoxical Approach. To provide significant breakthroughs in science often requires a change of orthodox thinking, hence the addition of heterodoxy in the title of the project to indicate a departure from existing knowledge and traditional electrochemical thinking. Practically the project focussed on 3 areas.

When an antibody recognises and transiently binds to its antigen there is a small electrode current produced in the supporting nanostructured matrix which can be measured and which is concentration dependant with respect to the antigen detected. The project investigated the nature and origin of the signal transduction mechanism observed in these nanostructured affinity-reagent based biosensors.

Using the knowledge obtained, immunosensor model prototypes were designed and optimised to give simple, novel, low-cost and reliable affinity sensors for a number of important clinical, environmental and related model analytes. These include cancer markers as a representative protein target (PSA), fluoroquinoline antibiotics as a representative hapten target (small molecule types) and other proteins.

The manufacture of electrochemical, label free immunosensors was also complimented by the development of dedicated electronics to provide specific interrogation protocols to deal with any non-specific binding events and to amplify the affinity event occurring.

The project was structured into 7 main sections, 1) Production of Antibodies; 2) Transducer Manufacture 3) Sensor Fabrication; 4) Immobilisation and Signal Generation; 5) Electronics Development; 6) Non-Specific Binding and Data Processing and 7) Prototype Instrumentation. All of these were completed by around month 24 with some intermittent work as new batches of transducers were needed and when more supplies of antibodies needed to be purified. The addition of molecular tags to antibodies also progressed throughout the project to allow new immobilisation methods to be explored.

Sensor fabrication, immobilisation methods and signal generation were the main project focus in the first half of the project. The production of immunosensors that exhibited the correct level of sensitivity, low non-specific binding and which are practical to manufacture were the main focal points. At its conclusion the project had identified several possible routes for immunosensor fabrication, all of which gave responses to the specific analytes that matched the antibody specificity. A good example is the cancer marker, prostatic specific antigen or PSA for short. This is used as a screen for prostatic cancer and is analyte within blood samples. The graph overleaf (figure I) shows that PSA can be easily detected at levels much lower than is present in blood.

In addition to this, two other protein analytes have been demonstrated to work using the ELISHA fabrication protocols. S-100 is a biomarker for trauma, such as stroke or heart attack and the antibody to this was used in an immunosensor format to give detection down to 1ng.ml⁻¹, (figure II). Haemoglobin is the main protein present in red blood cells. It is often used as a measure of microhaemoglobinuria, or very low levels being passed in the urine. Again the ELISHA technology enables immunosensors to be made that detect haemoglobin down to 5 nanomolar. This generic capability to obtain specific responses for many different antibodies has provided the evidence that the ELISHA method is a platform technology that can be developed into many areas where antibodies are used as diagnostic tools.

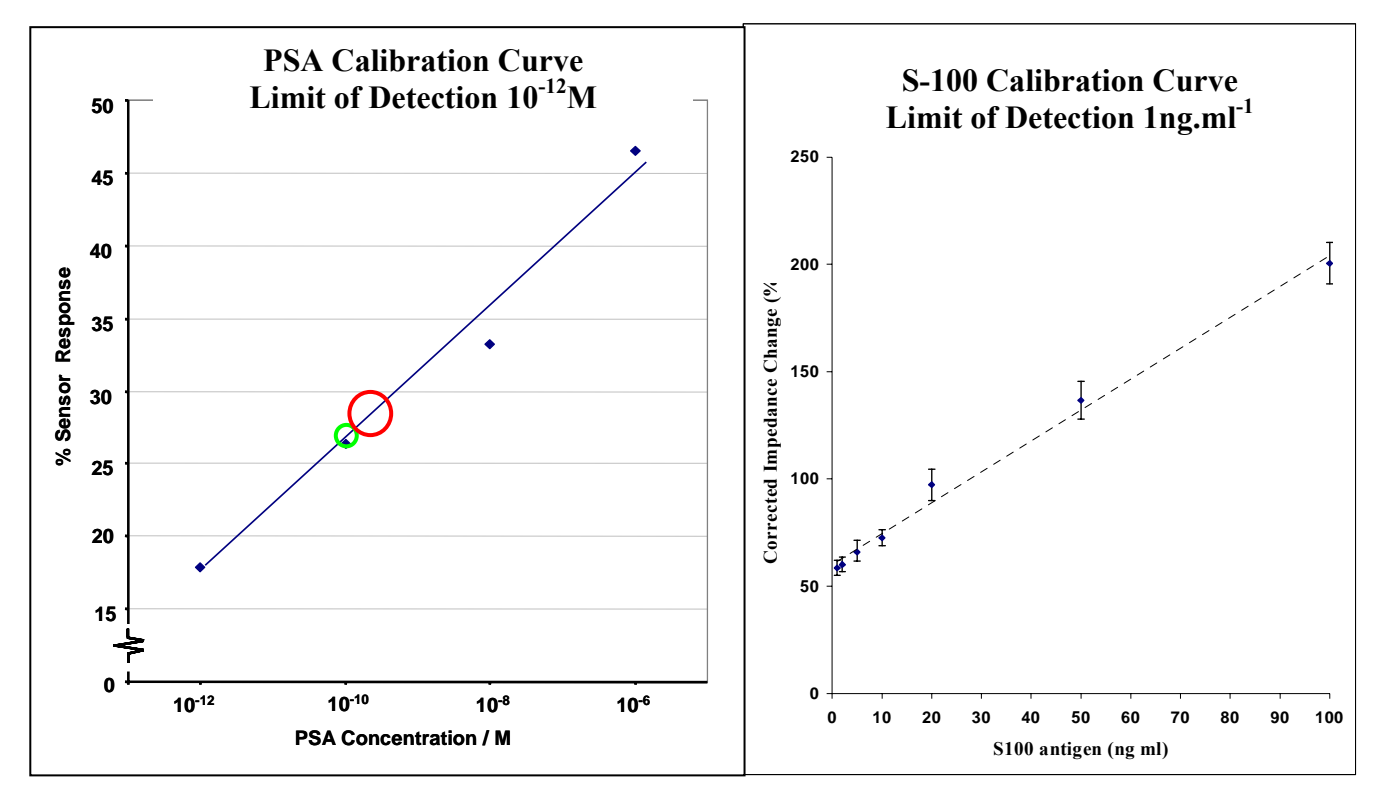


Fig.I Clinical levels of PSA used for diagnosis are: 4ng.ml⁻¹ or less normal O, benign prostate hyperplasia 4ng.ml⁻¹ to 10ng.ml⁻¹O, investigation into suspected Prostate cancer is done at levels above 10ng.ml⁻¹.

Fig II. S-100 protein biomarker for trauma. Stroke and heart attack elevate the protein in blood which can be measured using antibody based tests or immunosensors.

The speciality electronics designed for the instrumentation to interrogate and report the responses of the immunosensors are unique to the ELISHA project. This enables very low responses to be detected directly when coupled with the nanostructured immunosensor matrices, so the antibody recognising its antigen gives a measurable signal. The portable prototype device was constructed in the final year of the project for use at point-of-care or in field analysis and incorporates algorithms to enable rapid data processing and techniques to remove any signal due to non-specific binding to give specific antibody responses for the target analytes.

Exploitation, Market Interest and Competition.

In addition to the science of the project the market interest, potential competition and exploitation has been researched in some depth. The indications regarding market interest are extremely good provided nanostructured antibody based sensors can be manufactured that will give the same accuracy, sensitivity and precision as existing enzyme linked immunosorbant assays (ELISA's) and for the same price or less. The results for PSA and the trauma marker protein S-100 indicated that the sensitivity for ELISHA immunosensors will be at least as good as existing assays and that non-specific binding events can be virtually eliminated.

The exploitation potential of the project is enormous, as practical immunosensors that will work in the same manner as the most successful biosensor ever produced (i.e. blood glucose, having a worldwide yearly market turnover of \$5 billion) would make it very simple to test for a huge range of analytes. Competition in this particular field of low cost, electrochemical immunosensors is low, with just 4 companies being identified worldwide to date. Only one company makes an electrochemical device based on ion channel amplification and nobody makes simple, low cost immunosensor formats that are available as commercial products at the present time.

Section 1 Project Objectives and Major Achievements.

Molecular events occurring at the nanoscale impact on the macroscopic level in many different areas and rules for controlled manufacture at the nanoscale are important to understand. The ELISHA project was designed to improve knowledge in molecular interfaces and enable manufacture of new sensors, by interrogating the formation and signal generation by antibodies on electroconductive surfaces.

The main aim of the ELISHA project was:

• To produce a nanostructured immunosensor format that in practice works as simply the most successful commercial biosensors and which can be manufactured at high quality and low cost.

To do this effectively the project had three main objectives:

- 1) To provide detailed knowledge and understanding of a novel signal transduction mechanism observed in nanostructured affinity-reagent based biosensors.
- 2) To produce electronic, label free, immunosensor model prototypes that can then be further developed into simple, novel, low-cost and reliable affinity sensors for important clinical, environmental and related analytes.
- 3) The development of dedicated electronics.

The project was focussed on three representative analyte types, all of which are important in clinical, veterinary and environmental analysis. These are:

1) cancer markers, Representative protein target (Prostatic specific antigen - PSA)

2) fluoroquinoline antibiotics Representative hapten target (small molecule type)

3) prion type peptides. Representative peptide target (important small peptide analyte)

The range of these analyte types was designed to give specific model systems which are 1) useful and relevant to current applications as well as 2) representatives of large molecular size analytes, small molecular size analytes and a mid-sized peptide of particular structure. In addition to these initial targets, immunosensors for protein analytes which act as heart attack markers (myoglobin), and pregnancy (hCG) were also successfully constructed.

Current State-of-the-Art in Immunosensors.

Compared to the current state-of-the-art the ELISHA project remained throughout its operation at the cutting edge of immunosensor detection capability. It became clear that several other research groups world-wide were looking into rapid immunosensor devices as a step forward in point of care diagnostics, environmental and bioterrorism detection devices. There are new biomarkers being discovered for many diseases and most of these are assayed by antibody immunoassay. Just recently a new biomarker for prostate cancer has been discovered that enables more accurate detection and a reduction in non-specific interferences, Appendix 3, page 188.

The 8th World Congress on Biosensors held in Grenada, Spain in May 2004 was host to 637 refereed papers of which 117 were oral presentations and 450 were poster presentations. This is one of the largest biosensor conferences in the World and is a good conference to attend to glean the current status of World biosensor research and commercial development. Within this conference there were 2 oral sessions and 1 poster session dedicated to immunosensors containing 14 oral presentations and 63 posters respectively.

In addition there were several novel interrogation methods for sensor surfaces, including conductive polymer matrices and impedance spectroscopy. No mention was specifically made on the pulsing of surfaces for immunosensor development and this area is still remains very novel.

Despite numerous affinity biosensor presentations, the majority have reported the immunosensing event by an indirect method by the use of labels (e.g. enzyme activity, optical materials, quantum dots, etc.) Some academic laboratories are working on label free methods, particularly in the US and direct optical techniques have been described, also piezoelectric devices to detect mass change and similar to part of the ELISHA project direct interrogation of surfaces using impedance spectroscopy is being done. The use of conducting polymers is relatively low in immunosensors, however one group has pioneered novel organic electro-conductive polymer materials that can be used as molecular nano-wires and nano-transducers in PCR-less label-free DNA biosensors, immunosensors, biomimetic sensors and enzyme-based biosensors.

The 9th World Congress on Biosensors was held in Toronto, Canada in 2006 and 3 ELISHA partners presented new data obtained from the project. The new results obtained using the electronic test bed manufactured by partner 7 are completely different to any know immunosensor detection method and results from this were presented.

Despite all of the academic research, a simple commercial platform for a range of label free immunoassays remains to be produced, although this has now been addressed by ELISHA. One of the relatively new UK biosensor SMEs, Oxford Biosensors Ltd. have begun to explore the possibility of developing immunosensors to fit onto their generic detection platform, however the principles of detection are very traditional, using enzyme labels and standard electrochemistry techniques. Two other biosensor SMEs, Avacta Ltd and Swiss Precision Diagnostics (previously part of Unipath Ltd.) have also made approaches into the exploitation of the ELISHA technology into a fully operational immunosensor platform, indicating the level of commercial interest in affinity biosensors using antibody recognition is high. Initial meetings were made to consortium representaives covered by appropriate non-diclosure agreements, whilst later meetings have taken place with ELISHA Systems Ltd (ESL Ltd.) which has recently been formed to drive forward commercialisation of the ELISHA project outputs.

Information obtained from a commercially available biosensors report indicates that significant R&D effort in immunosensor devices is being done by several well known biosensor companies including: Bayer (in collaboration with Steag Microparts GmbH, now owned by Boehringer Ingelheim), Roche (acquired Igen in 2003 adding electrochemiluminescence immunoassay detection systems to company), TheraSense (now owned by Abbott) and Abtech Scientific Inc. Interestingly the principle of acquisition to get new technology into large company portfolios is clearly seen in these examples.

Major Achievements.

The major achievements of the whole project are as follows:

The production of several fluoroquinoline conjugates for inoculation to enable production of polyclonal antibodies for fluoroquinoline antibiotics. The synthesis of the hapten for immunisation has been optimised.

The production of model monoclonal antibodies has been completed for atrazine and terbutryn.

Model polyclonal antibodies for digoxin have been supplied to partners 2, 3 and 8.

A polyclonal fluroquinoline antibody has been produced in three separate rabbits and shows good sensitivity to ciprofloxacin down to 10nM.

The ELISA based on the fluroquinoline antibodies has been optimised and checked for selectivity and sensitivity with extremely good results and limits of detection 10-100 fold below levels required, including detection in the target matrix, mik.

The first monoclonal recombinant His-Tagged Fab fragment has been produced by fermentation, which recognises atrazine as a model for the immunosensors and has been supplied to partners 1, 3 and 8.

Gold on silicon transducers have been made and supplied to partners 1, 2, 3 and 8 (96 wafers = over 8,000 transducers). Connectors for the transducers have been manufactured and supplied.

Screen printed gold on alumina transducers have been produed and used by partner 1.

Platinum on silicon transducers have been fabricated and supplied to partners.

Microarray electrodes have been made, characterised and used by partners 1 and 2.

Photoactivated pyrrole derivatives have been synthesised as novel monomers for sensor production.

Chelation pyrroles, based on nitrilo-acetic acid – nickel complexes have been synthesised by partnre 8 and supplied to partners 1,2 and 3.

Seven potential immobilisation methods for antibodies on sensor surfaces have been developed and evaluated. (direct physical entrapment, electrostatic multicontact supra-molecular immobilisation, N-hydroxysuccinamide or N-hydroxyphthalamide, His-tag chelation, Neutravidin mediated attachment of biotin tagged antibody, glyco-immobilisation onto diboronic acid surfaces, photoimmobilisation, co-valent onto polyaniline, co-valent onto polyacrylic acid counter ions).

Surface blocking by long chain thiol compounds was shown to improv stability and reproducibility of pyrrole based immunosensors – this is an area that could become a patented process.

A calibration curve for PSA has been constructed using anti-PSA entrapped within polyaniline on microarray electrodes. Sensitivity is down to 10^{-12} M which is below the clinical requirement (normal levels are up to 10^{-10} M (4 ng.ml⁻¹).

A calibration curve for the stroke marker S-100 has been constructed using anti-S-100 entrapped within polyaniline on microarray electrodes. Sensitivity is down to 1 ng.ml⁻¹ and the immunosensor response is linear to 100 ng.ml⁻¹.

Non-specific binding on anti-PSA immunosensors has been reduced significantly using standard immunoassay blocking agents (BSA).

The first prototype electronics board has been constructed and evaluated on immunosensors with excellent results.

The laboratory prototype machine has been completed, the instrument has been constructed and evaluated.

Initial signal evaluation was completed ahead of time.

Early investigations into immunosensor signal generation has shown that the polyelectrolyte immobilisation method improves sensor output.

Direct proof of the faradaic component of the complex plane impedance of immunosensors being the important part of the antibody – antigen binding response has been conclusively demonstrated.

Pulsed interrogation of polyaniline - polyelectrolyte layers exposed to antibody and antigen has shown decreases in the amperometric transients recorded.

Antibodies immobilised onto mixed self assembled monolayers (SAMS) were evaluated using the test bed electronics constructed by partner 7 with excellent results initially using anti-atrazine Fab fragments – calibration curves for haemoglobin and PSA have been demonstrated. This was one of the most significant results of the first 24 months as it showed that nanoscale self-assembly could be used to produce working immunosensor devices. Subsequent work by partners, 1 and 7 showed that pulsed interogation of hCG immunosensors is possible.

Direct immunosensing of hCG in buffer and urine, of fluoroquinoline antibiotic in milkand of myoglobin in serum have been demonstrated.

Polymer immobilised antibodies have been successfully interrogated by the same test bed.

The ELISHA project web site became fully operational within the first year, with embedded instant update software and has the address www.immunosensors.com. It will remain operational for at least two years beyond the ELISHA project end date.

Section 2 Workpackage Progress for the whole 42 Months (36 + 6 extension).

Overview:

There were 9 workpackages in the ELISHA project which were effectively grouped into 6 major areas.

Table 1. Workpackage Area Grouping.

Workpackage number	Workpackage Title	Notes
W1A W1B	Affinity Reagent Production Purified Antibodies. Recombinant Antibodies and Fab Fragments with Affinity Tags.	Biological Affinity Reagent Production
W2	Electrochemical Transducer Production	Transducer Production
W3	Production of Matrix Precursors	G D 1 1 1
W4	Fabrication of Nanostructured Immunosensors. Sensor Production Operational Optimis	
W5	Development of Immobilisation Strategies and Matrix Construction	-
W6	Sensor Address Systems and Interrogation Electronics	Electronics (System and interrogation)
W7	Signal Generation and Non-specific binding optimisation	Knowledge generation for clear signal generation.
W8	Evaluation of Affinity Sensor Systems including Signal Processing	Instrument Construction,
W9	Laboratory Prototype System	Optimisation and Evaluation

Progress on all of the workpackage progressed well and was largely on-time (see progress chart on page 170).

Only one workpackage ran outside expected timescales. Workpackage 1B was slightly late due to the difficulties in generation of the rabbit primer library, the supply of first recombinant antibodies was delivered at month 15 rather than month 12. The first recombinant antibodies were finally made available at month 17. This workpackage was behind schedule by 2 months in regard to recombinant antibodies, but by the project end had fully caught up.

All milestones within the 42 month project period (36 +6 months extension below) have been fulfilled as specified;

- W1 Month 3: Supply of first antibodies from existing stocks; Month 6: Supply of first hapten derivatives; Month 9: Supply of first antibodies; the first polyclonal fluoroquinoline antibody were supplied in month 17. His-Tagged Fab antibody fragments were supplied to partners 1, 3 and 8 in month 23.
- W2 Month 2: Initial supplies of standard metal transducers; Month 6: Initial designed metal (gold) on silicon transducers both single and dual electrodes; Month 12: Micro-electrode transducers for evaluation (delivered month 10). All transducers were supplied on time by month 20.
- W3 Month 3: Initial supplies of monomers; Month 6: Initial designed monomers with specific binding characteristics; Month 18: Initial novel monomers made and available some delivered to partners 1, 2 and 3 for evaluation. Month 24. NHS, Biotinylated and NTA-pyrrole monomers supplied to partners. Month 36. Photoactivated monomers made and supplied to partners; polymerisable terbutyrin and ciprofloxacin monomers made and supplied to partner 6.
- W4 Month 12: Initial results for fabricated immunosensors formed by entrapment and post polymer deposition. Month 18: Feedback from other workpackages and partners has enabled modified immunosensors to be fabricated. Specific example is in polyaniline biotin neutravidin biotinylated anti-PSA fabrication format for blocked anti PSA sensors described on pages 70,71 Month 23 24. Anti-haemoglobin and anti-fluoroquinoline immunosensors constructed and tested. Months 24 42. Full immunosensors and calibration curves for myoglobin, haemoglobin, myelin basic protein, S-100 protein, Neuron Specific Enolase and Ciprofloxacin have been completed.
- W5 Month 6: Biotin loaded / hydrophilic pyrrole monomers for antibody immobilisation; Month 12: Pyrroles having photoactivation centres for antibody immobilisation. Months 18-24. immobilisation protocols based on SAMS, His-Tag affinity immobilisation, co-valent derivatisation of polyaniline and polyacrylic acid counterions have been done and tested. Months 24 42. Two new polyaniline immobilisation surfaces produced, using respectively the biotin:avidin couple and boronic acid:cis-diol (glycosyl) couple.
- W6 Month 18: The first version of the specifications of the dedicated electronics are done, page 50 and the specialised electronics test bed has been completed on time. Month 23-24 Evaluations of the test bed electronics done on anti-atrazine, anti-PSA and anti-haemoglobin based immunosensors. Early evaluations of anti-fluoroquinolines. Months 24 42. Laboratory prototype contructed and evaluated. Iterive improvements performed with partners 1 and 7 to develop measurement protocols, particularly for hCG (but also SAM formation and haemoglobin were tested.
- W7 Month 18: The first series of results to show reduction of non-specific binding have been produced, with a clear understanding of the signal generation. Further information on ion transport is shown on pages 116,117. Months 24 42 . evelopment of non-specific binding and subtraction protocols have been demonstreted for several analytes including myelin basic protein, S-100 protein, Neuron Specific Enolase and Ciprofloxacin
- Work was completed on signal processing algorithms and the evaluation of affinity sensor systems has been done. Month 24. Curve fitting and equivalent circuit interpretations were performed for model polypyrrole immunosensor systems. This explained the parameters that model the instability and destruction of non-stabilised polypyrrole films and will be the subject of a publication. Months 24 42. In depth evaluation of parameters that influence signal generation and transducer stability has been done. Specific parameters identified that predict transducer performance and breakdown.
- W9 Market and exploitation information was gathered to feedback into prototype design for the exploitation and commercialisation of the project deliverables. Month 24. Prototype design completed. Months 24 -42. Construction of the laboratory prototype finished. Several consulations with interested commercial entities have taken place.

The deliverables progress table on the next two pages gives a rapid 'at a glance' overview of the project.

 Table 2. Deliverables Progress Table

Del. number	Deliverable Title	WP N°.	Date Due	Actual Forecast Delivery Date	Estimated Indicative Person Months	Used Indicative Person Months	Lead Partner	Comments
D1	Supply of existing antibodies.	1a	Month 3	Month 3	3	3	6	Existing antibodies for early sensor work have been supplied for atrazine and digoxin. Others such as anti-BSA and anti-PSA were purchased.
D2	Supply of hapten derivatives.	1a	Month 6 to Month 24	Month 24	24	24	6	The supply of different haptens and conjugates is ongoing until month 24. Different ones being made available throughout the project. Done.
D3	Supply of purified antibodies.	1a	Month 9 to Month 30	Month 30	31	28	6	Purified antibodies to targets are expected throughout the project, terbuteryn being first. First polyclonal fluoroquinoline antibodies available month 17.
D4	Supply of recombinant antibodies and Fab fragments.	1b	Month 12 to Month 30	Month 30	40	34.5	4	The first polyclonal fluoroquinoline antibody is available and has been tested in ELISA immunoassay with good results to ciprofloxacin. His-Tagged Fab supplied to partners in month 23.
D5	Characterisation of antibodies and recombinant antibodies/Fab fragments.	1b	Month 36	Month 36	12	8	4	Some early characterisation of the first polyclonal fluoroquinolines antibody has already been done. Optimisation studies for fluoroquinoline ELISA's done.
D6	Initial supply of standard metal (gold) on silicon transducers	2	Month 3	Month 3	3	3	5	Single standard metal transducers were provided by month 3.
D7	Stocks of designed metal transducers on silicon substrates	2	Month 6 to Month 24	Month 24	11	11	5	Designed dual and interdigitated transducers supplied by month 6. Platinum transducers done and supplied to partners. Further gold on silicon done and supplied.
D8	Micro-electrode transducers	2	Month 12	Supplied Month 10	4	4	5	Micro-array electrodes were supplied and used by partner 2 to give early results in workpackage 4.
D9	Transducers having alternative geometries	2	Month 30	Month 30	6	2	5	Initial designs have already been conceived and should enter production ahead of time. Some supplied, redesigns being done ready for supply by month 30.
D10	Supply of existing monomers	3	Month 3	Month 3	3	3	8	Existing monomers have been supplied to partners.
D11	Designed monomers for specific binding:	3	Month 6 to Month 24	Month 30	24	24	8	Photoactivated monomers synthesised and supplied to partners. Di-pyrrole biotin and NHS pyrrole monomers available, NTA pyrrole monomers scaled up and supplied to partners.
D12	Alternative immobilisation materials	3	Month 18 to Month 30	Month 34	6	3	8	Alternative matrices will be explored on time. Some lipid SAM matrices tested with good results.

D13	Relationships between polymer formation, antibody type and deposition process for immunosensor fabrication	4	Month 12 to Month 30	Month 40	24	21	2	This started in month 9 and will continue through to month 30. Immobilisation of antibodies in a more structured orientation is beginning to give more detailed understanding. EQCM studies ongoing. SAMS deposition process tested.
D14	Detailed protocols for immunosensor fabrication	4	Month 30	Month 30	20	6	2	Some protocols designed. Work on immobilisation interfaces in progress. Direct co-valent immobilisation evaluated and affinity surfaces tested. Both good results.
D15	Nanostructures and Nanoelectronics of different immunosensor types	4	Month 36	Month 36	9	6	2	Electrostatic nanostructures being investigated. His-Tag linked antibodies and biotin linked antibodies being investigated as nanostructured films.
D16	Monomers, materials and methods for nanostructured immobilisation.	5	Month 6 to Month 33	Month 33	55	48	3	Monomers and materials have been available from month 6 and the methods of immobilisation are being developed. Novel attachment at the nanoscale has been done using DNA affinity surfaces and polyelectrolyte layering in WP5. Lipid SAMS and his-tag affinity structures done. Direct co-valent surfaces prepared.
D17	Knowledge-based protocols for reproducible immunosensor fabrication and operation	5	Month 36	Month 42	36	19	3	Early work suggests that antibody orientation on immobilisation will give better signal to noise ratios. Monolayers tested with good results.
D18	Specialised test bed electronics and rigs for sensor interrogation.	6	Month 18 to Month 30	Month 18	58	55	7	Preliminary demonstration of the electronic rig was carried out at the 12 month meeting. The electronics for interrogation test beds was done and disseminated at mid-term. Evaluations done an immunosensors done.
D19	Electronics for laboratory prototype.	6	Month 32 to Month 36	Month 34	12	0.5	7	In progress. Feedback from the project partners from the test bed electronics assisted in the final electronics design, which is done. Manufacture is in progress.
D20	Knowledge and understanding of the signal generation processes in the different nanostructured immunosensors produced.	7	Month 18 to Month 36	Month 36	34	24	1	The understanding of the signal generation is coming clear. Detailed experiments devised after some initial work which was inconclusive. Orientated immobilisation has been found to be important and the faradaic component of the total impedance signal has been conclusively demonstrated to report the antibody-antigen binding event in conducting polymer immunosensors. First derivative useful in the interpretation of affinity binding using the test bed electronics.
D21	Immunosensors exhibiting reduced non-specific binding	7	Month 32	Month 32	24	9	1	Non-specific binding protocols being investigated. The immobilisation types appear to be significant on the signals. Nano-orientation of antibodies is important and the first proofs of non-specific binding reduction have been demonstrated for PSA immunosensors. Further work done on S-100 and anti-haemoglobin immunosensors

D22	Evaluation reports of affinity sensor systems.	8	Month 36	Month 42	43	14	2	Early equivalent circuit modelling done. Equivalent circuit fitting for instability of polypyrrole immunosensors done, with modelling and parameters being affected understood.
D23	Working laboratory prototype.	9	Month 34	Month 34	24	5	7	Feedback has been given from the evaluations on the test bed electronics using three types of immunosensors. Designs finalised and manufacturing has begun.
D24 *	12 Month Report	-	Month 12	Month 13	6	6	1	Done on Time
D25 *	Mid-Term Report and Evaluation	-	Month 18	Month 18	3	3	1	Done onTime.
D26 *	24 Month Report	-	Month 24	Month 24	3	3	1	Within Time
D27 **	36 Month Report - Final Deliverable	-	Month 36	Month 42	6	0	1	Within the time for extension

^{*} Deliverables D24 to D27 inclusive have timescales that include the project management for years 1,2 and 3 of the 3 reporting periods. The actual time to compile and write the 12 month, mid-term, 24 month and final reports will be about 4 person months in total. The rest of the time is in running the project, partner contacts and visits, arranging and managing project meetings and web site management.

^{**} Project was extended for 6 months giving a final deadline of 30th June 2007, i.e. 42 months in total.

Project Meetings.

Eight project meetings have taken place as follows:

- 1. Kick-off meeting held at the University of Leeds, January 2004
- 2. Six Month meeting held at Technische University Munchen June 2004
- 3. Twelve Month meeting held at University of Barcelona, December 2004
- 4. Mid-Term meeting held after the Bioelectrochemistry 2006 conference in Coimbra, June 2005
- 5. Twenty Four Month meeting held in Cork, December 2005.
- 6. Thirty Month meeting held in Cranfield University, June 2006
- 7. Thirty Six month meeting held in University of Grenoble, January 2007
- 8. Final (42 month) meeting held in the Technische University Munchen, June 2007

In addition Steering Committee meeting were convened:

- After the 12 Month project meeting to review the first years work and direct the next 6 months progress towards the mid-term meeting.
- After the 24 month project meeting when we concluded that the project was proceeding to plan with very good scientific and potentially exploitable results.
- After the 36 month meeting, when plans for the final six months no-cost extension were discussed

Minutes of meetings are available on the web site and are reproduced in Appendix 1 of this report.

Workpackage number: W1. Affinity Reagent Production and Testing.

Objectives: To produce supplies of hapten derivatives for antibody production. To supply purified antibodies and recombinant antibody reagents for sensor production. To provide modified recombinant antibodies (tagged) for specific immobilisation protocols enabling simple sensor manufacture. Main targets are fluoroquinolines (antibiotic), prion peptides, cancer marker (prostate specific antigen), early models include atrazines.

Project Time	line	1 2 3 4 5 6 7 8 9 10 11 12 13 14 15 16 17 18 19 20 21 22 23 24 25 26 27 28 29 30 31 32 33 34 35 3	36
Workpackage 1	Antibodies		
Task 1.1	Purified Abs / Haptens		
Task 1.2	Recombinants / Fab's		

D2: Supply of hapten derivatives

Early work n the development of derivatives of pyrrole, through the conjugation to atrazine were done to compliment the early supply of existing anti-pesticide antibodies using aminopropylpyrrole (APP) and hydroxypropylpyrrole (HPP) as starting points. These compounds would be further used by Partner 8 (ICMG), Dr. Serge Cosnier, in the preparation of electropolymer films to test particular electrochemical transduction methods.

Initially, small scale syntheses were attempted in order to prove the reaction pathways for APP by the Active Ester and Mixed Anhydride Methods.

These consisted of use with dicyclodicarbodiimide (DCC) and i-butylchloroformate. The active ester method yielded a new product as shown by thin layer chromatography (TLC) but was inconclusive because of the small quantity of APP starting material used (ca. 5mg). This makes characterization difficult in methods such as proton NMR. A similar scenario was seen for the use of the mixed anhydride method. Following this approach, it was decided to use a model compound, similar in size and form of the APP. This would allow for better characterization of the reaction steps.

Through the use of DCC and N-hydroxysuccinimide (NHS) we attempted the conjugation. However using these conditions, the formation of N-acylurea unwanted by-product dominated. Alternatively, DmAP (dimethylaminopyridine) was used with the model compound. DmAP behaves as a catalyst in this case and highlighted the feasibility of this reagent for the proper conjugation of hapten atrazine to APP.

At this juncture, the reaction with the original starting material was scaled up and the conjugation performed under argon atmosphere. TLC showed the presence of two products of the reaction. In order to separate the two products flash chromatography was used which entails the addition of a solution of the reaction mixture to a column of silica and each product separates at a different rate. Elution at the end of the column and analysis of the eluent, at first, by proton NMR identifies the product structures. Using this method the unwanted by-product (acylurea) was also seen but the other product was verified by ¹H NMR and mass spectroscopy to be our desired product (aminopyrrole-atrazine 4a). The mass corresponding to

391 proves the conjugation worked. There was some small presence (3%) of isourea but this was deemed insignificant for the electropolymerisation process. Final product was found in 10% yield or 31 mg as amount using this procedure.

Further work to improve the product yield and purity continued after the mid-term meeting and a systematic study on the conjugation procedures potentially useful to prepare pyrrole derivatives was performed. The acid-activating agents such as DCC, EDCI, CDI, OCL chemistries were evaluated, typically used in peptide chemistry. As pyrrole analogues we used the corresponding aminopyrrolidines and aminopyrrolidones. The reaction and structures are shown below.

The use of CDI as activator yielded the best results with all the analogues assayed. The reaction product was almost 100% pure by HPLC and NMR, Figure 1 below. The characterized aminopyrrole conjugate was delivered to Partner 8 who could finally start the electrochemical characterization of this compound and its inclusion in the polypyrrole film.

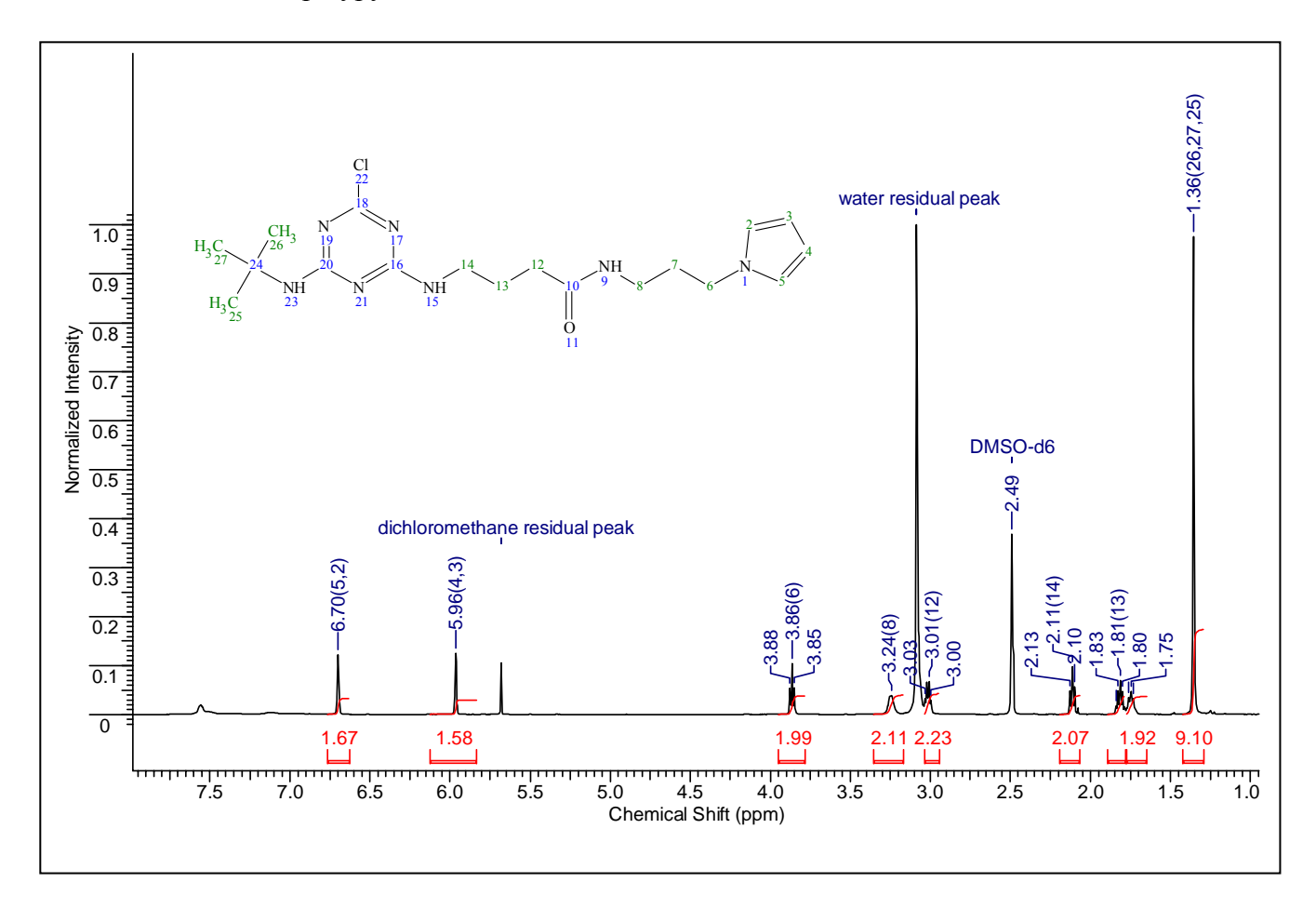


Figure 1. Purity of atrazine-pyrrole derivative by ¹H NMR.

In the same way, electroactive haptens for fluoroguinolines were developed.

The same strategy was followed as for the atrazine haptens and two pyrrole derivatives were synthesized. One was obtained using a method similar to that used for the synthesis of the fluoroquinolone haptens (aromatic fluorine displacement by an amine) and the second was a conjugation between the competitor hapten and a pyrrole containing a carboxylic acid.

When these compounds were used to build the electropolymerized polypyrrole layer it was found that no active fluoroquinolone would remain on it. In collaboration with Partner 8 a fluoroquinolone grafting procedure over the pre-grown polypyrrole layer was developed. This strategy was based on the copolymerization between pyrrole and a pyrrole bearing an activated carboxylic acid group and then, after the polymerization, the ethylenediamino-floroquinolone hapten was immobilized. This post-polymerization method finally yield the desired fluoroquinolone activated polypyrrole layer

Fluoroginoline hapten production.

The main objective in this task is the production of polyclonal antibodies with affinity towards fluoroquinolones used in foodstuff production.

Design of the hapten

To design the hapten we needed to know the most used fluoroquinolones in veterinary area, their chemical and physical properties, their metabolism and their maximum residue limits (MRLs). For this reason we made a large bibliographic search. In addition, we made a theoretical study using a computational chemical model (PM3 semi-empirical model) to see the geometry and the electronic properties and we observed that for the common fragment of the structure all the properties are very similar for all the studied compounds. We decided to attach the linker group to the quinolone nitrogen atom which masks the most variable group, and we kept the most important and common epitopes, chemical, physical, conformational and electronic properties intact. Also, for the protein coupling

procedure we needed a group with orthogonal chemistry versus amino and carboxyl groups and we have chosen a reactive thiol group (**GRP**) for the linking. However, due to its reactivity it required protection throughout the synthesis. The proposed hapten was the following compound:

Synthesis and Characterization of the hapten

The next step was to make a bibliographic research to see the various pathways of synthesis of fluoroquinolones. Wwe found two different pathways and proceeded with the one that needed fewer reaction steps and had better yields of reaction. We modified this pathway to synthesize our hapten; the retrosynthesis is the following:

We started the synthesis with good yields in the first steps and found the first problem when we added the linker to the nitrogen of the fluoroquinolone; this problem was easily solved by changing the chlorine atom for an iodine atom.

The main problem appeared when we added the piperazine ring since we obtained two regioisomers in a 4:1 ratio in the position 7 and 6 respectively. We attempted several purification methods and still could not separate the regioisomers. For this reason we decided to change the synthesis and we started the new synthesis with the aniline with a fluorine atom in the 7 position instead of a chlorine atom. All the reactions proceeded similarly with high yields and the piperazine ring was added with high yield and purity.

The next step was de-protection of the thiol group. The literature reported several de-protection methods but all of them used strong conditions incompatible with bio-reagents. For this reason we used a model reaction using ethylmaleimide that mimics the linker group in the protein moiety. The de-protection reaction was optimized using trifluoroacetic acid, various scavengers and different temperatures followed by HPLC-UV and finally the model compound was obtained in good yield and isolated. All of the products were characterized by proton nuclear magnetic resonance (NMR).

Synthesis of the immunogen

The next step was the coupling of the synthesised hapten and the protein carrier. We needed a heterobifunctional linker to modify the protein and link the hapten. We chose the maleimide group because it is most frequently used and we synthesised the heterobifunctional linker with that group with high yield and purity.

For the conjugation, we made, in parallel, the de-protection reaction of the hapten and the protein derivatisation. We then purified the hapten and the protein separately and finally added the hapten to the derivatised protein.

The main problem during the first attempts was the solubility of the hapten in buffer and so the co-solvent and the pH were changed. We then made extractions of the crude de-protection mix with different solvents and finally, at pH=7 extracted with dichloromethane. These steps yielded 12 residues of hapten linked to the protein as confirmed by MALDI-TOF. The problem however was that the maleimide group (linker) was in excess (35% of hapten respect to the linker). As it could be immunogenic, we could have obtained two different families of antibodies if it was used this as immunogen. For this reason we decided to change the maleimide linker group for an iodoacetic one that was smaller and that could subsequently be capped with a cysteine derivative. These steps allowed for a non-immunogenic moiety and specific antibody formation.

At the 12 month point the preliminary characterisation of the immunogen by UV absorption was done but the immunization to produce the antibodies was just starting. Also the actual synthesis of the hapten was not optimised.

Optimisation of Hapten Synthesis.

Thiol nucleophylic reactions are very sensitive to the pH conditions. At acidic pHs it is very slow and in alkaline conditions the disulfide formation is also fast. On the other hand, the solubility of the hapten is higher in acid media than in other. Due to these problems we decided to run a battery of reactions at micro scale to fully optimise the conjugation protocol. Finally we obtained a set of conditions which allowed us to prepare the hapten conjugated to BSA in a molar ratio of 17:1 characterized by MALDITOF and by UV-Visible spectrocopy. In a similar way the hapten was conjugated to Keyhole Limpet Haemocyanin (KLH) to prepare the final immunogen. These two conjugates were delivered to Partner 4 to develop their monoclonal antibodies.

Rabbit immunization

At this point work proceded in two parallel directions. One approach was to raise the immune response in rabbits to get the desired antiserum and the second was to prepare a wide set of structurally related haptens to be used as competitors after their conjugation to the corresponding protein carries or enzymes.

Three New Zealand white rabbits were immunized with the fluoroquinolone immunogen following our standard protocol (1 immunization and 5 boosting injections) taking periodic blood samples to control the process.

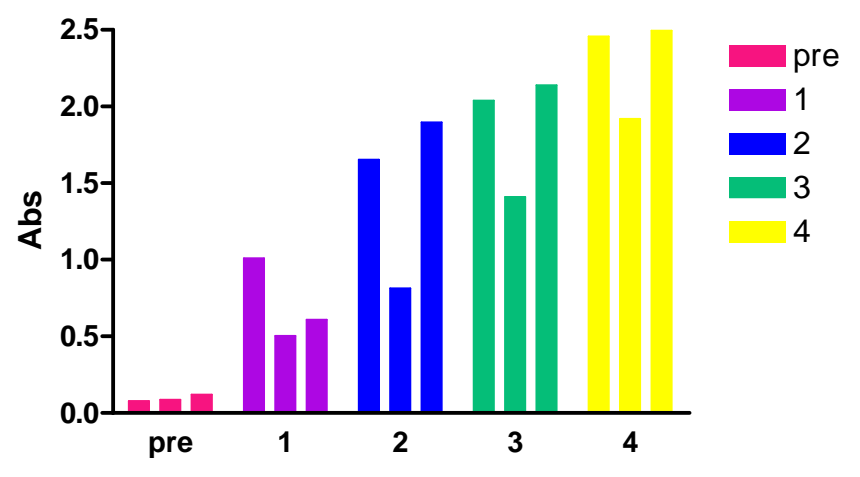


Figure 2. Fluroquinoline Immunization Results.

As is evident from figure 2, all three rabbits showed a good response against the hapten conjugated to BSA via maleimido and via iodoacetic comjugated hapten with no signal against the cysteine derivative. These two facts showed us that the antiserum reacted against the fluoroquinolone structure but not with cysteine and the linker group which had a very low effect, if any.

Final antiseras were collected and the rabbit's spleen's were sent to partner 4 to develop monoclonal antibodies starting with rabbits B-cells. The theory was that if these monoclonal antibodies could be developed, they would be better than the standard mouse monoclonals.

Antiserum characterization.

In a test with the 3rd bleed we observed an inhibition of the signal when the antiserum was titred in the presence of ciprofloxacin. This data suggested that we could develop a competitive assay using as competitor the immunizing hapten conjugated to BSA.

To develop an ELISA assay the first step must be the characterization of the affinity response between antiserum and the competitor. The usual way is run a 2D experiment, where several relative binding curves are obtained simultaneously with systematic changes in the relative concentration of the reactants.

The result was very good for the three antiserums produced, shown in figure 3.

Clearly the antiserum dilution lower than 1/64000 yielded signal saturation (Abs. higher than 1.8 units) and the ideal dilution for the ELISA assay varies from 1/256000 to 1/512000. This antiserum dilution factor reflects the affinity of the antibodies produced and the amount of the specific antibodies in the antiserum. The second important fact was the competitor dilution needed to get a good signal out of the binding curve plateau. For the three antisera, a competitor dilution of 60 ng/ml yielded a good signal. The results of these experiment were very promising if we remember that the competitor was the homologous hapten linked by the maleimido chemistry to BSA whereas the immunogen used the iodoacetic chemistry. Then the affinity showed would be directed to the fluoroquinolone structure giving an easy route to development of a competitive assay for quantitative purposes.

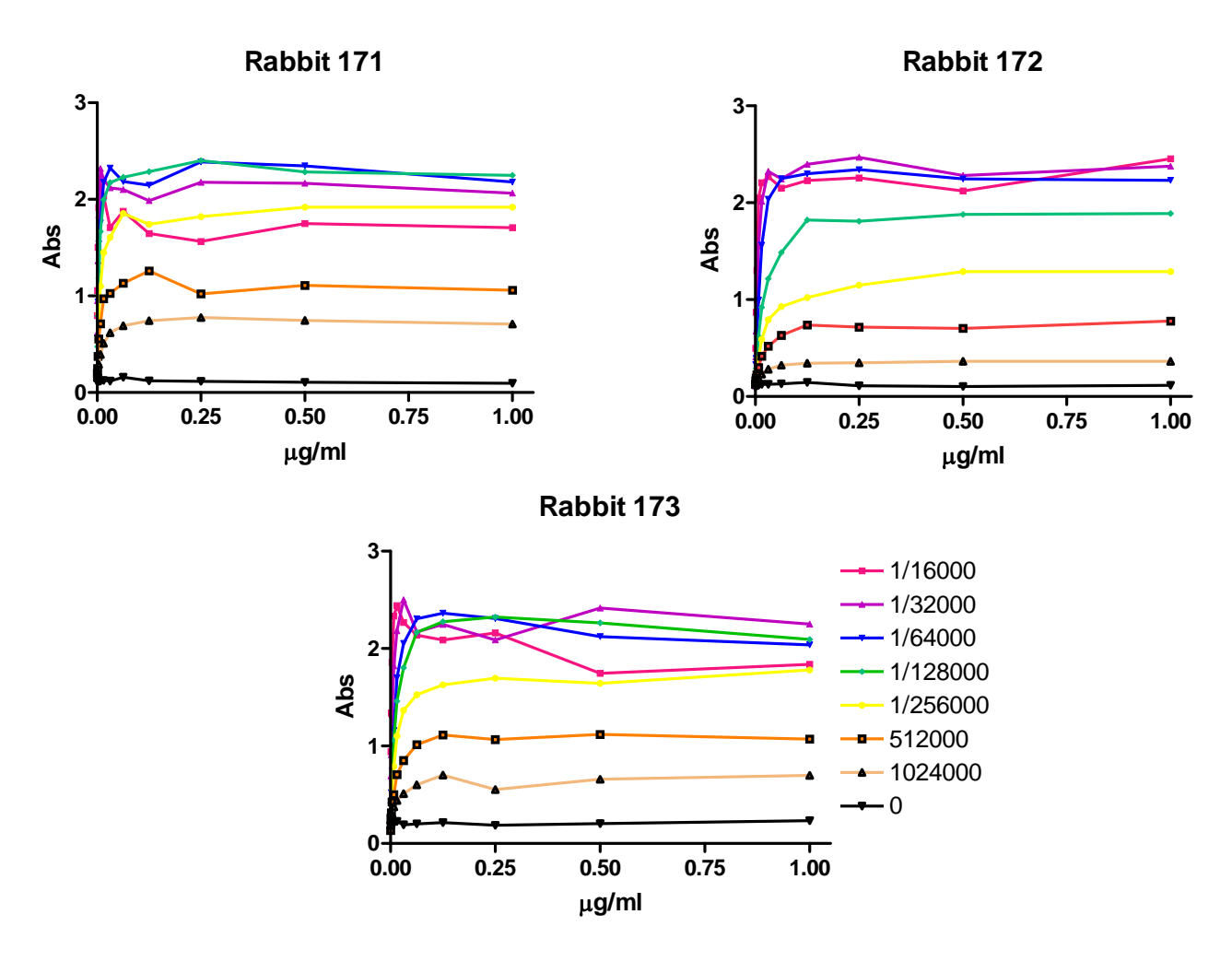


Figure 3. Binding Curve Responses for Polyclonal Fluroquinoline Antibodies

Development of ciprofloxacin competitive ELISA assay.

In a preliminary experiment without any assay optimization very good result were fond in terms of IC50, limit of detection and response line (figure 4 and table 3).



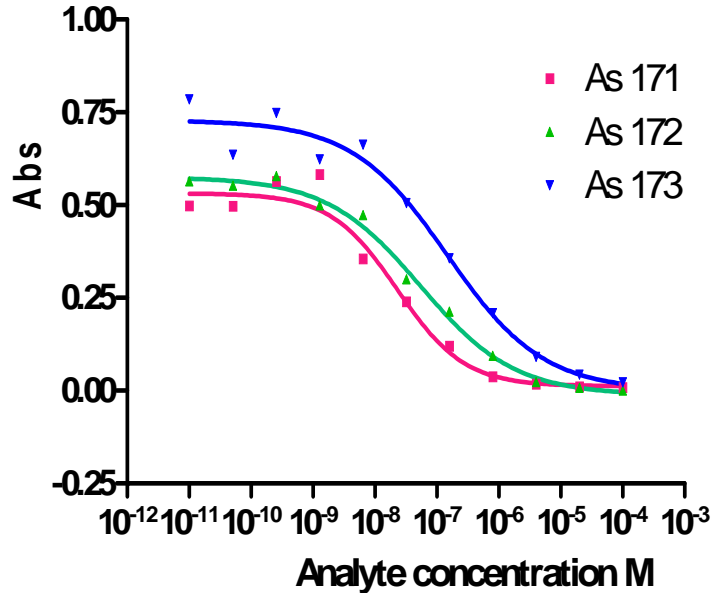


Figure 4. Competitive Immunoassay Curves for Ciprofloxacin using Polyclonal Antibodies from Rabbits 171, 172 and 173.

Table 3. Characterisation of Anti-Fluoroquinolines.

Rabbit	171	172	173
BOTTOM (Abs)	0.01196	-0.01161	0.000332
TOP (Abs)	0.5323	0.5756	0.7285
SLOPE	-0.8048	-0.5713	-0.563
EC50 (nM)	23.08	54.45	148.5
EC50 (ppb)	7.6	18.1	49.1

One other important factor was the very slow non-specific signal reflected by the low bottom value (the assay noise).

With these results (the limit of detection is one order of magnitude lower) we concluded that the obtained antisera were appropriate to develop analytical assays (ELISA) and sensors to detect with high sensitivity some fluoroquinolone antibiotics as planned for the mid-term milestone in WP1.

Fluoroquinoline Assay Optimisation.

The first task in this stage was the synthesis of a collection of potential chemical competitors, Figure 5. The competitor structure could shift the assay properties from a high selectivity to a broad selectivity and/or the final detectability.

Figure 5. Fluoroquinoline Competitor Analogues

These competitors were conjugated to several carrier proteins or enzymes (HRP, APs, BSA, OVA, CONA). Most of the competitors (combinations of 1 hapten-1 protein) yielded competitive assays (Table 4), with good limits of detection, (see Figure 6). Finally we chose the competitor CFQ1Pro7EDA-BSA due to the extremely low detection limits and the broad reactivity shown. Figure 7 shows the calibration curves for four different fluorquinolines using the optimised assay system.

Table 4. Optimisation of Fluoroquinoline ELISA's. Features of the 8 best ELISAs developed (Total: 18 ELISAs)

Competitor	As	[AT]	[As]	Abs max	Abs <i>min</i>	IC50, nM	Slope	R2
SPrPP	171	0.0156	1/128000	1.615	0.0732	14.39	-0.6613	0.9985
SPrMF	171	2.5	1/16000	1.767	0.1371	49.07	-0.8577	0.9980
PrPP	171	0.25	1/16000	1.464	0.1249	21.4	-0.5999	0.9928
	172	0.25	1/4000	1.423	0.0668	68.7	-0.7167	0.9689
CPrPP	171	0.25	1/64000	0.6264	0.0603	15.69	-0.5096	0.996
PrEDA91	171	0.25	1/4000	1.088	0.2523	5.123	-0.7035	0.9154
PrEDA28	171	0.25	1/16000	1.360	0.0982	4.973	-0.7930	0.9691
	172	0.25	1/4000	1.427	0.0791	34.56	-0.8451	0.9939
				т			п	

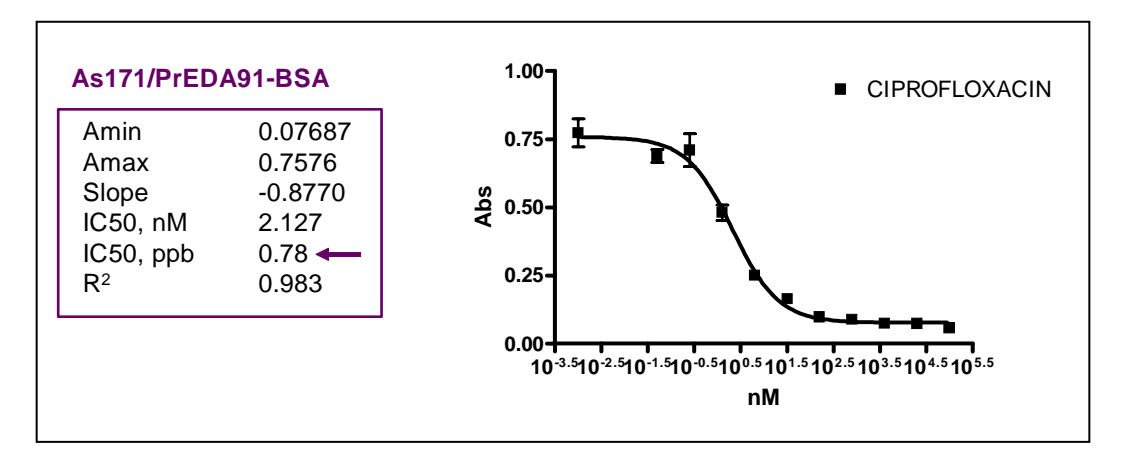


Figure 6. Optimised Competitive ELISA for Ciprofloxacin.

The chemical structures of the common fluoroquinoline antibiotics are shown below in Figure 7. The optimised ELISA was tested on all of them to give calibration curves showing limits of detection at the nanomolar level.

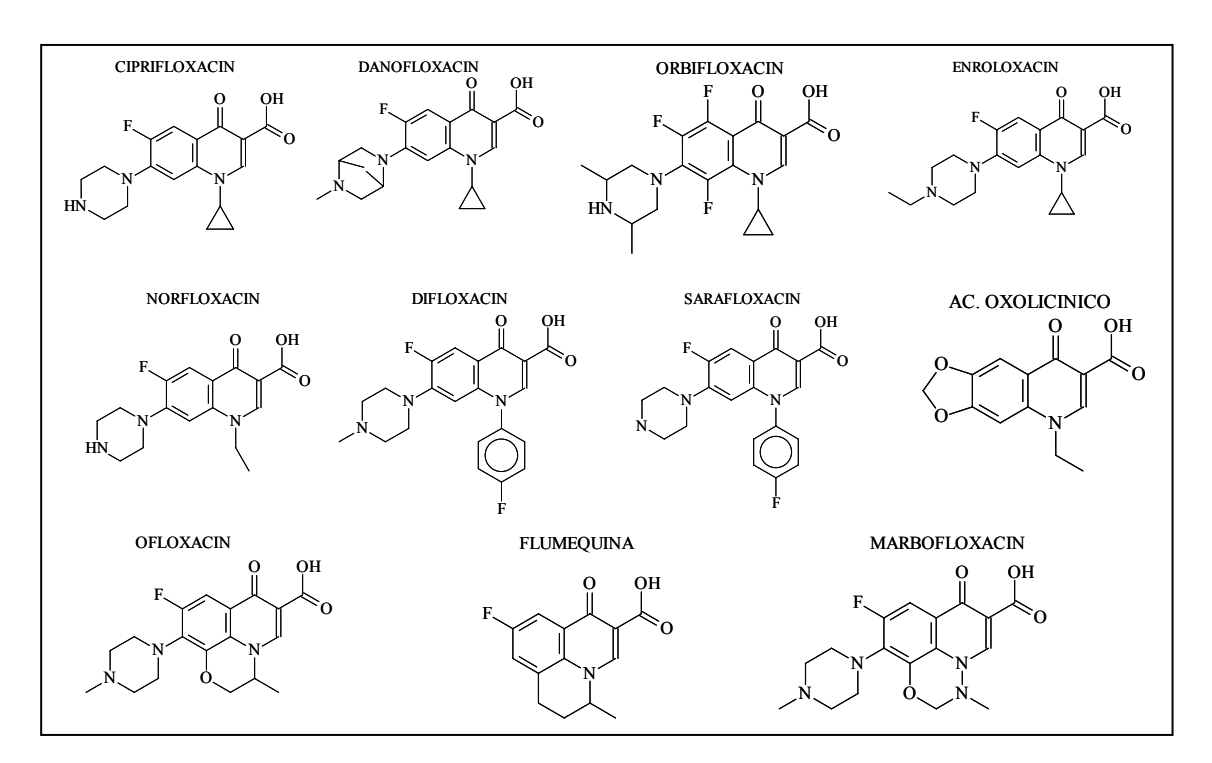
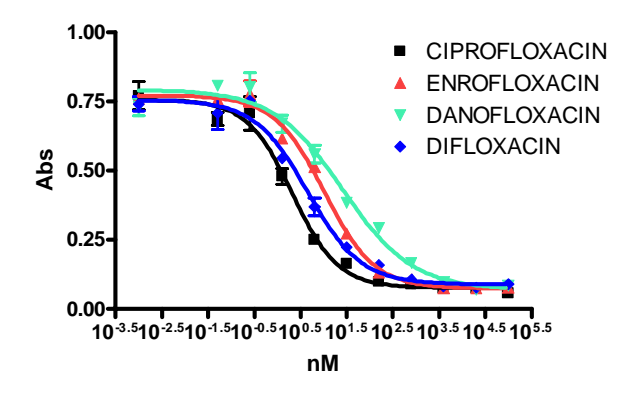
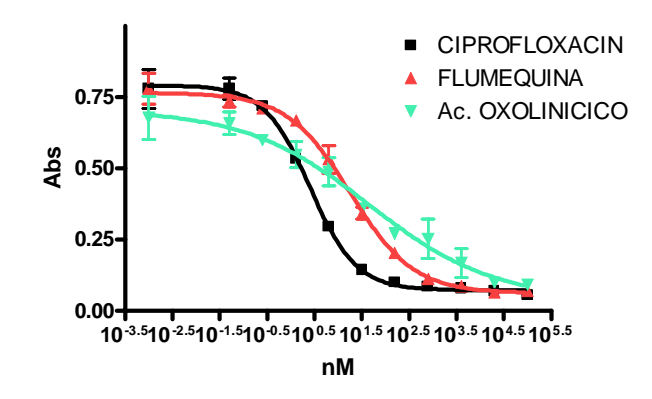


Figure 7. Chemical Structures of the Common Fluoroquinoline Antibiotics





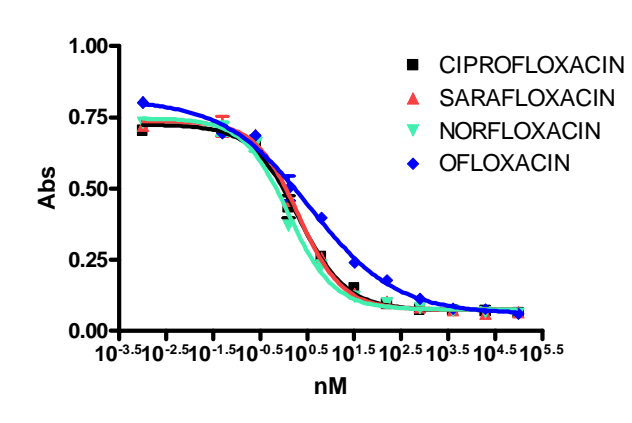


Figure 8. Calibration curves of the different fluroquinolines using the optimised ELISA.

	CIPROFLO	XACIN E	ENROFL	OXACIN	DANOF	LOXACI	N DIFLO	OXACIN	
EC50 nM		2.13		10.43		26.	16	4.59	
EC50 ppb		0.78		3.75		9.	35	2.00	
%CR		100		20			8	46	
PM		367.8		359.4		357.	38	435.85	
	CIPROFLO	XACIN	SARAFLO	OXACIN	NORFL	OXACIN	I OFLC	XACIN	
EC50 nM		2.09		2.10		1.	28	3.58	
EC50 ppb		0.77		0.89		0.	41	1.29	
%CR		100		99		1	64	58	
PM		367.8		421.83		319.	33	361.37	
	CIPROFLO	XACIN F	FLUMEQ	UINA	Ac OXO	DLINICIC	O		
EC50 nM		2.58		18.19		44.	95		
EC50 ppb		0.95		4.75		11.	74		
%CR		100		14			6		
PM		367.8		261.25	5 261.23				
Campaiin	d Cipro *	Enro *	Dano	Diflo	Flume	Marbo	Sara #	Oxoli	
Compoun									
MRL ppb	100	100	200	400	200	150	30	100	

Table 5. Analytical Parameters of the Different Antibiotics in the Optimised ELISA.

MRL for bovine muscle in ppb. Council Regulation n°2377/90 Updated up to 22.07.2003

The MRL or maximum recommended limit of the different fluoroquinolines in bovine muscle or fish muscle are listed at the bottom of table 5. Note that most are in the 100's of ppb except one, sarafloxacin which is set at 30 ppb. The sensitivity of the ELISA was much lower in most all cases ranging from 0.45 ppb to 11.74 ppb at mid-point of the curve.

Fluoroquinoline Competitors

Free or protein conjugate haptens for fluoroquinolone antibiotics immunoassay were prepared and delivered to ELISHA partners as required. The set of potential competitors for fluoroquinolones immunoassay prepared are shown below. These were assayed in the competitive format in order to find the best sensitivity or a wider fluoroquinolone family recognition (figure 9).

Figure 9 Fluoroquinilone competitor structures.

Gray arrows show haptens which could be linked using an amino group, purple arrows show haptens to be linked using thiol chemistry and blue arrows those using carboxyl group chemistry. The boxed structure shows the homologous to the immunogen compound whilst the boxed named compound shows the competitor which yielded better results in sensitivity and family recognition. The synthesis of these haptens was performed using similar procedures to the method used for the immunogen synthesis.

The CFQ1Pro7EDA* haptens were delivered to the partners developing the fluoroquinolones immunosensors (Partners 1, 2, 3).

Sulfonomide Antibodies and Haptens

New sulfonamide antibodies were raised in the context of other AMRg projects and were supplied as an extra item for ELISHA project. In the ELISHA 3rd year we characterized these antibodies priors to delivering them to Partner 4. The immunization protocols and antibodies titer evaluation were performed using the standard protocol developed by AMRg group and used to raise the anti-fluoroquinolones antibodies.

New antibodies against sulfonamide antibiotics were also raised in this project following a similar immunogen and competitor design rules that was used in the case of anti-fluoroquinolones antibodies.

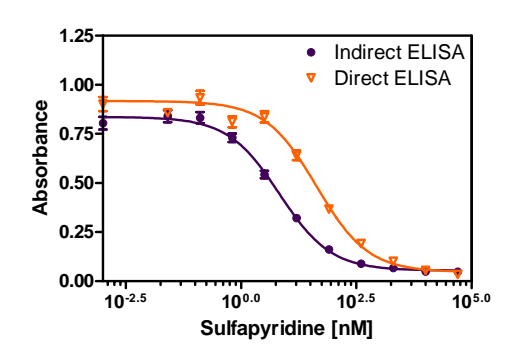
The immunogens developed and used, kept at maximum the common structural features for all the sulfonamides and try to reduce the variable part. The haptens were finally linked to KLH as a carrier protein and to BSA to check the derivative and as a hapten to control the antibody titer while immunization is in progress. As for fluoroquinolones a set of potential competitors to be used in the

ELISA assay were prepared. After checking the whole hapten set, the two best haptens and competitors were those shown in figure 10.

The whole set of immunizing and competitor haptens as well as their protein conjugates were delivered to Partner 4 to be used to raise monoclonal and recombinant antibodies for sulfonamides.

Figure 10 Optimum sulfonamide haptens and competitors.

After classical characterization process (1D-antibody titration against the competitor hapten, and 2D-binding optimization) we selected the antibody-competitor (direct or indirect format) combinations that yielded the best results and checked them in the competitive format. Finally two assays were developed, one direct and one indirect that showed enough sensitivity and good assay characteristics in buffer to detect sulfapyridine as a representative compound (figure 11 and table 6)



	Direct ELISA	Indirect ELISA
Amax	0.047	0.836
Am <i>in</i>	0.917	0.054
Slope	0.78	0.77
IC50, µg L ⁻¹	11.1 ± 1.3	1.69 ± 0.23
LOD, µg L ⁻¹	0.49 ± 0.15	0.10 ± 0.06
N	11	11

Figure 11. Direct and indirect sulfapyridine ELISA

Table 6. ELISA paramters (from Figure 6)

D3: Supply of purified antibodies

Prior to the supply of antibodies, tracers or coating reagents to the other partners it was necessary to assess the performance of these compounds and determine the best combinations for successful assaying. The sensor development groups then used the reagents for successful preparation of their particular sensing platforms. Therefore it is essential that the reagents function in such a manner to give sensitive, specific methods. The evaluation protocols are given in Appendix 1.

Affinity purified recombinant Fab-fragments (K411B Atrazine-Antibody) and corresponding hapten-derivative were delivered to partner 3 (Lyon) and 1 (Leeds). Monoclonal antibodies against the s-triazine pesticide terbutryn, prepared in hybridoma culture and affinity-purified using protein A-column chromatography was made available at mid-term.

The polyclonal anti-fluoroquinolones antibodies were obtained and fully characterized by month 24 and then by month 36, antiserum or partially purified (ammonium sulphate precipitation or protein A affinity chromatography) antibodies was delivered to Partners 1, 2, 3 to develop the immunosensor platforms.

Design of expression vector pJuKa

For large scale production of K411B-Fab, proline auxothroph E.coli JM83 strain was chosen because of its suitability for high cell density-fermentation. Therefore the existing plasmid pASK85 had to be changed in so far as the proline genes proA (γ -glutamyl kinase) and proB (γ -glutamyl phosphate reductase) had to be cloned into pASK85. The designed vector was called pJuKa (Figure 12).

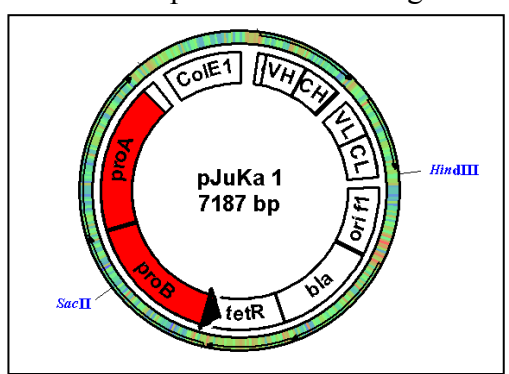


Figure 12: pJuKa

pJuKa was transformed into E.coli JM83 by electro-transformation. The successful cloning was proven by PCR and enzymatic digestion and the vector's functionality was tested by growth in minimal medium M9. The comparison of the OD_{600} of JM83pASK with supplemented proline and JM83 pJuKa in the fermentor after 16 and 48h of growth in minimal medium M9 showed, that the introduction of proAB adds the ability of growth in minimal medium as a consequence of proline production. This fact was supported by the growth behaviour of JM83 with pASK versus JM83 with pJuKa on minimal agar M9 (Figure 13).

growth in high cell density fermenter

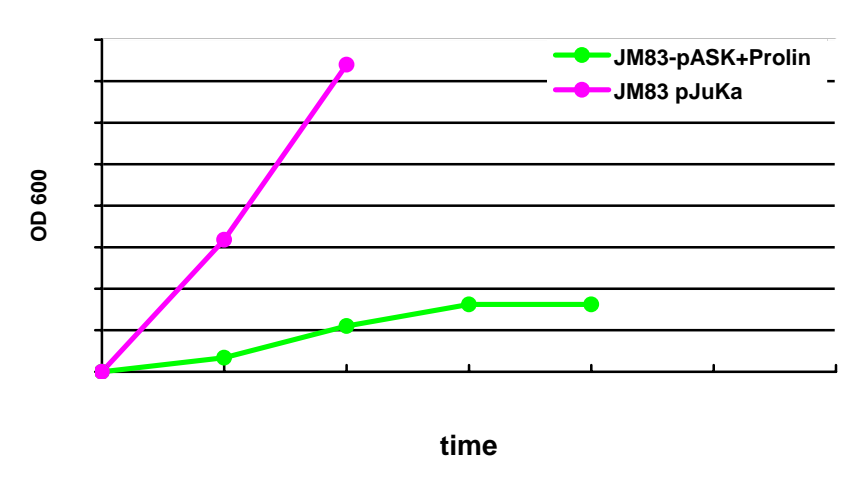


Figure 13. Growth of JM83 with pASK/pJuKa

After high density cell fermentation to an $OD_{600} = 22$ the production of K411B Fab (Atrazine-Antibody) was induced by addition of anhydrotetracyclin, as the production of the Fab is controlled by a tet-promoter dependent of a tet-repressor. The resulting protein was purified by IMAC, based on the affinity of the HisTag molecules for Cu^{2+} ions (Figure 14a). The HisTag is ligated to the constant region of the heavy chain (CH) of the Fab (Figure 14b). In a SDS-PAGE the expected size of the protein of about 45kDa could be shown (Figure 14c) and by means of an ELISA the functionality of the Fab could be proven.

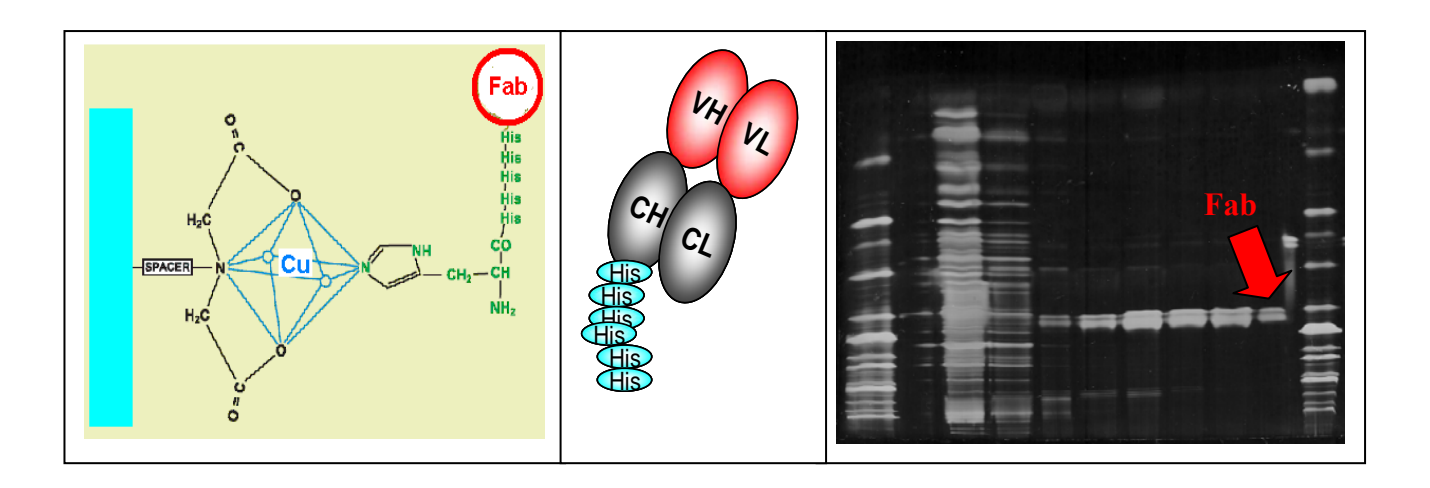


Figure 14. a) Metal chelate column with Cu²⁺ ion; b) Fab-fragment with HisTag; c) Result of purification on SDS-Gel

D4: Supply of recombinant antibodies and fragments

Design of pCaJo-vector-series

To make pASK85 suitable for phage display, additional restriction sites (pCaJo1) and parts of gene 3 had to be amplified from PCANTAB5 and cloned into pASK, which was designated pCaJo3 (Figure 15)

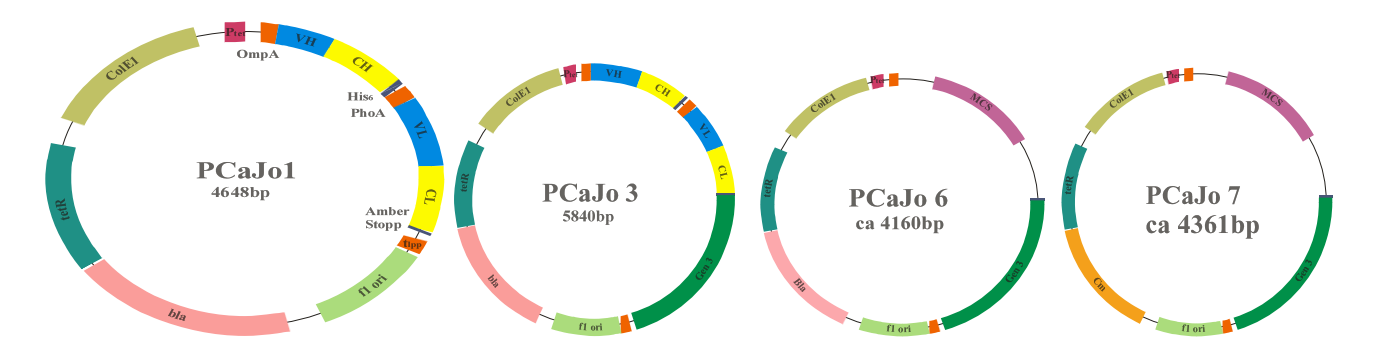
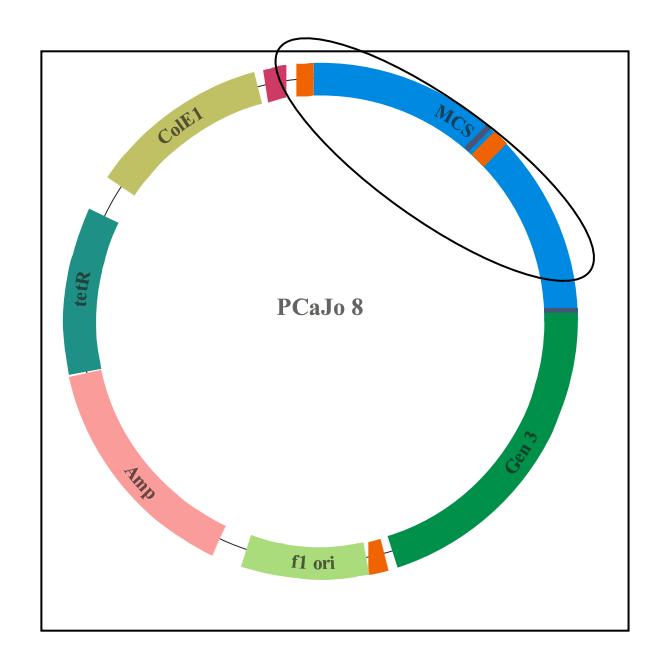


Figure 15: pCaJo1, pCaJo3, pCaJo6, pCaJo7

For optimisation of the new phage display vector, a new Multiple Cloning Site (MCS) was needed. The most common restriction enzymes, for which commercially available MCS exist, differ from the enzymes found in rabbit, therefore a rabbit adapted MCS was designed and ordered. This MCS was then cloned into pCaJo5, representing pCaJo6.

To gain the gene for chloramphenicol acetyltransferase CAT, which leads to the antibiotic resistance, primers were designed using the cloning vector pACYC184 as template DNA.

The CAT gene was successfully amplified and was introduced into pCaJo6, while the existing antibiotic-resistance bla (for Ampicillin) will be removed. The new vector produced by Month 12 was pCaJo7. Subsequently the final vector pCaJo8 was produced by mid-term and showed a specific pattern after being digested with different enzymes (EcoR*I*, Kpn*I*) proving the existence of the rabbit-specific MCS, Figure 16.



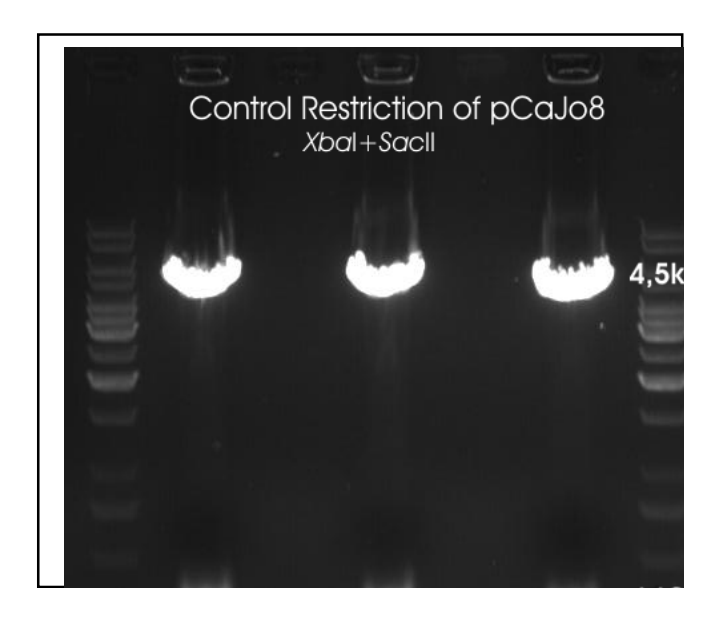


Figure 16. Final pCaJo8 vector and enzymatic digest showing Rabbit specific MCS.

Design of pCaJo/pASK111-vector-series

The cloning strategy for our selection vector was then changed pASK111 (from A. Skerra) were used and pCaJo3 instead of pCaJo8. pCaJo8 contains the non truncated version of gene III (green) from pCANTAB 5E and an ampicillin-resistance. pASK111 contains no gen3 but instead of ampicillin resistance bla (blue) contained chloramphenicol resistance (red). This marker was advantageous because of the selection pressure on antibody producing bacteria. pASK111 is a tested selection vector. To get pASK-111-CJ the cloning site and gen3 from pCaJo3 was fused with pASK111, before cloning the antibody-DNA into the new cloning site, Figure 17.

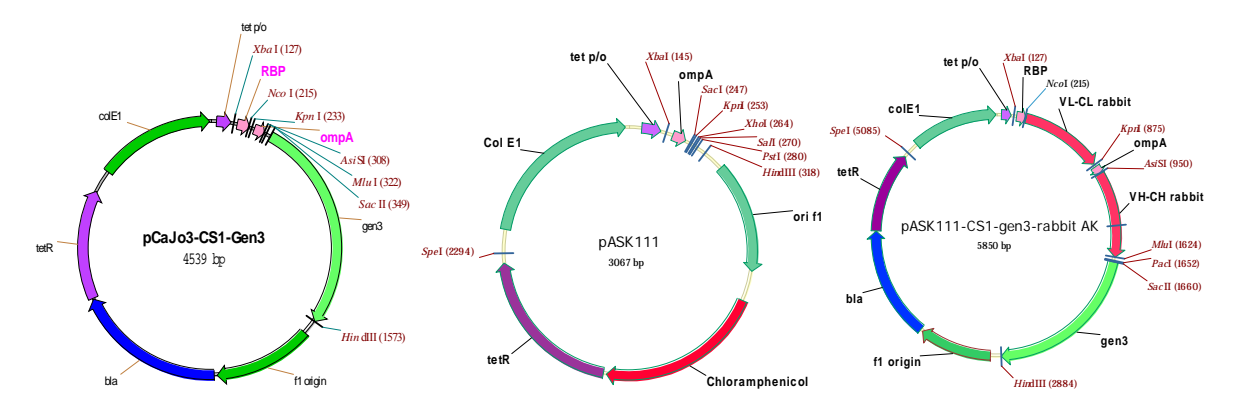


Figure 17: pCaJo3, pASK111 and pASK111-CJ

Sequencing of selection vector (phagemid)

To confirm the correct sequence of pASAK111 it had to be sequenced. Therefore we designed the indispensable primers, covering the complete vector.

Design of specific primers and MCS

The cloning strategy was reworked in order to optimize the antibody expression. New primers based on literature research of rabbit Ig-genes were designed as well as a new cloning site with different leader sequences, Figure 18. Also, bioinformatic analysis of restriction site frequencies was rendered to choose the most appropriate restriction sites for the primer design.

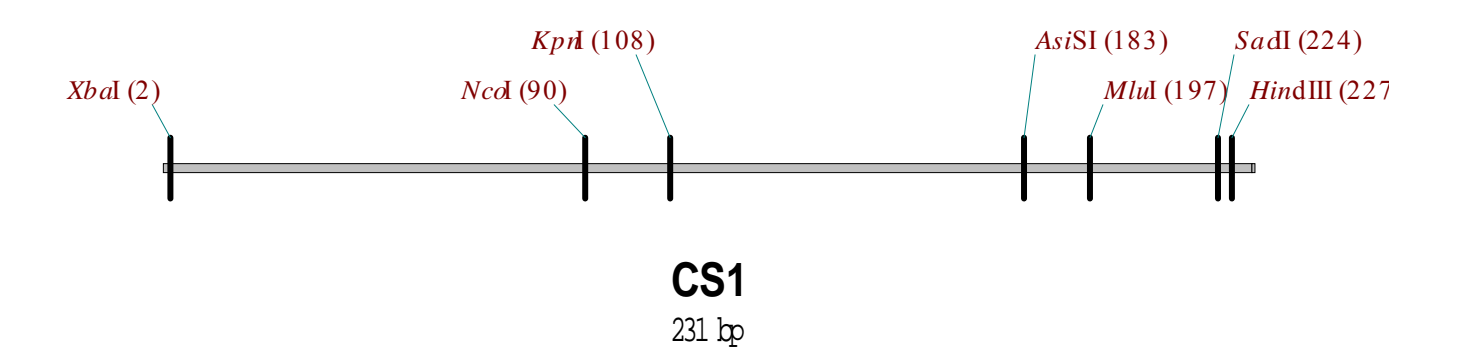


Figure 18: New Cloning site

Design of specific primers

Before starting the production of recombinant antibodies based on the mRNA/cDNA of light and heavy chain of rabbit B-cells, specific primers had to be designed. Literature research of rabbit Ig-genes was been carried out supported by different data-bases. Differences in number and organization between human/mouse and rabbit Ig heavy- and light-chains genes was much higher than expected and existing information found to be very limited. A statistical screen of restriction site frequencies was performed to choose the most appropriate restriction sites for the primer design.

From the statistical results the following 4 restriction sites were chosen for primer design:

 V_H : FseI C_H : PacI V_L : AsiSI C_L : MluI

It was possible to identify, from 350 antibody sequences, 40 primer sequences against the variable light and heavy chains as well as against the constant light and heavy regions of antibody-cDNA. The primers were tested in PCR, antibody mRNA was isolated and specific rabbit cDNA amplified (Figure 18).

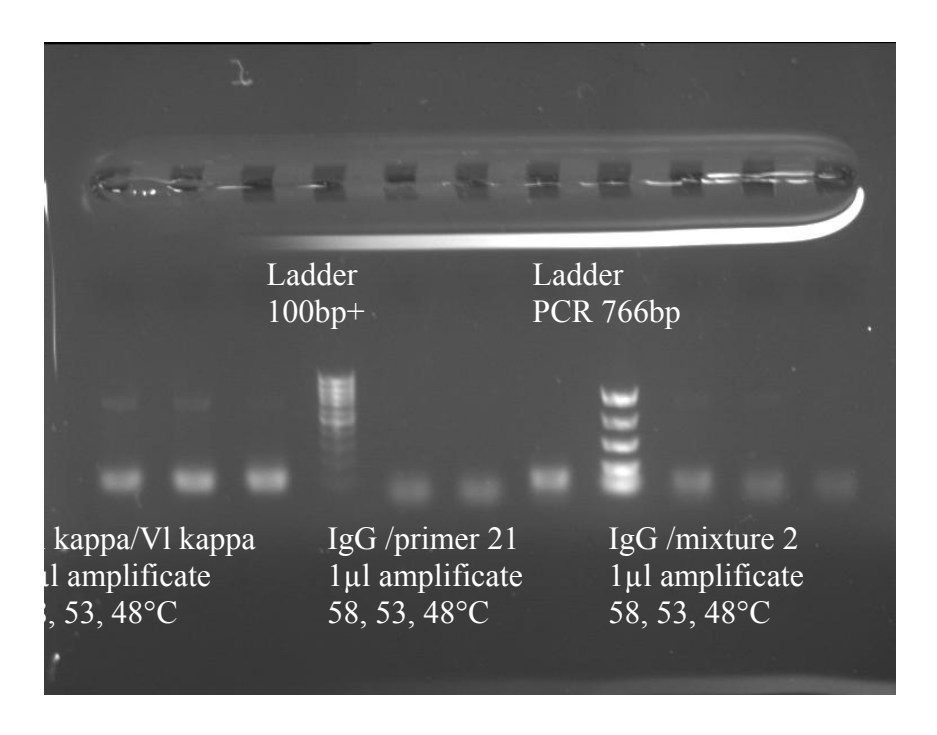


Figure 19. Amplified specific rabbit cDNA

Sequencing of expression vector (plasmid) and selection vector (phagemid)

To confirm the correct sequence of the vectors they needed to be sequenced. Therefore we designed the indespensable primers, covering the complete vector. pCaJo8 and pJuKa were also sequenced.

Test of primer sequence functionality on sulfonamide-rabbits

After the design of 40 primers against the variable light and heavy chains as well as against the constant light and heavy regions of antibody-cDNA, the primers were tested group wise in PCR. Antibody mRNA was isolated from spleen and specific rabbit cDNA was amplified for five sulfonamid-immunised rabbits. Then, different cDNA-kits were tested and after initial problems, yield wasd finally be enhanced for almost all of the primer-groups by touchdown-PcR to 1-6µg cDNA for IgG, IgM and IgA depending on the Ig-subclass (Figure 20).

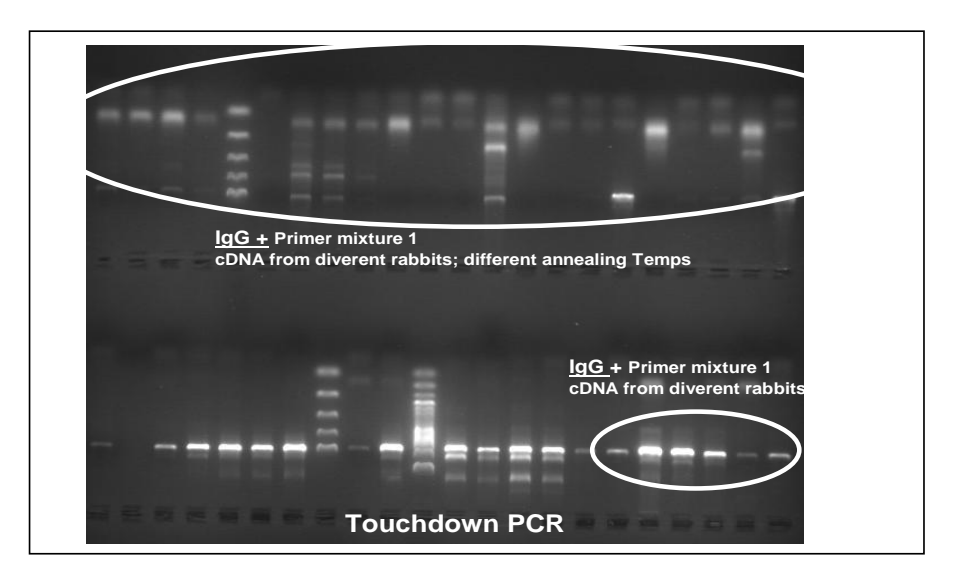


Figure 20: IgG cDNA PCR-Amplificate yield with conventional and touchdown-PCR

Fluoroguinolone-Hapten Immunised Rabbit Material for Recombinant Antibody Production.

After 7 months of immunisation and boosting with fluoroquinolone-haptens from partner 6, the blood-serum of rabbit showed specific antibody production against the fluoroquinolone-hapten-BSA, as we confirmed by competitive ELISA with ciprofloxacine. The antibody-concentration did not to grow any futher, which is not suprising, as rabbit B lymphopoiesis begins during fetal development and decreases soon after birth. The antibody repertoire is established during these first 3 weeks of life and the specificity of antibodies is only changed by diversification and somatic hypermutations in gut-associated lymphoid tissues (GALT). Therefore the rabbitwasn killed and spleen and blood saved. Two fluoroquinolone-immunized rabbits and, separately, three spleens arrived from partner 6 at the end of May 2005. mRNA was isolated from blood in sufficient amounts for subsequent antibody cloning. The recovery of mRNA from bone marrow and spleen cells was more difficult and less satisfying with respect to the yield of mRNA. Therefore, work onh the blood isolates was continued. In addition the blood of a non-immunized rabbit, was received and functioned as a control besides material from the immunized animals.

Fermentation to Produce His-Tagged Fab.

After high density cell fermentation to an $OD_{600} = 22$ the production of K411B Fab (Atrazine-Antibody) was introduced by addition of Anhydrotetracyclin, as the production of the Fab is controlled by a tet-promoter dependent of a tet-repressor. The resulting protein was purified by IMAC, based on the affinity of the HisTag molecules for Cu^{2+} ions . The HisTag is ligated to the constant region of the heavy chain (CH) of the Fab . In a SDS-PAGE the expected size of the protein of about 45kDa could be shown (Figure 18) and by means of an ELISA the functionality of the Fab could be proven.

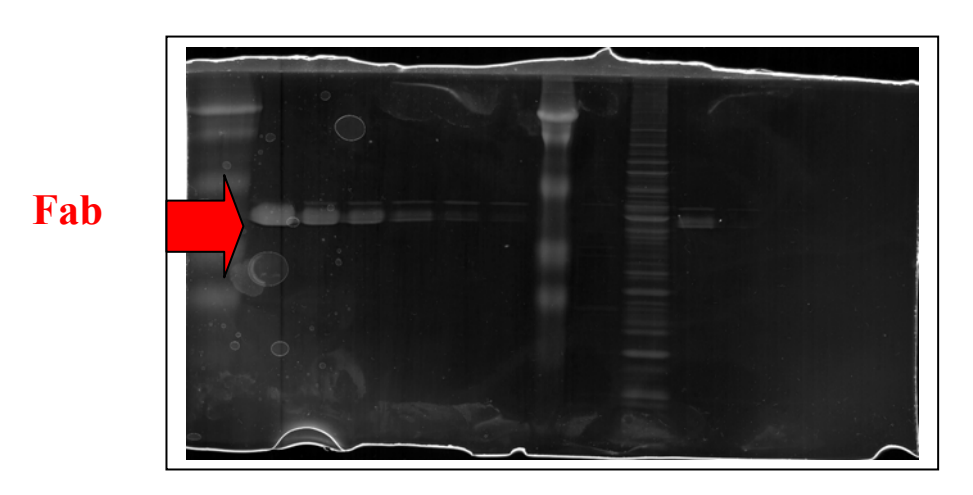


Figure 21. Purification of His-tagged recombinant Fab on SDS-polyacrylamide gel

Examination by Western Blot with Atrazine-POD tracer confirmed the functionality of K411B even after SDS treatment (Figure 22). The weak second band could have resulted from a degradation of the CL-region of the antibody, as it neither disturbed the His-tag nor the specific variable region.

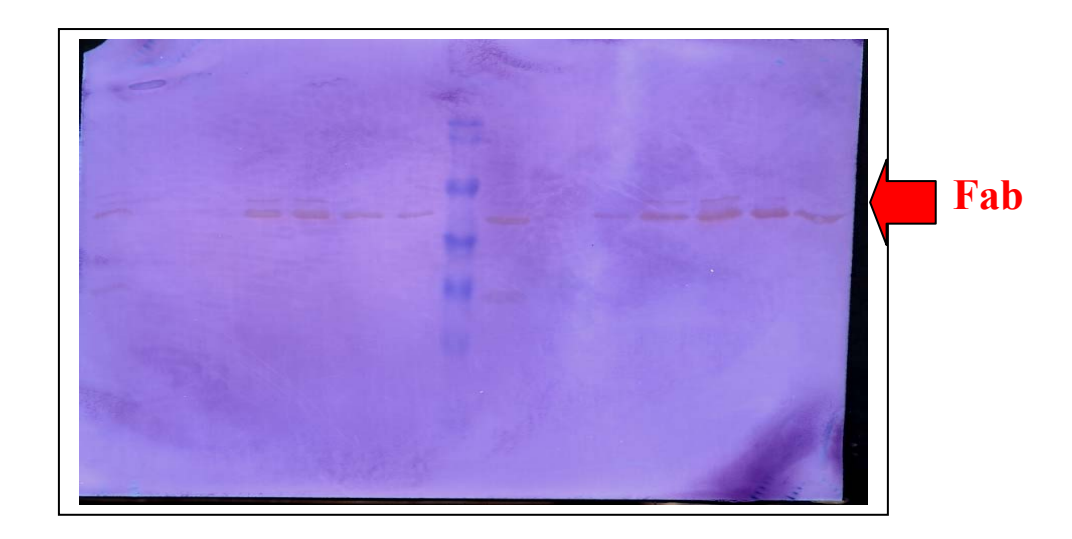


Figure 22. Purified recombinant His-tagged Fab western blot

To optimize the protocol of fermentation, each batch was started by different sugar-concentrations and innoculated with different optical density starter cultures. Antibody production induction by different optical densities had been carried out and growth-rate, dry cell mass production and sugar concentration during batch and fed batch and their influence on antibody output had been compared (Figure 23). To date about 1.5-2.5 mg atrazine-antibody per 50 ml fermentation has been achieved using affinity-purification via IMAC. Each fermentation produced between 150-400 ml depending on the final dry cell mass of the batch. Figure 23 shows the difference in culture optical density depending on initial sugar concentration and absorption of inoculation culture.

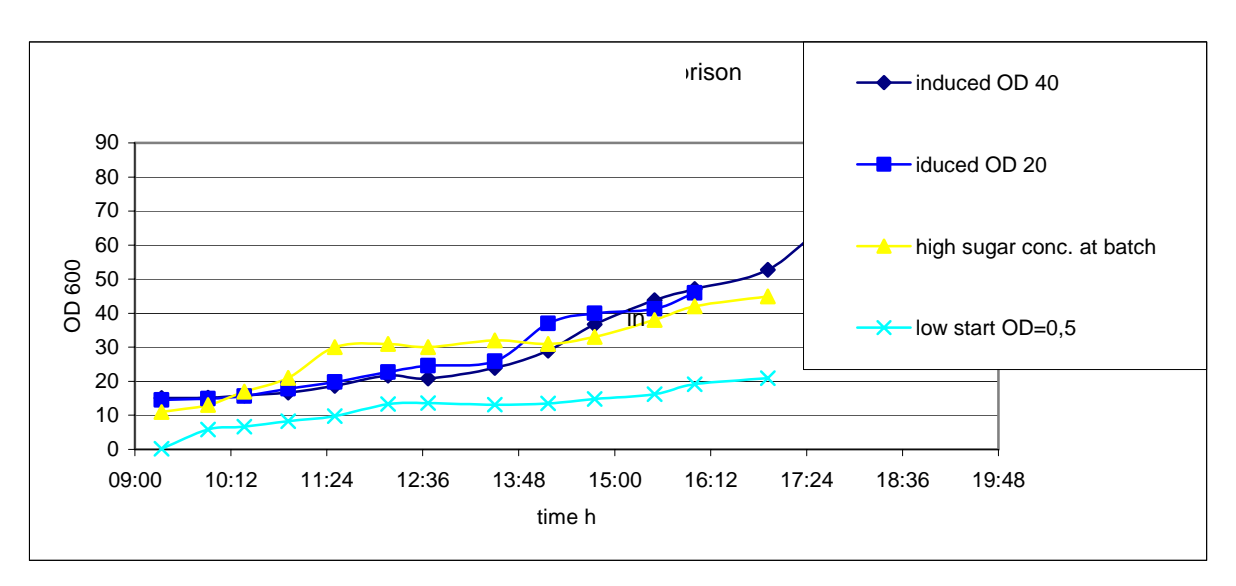


Figure 23. Effect of sugar and starting concentration on fermentation.

Design of pJuKa expression vector series

For large scale production of K411B-Fab in the fermenter, proline auxothroph E. coli JM83 strain was chosen because of its suitability for high cell density-fermentation. For expression of antibody-DNA pJuKa-plasmid (Fig.24) which is based on pASK85 (kindly provided by A.Skerra) was cloned, with the additional proBA genes (light blue, proA:γ-glutamyl kinase, proB: γ-glutamyl phosphate reductase). It contains the mouse atrazine-antibody-DNA (yellow) and was used for the atrazine antibody production in the fermenter.

To make pJuKa suitable for high density fermentation of rabbit antibodies, the rabbit cloning site (CSR2, Figure 26) was introduced into pJuKa (Fig. 24), which resulted in the new vector pJuKa-CSR2. Sequencing of the vector proved the anticlockwise orientation of the proBA genes. The rabbit antibody genes from phagemid pASK111-WKRn-13 were introduced into the rabbit cloning site of pJuKa to obtain pJuRab13 (Fig. 25), a plasmid for high-density production of rabbit Fab fragments. Expression of pJuRab13 allowed comparison of rabbit Fab-fragment production in the expression plasmid with the expression characteristics of the phagemid pASK111-WKRn13. The pJuRab13 plasmid thus served as a vector for large scale production of rabbit Fab fragments against fluoroquinolones. As a control, mouse anti-atrazine heavy chain (HC) and light chain (LC) genes were introduced into pJuKa-CSR2 (resulting in pJuAR, Figure 25) to compare atrazine production in pJuKa containing the standard CS for mouse with pJuKa containing the rabbit cloning site (CSR2).

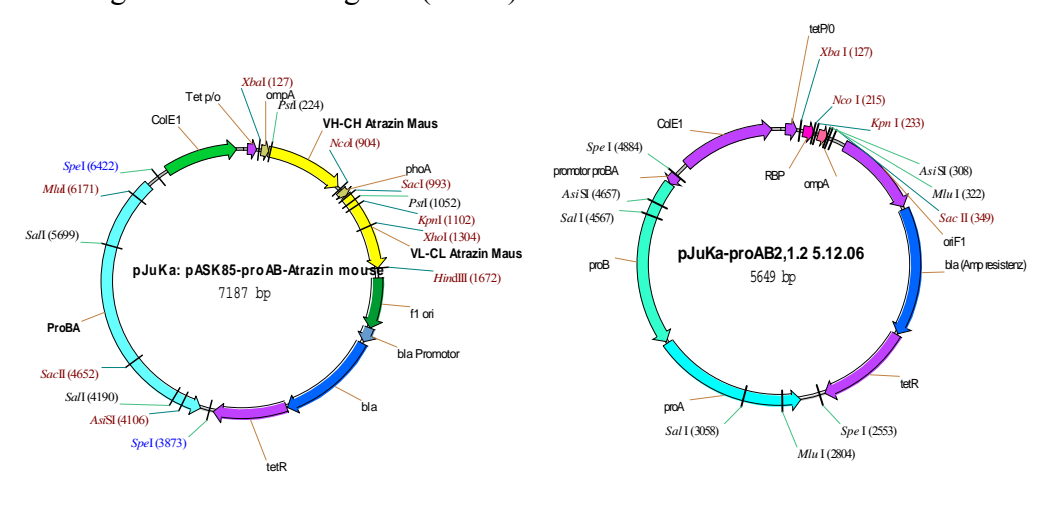


Figure 24: pJuKa mouse, pJuKa-CSR,

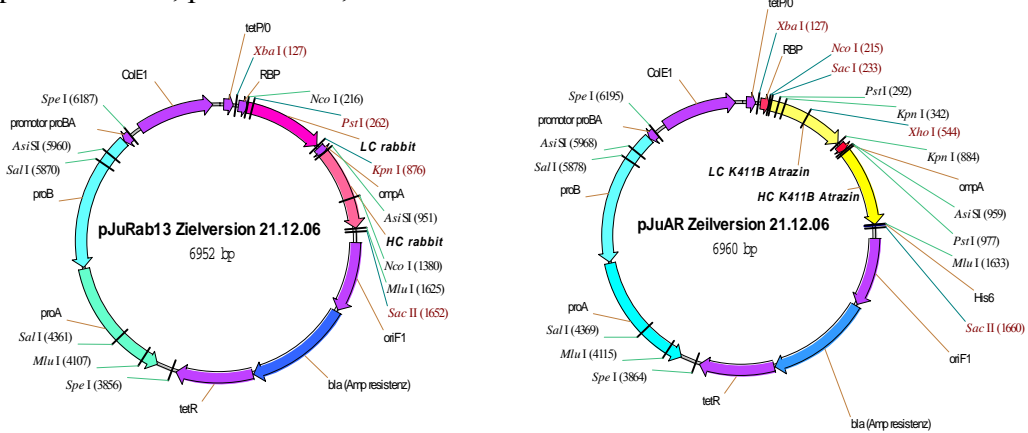


Figure 25: pJuRa13, pJuAR

Sequencing of selection vector (phagemid)

To confirm the correct sequence of pASK111 (kindly provided by A.Skerra) the plasmidwas sequenced. Therefore we designed the indispensable primers, covering the complete vector.

Design of specific primers and MCS

The cloning strategy was reworked in January 2005 in order to optimize antibody expression. New primers based on literature search of rabbit Ig-genes were designed as well as a new cloning site (CSR2) with different leader sequences (RBP and ompA, Figure 26). The new primers were tested and the amplification of naive and immunized rabbit antibody genes was performed for fluoroquinolone.

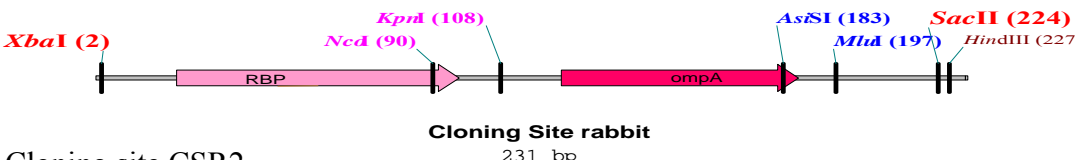


Figure 26. Cloning site CSR2

Design of pASK111 selection vector

Out of pASK111 (figure17,27) and pCaJo3 (pASK85 containing gene3, figure 17) we constructed pASK111-CSR2, which contains a chloramphenical resistance marker, the non truncated version of gene III (green) from pCANTAB 5E and the rabbit cloning site CSR2.

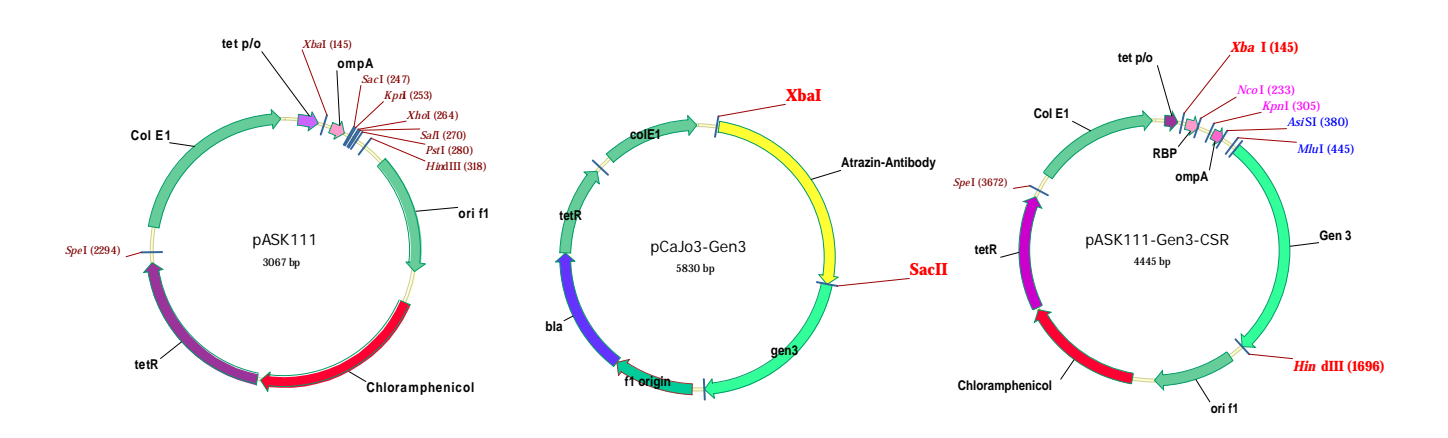


Figure 27. pASK111, pCaJo3, pASK-CSR2

Expression of naive rabbit IgG

Instead of cloning immunized rabbit antibody-cDNA directly into pASK111-CSR2 we decided to first clone naive antibody-DNA into the new cloning site to ensure functionality of this new phagemid (figure 28). The resulting clones pASK111-WKRn 2,5 and 13 was sequenced and turned out to contain rabbit IgG antibody Fab fragment.

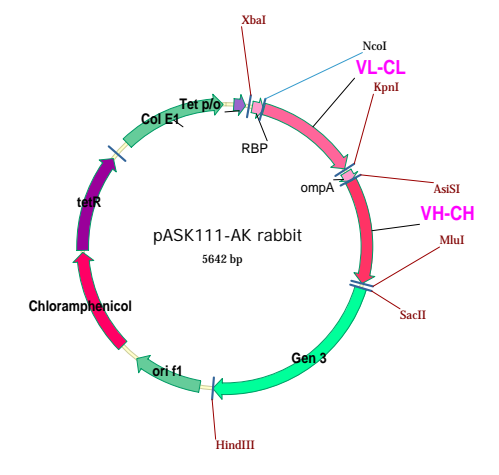


Figure 28. pASK111-WKRn

A diagnostic restriction site was introduced in each antibody chain to simplify the distinction between naive and immune rabbit DNA while cloning the library. All three pASK111-WKRn vectors were tested in expression experiments to reduce the possibility of failure based on the protein sequence of one of the three proteins. After expression, SDS-PAGE and Western Blot analysis indicated either dificulties of protein folding or of translocation from bacteria cytoplasm to periplasm, since we could only show the heavy chain in the periplasm, but not the Fab fragment.

Anti-atrazine in pASK111-WKRn

To check functionality of pASK111-WKRn, especially of the leader sequence RBP, the rabbit LC and HC were exchanged against the ones of the anti-atrazine antibody K411B (figure 29). This protein has already been expressed in pJuKa and was therefore assumed to have no problems in correct protein folding.

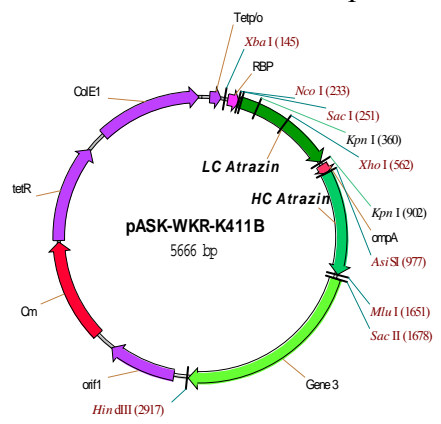


Figure 29. pASK111-WKR-K411B

After expression, analysis by Western Blot showed that the anti-atrazine was expressed in phagemid pASK111-WKR-K411B as good as in plasmid pASK85. Hence it could be concluded that expression difficulties could probably be explained by rabbit Fab fragment's protein characteristics. Compared to mouse IgGs, rabbit Fab fragments contain additional disulfide bonds bridging constant and variable domains within each antibody chain, which could complicate the folding process in the periplasm. Co-expression of the rabbit Fab fragment with an additional chaperone expressing vector (pTUM4, kindly provided by M.Schlapschy) supported this hypothesis. Promoted by four additional folding helper proteins in the periplasm, rabbit Fab fragments could be detected with this system in Western Blot analysis.

It has also to be considered that we only expressed three different HC-LC combinations. It is possible, that none of these accidental combinations turned out to result in a functional antibody. Expression of Fab fragments selected through several rounds of panning woud probably result in functional Fab fragments. Another explanation remains the new leader sequence, RBP, which might be a less effective than we expected. To make sure that RBP was not the problem - it worked well for mouse anti-atrazine Fab fragment- RBP was exchanged into pASK111-WKRn-13 against pelB, a common signal sequence (figure 30).

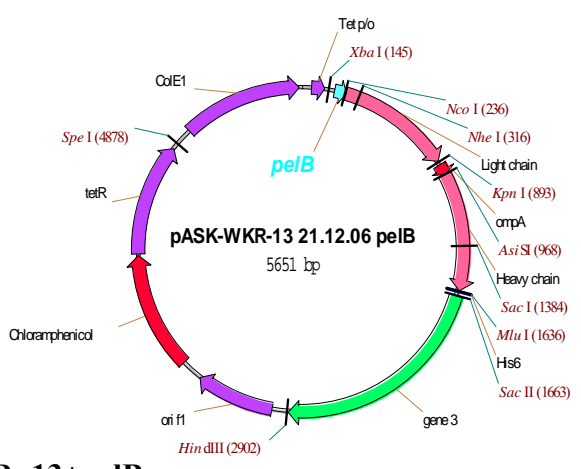


Figure.30. pASK111-WKRn13+pelB

Library construction

For cloning of the immunised rabbit antibody library, digested IgG of fluorochinolone immunized rabbits heavy chain DNA out of PCR was introduced into AsiSI/MluI digested pASK111-WKRn and, separatly, light chain DNA was introduced into NcoI/KpnI digested pASK111-WKRn.

Phage display and panning of anti-sulfonamide Fab fragments

Investigation of the functionality of the final phage display system was performed by by using a control library for selection, which was obtained by cloning rabbit antibody genes from sulphonamide immunized rabbits into our phagemid. After rescue of phagemid particles by infecting the bacterial library (size 1.3×10^{10}) with $2x10^{11}$ M13KO7 helper phage, phagemid particles were percipitated. The phage titer of the sulfonamide library was 1.4×10^{10} phage particles.

Rabbit anti-sulfonamide F_{ab} containing phage particles were enriched from the library by phage display selection and applied to polystyrene strips coated with 2.5 µg/ml BSA/OVA sulfomamide conjugates and incubated. Enriched particles were eluted and used for TG1 F^+ infection. The eluted phage fraction was amplified and applied for a subsequent round of phage selection under comparable conditions. This was repeated up to a total of four rounds of panning. Depending on the coating conjugate a 10 fold increase of reinfectants was observed after panning round three and four.

From each round of panning up to 200 clones were investigated with respect to their binding capability to sulfomamide antibiotics by competitive ELISA. Therefore a mixture of eight different sulfonamide antibotics was used for competing with the coating conjugate in order to bind specific rabbit F_{ab} fragments. 64 out of a total of 800 clones showed a selective binding to the conjugate. Out of these a subpopulation of 11 clones proved to provide reproducable increase in signal intensity of 30-70% above background signal.

D5: Characterisation of antibodies and recombinants and fragments

Commercial sources of PSA-antibodies were provided to project partners.

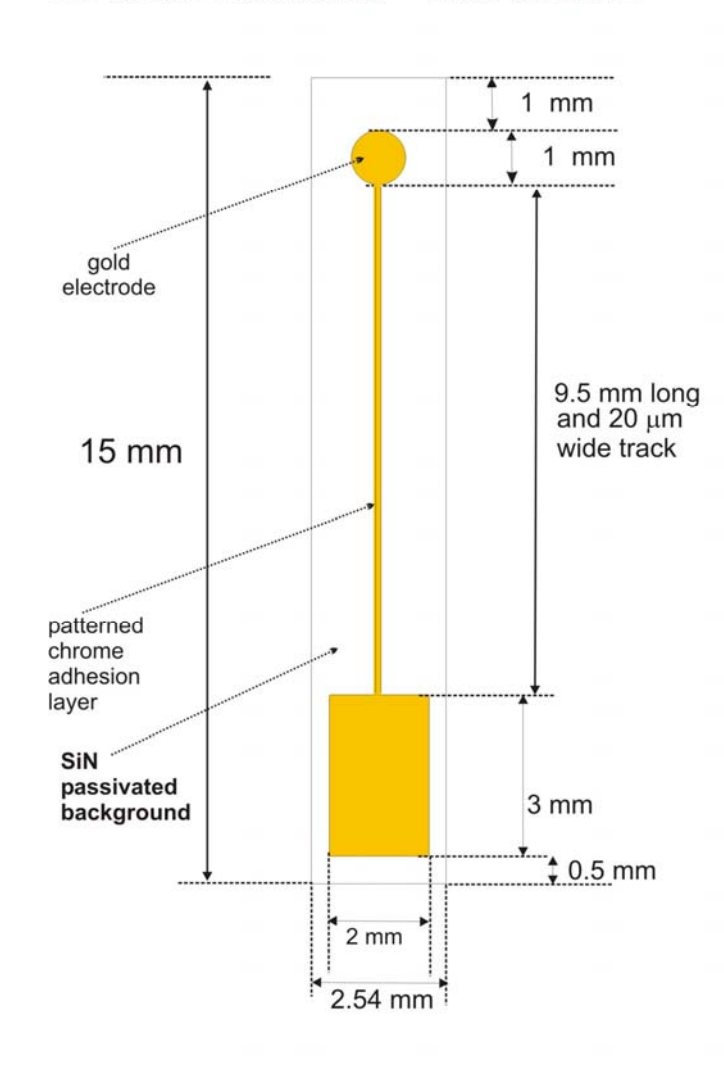
Workpackage 1 progressed to time with the milestones and deliverables approximating to the estimated timescales. In addition the decision to analyse a rabbit database and design rabbit primers is potentially very useful commercially, as no existing rabbit primers are commercially available. Also this means that the primers designed are free of any external restriction to use and the benefit goes directly to the partners in the consortium, especially partner 4 who is exploring the possibility of patenting the rabbit primers.

Objectives: To produce metal (gold and platinum) transducers, using silicon or plastics as the substrates, with corresponding mounting connectors. To produce a range of metal transducers with different geometries. To produce micro electrode transducers.

Project Timeline		1 2 3 4 5 6 7 8 9 10 11 12 13 14 15 16 17 18 19 20 21 22 23 24 25 26 27 28 29 30 31 32 33 34 35 36
Workpackage 2	. Transducers	
Task 2.1	Standard Transducers	
Task 2.2	Designed Transducers	

Device Design and Mask Production

P3 and P4 electrode PAM 04/02/04



Substrate
Silicon/silicon oxide -suggest 800-1000nm SiO₂ then

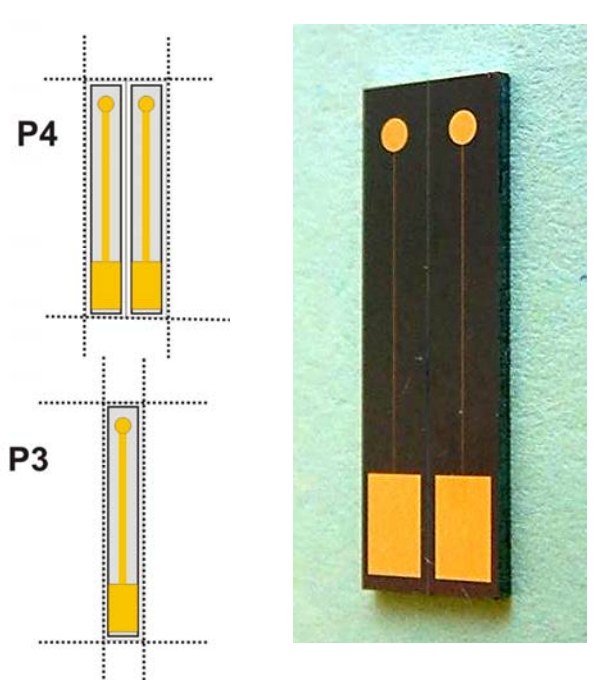
adhesive layer - 50 nm Cr electrode layer -100 -150 nm Au

Delivery

7 wafer run - 4 wafers diced as double electrodes 3 wafers diced as single electrodes Electrodes were designed by Partner 1 in collaboration with Partner 5. Two discrete electrode designs were chosen, P3 and P4 (Figures 31 and 32) and a third option was introduced by dicing the devices on design P4 into a dual device per die format (see Figure 33) in order to incorporate 2 electrodes on one die.

The gold fabrication process involved two lithography steps, two masks were drawn for each design. The mask sets were drawn using Mentor Graphics software program, which allowed for easy conversion of the file into Gerber format. The designs were forwarded to the manufacturer (Delta Masks) for production of glass masks.

Figure 31. Device design P4- for single and dual based electrodes.



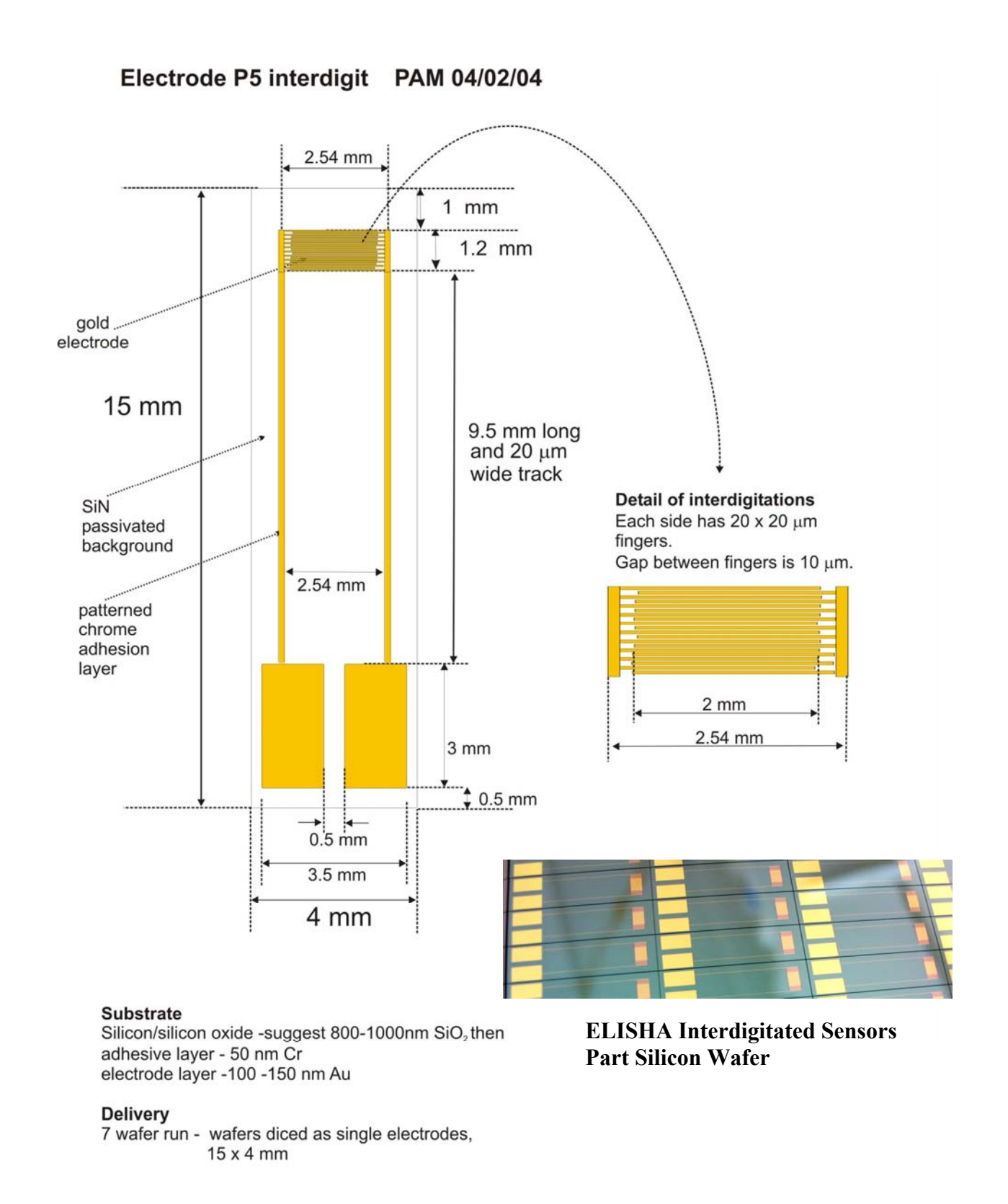


FIGURE 32. Device design P3- for interdigitated based electrodes.

The three gold metal on silicon electrode structures were fabricated in two modifications (with Cr or Ti stiction layers for Au adhesion). In total 96 gold wafers of electrodes were produced. This was the required amount of electrodes for sensors development and evaluation which were shipped to the respective ELISHA partners to complete D6.

Between month 13 and 18, redesigns of P3, P4 and P5 were undertaken as a result of high resistance values reported by some partners. Partner 1 sent new designs and new layout were created and sent for mask production. In addition an alternative design P10 was also sent for mask production.

Wafers 7& 8 of X-2777 with gold P4 rev A design sent to Partner 1 on 14.3.05. X-2777 W11 & 12 (blanket gold on Palladium) W13 & 14 (blanket gold on Titanium and palladium), there was poor gold adhesion due to the underlying stiction layer these wafers were scrapped.

Blanket gold on Ti was decided upon and X-2777 W9 & 10 blanket gold on Ti X-2832 were sent to Partner 3 on 14.3.05.

Platinum electrode fabrication

Wafers 1&24 from batch X-2777 platinum on titanium with the P4 revA design and wafers 2 & 23 from X-2777 platinum on titanium with the P3 revA design were fabricated using the evaporation process were sent to Partner 1 on 11 5 05

Some 14 out of 20 wafers from X-2832 platinum P4 revA many failed devices due to poor processing at the platinum lift off stage, these have been scrapped, the wafers that passed microscopic inspection; wafers 1, 2, 3, 4, 9&12 are ready for shipping.

An alternative evaporation process was employed and currently in process are 21 wafers X-2799 platinum of P3, P4 and P5 rev B designs are at the saw dicing stage. From X-2824 20 wafers platinum P3 rev A and P10 revB were also due produced.

Photolithographic gold electrode fabrication

Redesigns of P3, P4 and P5 electrodes were undertaken as a result of high resistance values reported by some partners. New designs were created in collaboration with partner 1 and a new mask set was produced. P10 electrode was also redesigned. In order to create the desired electrode structure a process flow had to be developed. This involved the deposition of multiple metal layers subsequent photolithographic processing techniques. A flowchart of the process is shown in Figure 33. Initially, single crystal silicon wafers were thermally oxidised to create an oxide layer of 1000 angstroms (figure 23(1)). A 35nm layer of titanium was evaporated onto the oxide and finally 100 nm of Pt or 200 nm of gold was evaporated onto the surface. The Ti metal acts primarily as an adhesion layer between the metal electrode and the wafer surface.

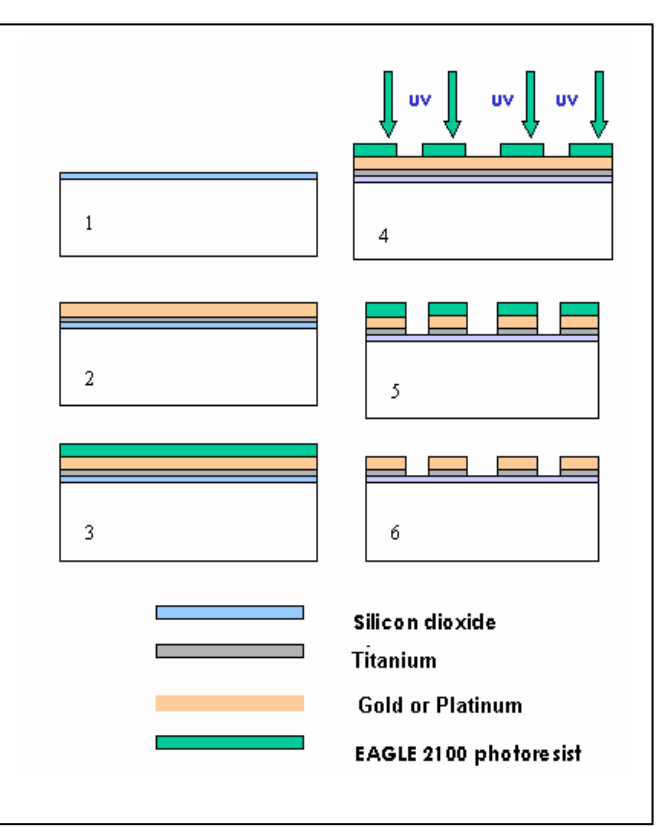


Figure 33. A schematic of the photolithographic process to define the gold electrode array.

The wafer was prepared for the subsequent photolithographic process to create the desired electrode pattern. Initially, a negative photoresist, EAGLE 2100, was electroplated onto the surface of the gold or platinum (figure 33(3)) and exposed to UV light at 60mw/sec, through the desired mask (figure 33(4)). Due to the nature of negative resist, it is the areas exposed to the UV light that polymerise and the non-exposed areas were removed using a developer solution. A gold lift off process was performed, which required etching the gold in a KI, I₂ and water solution at 40°C (figure 23(5)). Following an etch inspection to ensure successful removal of the gold, the titanium adhesion layer was etched using potassium ferrocyanide (figure 33(5)). Following the titanium etch it was possible to remove the

remaining photo resist using EAGLE 2100 photo developer (figure 33(6)) and a final nitride passivation layer was deposited and subsequently patterned with the required design. As a result of this work the required amount of electrodes for sensor development and evaluation were shipped to ELISHA partners in accordance with Deliverable 6. Listed below is an itinerary of processed wafers involved with this work.

Problems Encountered.

The mask sets received from Delta Masks underwent an in-house micro scale inspection which revealed significant artefacts on the masks in the areas of the interdigitation. It appeared that the final manufacturing cleaning steps had not been sufficient. The NMRC Central Fabrication Facility were in contact with Delta Masks regarding this issue and the manufacturer instructed us to perform the cleaning step in-house at the NMRC Central Fabrication Facility, this was performed and further micro scale inspections revealed that the masks had been cleaned perfectly. This delayed the progress of our deliverables in a total by one calendar month.

Listed below is an itinerary of processed wafers involved with this work.

Gold Electrodes

X-2777	W 7-8 with gold P4 revA design						
	W11 & 12 (blanket gold on Palladium)						
	W13 & 14 (blanket gold on Titanium and palladium), there was poor gold adhesion due						
	the underlying stiction layer and these wafers were scrapped.						
	W9 & 10 blanket gold on Ti						
X-2832	Au on Ti						
X-2925	21 wafers gold processed on Ti with P3 P4 and P5 rev B.						
X-2129	W 19-22 gold processed on Ti with P10 revB						
X-2777	W3-6 + 25 gold processed on Ti with P10 revB						
X-2949	W5-25 gold processed on Ti with P4 revB						
X-2799	W2-4, 8, 10 gold processed on Ti with P10 revB						
X-2949	W 1-4 gold processed on Ti with P10 revB						
Platinum Elec	etrodes						
X-2777	W1 + 4 platinum on titanium with the P4revA design						
X-2777	W2 + 23 platinum on titanium with the P3revA design						
X-2832	W $1 - 14$ platinum P4 revA many failed devices due to poor processing at the platinum lift						
	off stage, these wafers were subsequently scrapped, the wafers that passed microscopic						
	inspection; wafers 1 2 3 4 9&12 were shipped.						
X-2799	An alternative evaporation process was employed and 21 wafers platinum of P3, P4 and P5						
	rev B designs were fabricated and diced.						
X-2824	There were 20 wafers platinum P3 revA design fabricated and diced.						
X-2959	W1-14 Pt processed with P10 revB						

Screen printed micro-electrode arrays

To facilitate commercialisation of the immunosensors, partner 2 produced screen printed transducers of the format shown opposite (figure 34). These can be made in large sheets with 600 transducers per sheet and up to 40 sheets can be processed at one time.

These transducers were used in the sensor fabrication and evaluations in WP4 and WP5, also in WP 7 for the non-specific binding optimisation.

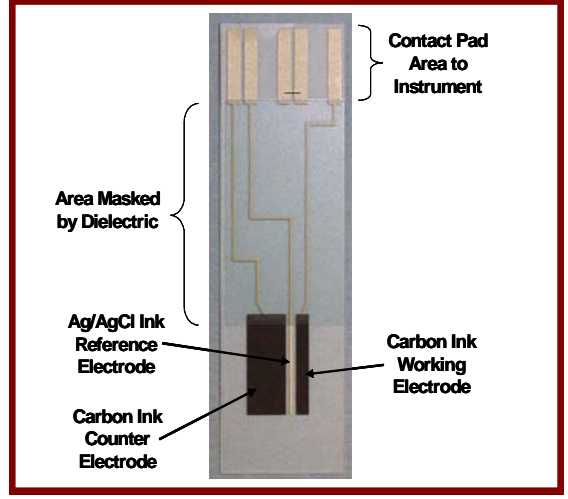


Figure 34 Screen printed transdsucer

Dual sensors

To further facilitate commercialisation of the immunosensors, partner 2 also produced screen printed dual transducers of the format shown below (figure 35). These can be made as before in large sheets with 600 transducers per sheet and up to 40 sheets can be processed at one time.

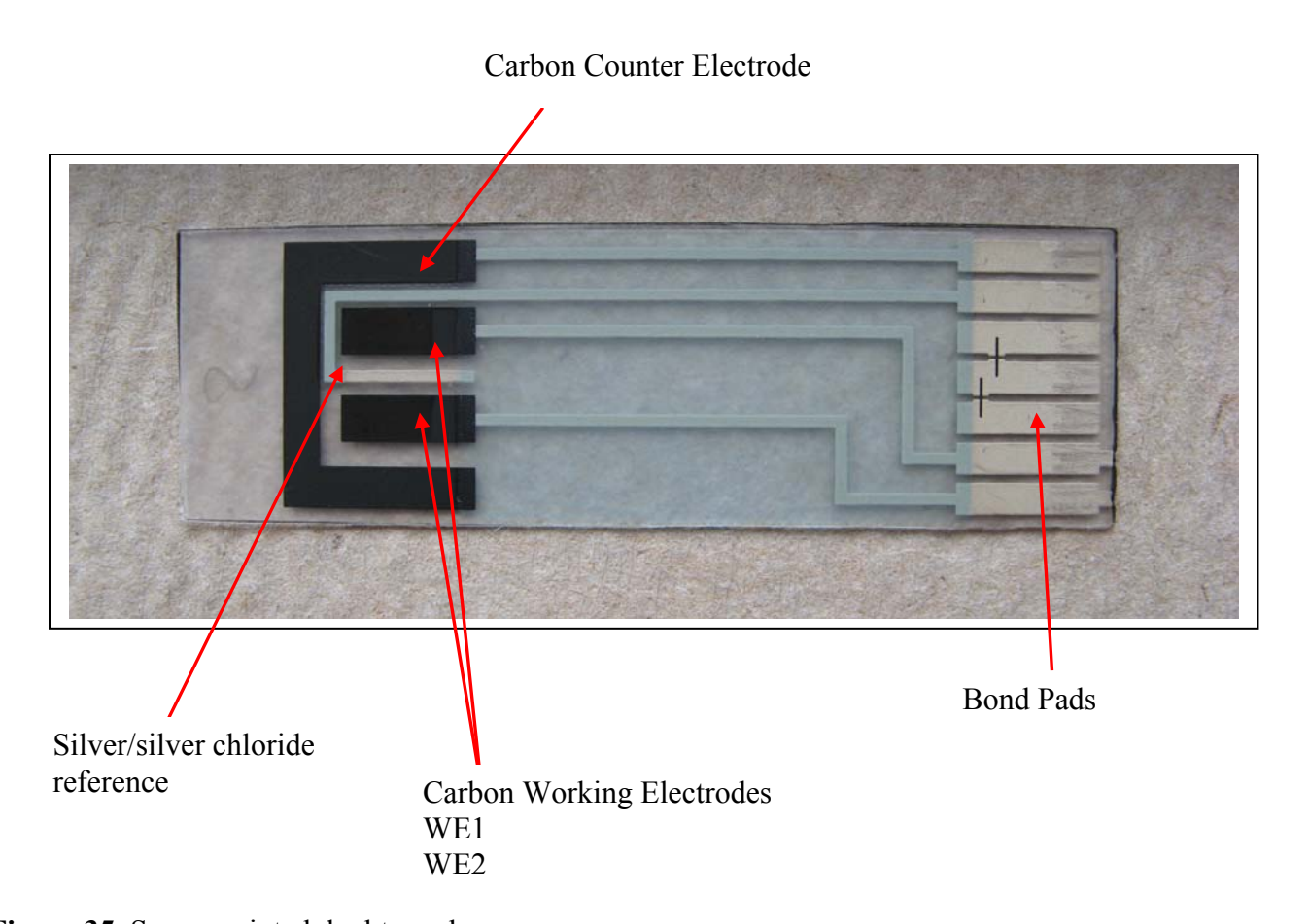


Figure 35. Screen printed dual transducers.

The dual sensors were made in two types; planar carbon and micro-aaray using polyaniline as the base microarray layer.

WE 1 usually has the specific antibody immobilied and WE 2 has a non-specific antibody. Interrogation of WE1 and WE2, followed by subtraction of the WE2 signal from the WE1 signal corrects for non-specific binding.

Workpackage number: W3. Production of Matrix Precursors.

Objectives: To produce a range of electropolymerisable monomers or electrodepositable materials having specific chemical characteristics to enable entrapment or co-valent immobilisation of bioactive antibodies and fragments.

Project Timeline	1 2 3 4 5 6 7 8 9 10 11 12 13 14 15 16 17 18 19 20 21 22 23 24 25 26 27 28 29 30 31 32 33 34 35 36
Workpackage 3. Matrix Precursors	

By using chemically tailored monomers, the reproducibility of manufacture can be improved. Consequently, different monomers were synthesised during the first year of the ELISHA project. The list of these monomers is provided on figure 34. They all bear an electropolymerisable group (pyrrole) in order to get a conductive material at the surface of the electrode. Monomers 3 and 4 contain a photoactivable group (benzophenone group) in order to immobilize antibodies under UV irradiation. Momomers 2 and 3 have a complexation site (biotin) in order to get nanostructured films using the strong biotin-avidin interaction. The other monomers synthesised allow the immobilisation of the biomolecule by entrapment.

Figure 36. Scheme of the synthesised monomers with the respective yield of synthesis

These monomers were sent to partners. In particular, monomers 6 and 8 were produced at large scale for partner 6 as intermediates in the chemical synthesis of electropolymerisable pesticides.

The synthesis of these monomers was by a multi-step synthesis. The purity of all these compounds were checked by different spectroscopic methods (¹H NMR, FAB mass) and by electrochemical methods. The electropolymerisation of these monomers was achieved in organic or aqueous solution depending on the solubility of the monomer. For example, monomers (1, 6, 7, 8) which were poorly soluble in aqueous solution, were firstly dissolved and dispersed under ultrasonication in aqueous solution and then electropolymerised at a controlled potential in an aqueous solution. On the other hand, for the monomers soluble in organic solvent (CH₃CN), they could be be electropolymerised by the cycling potential method or by a potentiostatic method. This last method of electropolymerisation provided the advantage to control the thickness of the film deposited onto the surface of the electrode.

To illustrate the report, the electrochemistry of the monomer 4 which is an association of an electropolymerisable group and a photoactivable group is shown on figure 37. The cyclic voltammetry exhibits two monoelectronic reversible peak systems at $E_{1/2} = -1,90$ V and $E_{1/2} = -2,40$ V. These systems are attributed to the 2 successive reductions of the benzophenone group. Moreover, in the positive part, the irreversible oxidation of the pyrrole was detected at a potential of 0.90 V.

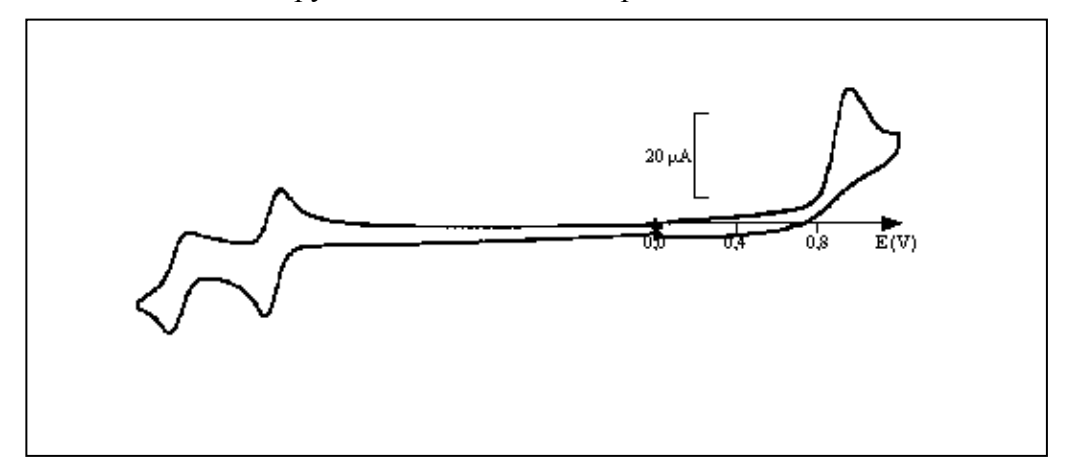


Figure .37 Cyclic voltammetry of the monomer 3 1,8 mM in CH₃CN+TBAP 0,1M on glassy carbon (3mm). Scan rate : 100 mV/S. Reference electrode: Ag/Ag⁺ 10mM in CH₃CN+TBAP 0,1M

The monomer was electropolymerised by the potentiostatic method giving a yield of polymerisation of around 20 %. The modified electrode transferred to a monomer-free solution kept the electroactivity of the monomer in solution. This new polymer was checked to immobilise firstly enzymes. In this context, a new experiment device was designed for the irradiation of conductive materials under an inert atmosphere (glove box). After irradiation in presence of alkaline phosphatase, UV tests confirmed the grafting of a monolayer of the biomolecule at the surface of this polymer. No difference between polymer 4 and 5 was noticed.

Moreover, these new polymers were used with success to immobilize antigens. After irradiation of the polymer immobilised onto optical fibers in the presence of antigens, the photografting was evaluated by fluorescence spectroscopy using a fluorescent secondary antigen.

In addition, the molecular assembly biotin-avidin was evaluated by impedance spectroscopy and by cyclic voltammetry by using the conductive electrodes recovered with derivative biotin polypyrroles (monomers 2 and 3). The data showed that the biotin groups were accessible to avidin and the surface of the polymer was completely covered by proteins. The presence of avidin at the surface of the electrode however did not favour electrode performance and increased the internal resistance of the system.

A complex synthesis of pyrrole-nitrilo acetic acid derivative was also been carried out and this was electropolymerised to give a poly(pyrrole-NTA) film which was able to chelate nickel ions and subsequently to immobilise histidine – tagged glucose oxidase. This material could have a very useful

role in immobilisation of his-tagged Fab fragments being produced by partner 4. A manuscript has been submitted for publication, see Appendix 6 for patents, publications and conference abstracts.

The scale up of the synthesis of pyrrole-nitrilo acetic acid (monomer10) as well as monomers 9 and 11 became part of the work up to the mid-term. These monomers were designed to improve the immobilisation protocols for antibodies to produce sensors.

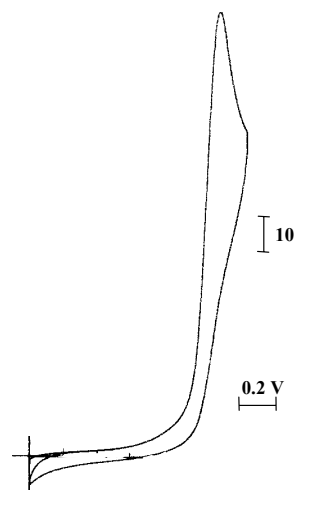
Figure 38: Structures of Monomers 9, 10 and 11.

Monomer 9 contains n-hydroxysuccinamide reactive groups to allow co-valent linking to amino functionalities of the protein structure. Moreover, the bis-pyrrole derivative of biotin (figure 38, monomer 11 was more effective in producing biotin loaded surfaces after polymerisation.

The purity of all of the monomers was checked by different spectroscopic methods (NMR ¹H, FAB mass) and by electrochemistry.

The cyclic voltammetry of the monomer $\bf 9$ shown on the right (figure 39), carried out in CH₃CN + 0.1 M TBAP exhibits an irreversible peak at Epa = 1.0 V attributed to the irreversible oxidation peak of pyrrole.

Figure 39: Cyclic voltammetry of monomer 9 (5mM) in $CH_3CN + LiClO_4$ 0.1 M on Platinum electrode (5mm). Scan rate : 100mV/s. Eréf : Ag/Ag^+ 10 mM in $CH_3CN + LiClO_4$ 0.1 M



Monomer 9 could be electropolymerised by repeated potential scanning over the range 0-1 V (figure 40). The modified electrode transferred to a solution exempt of monomer showed the electro-activity of the polypyrrole at $E_{1/2} = 0.7 \text{ V}$ (figure 40).

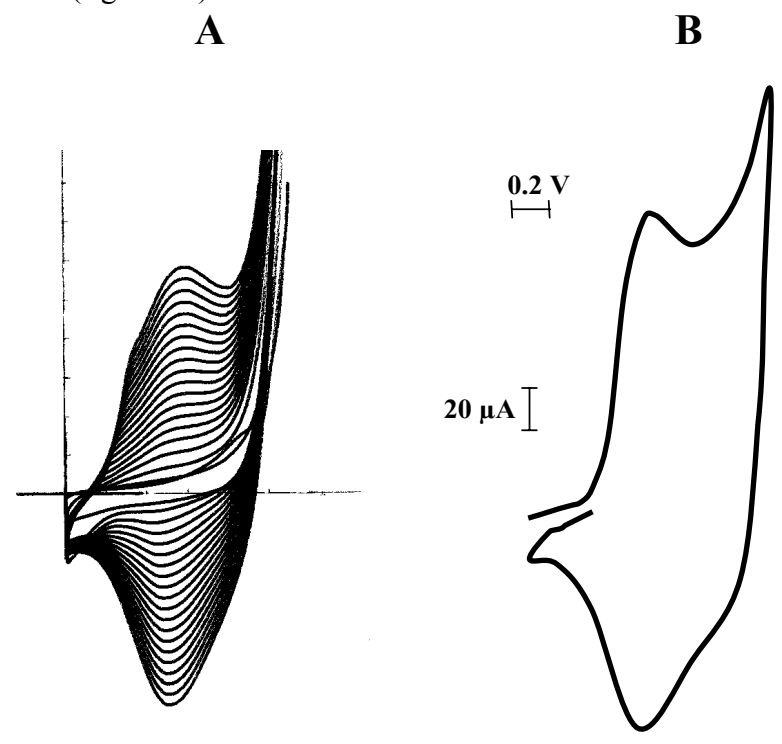


Figure 40. A) Cyclic voltammetry of monomer 9 (5mM) in CH₃CN + LiClO₄ 0.1 M on Platinum electrode (5mm) by cycling potentials. Scan rate: 100mV/s. Eréf: Ag/ Ag⁺ 10 mM in CH₃CN +LiClO₄ 0.1 M. **B).** Cyclic voltammetry of the modified electrode transferred in a solution free of monomer (CH₃CN + LiClO₄) (same conditions as A)

In the same way, the monomer 10 exhibited in the anodic part an irreversible anodic peak due to the oxidation of pyrrole into polypyrrole. It could also be electropolymerised by cycling potentials in the range of 0.0 V to 0.8 V or by potentiostatic method at a potential of 0.8 V.

The polymer electrogenerated with the monomer 10 allowed the anchoring of histidine-tagged proteins. Indeed, after immersion of the modified electrode in a solution of CuCl₂, the metallic cation was complexed to the polymer via the NTA (nitrilotriacetic acid). This new material was then used successfully for the detection of glucose after coordination to the histidine-tagged glucose oxidase. These results have been recently published. Moreover, results using QCM showed the reversibility of this sensor. Concerning the protein immobilization by biotinylated polymers, several synthesises were performed providing the pure product that sometimes does not polymerize. We found no explanation for this erratic behaviour. Due to the difficulties encountered with the electropolymerisation, a new biotin-pyrrole monomer (monomer 11) bearing 2 pyrrole groups was designed

The monomer 11 was successfully electropolymerised by cycling potentials from 0.0 V to 0.8V. Compared to the monomer previously synthesised bearing only a single pyrrole group, the yield of polymerisation was greater. The work on immobilisation of enzymes by photografting was continued and these results have been accepted for publication.

Subsequently, monomers 9, 10 and 11 were synthesised in greater quantities to provide the different partners with samples. The first synthesis was done in small quantities to check the synthetic route.

Monomer 12 (Figure 41) synthesized by the partner 6 (CSIC) was characterized by cyclic voltammetry in organic medium (acetonitrile under an argon atmosphere).

Figure 41 Structure of monomer 12.

An irreversible anodic peak appeared clearly at 920 mV vs Ag/ 10 mM Ag⁺ corresponding to the formation of pyrrole radical followed by their polymerization. After several sweeps in the potential range: 0 - 0.85 V, the appearance and the growth of a reversible signal at $E_{1/2}$ = 0.4 V, indicated the formation of a polypyrrole film on the electrode surface, Figure 42.

After transfer into an acetonitrile electrolyte without monomer, the modified electrode exhibited a signal corresponding to the polypyrrole electro-activity. Elaboration of films by controlled potential electrolysis allowed the determination of an electrochemical yield of 73%.for the polymerization process.

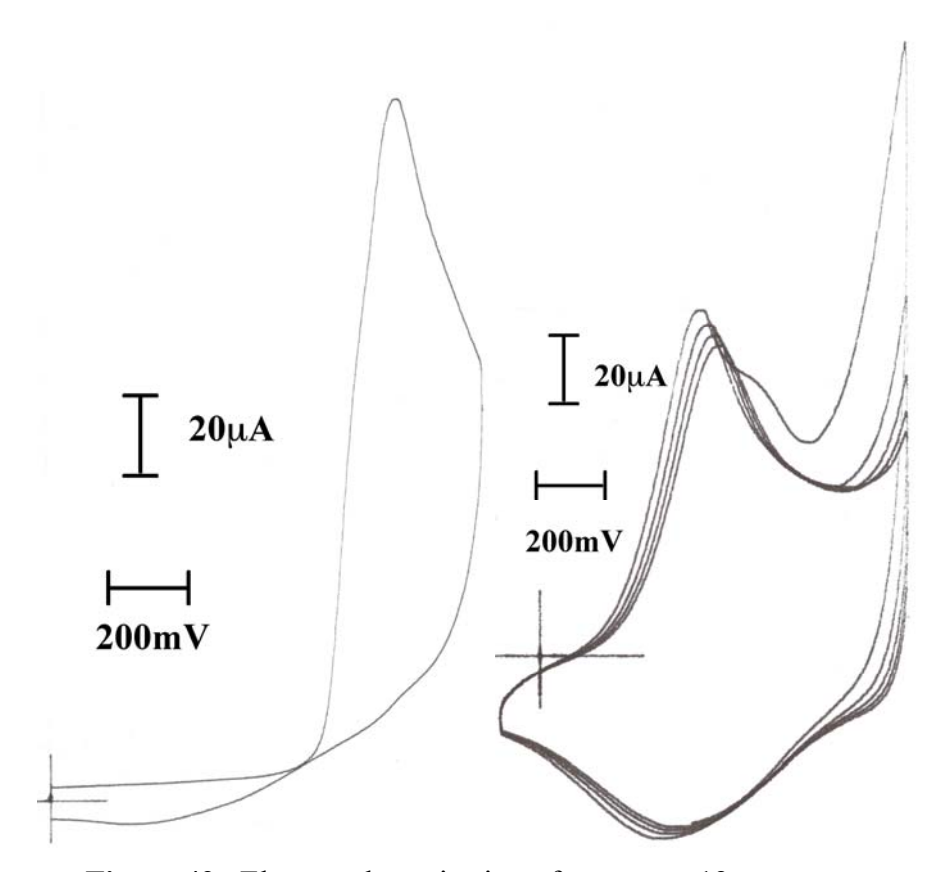


Figure 42. Electropolymerisation of monomer 12.

This polymer was exploited for the specific anchoring of atrazine antibody prepared by the Partner 4 from the Technical University of Munich. Preliminary attempts seemed to indicate that such film was able to anchor antibody and the latter could be displaced by atrazine.

Synthesis of pyrrole –adamantane conjugate

In order to develop an alternative affinity system to the well known avidin-biotin complex for the immobilization of Ab or Ag on polymer surfaces, the strong association between adamantane and β -

cyclodextrin was investigated via the synthesis of a new monomer. The synthesis is described below (figure 43). The electro-oxidation of this new pyrrole-adamantane should provide a functionalized polypyrrole film able to anchor proteins bearing β cyclodextrins. The electrochemical characterization of this monomer and the related polymers were investigated.

Figure 43. Scheme 1 for synthesis of the monomer pyrrole-adamantane

This new monomer was electro-polymerized in a three electrode electrochemical cell. To test the affinity properties of the electropolymerized films for the anchoring of biomolecules modified by cyclodextrin groups, glucose oxidase was modified with mono-6-deoxy-6-amino β -cyclodextrine (figure 44). The resulting activity of the modified enzyme was tested due to its activity with amperometric methods before its immobilization onto the polymer film.

Figure 44: Schematic presentation of the synthesis of electropolymerizable adamantane and its formation of a polymer film (top). Schematic presentation of mono-6-deoxy-6-amino β -cyclodextrine (bottom).

After incubation of the adamantine polypyrrole modified electrode into a PBS (0.1 M, pH 7.0) solution containing 2.5 mg/ml cyclodextrine modified glucose oxidase, the sensitivity of the resulting bioelectrode (see figure 45) was tested amperometrically using a standard three electrode electrochemical cell. Sensitivities around 200 μ A.M⁻¹cm⁻² could be obtained. These relative low sensitivities can be explained by the highly hydrophobic surface of the adamantane polypyrrole film which reduced drastically the permeability of the enzymatically produced hydrogen peroxide.

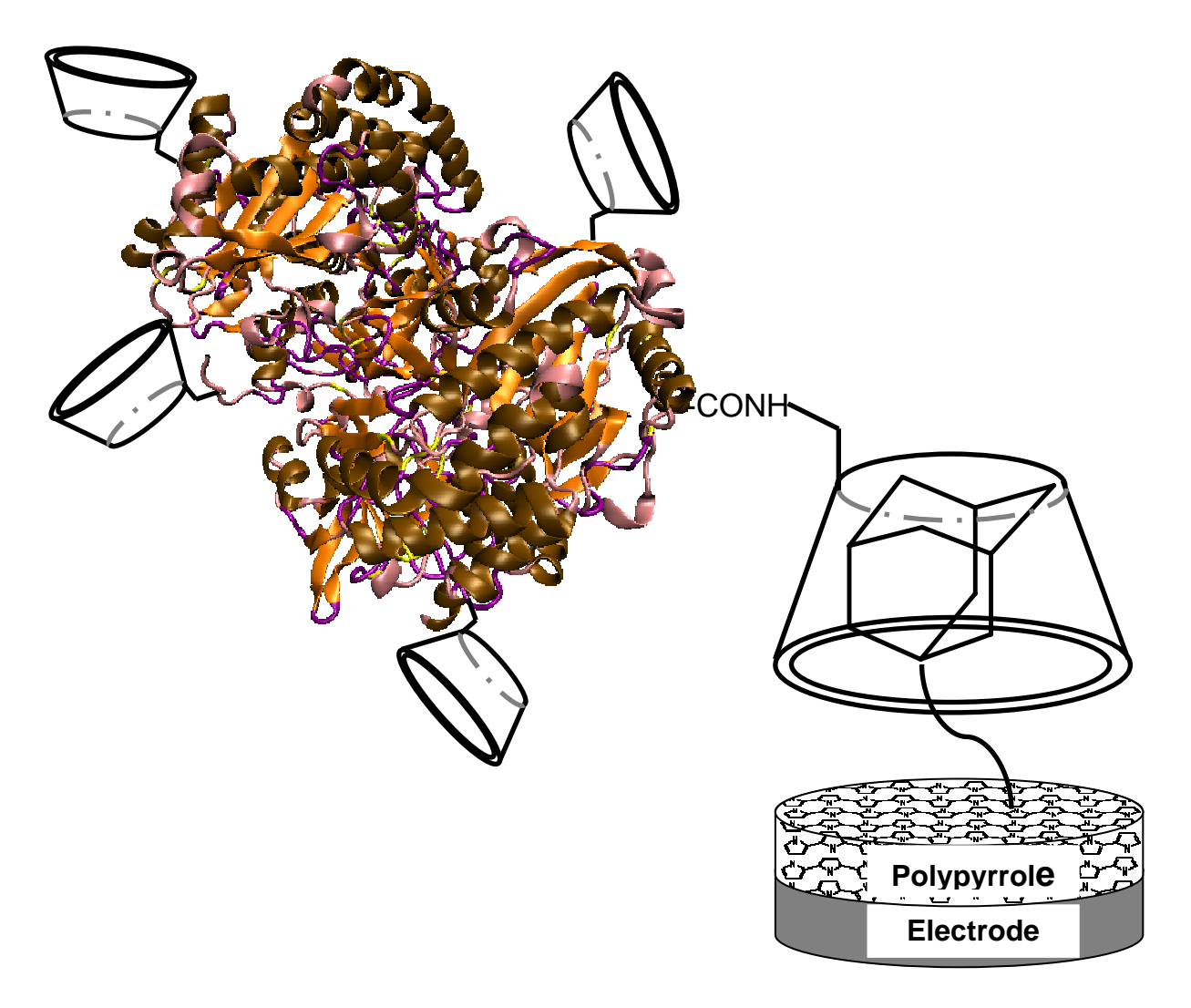


Figure 45 : Schematic presentation of the immobilization of cyclodextrine modified glucose oxidase onto adamantane functionalized electrodes.

Synthesis of the pyrrole-viologen-biotin derivative as an impedance amplifier.

This redox monomer led to an electropolymerized polymer for the immobilization of proteins by affinity interactions (system avidin-biotin). The polymerized redox group was thought to be a potentially interesting electrical probe for impedance measurements of the recognition process occurring at the polymer-solution interface. However, the synthesis was rather complex and time-consuming. Therefore, we tried to improve the synthetic pathway as well as to enhance the reaction yield (figure 46).

OMe
$$OH_{2}N \longrightarrow Br \longrightarrow N \longrightarrow N$$

$$CH_{3}CO_{2}H \longrightarrow N$$

$$OMe$$

$$OH_{2}N \longrightarrow N$$

$$CH_{3}CO_{2}Na$$

$$OH_{3}N \longrightarrow N$$

$$OH_{4}N \longrightarrow N$$

$$OH_{5}N \longrightarrow N$$

$$OH_{5}N \longrightarrow N$$

Synthesis of the biotin moiety:

Coupling step and counter anion exchange:

Figure 46. Scheme for synthesis of pyrrole-viologen-biotin derivative.

A stoichiometric amount of 3-bromopropylamine hydrobromide (10.944 g, 50.0 mmol) and dimethoxytetrahydrofurane (6.5 ml, 50.0 mmol) was stirred at 70°C for 2.5 hours with 1.1 equivalent of sodium acetate (7.534 g, 55.4 mmol) in 100 mL of a H₂O/acetic acid mixture (3/2, v/v). The aqueous layer was separated and extracted with Et₂O. The organic layers were collected, washed with water and brine and dried over sodium sulfate. After evaporation to dryness, the crude residue was purified by filtration on silica gel using hexane as eluant. After evaporation of hexane, the pure bromo-pyrrole (5.965 g, 31.7 mmol) was obtained in 63% yield.

A mixture of bromo-pyrrole (0.472 g, 2.5 mmol) and 2 equivalents of 4,4'-Bipyridine (0.782 g, 5.0 mmol) was stirred at 85°C for 20 hours in DMF (5 mL). After evaporation of the DMF, H₂0 was added and the aqueous layer was extracted three times with CH₂Cl₂. After evaporation of water, the mono-alkylated product was dried under vacuum and thus obtained in 87% yield (0.754 g, 2.19 mmol).

A mixture of biotin (0.488 g, 2.0 mmol) and 3-Bromopropan-1-ol (1.3880 g, 10.0 mmol), *p*-toluene sulfonic acid (0.0380 g, 0.2 mmol) was stirred and refluxed at 120°C in toluene (12 mL) for 72 hours under nitrogen atmosphere. The reaction mixture was cooled at room temperature and the toluene was evaporated under vacuum. The residue was dissolved in CH₂Cl₂, precipitated by adding Et₂O and filtered off. The solid was dissolved in CH₂Cl₂ and purify by silica gel column chromatography (CH₂Cl₂/MeOH, 9/1) to give a white solid (0.5893 g, 1.61 mmol) in 81% yield.

A stoichiometric amount of bromo-biotin (0.1434 g, 0.39 mmol) and Pyrrole/bipyridine conjugate (0.1248 g, 0.39 mmol) was stirred at 60°C in EtOH (5 mL) for 12 days. The reaction mixture was cooled at room temperature and the ethanol was evaporated under vacuum. The residue was dissolved in MeOH (1 mL), precipitated by adding CH₂Cl₂ and filtered off. After anionic exchange, the Bipyridinium with

BF₄ counter anions was thus obtained in 45% yield (0.1484 g, 0.21 mmol). The product has been characterized by NMR and ESMS before anionic exchange.

Work also focused in the development of electrochemical immunosensors allowing the direct detection of specific proteins such as lectins. The approach consisted to immobilise saccharidic structure onto electrodes via the electrogeneration of polymer films. In this context, 2 new monomers were synthesised. (figure 47) They are functionnalised by lactose and siallylactose (pyrrole-lactosyle named pyr-lactose) and (3'-sialyl)- β -lactoside allyl (pyr-sialyllactose). The yields of synthesis were 66 % and 94 % respectively.

Figure 47 Structures of the oligosaccharide-pyrrole(pyr-lactose and pyr-sialyllactose) monomers synthesised

The 2 compounds bear an electropolymerisable group in order to provide conductive polymer at the surface at the electrode. The first monomer was designed for the detection of *Arachis hypogaea* (PNA) lectin and the second one for the detection of *Maackia amurensis* lectin. The schemes for the syntheses are described below (figires 48 and 49).

Figure 48. Scheme of the synthesis of pyr-lactose

Figure 49. Scheme for the synthesis of and pyr-sialyllactose

The electrochemical behaviour of these 2 monomers was studied in aqueous solution under an inert atmosphere. The irreversible oxidation of the pyrrole group was detected at a potential of 1.1 V and the film was developed at the surface of the electrode at a potential of 0.95 V. The permeability of these poly(pyr-lactose) and poly(pyr-sialyllactose) were checked in presence of hydroquinone and Ru (III) hexamine. Then, by immersing the electrode in a solution of proteins, the permeability values decreasd (see figure 50).

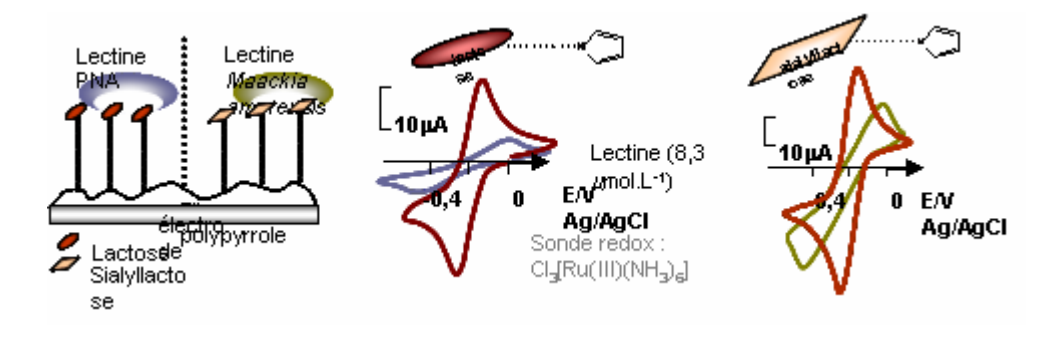


Figure 50 : Curves of permeability in presence of lectin for the modified electrodes Pyr-lactose and Pyr-sialyllactose

The interactions between the proteins and the polymers were detected by impedance measurements in the presence of a 2 mM of hydroquinone. The module of impedance as can be seen in the figure 51, increased because of the protein interaction.

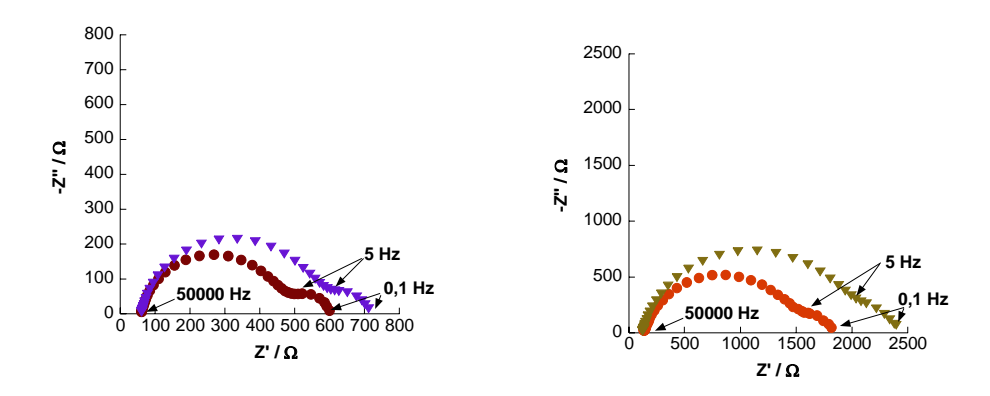


Figure 51. Impedance spectra of the modified electrodes poly[pyr-lactose] and poly[pyr-sialyllactose] in presence of 8.3 μM lectin at a potential of 0.45 V/ ECS in presence of 2 mM hydroquinone.

In order to enhance the recognition phenomena, a new monomer was designed with an internal redox probe, namely a viologen group. The synthesis of this new monomer gave a yield of synthesis of 80 %.

New Pyrrole viologen derivative

This monomer was characterised by cyclic voltammetry in CH₃CN + TBAP 0.1 M (see figure 52). In the reduction part, two reversible monoelectronic systems are detected at $E_{1/2} = -0.72$ V, $E_{1/2} = -1.14$ V due to the monoelectronic and bielectronic viologen reductions. In the positive part, the pyrrole oxidation was detected at a potential of 1.08 V. The electropolymerisation was achieved by potentiostatic method at a potential of 0.96 V.

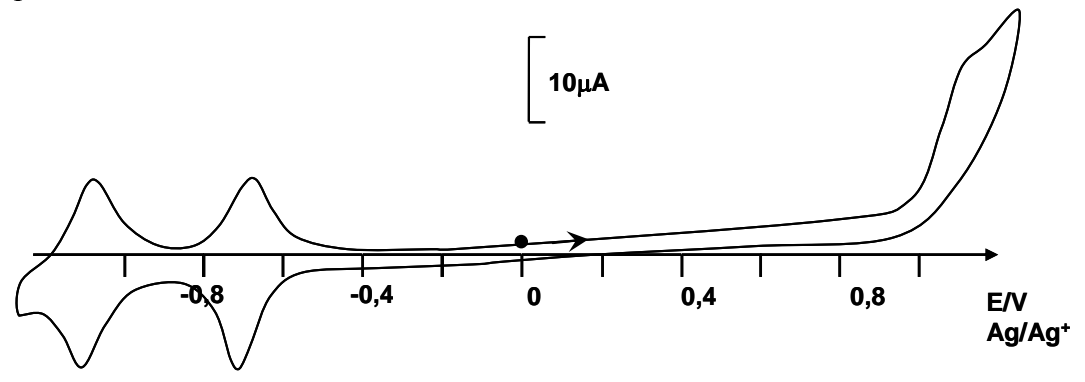


Figure 52. Cyclic voltammogramm of a Pyr-viologen-lactosyl (3 mM) on a vitreous carbon (diameter 3 mm) in CH₃CN + TBAP 0.1 M

As previously described, the permeabity curves were measured in the presence of hydroquinone. By impedance measurement, injection of PNA in the solution allowed the construction of a calibration curve with a limit of detection of 1.5 nmol/L (figure 53). Compared to the results obtained with SPR measurements, the electrochemical method is more sensitive.

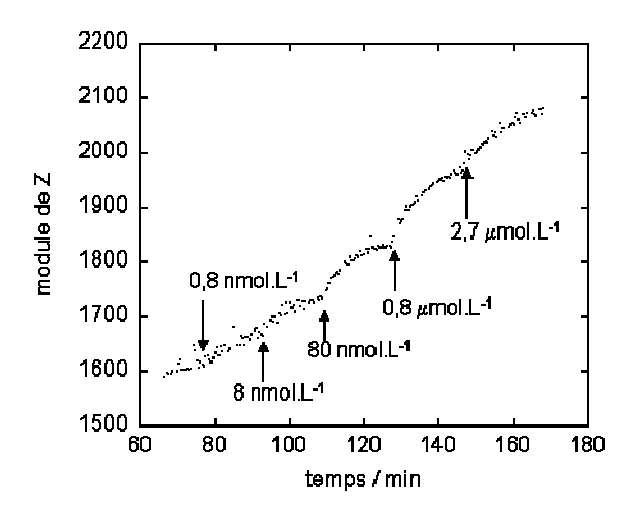


Figure 53. Impedance module variation for different concentrations of lectin-PNA

Single Walled Carbon Nanotubes

With the aim of enhancing the sensitivity of impedance measurements of immuno reactions occurring at the interface polymer-solution, improvement of the polymer permeability and conductivity was attempted via the coimmobilization of single walled carbon nanotubes (SWCNT).

In order to keep the intrinsic conductivity of SWCNT, the latter should not be oxidized or chemically modified. However, pure SWCNT were not soluble in water. A possibility was to disperse these nanotubes with the detergent Tween-20, but the resulting aqueous solution led to an unstable coating on the electrode surfaces. Accordingly, it was attempted to make soluble SWCNT with an aqueous solution of the amphiphilic pyrrole monomer pyrrole-alkylammonium (PAlk) used as a surfactant. Thus, carbon nanotubes were for the first time highly solubilized in a monomer aqueous suspension and used in the construction of enzyme electrodes to investigate the effect of their presence on the electro-enzymatic transduction step. For this purpose, glucose oxidase and tyrosinase were mixed with aqueous suspension of SWCNT and PAlk, then, these solutions were spread and dried on electrode surfaces (platinum and glassy carbon). The adsorbed coatings containing carbon nanotubes and enzymes (glucose oxidase or tyrosinase) were then electropolymerized onto platinum and glassy garbon electrodes, respectively. Their amperometric current response to glucose or catechol were recorded and compared to those recorded for the same biosensor configuration without SWCNT.

The SWCN-biosensors showed higher sensitivity (140 mA.M⁻¹.cm⁻² glucose and 800 mA.M⁻¹.cm⁻² catechol) than those fabricated without SWCNT, illustrating the beneficial effect afforded by these nanotubes on the permeation of substrates and the conductivity of the polymeric material. These preliminary experiments demonstrated the value of incorporating SWCNT within the polymer structures used for the fabrication of electrochemical immunosensors.

Other work concerned tests to exploit the structural uniqueness of single-walled carbon nanotubes (SWCNTs) having in average an aspect ratio of 1:1000. As produced pristine SWCNTs, furnished by Nanoledge SA (grate A; sample-number: Poh47H; 18.11.04), weren purified and oxidized by 3h reflux with 69 % (v/v) nitric acid and several subsequent washing steps. The obtained SWCNTs were further modified with 11-(1-pyrrolyl)-undecanol under standard Steglich conditions (DMF, DCC, DMAP) to give the pyrrole esters. The modification cheme is shown in figure 54 whilst an electrochemical comparison of the modified and unmodified SWCNTs is shown in figure 55.

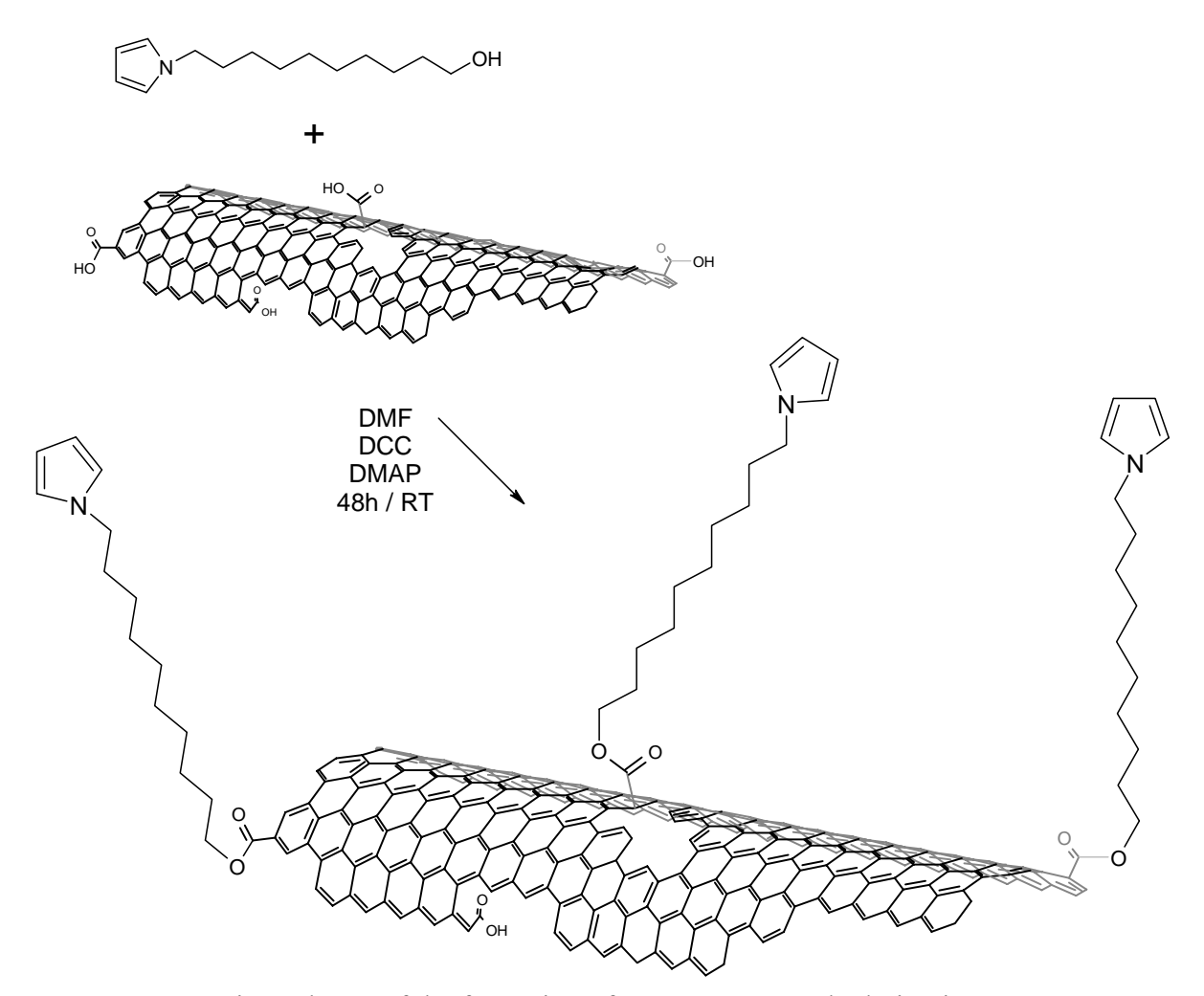


Figure 54. Reaction scheme of the formation of a SWCNT-pyrrole derivative.

This compound could be dissolved with sufficient high concentration in THF_{abs} and polymerized with a standard three electrode electrochemical set-up.

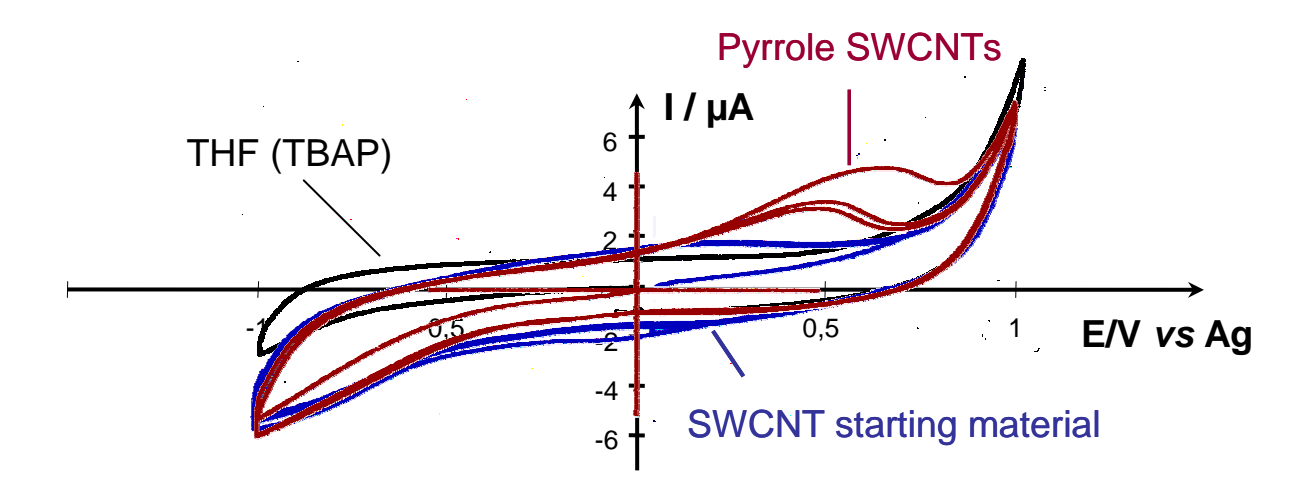


Figure 55. Cyclic voltamograms of pyrrole functionalized SWCNTs (red) and pristine SWCNTs (blue), dispersed in a THF_{abs} / electrolyte (TBAP) solution (black).

Impedimetric immunosensor for specific label free detection of ciprofloxacin (Partners: 5, 6 and 8)

The design of the electrochemical immunosensor was based on the chemical grafting of an antibody on an electropolymerized film and the detection of the antigen was performed by impedance.

In this context, the synthesis of pyr-NHS was carried in greater quantities than merely pilot scale. Impedance spectroscopy approaches combined with the immunosensor technology have been used for the determination of trace amounts of ciprofloxacin antibiotic. The sensor electrode was based on the immobilization of anti-ciprofloxacin antibodies by chemical binding onto a poly(pyrrole-NHS) film electrogenerated on a solid gold substrate. The gold surface modification: electropolymerization of pyrrole-NHS, antibody grafting and ciprofloxacin immunoreaction was characterized by cyclic voltammetry (CV) in the presence of $[Fe(CN)_6]^{3-/4-}$ as a redox system as well as by atomic force microscopy (AFM) imaging.

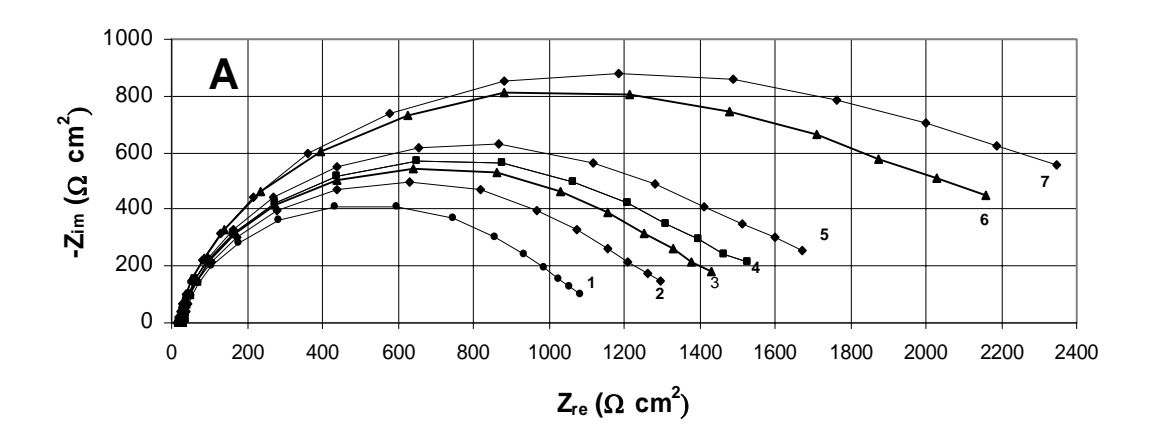


Figure 56. Nyquist plane impedance spectra obtained for an antibody modified gold electrode at apotential -1.4 V versus SCE and ac signal 10 mV, in PBS (1)-poly(pyrrole-NHS) electrodeposited on gold, (2)-antibodies deposited onto poly(pyrrole-NHS) electro-deposited on gold, (3)-10 pg/ml ciprofloxacin (CAP)deposited onto antibodies-polypyrrolic-NHS films, (4)-100 pg/ml CAP, (5) 2 ng/ml CAP, (6) 100 ng/ml CAP, (7) 1 μ g/ml CAP.

The immunoreaction of ciprofloxacin on the grafted anti-ciprofloxacin antibody directly triggered a signal via impedance spectroscopy measurements (Figure 56) which allowed the detection of the antigen target, ciprofloxacin down to 10pg/ml.

Other work was focused on the detection of fluoroquinolones: Dr DG Pinacho from the Applied Molecular Receptors group AMRg-CSIC (partner 6) came to our laboratory. We worked on the electropolymerisation of pyrrole-fluoroquinolone model derivatives (Figure 57). The yields of polymerization were very low (\leq 3 %) and difficulties were encountered to solubilise these compounds in a solvent favorable for the electropolymerisation of pyrrole groups.

Figure 57. Chemical structure of pyrrole-fluoroquinolone model derivatives

In this context, another alternative to immobilize the fluoroquinone was examined. The first step was to obtain the polymer by electropolymerisation of Pyr-N-hydroxysuccimide. Then a chemical grafting step was performed with the fluoroquinolone competitor. Each step was controlled by making permeability measurements with 2 mM [Ru^{II}(NH₃)₆] in aqueous solution (figure 58). The permeability value decreasd as expected from 1.6 x10⁻² cm².s⁻¹ to 1.1 x10⁻² cm.s⁻¹ after the chemical grafting. The concept of the immunosensor for the detection of fluoroquinolone compounds consists first in the immobilization of the fluoroquinolone Ab by immunoreaction with the polymerized model. Then, the presence of the target should displace the immobilized Ab generating thus a decrease of the module of impedimetric signal. To optimize the concentrations of the fluoroquinolone antibody sensor, anamperometric test with hydroquinone was carried out by anchoring the secondary antibody-HRP conjugate. The latter catalyses the production of an electroactive compound "quinine" which could be detected at the underlying electrode surface (figure 59). This amperometric signal must be proportional to the amount of secondary Ab-HRP and hence to the attached amount of fluoroquinolone antibody.

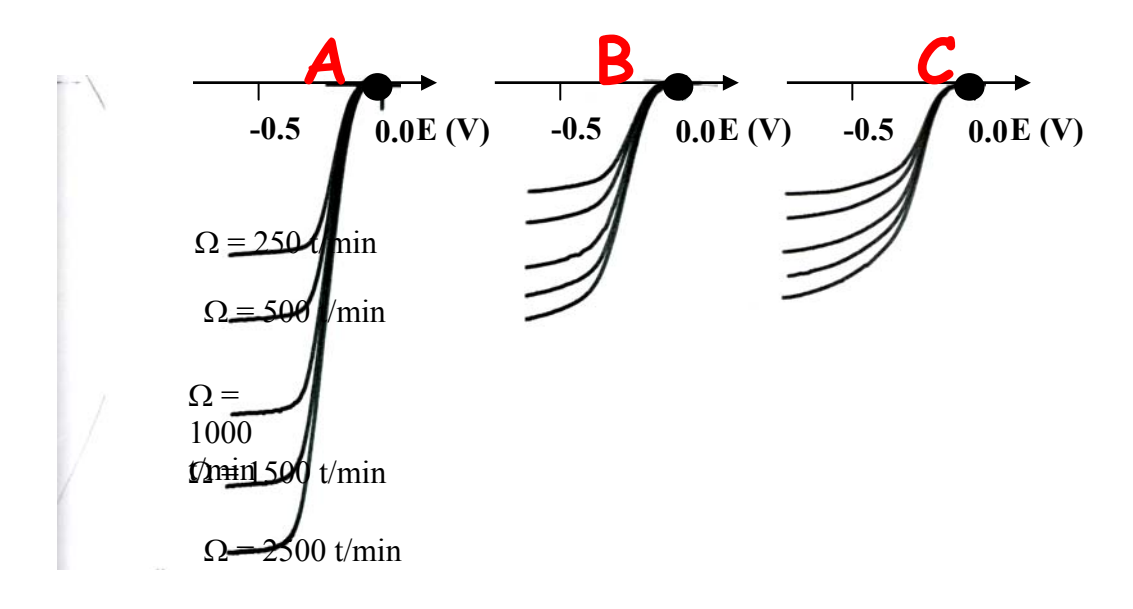


Figure 58. Experiments of rotating electrode of $Ru^{III}(NH_3)_6$ (2 mM) on vitreous electrode diameter 5 mm (A) after electropolymerisation of Pyr-NHS (B) (Q = 0.5 mC), after chemical grafting (C)

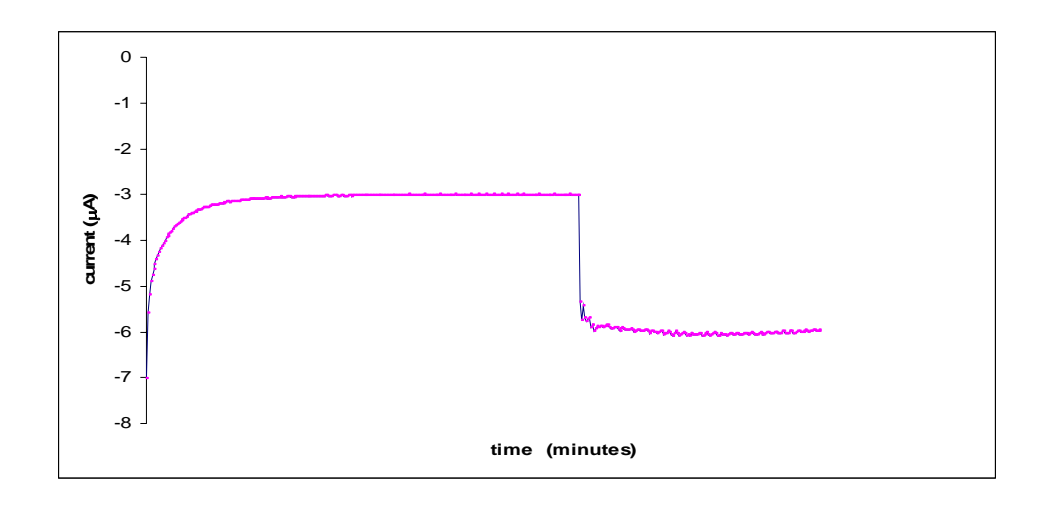


Figure 59. $E = 0.5 \text{ V.Addition of H}_2\text{O}_2 (10 \text{ mM}) \text{ and hydroquinone (2 mM) in 10 mM PBS, pH} = 7$

New methods of transduction

A tris(bipyridinyl) ruthenium(II) polymer was used to both immobilize biotinylated cholera toxin through avidin-biotin interaction and detect the corresponding antibody free of label via the change of electrochemical and photophysical properties of the polymer (figure 60).

With the aim of developing a new label-free photoelectrochemical detection concept for immunosensors, the formation and characterization of a novel ruthenium tris(bipyridine) polymer film was carried out. This allowed both the immobilization of proteins and the direct transduction of immunoreaction via its photoelectrochemical properties. The quality of both the photosensitive layer and the immobilized antigen layer at which the molecular recognition process takes place, is of extreme importance in the achievement of suitable immunosensor sensitivity. Consequently, the ruthenium complex was functionalized by electropolymerizable pyrrole groups with biotin as the affinity binding group.

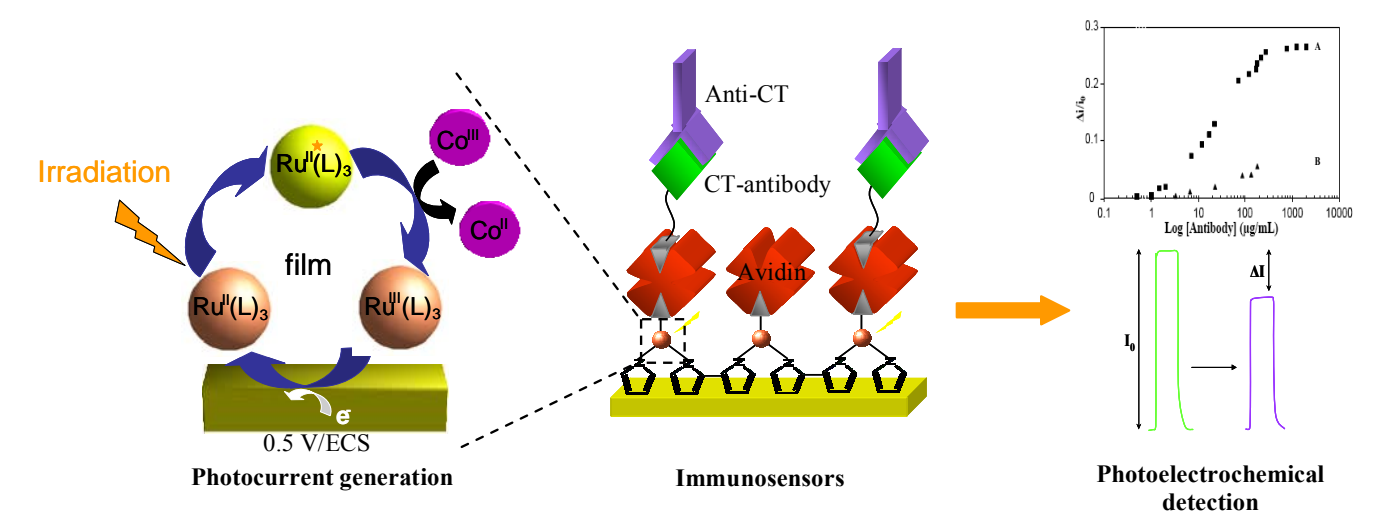


Figure 60. Scheme of the transduction of the immunoreaction from a ruthenium tris(bipyridine) polymer film based immunosensor.

Workpackage number: W4. Fabrication of Nanostructured Immunosensors

Objectives. To identify the correct techniques and conditions to enable reproducible manufacture of immunosensors based on the antibodies, recombinant antibodies and Fab fragments. To investigate the effect of different fabrication protocols on the loading and the sensitivity of the immunosensors produced.

Project Timeline	1 2 3 4 5 6 7 8 9 10 11 12 13 14 15 16 17 18 19 20 21 22 23 24 25 26 27 28 29 30 31 32 33 34 35 36
Workpackage 4. Sensor Fabrication	

Key results and discussions are detailed below:

Sensor Fabrication and Immobilisation of Antibodies:

Partners 1 and 2 were particularly active in the development of immunosensor devices during the first 12 months. Partner 1 used simple planar gold transducers and defined the techniques to produce reproducible sensor fabrication using polypyrrole matrices and impedance analysis to check the viability and activity of the antibodies in the conducting films. Partner 2 looked at the screen printed microelectrode approach using polyaniline matrices and impedance analysis to check activity.

Partner 1 - BBG, Leeds

Initial studies focused on the stabilisation of polypyrrole layer to enable reproducible manufacture of immunosensors. The data is linked to monomers from W3. Two electrodepositable systems were investigate initially—pyrrole and two different anions, chloride (Cl) and polystyrene sulphonate (PSS).

The type of transducer used was the simple gold on silicon structure depicted in figure 31 (page 36) and shown below as a photomicrograph (figure 61). Electrodeposition of the pyrrole – anion loaded films gave a slightly rippled effect indication potential problems with adhesion of the sensing layer.

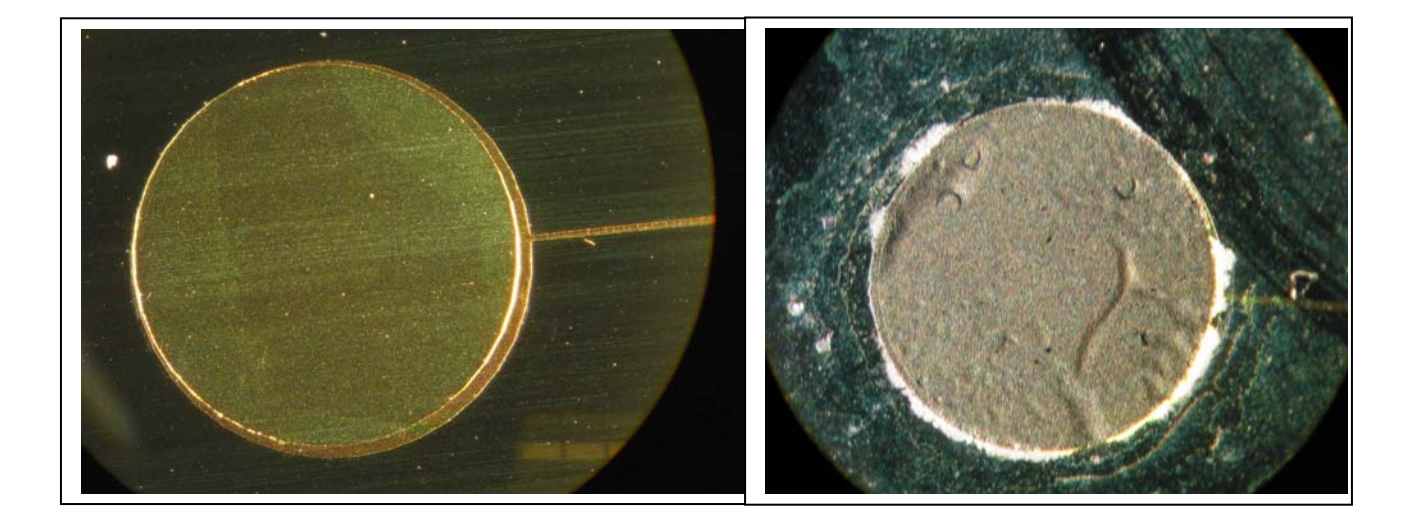


Figure 61: Photomicrographs of gold transducer and electrodeposited pyrrole – PSS film.

It was found using cyclic voltammetry that the adherence of the films to the transducers was generally poor at this stage and the physical stability was unpredictable with some sensors being relatively well adherent and others poorly adherent, figure 62.

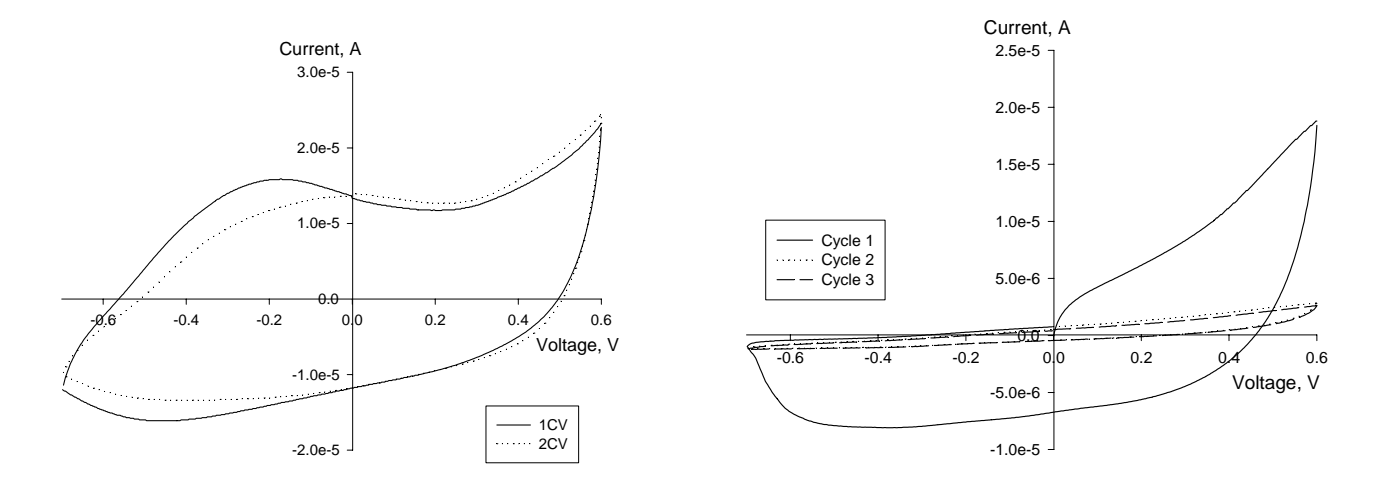


Figure 62. The left figure is for a polypyrrole-PSS film that is relatively stable and well adherent to the gold transducer showing the first (1CV) and second (2CV) cyclic voltammagrams. The right figure

shows an example of destructive cyclic voltammetry where the polypyrrole-PSS film was detached from the transducer during analysis. The adjacent photomicrograph shows detachment of the sensing layer.



Simple polypyrrole films were found to be not stable to storage in solution as revealed by electrochemical impedance spectroscopy (figure 63).

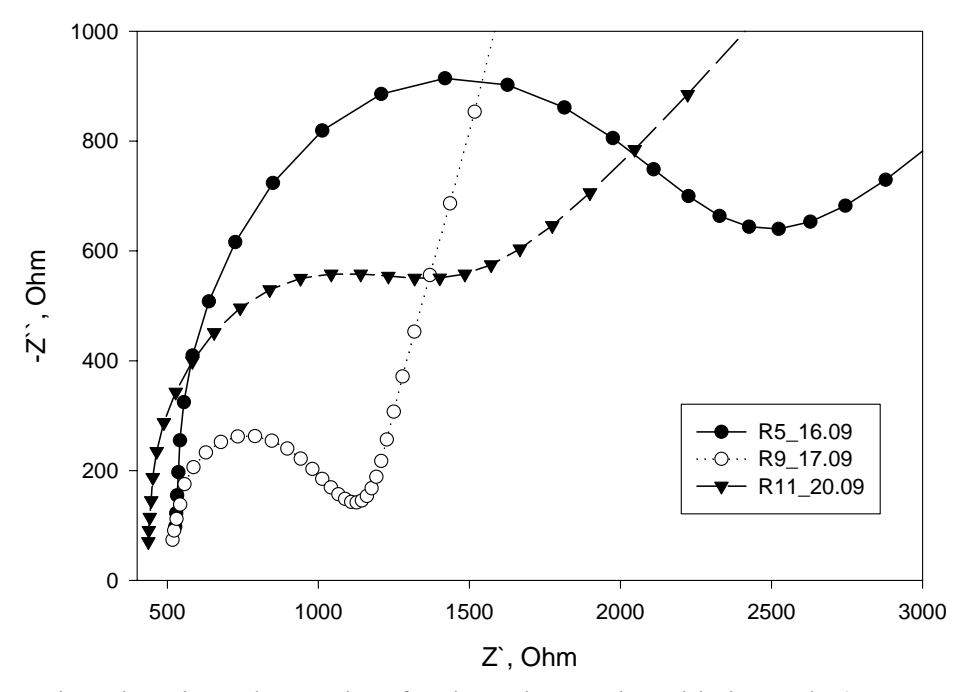


Figure 63: Complex plane impedance plots for the polypyrrole gold electrode (x-2546-10 single) number 5.

Impedance measurements were performed at 0.1~V vs Ag/AgCl and 0.5~V oscillation amplitude in 0.1~M NaH₂PO₄ and Na₃Fe(CN)₆-Na₄Fe(CN)₆ 10mM solution (pH 8.0). R5, R9 and R11 are repetitions number 5, 9 and 11 accordingly. The electrodes were stored in pure water between the measurements R5 and R9 during one day and between r9 and R11 during three days. Frequency range was 25 kHz – 25 mHz. Polypyrrole was prepared using 0.1 M pyrrole and 0.1 M poly-4-styrenesulphate solution at 700 mV vs Ag/AgCl by passing 1.5 mC charge.

Stabilisation of the polypyrrole layer was studied to enable reproducible manufacture of immunosensors. The two electrodepositable systems – pyrrole-PSS and pyrrole-Cl were used for these experiments. Polypyrrole electrodes produced with KCl were not reproducible or stable to storage. Traces show repetitions of single electrode at 'time 0' and 1 day later (figure 64). Polypyrrole electrodes produced with PSS were more reproducible but still not very stable to storage (figure 64).

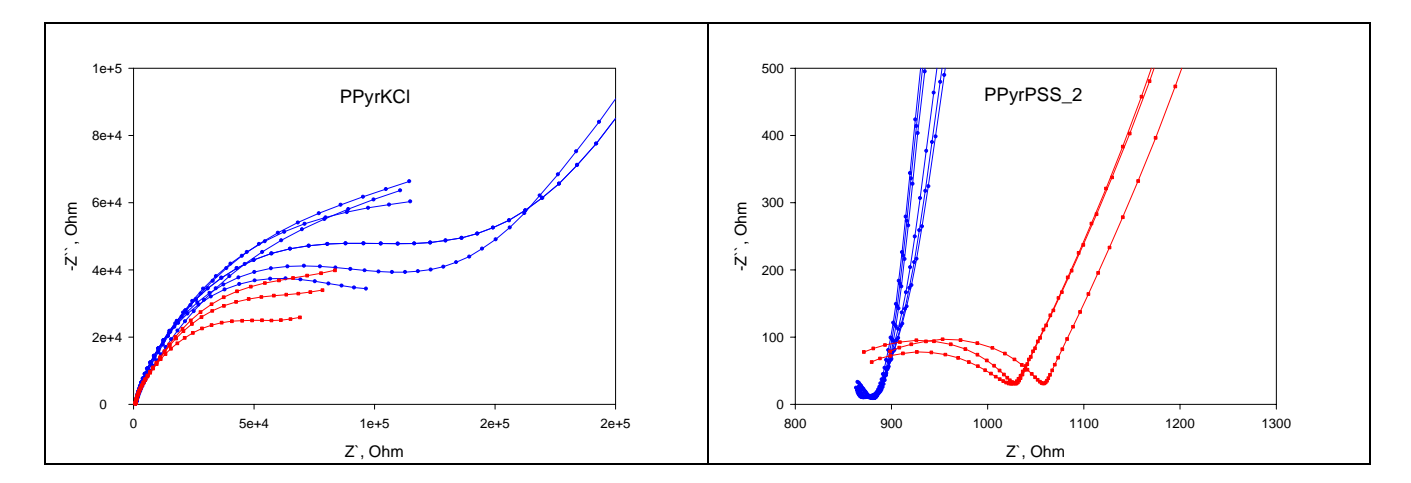


Figure 64. Complex plane impedance plots for the polypyrrole gold electrode.

Impedance measurements were performed at -0.4 V vs Ag/AgCl and 0.21 V oscillation amplitude in 0.1 M NaH₂PO₄ solution (pH 8.0). The electrodes were stored in 0.1M aqueous KCl solution during one day between measurements (blue circles and red squares). Frequency range was 25 kHz – 25 mHz. Polypyrrole was prepared using 0.1 M pyrrole and 0.1 M KCl solution at 800 mV (left plot) and using 0.1 M pyrrole and 0.1 M PSS solution at 700 mV (right plot) vs Ag/AgCl by passing 1.0 mC charge.

The possibility of stabilising of gold-polyrrole surfaces with alkanethiols was tested, as these materials form self-assembled monolayers on gold surfaces and it was thought that such self-assembly may have assisted in the blocking of 'gaps' or defects in the polypyrrole film (figure 65).

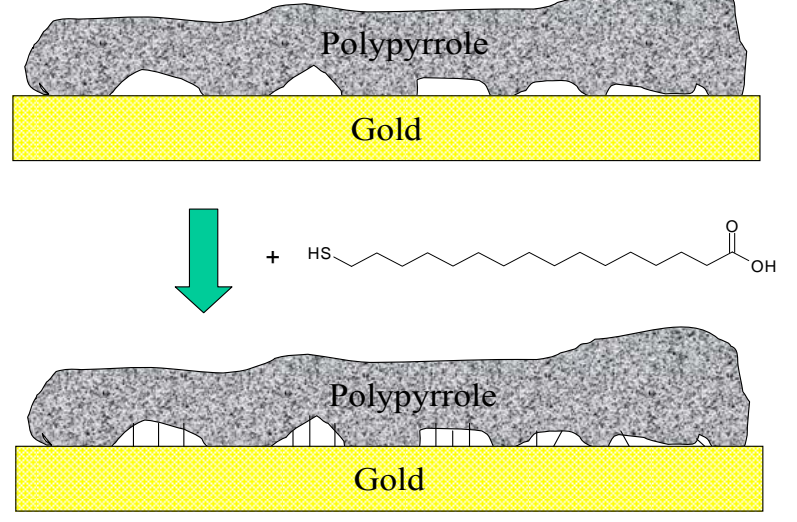


Figure 65. Schematic of thiol blocking on existing an electrodeposited polypyrrole matrix.

Treatment of polypyrrole electrodes with different thiols showed stabilising or destabilizing effects depending on properties of the alkanethiol (table 3). A stabilising effect was observed in the case of long chain thiols having polar end groups, for example, 11-mercaptoundecanoic acid (MUDA), 11-mercaptoundecanol (MUDO). Mercaptododecane having a long chain but no polar end group was not effective for stabilisation. The short chain thiols 6-mercaptohexanol (MHO) and 3-mercaptopropionic acid (MPA) had destabilising effect on the polypyrrole electrodes.

MHDA		MUDA		MUDO		MDD		МНО		MPA	
Ppyr/											
KCl	PSS										
(+)	(+)	(±)	(±)	(±)	(±)	N	N	(-)	(-)	(-)	(-)

Table 3. Stabilizing effect of different thiols ((+) – positive; (±) – less positive; N – not effective; (–) – negative effects (ppyr destroyed)). MHDA,mercaptohexadecanoic acid; MUDA, mercaptoundecanoic acid; MUDO, mercaptoundecanol; MDD, mercaptododecane; MHO, mercaptohexanol; MPA, mercaptopropionoic acid.

In particular, MHDA appeared to increase the reproducibility and stability of polypyrrole/KCl and polypyrrole/PSS films when incubated over several days in solution (figure 66).

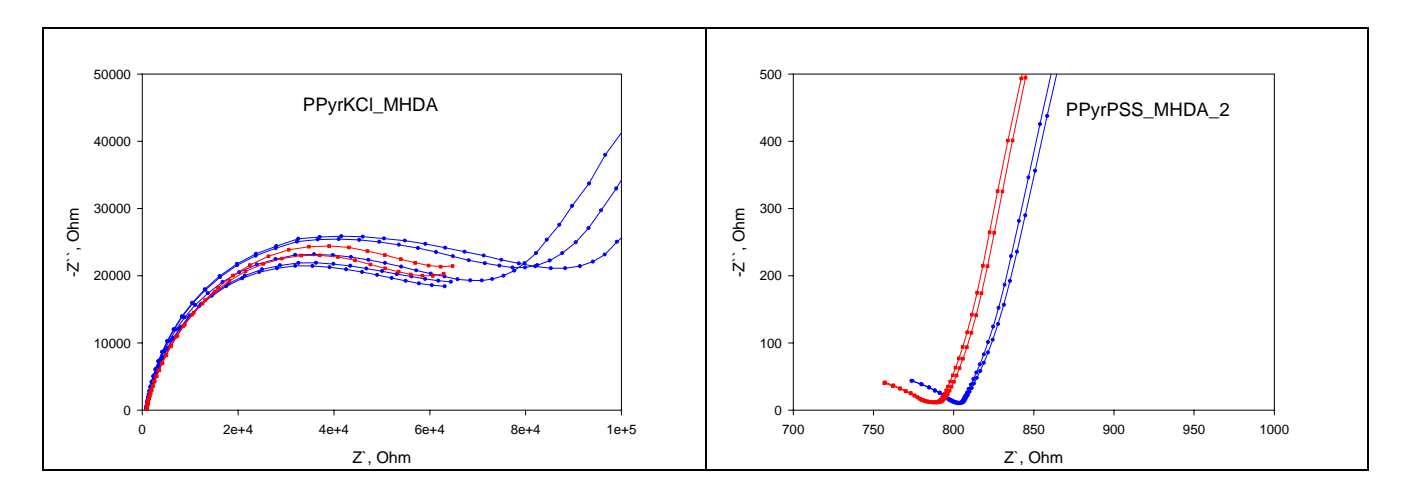


Figure 66. Complex plane impedance plots for the polypyrrole gold electrode. Impedance measurements were performed at -0.4 V vs Ag/AgCl and 0.21 V oscillation amplitude in 0.1 M NaH₂PO₄ solution (pH 8.0). The electrodes were stored in KCl water solution 0.1M during one day between measurements (blue circles and red squares). Frequency range was 25 kHz – 25 mHz. Polypyrrole was prepared using 0.1 M pyrrole and 0.1 M KCl solution at 800 mV (left plot) and using 0.1 M pyrrole and 0.1 M PSS solution at 700 mV (right plot) vs Ag/AgCl by passing 1.0 mC charge. Polypyrrole electrodes were treated with 0.1 mg/mL solution of thiols in ethanol.

Further experiments carried out using extended CV interrogation of both unmodified polypyrrole and MHDA modified polypyrrole layers clearly indicated an increase in the stability of the polymer, (figure 67).

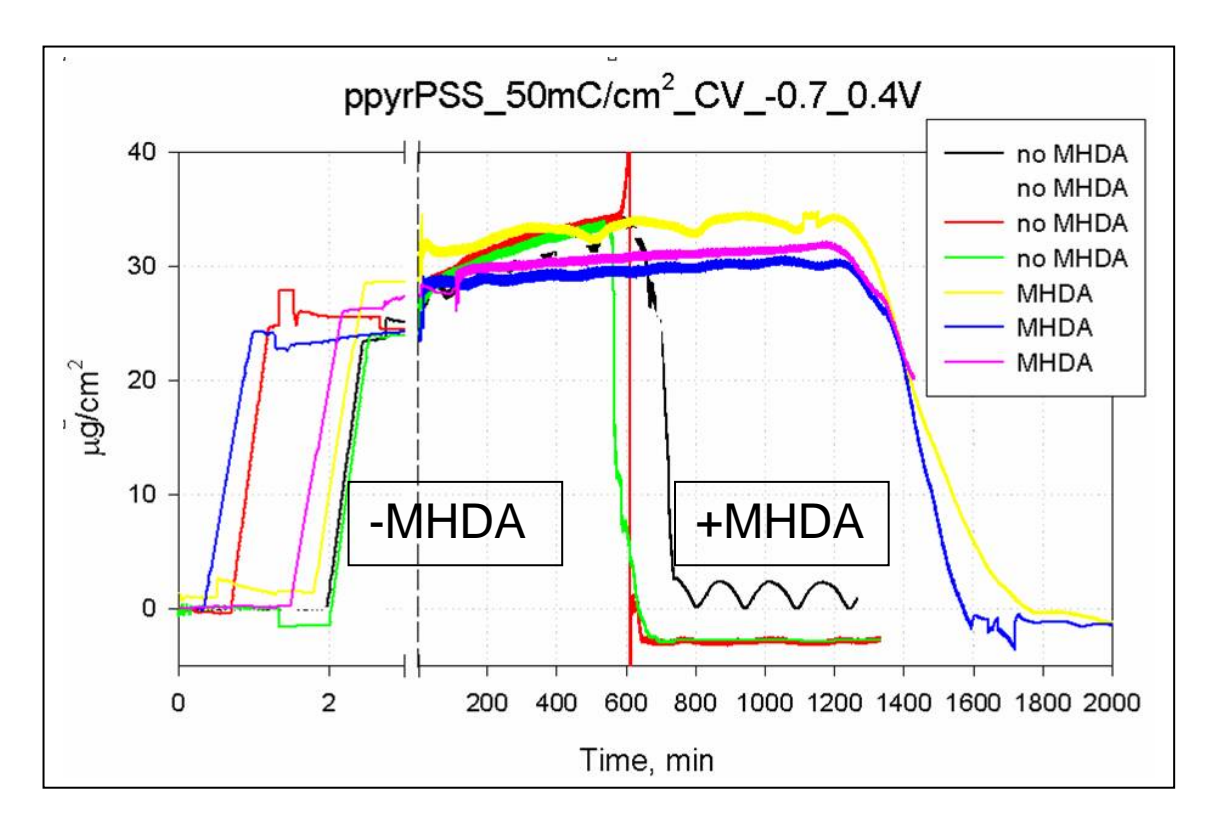


Figure 67. Succesive electro-QCM of polypyrrole-PSS deposited and destroyed by CV (-0.7V to 0.4V , cycle rate 50 mV/s) in the absence or presence of MHDA.

Whilst the addition of MHDA clearly stabilised polypyrrole films, an alternative method was investigated that used the properties of a cross linker to rigidify the electroconductive film in much the same way as polyacrylamide gels are stabilised. Such a route allows the direct formation of a cross-linked electroactive matrix by electropolymerisation. The monomer used was an aniline derivative – N-phenyl ethylene diamine and the cross linker was diphenyl-ethylene diamine, the structures are shown below, figure 68 and the synthesis of the electroactive film is shown in figure 69 by E-QCM.



Figure 68. Structures of N-phenyl ethylene diamine and diphenyl-ethylene diamine

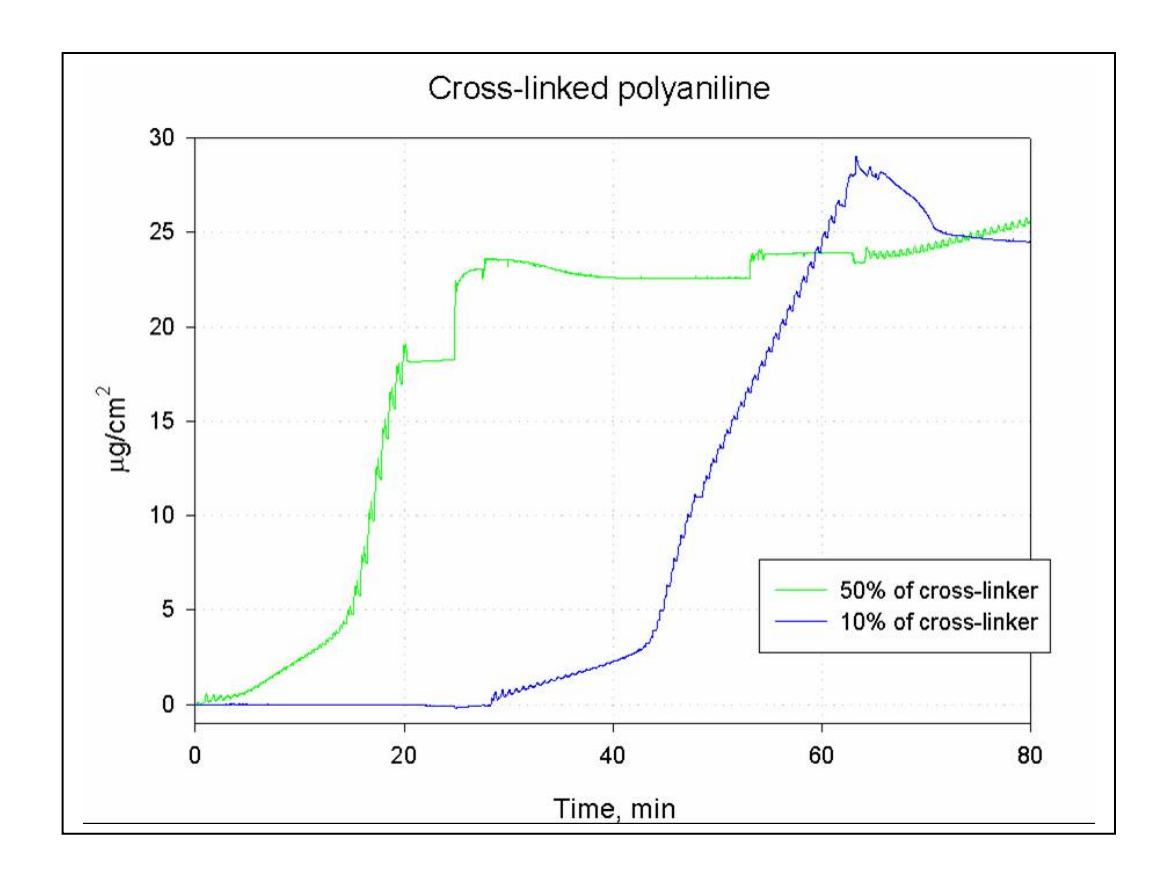


Figure 69. Electrosynthesis and deposition of cross-linked polyaniline matrix measured by E-QCM. This clearly shows deposition of the polymer on the electrode surface by the mass change measured. Note the rapidity of polymerisation increased when more cross-linker was added.

The stability of these cross-linked polyaniline films was tested in the same way as the polypyrrole film by using repeated cycles of voltage and measuring the remaining mass change on the E-QCM. No destruction of the layer was seen over a period of 4,000 minutes (66.7 hours) continuous cycling. Also the electroactivity of the film was maintained, shown by the oscilation of mass change caused by ion transport in and out of the film as the voltage was cycled (figure 70).

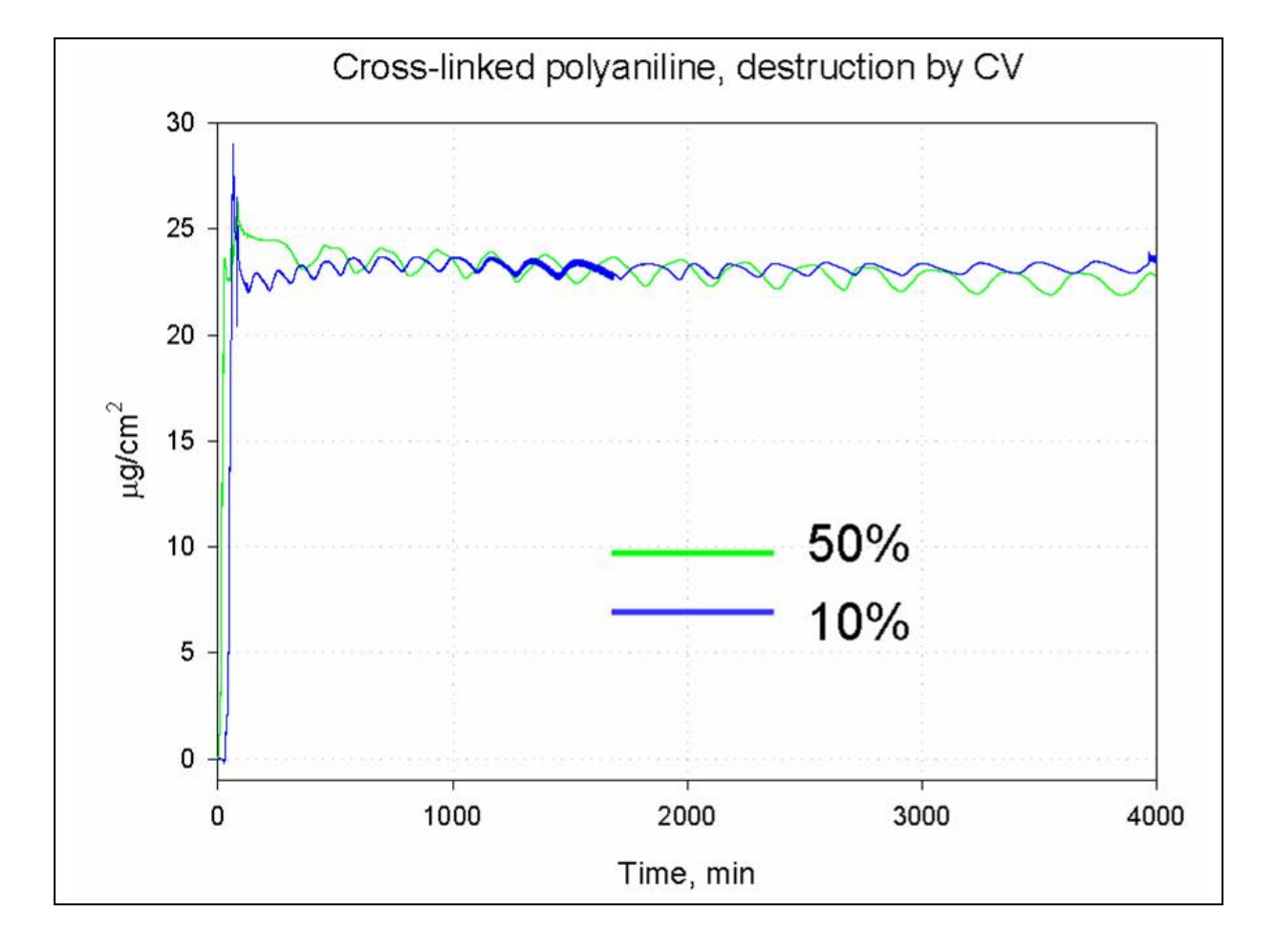
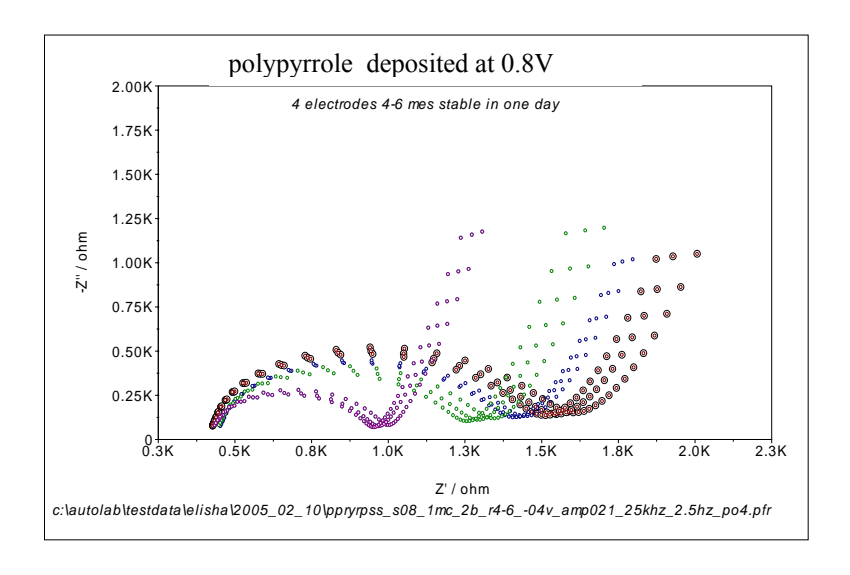


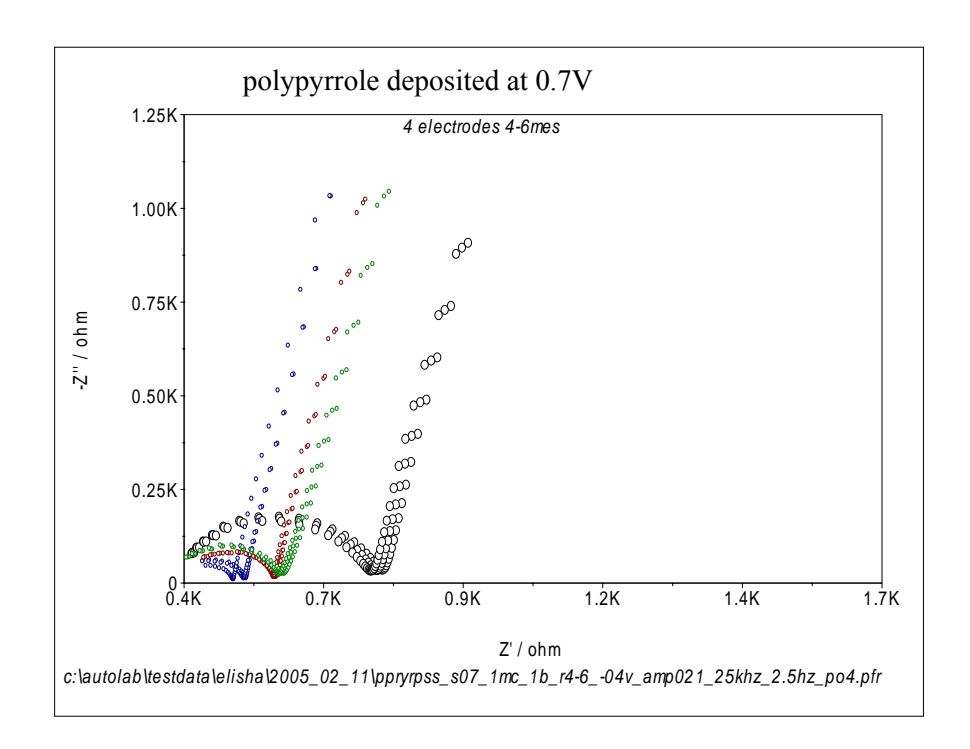
Figure 70. Continuous CV on the cross-linked polyaniline films measured by E-QCM. No material breakdown is seen and electro-activity is maintained for these cross-linked films.

Reproducibility of polypyrrole films.

Detailed experiments done after the 12 month meeting confirmed that simple electrochemically deposited polypyrrole immunosensors (formed from underivatised pyrrole) on gold transducers were difficult to produce in a reproducible manner and showed significant instability when stored in aqueous buffers, (figure 71 - bottom, and next page). Polypyrrole films deposited onto graphite electrodes were similar with respect to reproducibility. This indicated that pyrrole in its underivatised state was easy to polymerise but formed polymers with irregular properties which were susceptible to changes over time when stored.

The different derivatised pyrroles generated by partner 8 were then investigated in detail. however some difficulties in polymerisation were found transferring techniques between the different laboratories.





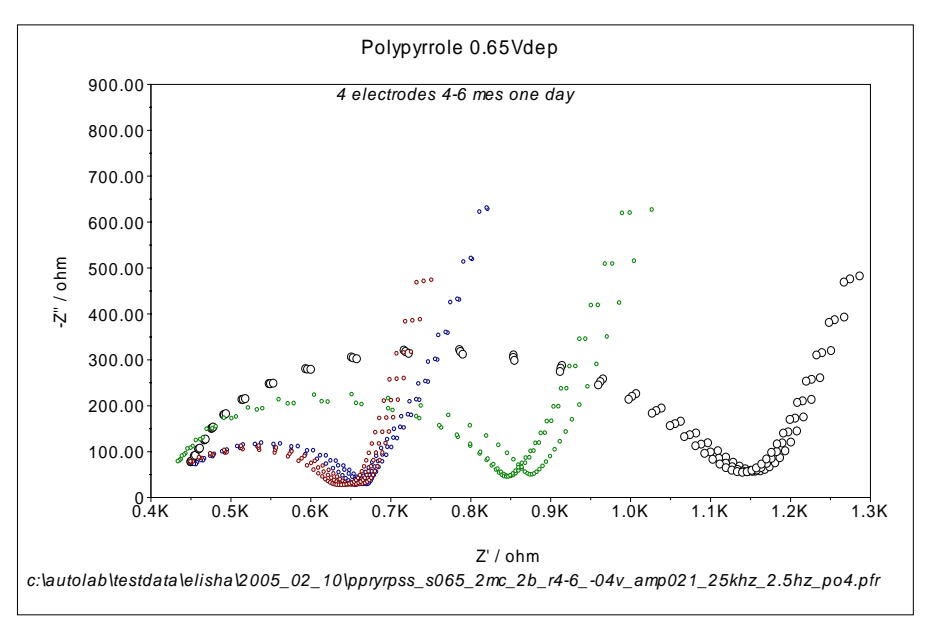


Figure71. Polypyrrole matrices produced at different oxidation potentials. In each case the impedance analysis of the deposited film indicated differences due to the deposition process. This type of result is attributed to the actual process of polymer initiation, as this is not a reproducible phenomenon and the polymer formed depends on the initial formation of oligo-pyrroles which then associate to produce the polymer.

Polythiophenes were found to bemuch more reproducible (figure 72). However, they were not very water compatible and in many cases therefore post-deposition immobilisation would have to be carried out if polythiophenes were used.

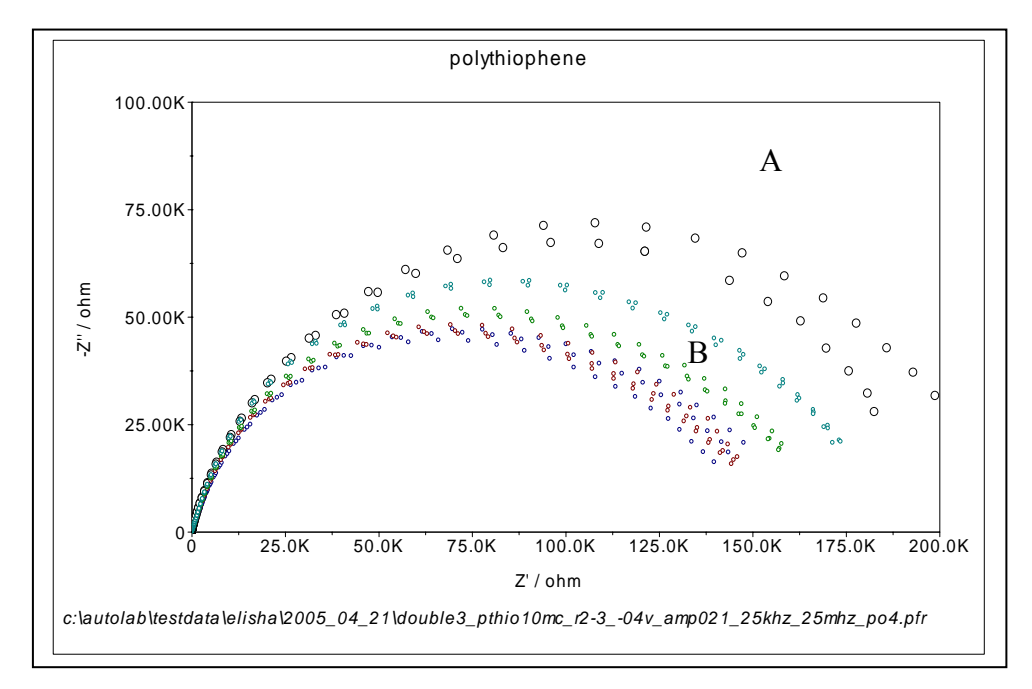


Figure 72. Complex plane impedance plots for four polythiophene gold electrodes

Impedance measurements were performed at -0.4 V vs Ag/AgCl and 0.21 V oscillation amplitude in 0.1 M NaH₂PO₄ solution (pH 8.0). Frequency range was 25 kHz – 25 mHz. A: First repetition; B: Repetitions before CV (-0.7 – 0.6 V, 10 cycles). Polythiophene was prepared using 0.1 M thiophene and 0.1 M NBu₄BF₄ solution in acetonitrile at 1700 mV vs Ag/AgCl by passing 10.0 mC charge. Gold ELISHA electrode, design P4 was used.

Partner 2 – ISBT, Cranfield - Microarray electrodes

The first stage in the fabrication of microarray sensors is to electropolymerise and thereby insulate electrode surfaces with o-phenylenediamine. This was achieved by cyclic voltammetry as depicted in Figure 73. The deposition is self limiting, eventually reaching and insulating state.

O-phenylenediamine deposition: (0 to 900mV at 50mVs⁻¹)

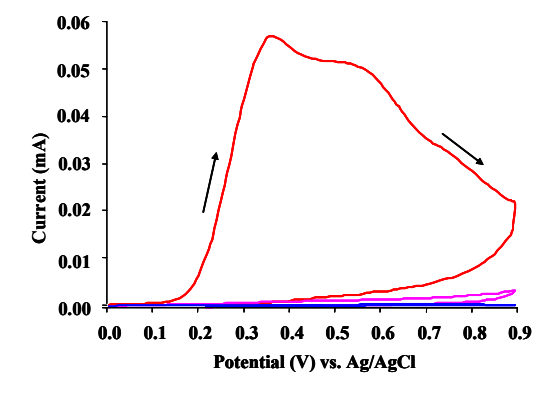


Figure 73: Electro-deposition of *o*-phenylenediamine at screen-printed carbon electrodes. Red trace, inital scan; purple trace, self limited (insulating) film.

The insulated electrodes were sonicated to ablate the insulating surface giving rise to micro-electrode templates with population densities of up to 2.5 x 10⁵ micro-electrodes.cm⁻². The voltammetry of these was evaluated via cyclic voltammetry of a redox couple such as ferri/ferrocyanide or ferrocene carboxylic

acid. The plateau regions seen within the current transients provided confirmatory evidence of characteristic micro-electrode performance (figure 74).

Cyclic Voltammetry of Fe(CN)₆3-/4-

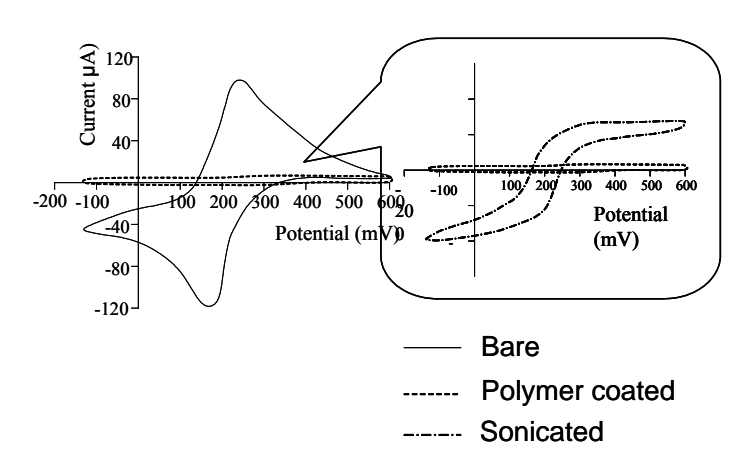
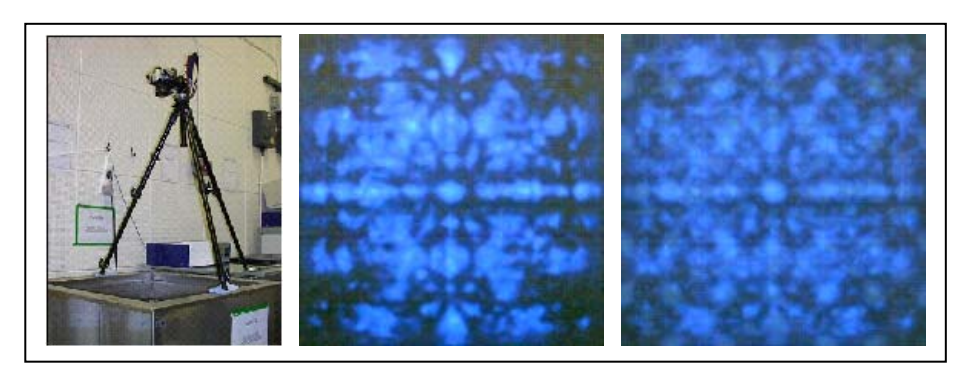


Figure 74: Cyclic voltammetry of sonochemically fabricated micro-electrode array showing confirmatory evidence of plateau within current transients - and so classical micro-electrode behaviour.

The reproducibility of the micro-electrode production was progressed to further improve the manufacturing capability of the micro-electrodes. One of the early problems was reproducibility of the sensors. It was thought that this could be due to the fact that inside the tank, ultrasound was produced by 12 horns (a new tank with 48 ultrasonic horns will became available in 2006). However, constructive and destructive interference occurs and cause formation of nodes and anti nodes within the tank. Therefore a sensor that was located at a node would be subjected to more energy than one located at an antinode.

Two complementary approaches were utilised to minimise this effect. The first involves placing a perforated metal baffle in the tank to disrupt the formation of standing waves within the tank and "smear out" the nodes and antinodes. However a method was required to determine whether the baffles were having any effect. It is known that the dye luminol fluoresces when irradiated with ultrasound. Therefore the tank was filled with a dilute solution of luminol and a camera mounted as shown in Figure 75. The laboratory was then blacked out and a long-term exposure photograph taken of the tank whilst sonochemical irradiation of the contents was occurring. As can be seen from the photographs a series of standing waves forms within the tank, causing different levels of emission from the luminol. Addition of the baffle disrupted these standing waves somewhat, with the profile being less pronounced when the baffling was present.

Figure 75. Sonoluminescence profiling of the transducer manufacturing tank.



The standing waves formed in the tank are clearly seen in the centre picture. The picture on the right is more diffuse due to the baffling being present.

The second stage of the process was to move the sensors themselves whilst irradiation took place, so as to average out the amount of sonochemical energy each sensor received. Therefore a device was constructed (Figure 76) which moved a sheet of sensors within the tank during irradiation whilst keeping them in the same phase.

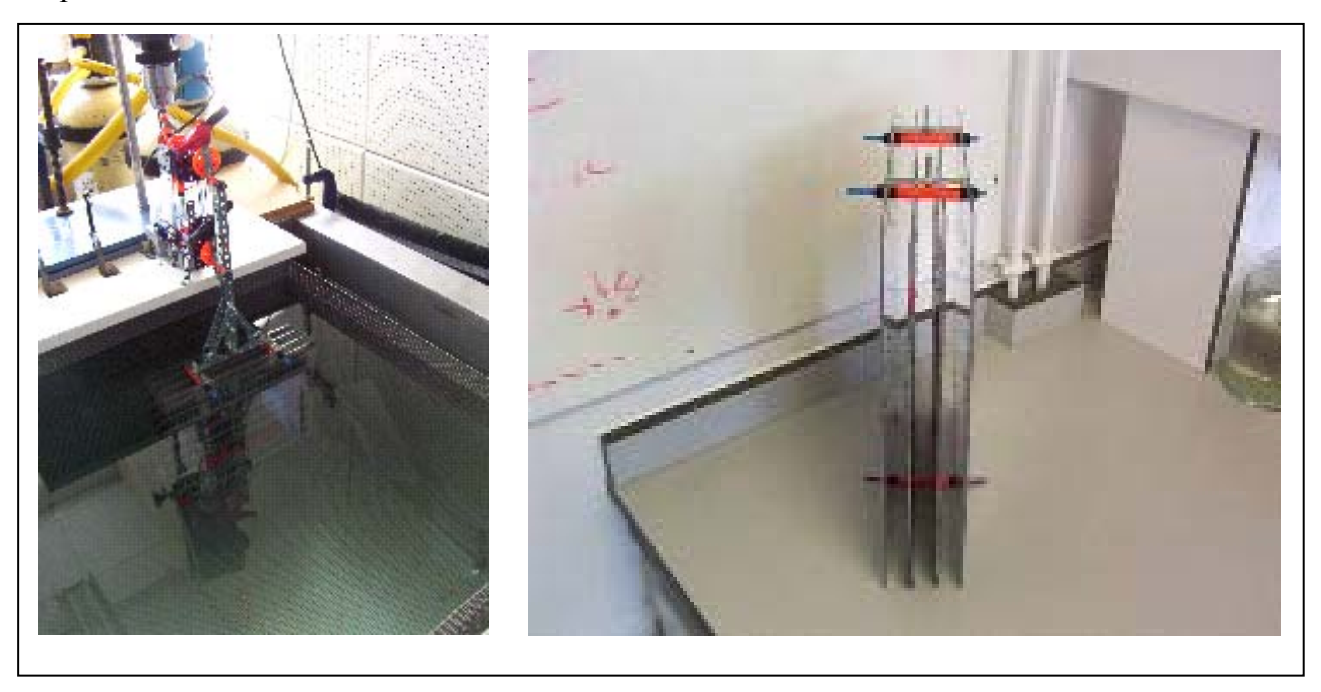


Figure 76. Movement of transducer sheets within ultrasound field.

The reproducibility of sensors obtained using baffling and sensor movement were evaluated via measuring the current transient of a redox species such as Ru(II)/Ru(III). As can be seen the current passed after one minute for a batch of 400 sensors varied by less than 2% (figure 77).

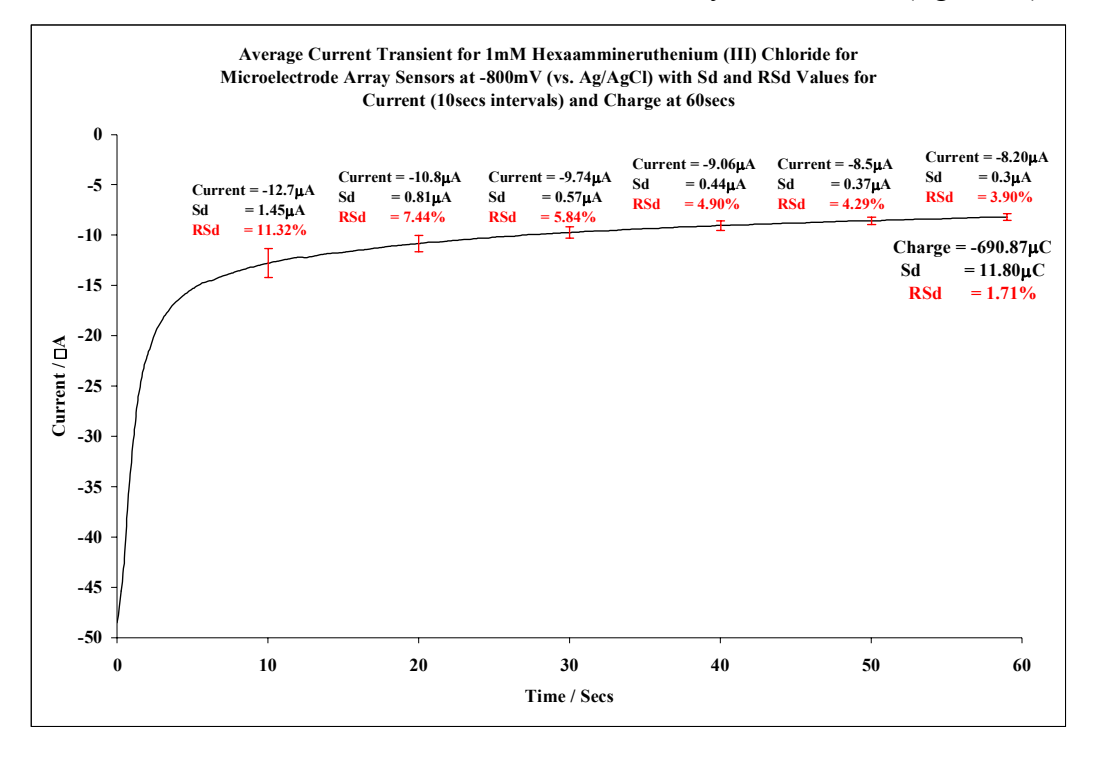


Figure 77. Current Transients and Reproducibility of Micro-Array Transducers.

Antibodies, such as anti-BSA could then be deposited within in-situ polymerised conducting polymer protrusions (e.g. of polyaniline) via cyclic voltammetry (figure 78).

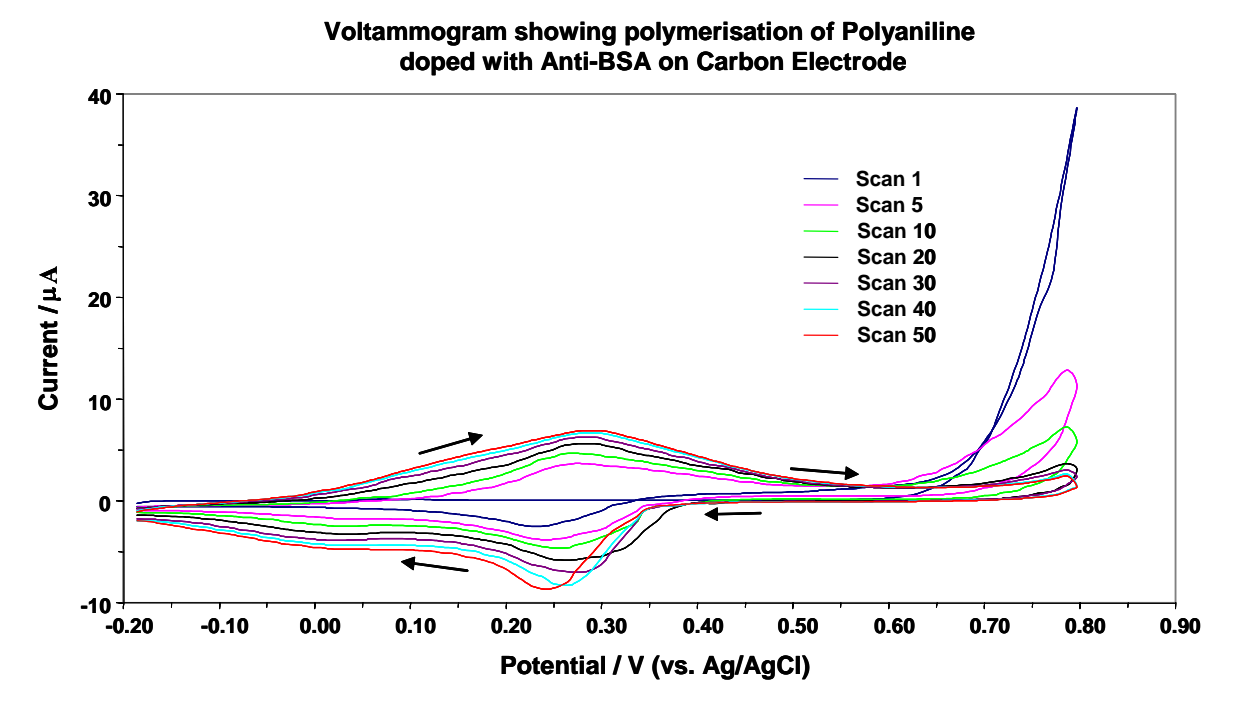


Figure 78: Immobilisation of anti-BSA within conducting polyaniline protrusions at sonochemically fabricated micro-electrode arrays.

Interrogation of Antibody / Antigen Sensors:

These sensors were interrogated via *ac* complex plane impedance using a frequency range of 0.1 through to 10 kHz. The impedance was found to be dependent upon antigen (BSA) concentration so allowing the basis of a sensor. The greatest change in impedance in response to antigen was seen at the lowest frequencies (figure 79).

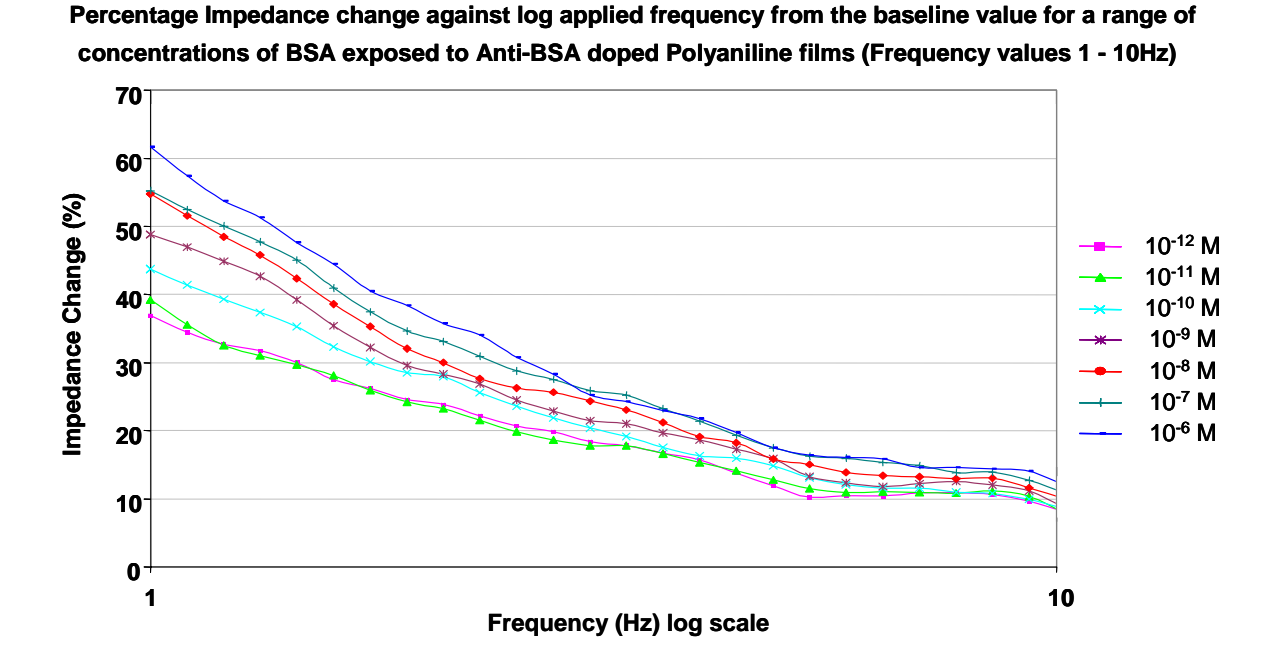


Figure 79: Impedance of antibody/polymer sensors with differing concentrations of antigen.

This approach allows for a calibration plot to be established as shown within figure 80.

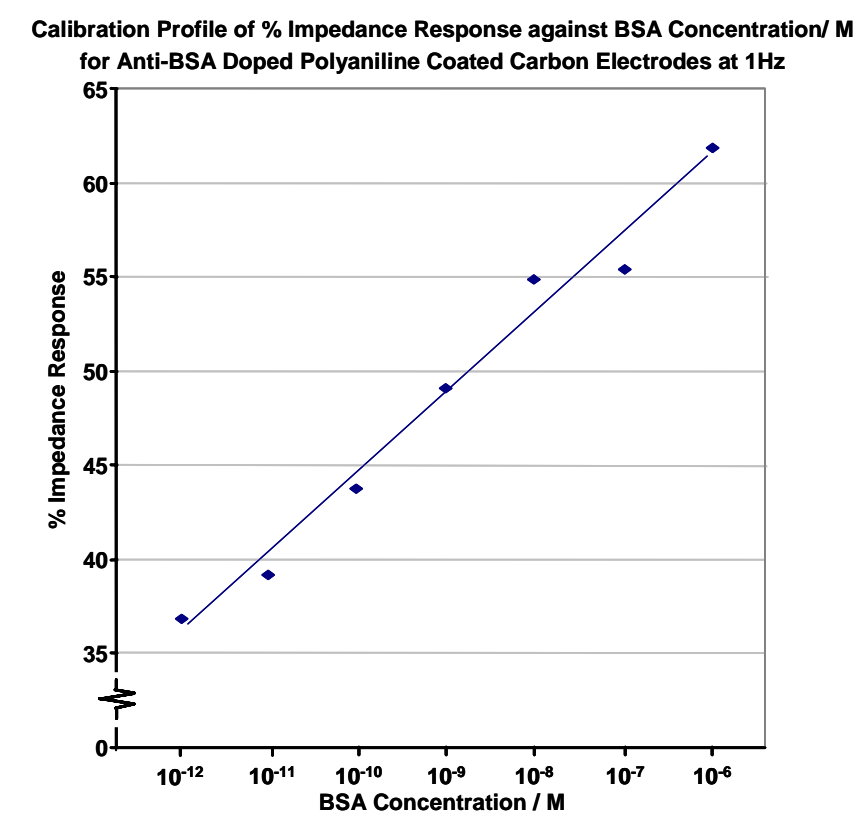


Figure 80: Calibration profile for BSA antibody based impedimetric sensor.

In a similar way a calibration plot for prostrate specific antigen (PSA) was also determined (figure 81.

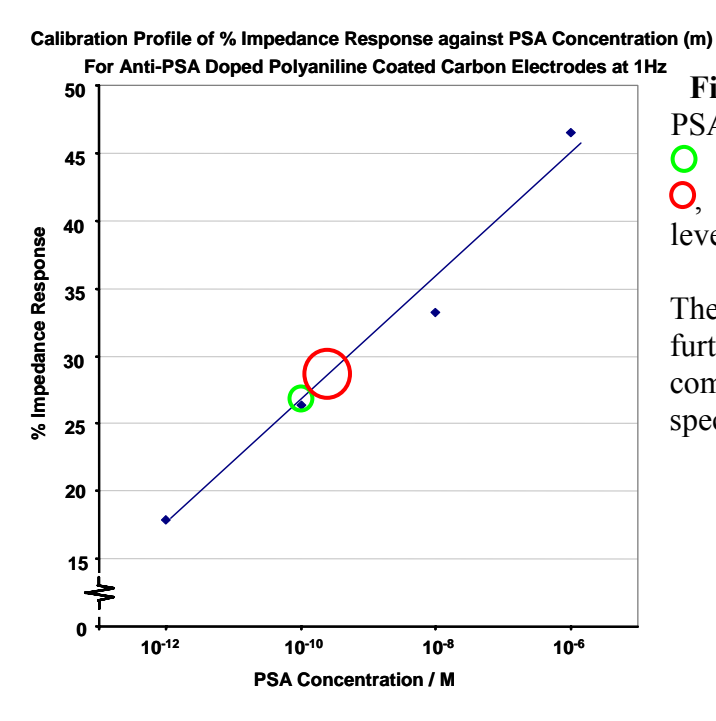


Figure 81: Calibration profile for PSA. Clinical levels of PSA used for diagnosis are: 4ng.ml⁻¹ or less normal , benign prostate hyperplasia 4ng.ml⁻¹ to 10ng.ml⁻¹, O, investigation into suspected prostate cancer is done at levels above 10ng.ml⁻¹.

The impedimetric responses of the electrodes could be further differentiated into the real (z') and imaginary components contributing to the total (Z) complex impedance spectrum, (figure 82).

Plot showing Faradaic Component against Capacitive Component (Z' vs. Z" - Nyquist Plot) for Polyaniline doped with Anti-PSA on Carbon Electrode after Exposure to

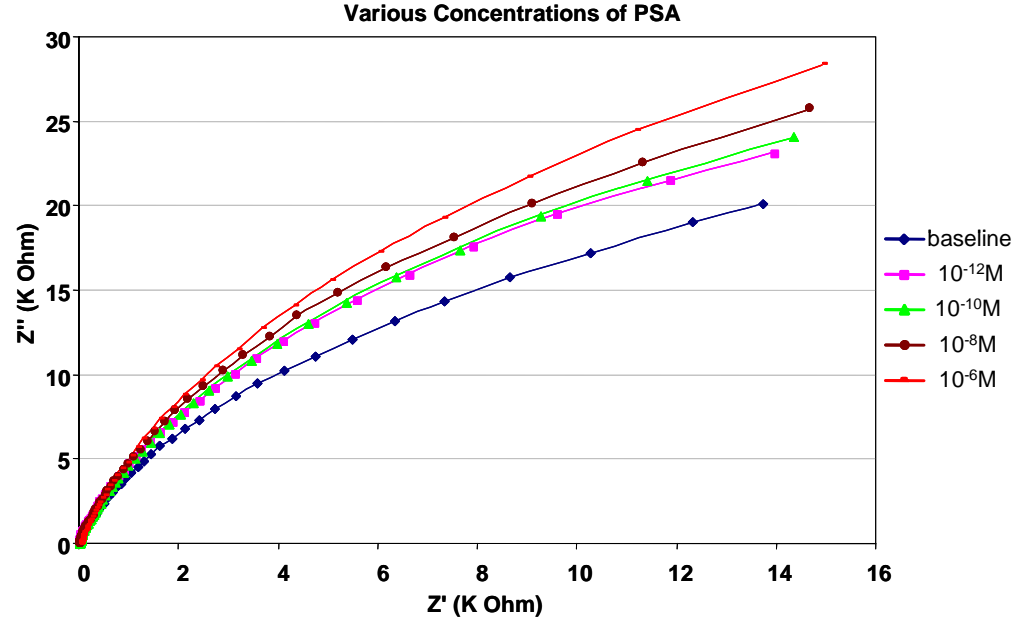


Figure 82. Complex plane impedance spectrum for anti-PSA/PSA sensor in response to differing concentrations of antigen (analyte).

Immunosensor for S-100 stroke marker protein.

Further work studied the development of a selective sensor for the S100 antibody. Unlike the direct entrapment techniques used to produce and evaluate anti-PSA based immunosensors, a new biotin-avidin immobilisation protocol was used to immobilise anti-S100 on carbon micro-array electrodes. This is described for antibody immobilisation onto polyaniline in WP5, (page 74). The sensors were then exposed to BSA solution to block unspecific binding as described in WP7. Finally these were exposed to solutions of S-100 in phosphate buffer and AC impedance studies made. Control tests were made using non-specific IgG solutions.

The results (figure 83 overleaf) showed clear changes in the total impedance of the systems when exposed to S-100 (Figure 83c). There were still some changes in the control samples but these were much smaller in magnitude (Figure 83a). Calibration plots relating change in impedance to antigen concentration can be drawn for IgG (Figure 83b) and S-100 (Figure 83d). As can be seen the specific response was much larger than the non-specific response.

Unfortunately, it didnot proved possible to completely block unspecific binding by use of BSA. However, this does not invalidate the sensor since sensors can be made in such a format that it is possible to separately detect specific and non-specific responses and subtract one from the other. Figure 84 shows the corrected calibration curve for S-100 detection.

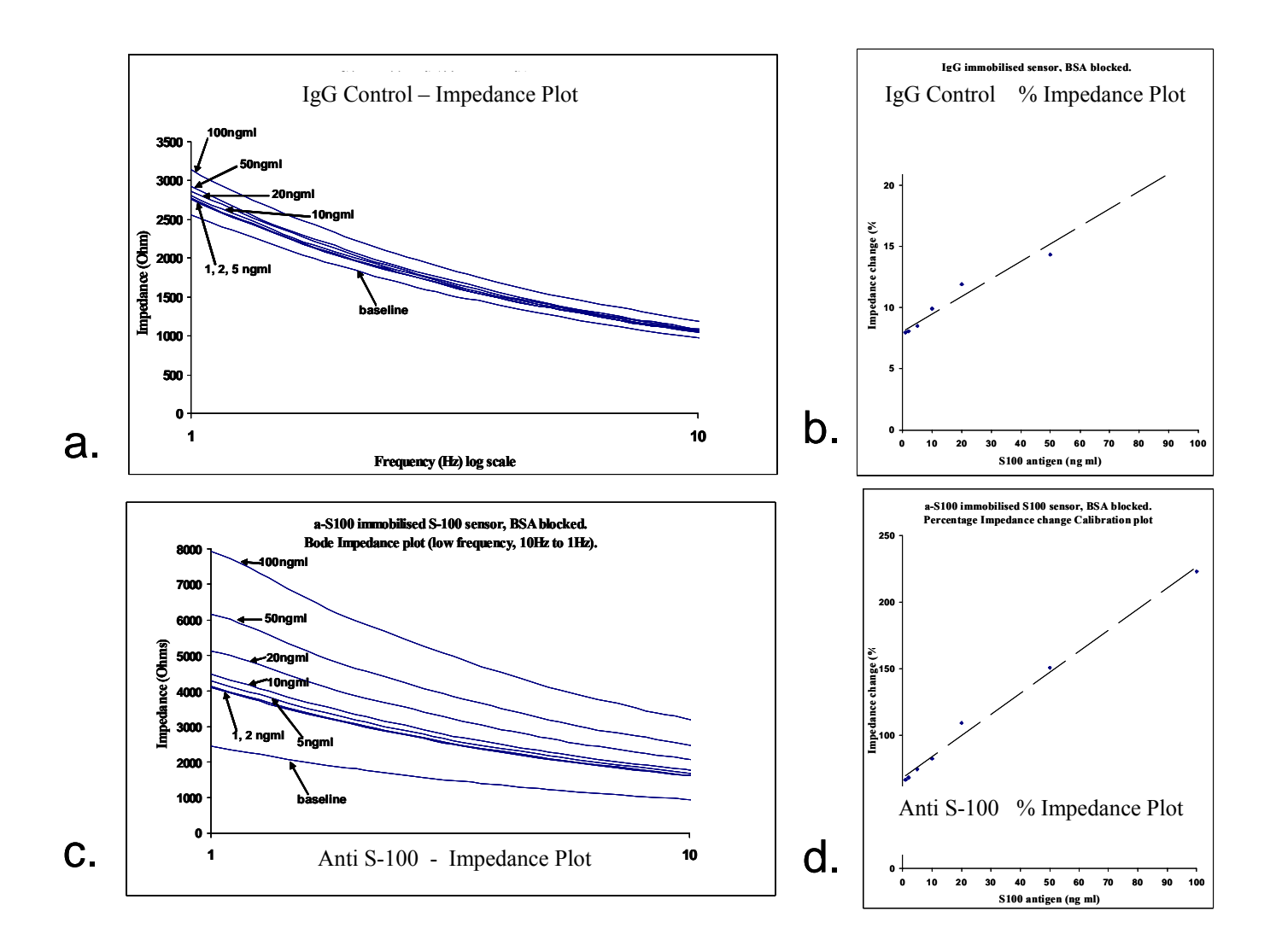


Figure 83 IgG control and Anti-S-100 Impedance Plots and Calibration Curves. Results were obtained between 1 and 10Hz. The calibrations are in nanograms per millilitre of S-100 protein added. Responses are in % total impedance changes on binding. Non-specific responses were around 10% of specific ones.

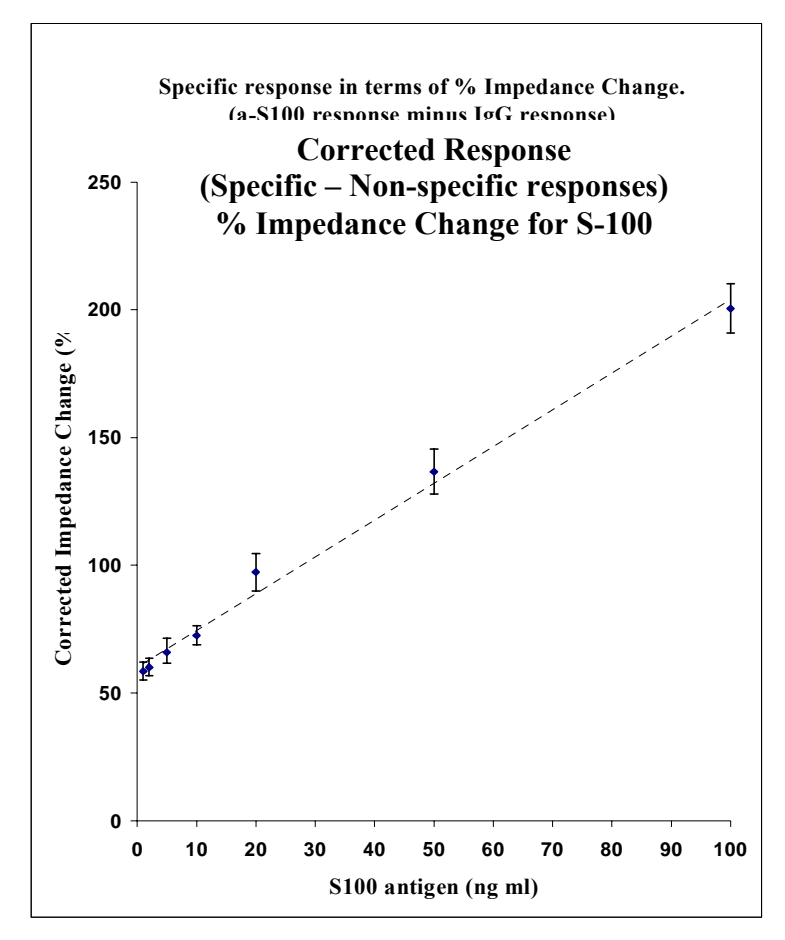


Figure 84 (left). Corrected Anti S-100 Calibration Curve. The non-specific responses were subtracted from the specific responses to give the corrected figures.

Interrogation of immunosensors constructed using test bed electronics produced in WP6.

The test bed electronics made available at mid-term in WP6 was tested on several different immunosensors types. These are mainly reported in WP5 under the immobilisation section of the report. The test bed was used in pulsed waveform mode to deliver a 10 millisecond (ms) voltage pulse followed by 40ms recording cycle. The results for a polypyrrole – covalently immobilised anti haemoglobin immunosensor (method described in WP5, page 74) are shown below (figure 85) and the differential responses are seen in figure 86.

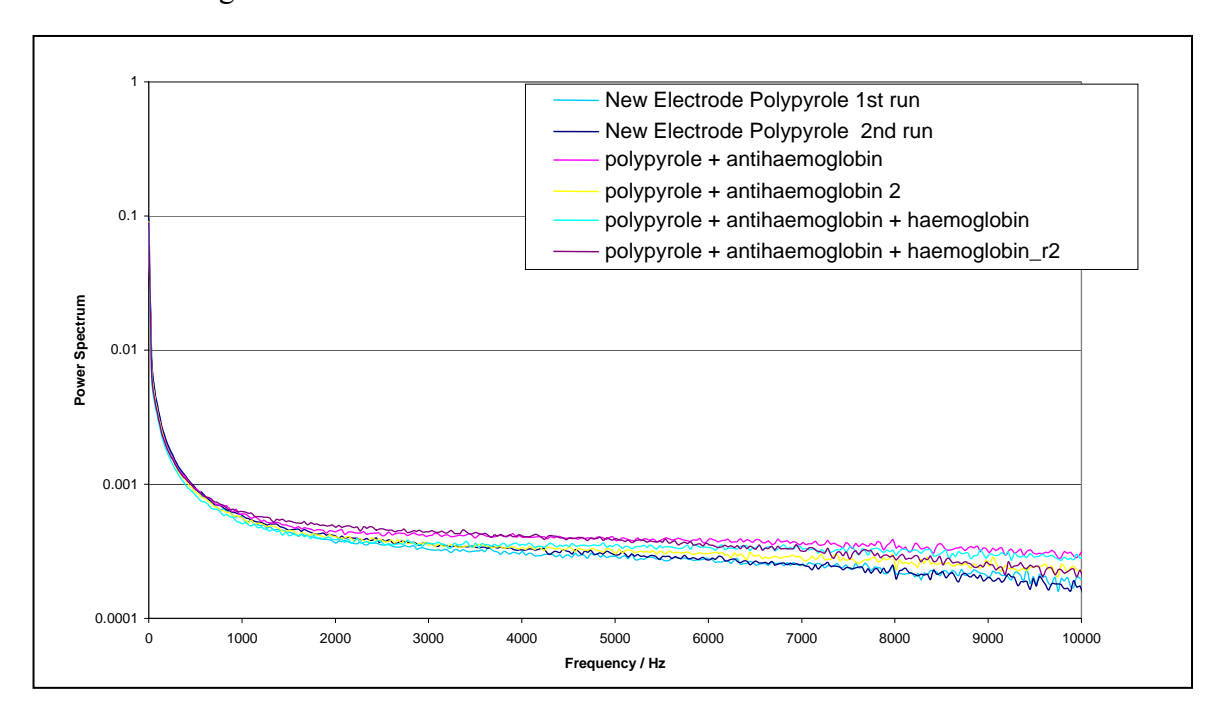


Figure 85. Responses of a polypyrrole – Anti Hb immunosensor using the Pulsed Waveform Test Bed.

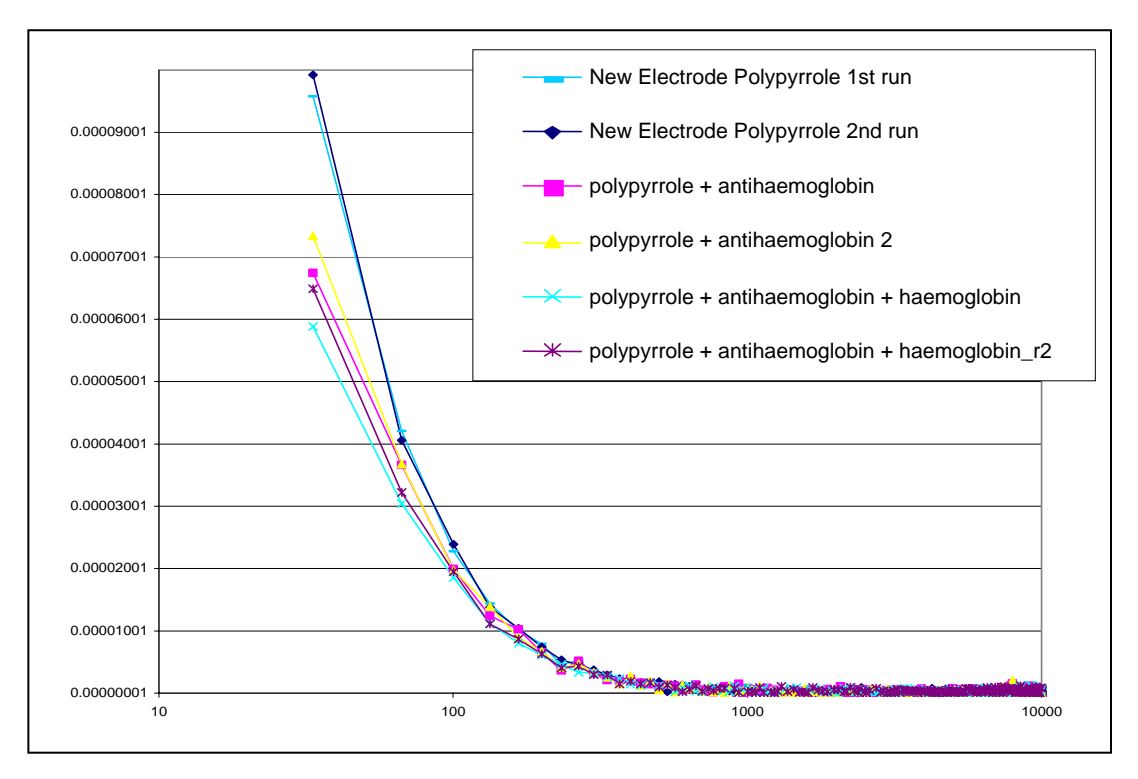


Figure 86. Differential Responses of a polypyrrole – covalently immobilised Anti Hb immunosensor using the Pulsed Waveform Test Bed. Small but significant responses are apparent on the binding of haemoglobin, proving the test bed performs on standard immunosensors.

Objectives. To investigate the immobilisation events themselves and develop understanding on the chemistry - biochemistry of the immobilisation processes to feedback into W4 for effective fabrication. To characterise the nanostructural properties that produce the micro and nano-environments required for device production. To evaluate different matrices in regards to sensitivity and stability.

Project Timeline		1 2 3 4 5 6 7 8 9 10 11 12 13 14 15 16 17 18 19 20 21 22 23 24 25 26 27 28 29 30 31 32 33 34 35 36
Workpackage 5.	Ab Immobilisation	
Task 5.1	Entrapment Strategies	
Task 5.2	Covalent Strategies	
Task 5.3	Alternative Matrices	

Partner 3.

In parallel different electrodes designs, or substrates have been tested for their suitability for impedance measurement. Functional requirements for the instrumentation to be developed for the ELISHA project have also been examined in relation with Partner 7. Thus feasibility of impedance measurements on silver substrates with SAMs layers including immunospecies have been proved. It appears also, that obtaining reproducible gold micro-electrodes is not so easy, misalignment of layers or diffusion phenomena from the anchoring layer can induce interferences in electrochemical characteristics of electrodes.

Entrapment strategies and impedance measurements

1. The first strategy explored was based on co-electro polymerisation of a mixture of pyrroles on gold substrates. Through the strong interaction involved in the biotin/avidin system a "lego" like strategy can be used to build layers entrapping immunospecies. One pyrrole is biotinylated, the second one, is amphiphilic. Such reagents were provided by Partner 8. The building-up of successive layers involved is represented below (figure 87).

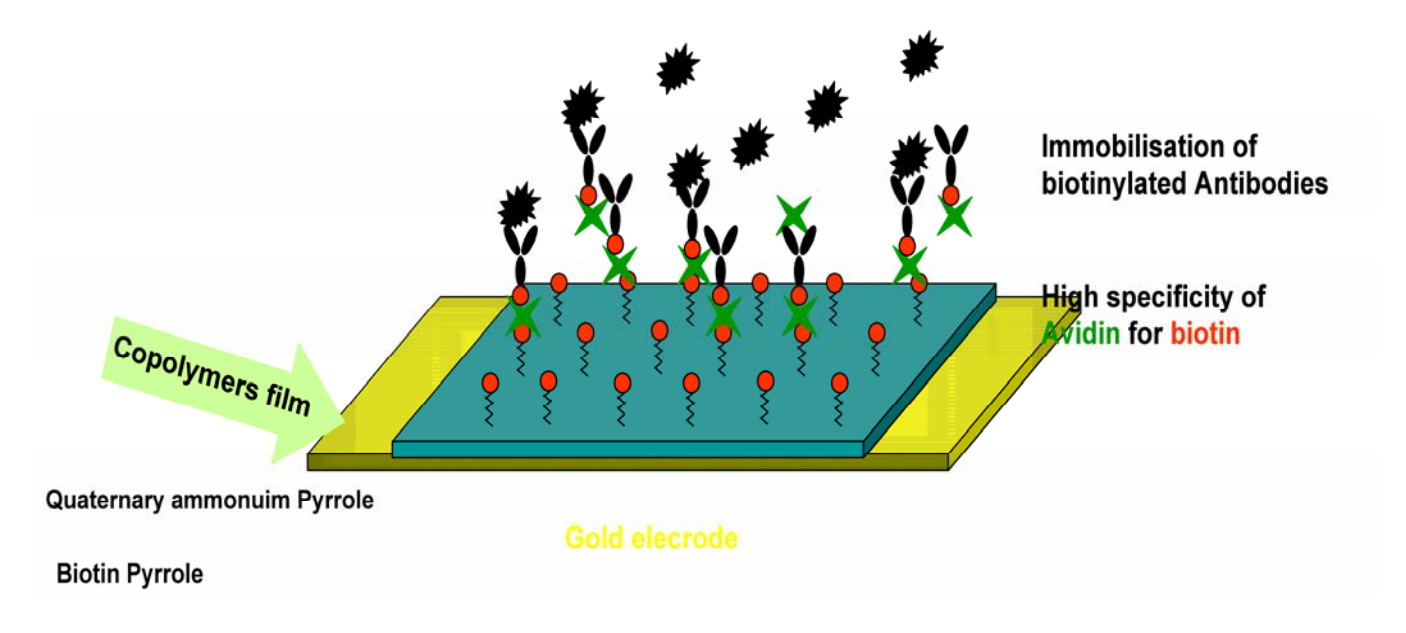


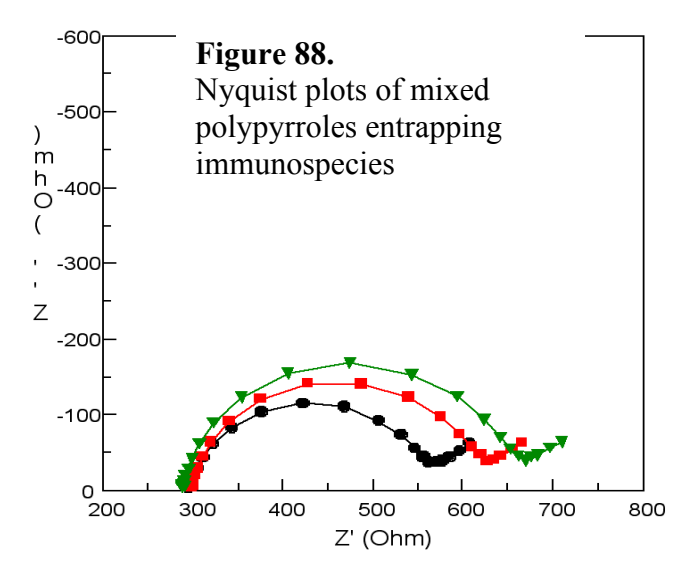
Figure 87. Co-polymerised pyrrole layers using biotin – avidin immobilisation protocols.

Impedance spectra, acquired at -1,2V vs (SCE) in PBS electrolyte, pH 7,4 in a.Nyquist plot representation obtained for the successive building-up steps are shownd in figure 88.

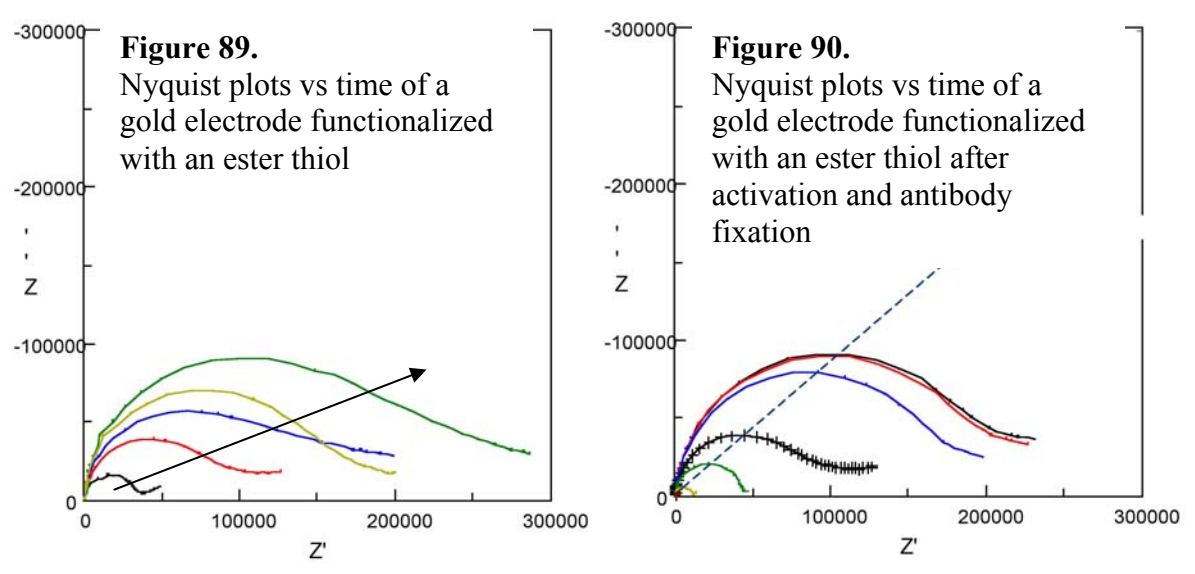
The three steps of layers formation:

- pyrroles electropolymerisation ($\bullet \square$)
- fixation of avidin (■□)
- immobilisation of biotinylatedantibodies($\triangle \square$).

are well characterized. Such a strategy seemed promising as the different building-up steps are clearly evident.



2. The second approach used was based onto anchoring antibodies onto an activated thiol ester fixed onto a gold electrode by incubation in a 1mM solution in ethanol. As shown on figure 89 such a layer was not stable. A similar situation was observed (figure 90) with thiol activated electrodes after incubation (4 hours at 4°C°) with an antibody (anti-digoxin).



During the subsequent months several strategies to improve the SAM anchoring layer, i.e. an activated ester thiol fixed on a gold electrode were attempted. Improving the layer's behavior, by the use of antioxidant agents, such as ascorbic acid, were more successful in giving a good stabilization effect. Physicochemical characterization of these molecularly engineered layers including immunospecies were performed using XPS, IR and cyclic voltammetry experiments. Responses of such layers after addition of antigen were also tested using impedance measurements.

3. The first step of an innovative way for the entrapment of immunospecies based on oligonucleotide functionalized polypyrrole was also validated. This approach used DNA probes bearing amine groups immobilized on a supporting polypyrrole matrix by covalent grafting. Such surfaces are able, by hydridation, to recognize DNA targets and thus could be used to attach antibodies modified with such DNA targets. The scheme in figure 91 shows the reactions involved on the electrode surface after formation of the polypyrrole layer. This precursor copolymer poly [3-acetic acid pyrrole, 3-N-hydroxyphthalimide pyrrole)] was electropolymerized in acetonitrile containing the monomers 3-acetic

acid pyrrole (0.06 M) and 3-N-hydroxyphthalimide pyrrole (0.04 M) at a fixed potential of 1V versus Ag/AgCl during 15s

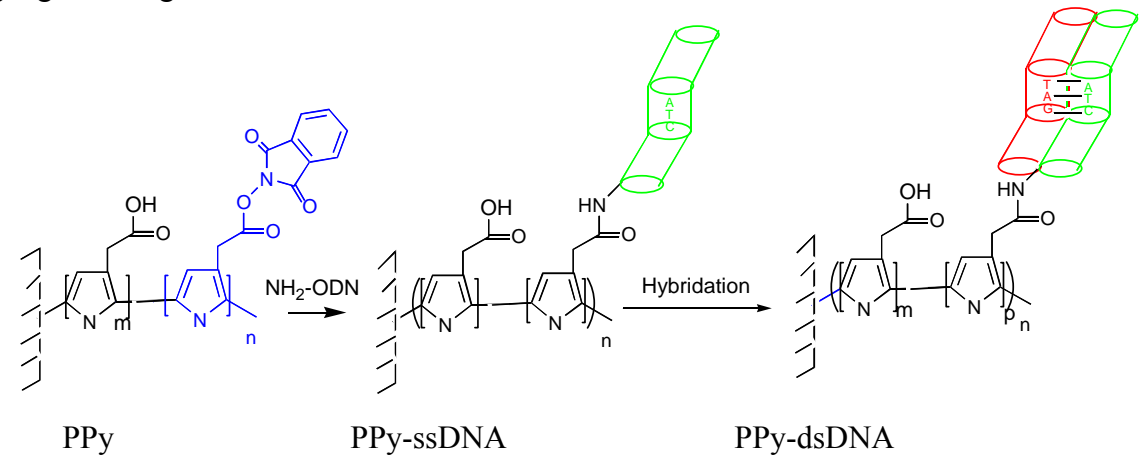
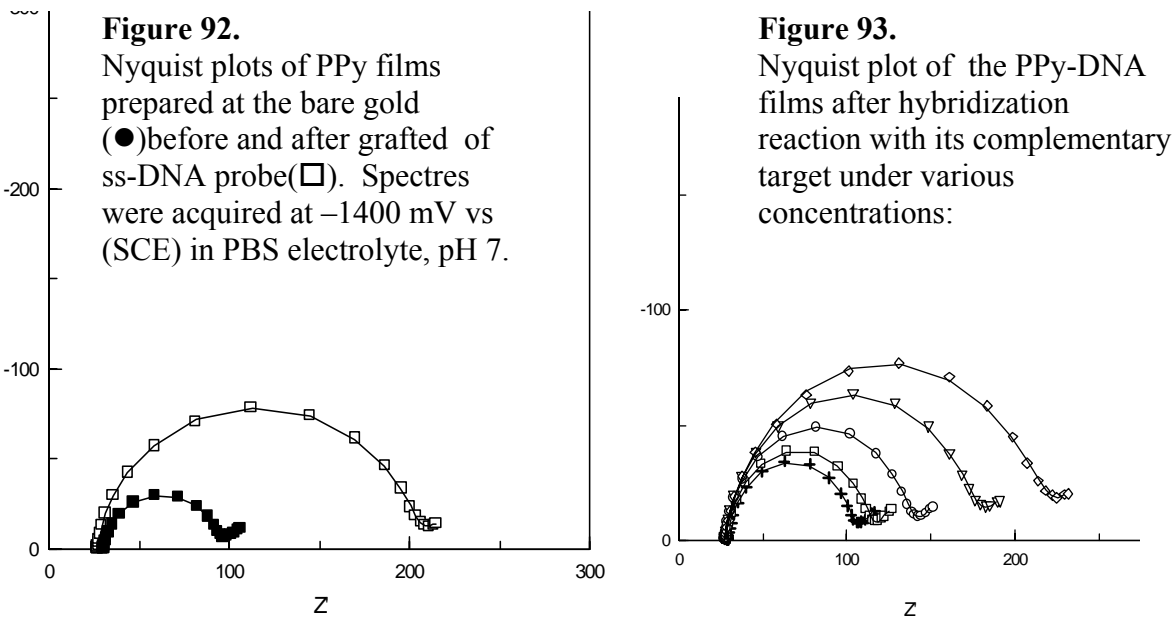


Figure 91. Formation of polypyrrole-ssDNA and subsequent hybridisation of complimentary DNA.

Such layers were characterized by non faradaic impedance measurements. Figure 92 presents the Nyquist diagram of the copolypyrrole films on gold electrode obtained after polymerisation reaction and grafting of the ssDNA probe measured in the same experimental conditions. These results show a large modification of the Nyquist diagram after the grafting of ss-DNA on the copolymer film. The resistance of the charge transfer (electronic and ionic) decreased from 175.9 Ω cm² for PPy film to 63.9 Ω cm² for PPy-ssDNA. The modified PPy-ssDNA electrode was then incubated for 1h 30mn in PBS solution containing complementary ss-DNA target, and the impedance measurements are shown in figure 93. With complementary ss-DNA, hybridisation took place with the probe immobilized on the polypyrrole, producing an obvious enlargement of the Nyquist diagram However, with non complementary ss-DNA target, the impedance measurements showed a quite small variation in the Nyquist plot proving the specificity of this new detection method.



A quantitative study of the sensitivity was done through analysis of the charge transfer resistance (R_{2}) with continuous addition of the ss-DNA complementary target from 0 to 5.5 nmol/ml. The sensitivity obtained corresponding to the lowest concentration actually detected showed a quantifiable resistance measured for 100 pmol/ml.

Calibration curves from amperommetric and impedance measurements

A quantitative study of the sensitivity was made by analyzing both the variation of current density at a constant potential of -0.2 V/SCE and the charge transfer resistance R2, with continuous addition of the ss-DNA complementary target from 0 to 5.5 nmol/ml. These results are presented in Figure 94 and Figure 95, both these curves showed large variations a function of the concentrations of DNA target.

Figure 94 shows that upon addition of the complementary DNA, the electrode current decreased linearly as a function of the DNA concentration and this variation show a current variation that was asymptotic when 5 nmoles were added. The sensitivity of the detection of complementary target was calculated from the slope at the origin of this curve and the value obtained is $80~\mu\text{A.cm}^{-2}.\mu\text{M}^{-1}$. A quantitative determination of the detection limit of the complementary ODN in solution can be calculated taking into account of a signal to noise ratio of 3 and using a conventional method. The detection limit of this ODN-functionalized polypyrrole electrode found to be of 10 pmoles of target ODN.

Figure 95 shows that the R2 increase linearly as a function of the concentration of the DNA target. The sensitivity of complementary ODN was calculated from the slope at the origin of this curve, and the value obtained was $21.6~\Omega~cm^{-2}~\mu M^{-1}$. The detection limit was determined as 1 pmol of DNA target. These results show first that the obtainable detection limit by impedance measurement was one order of magnitude lower than that obtained using amperometric measurement. Secondly, the charge in transfer resistance showed a continuous variation as function of the concentration of the DNA target, contrary to the amperometric variation which reachedan asymptotic value. Comparing this detection limit to the values obtained by other systems: 1 nmol for the electrochemical response of polythiophene , 1 nmol using the system with fluorescence probes, 10 nmol using nanoparticle probes and 20 pmol given for a system using the catalytic activity of enzyme, the value of 1 pmoles obtained in this system using an DNA-functionalized polypyrrole as interface and electrochemical impedance spectroscopy as direct electrical method of detection, appeared to be a very promising tool for use in DNA and protein chips. The large surface area obtained by using porous polypyrrole lead to an increase in the density of immobilized DNA probes, which helped to monitor more easily the DNA hybridization reaction.

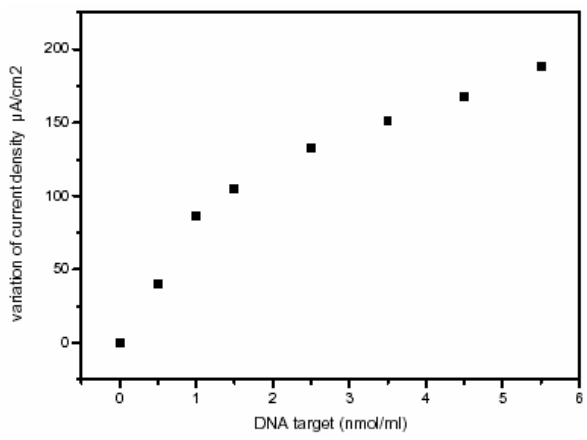


Figure 94: Variation of electrode current density at a constant potential of - 0.2 V/SCE, as a function of the complementary ss-DNA target concentration

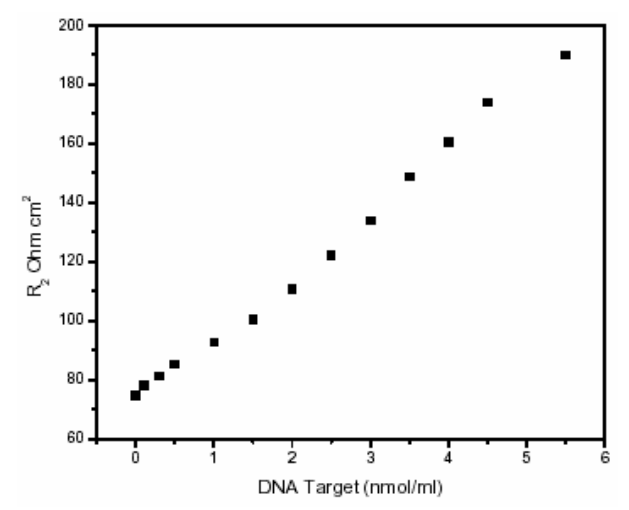


Figure 95: Calibration plot (variations of the resistance R2 vs the complementary target concentrations.)

The importance of this work to detect DNA may have been slightly outside the main scope of the project, but it is important to note that the work here provided insights into perhaps the most difficult part of the project, the understanding and proof of the signal generation in electroconductive polymeric – biological matrices at the nanoscale. Some explanations for this are given in workpackage 7, based on the cyclic voltammetry of the polypyrrole- ssDNA nanostructured films. In addition oligonucleotide tagged materials should be able to be immobilised by complimentary hybridisation onto the DNA surfaces.

Alternative immobilisation strategies were investigated by partners 1 and 2, where direct entrapment was used into growing polypyrrole or polyaniline layers was the original method of choice. These gave the results described in W4 mainly from partner 2 and in W7 from partner 1. The non-covalent layer by layer technique using polyanion / polycationic alternate matrices gave some significant improvements in sensor fabrication described below.

Alternative layers of polystyrene sulphonate (PSS) and poly(diallyldimethylammonium)chloride (PDDM) were deposited using the scheme below (figure 96) and anti-digoxin as a model antibody was then deposited into the matrix by incubation in buffered solution (30 minutes incubation time of 1mM antibody in pH 8 sodium phosphate buffer). The results obtained from radiolabelling the anti-digoxin model clearly showed improved immobilisation when the polycation was the uppermost layer in the nanostructure.

ANTIBODY ENTRAPMENT USING POLYANION/POLYCATION **OVERLAYERS PSS PDDM** + Protein Polypyrrole Gold 250 ¹²⁵I-anti-digoxin binding, 30 min incubation 1 μM of anti-digoxin, NaH₂PO₄, 50 mM, pH 8 200 polyanion 150 polycation no PE 100 50 0 0 2 3 1

Anti-digoxin (protein), ng

Figure 96. Polyanion and polycation overlayer schematic and [¹²⁵I]-anti-digoxin binding after 30 min incubation in 1 mM of anti-digoxin, NaH₂PO₄, 50 mM, pH 8. Polyelectrolyte layers made by incubation of the electrode in solutions of polyanion (PSS) and polycation (PDDM) respectively. First incubation was made with polyanion. Blue bar indicates last treatment was with the polyanion. Red bar means last

Number of polyelectrolyte layers

treatment was with the polycation. It is clear that the best results came from the polycation indicating that the antibody is negatively charged at the pH of the incubation.

The effective immobilisation of the model anti-digoxin antibody to a polypyrrole gold electrode with polyectrolyte multilayers and binding of antigen to antibody-polypyrrole gold electrode with polyectrolyte multilayer always resulted in increase of impedance parameters in the low frequency region. The quantity of this increase and the reproducibility required further work to improve fabrication and was be investigated further as the project progressed. The traces below (figures 97, 98) show repetitions of single electrode at position 'No AntiDigoxin', (control) '+AntiDigoxin' (control) and '+AntiDigoxin' (active sensors). Binding of digoxin to polypyrrole gold electrode with polyectrolyte multilayer was negative (negative control). The electrode with co-polymerized antibody into polypyrrole layer showed low effect and was unstable. (Table 4)

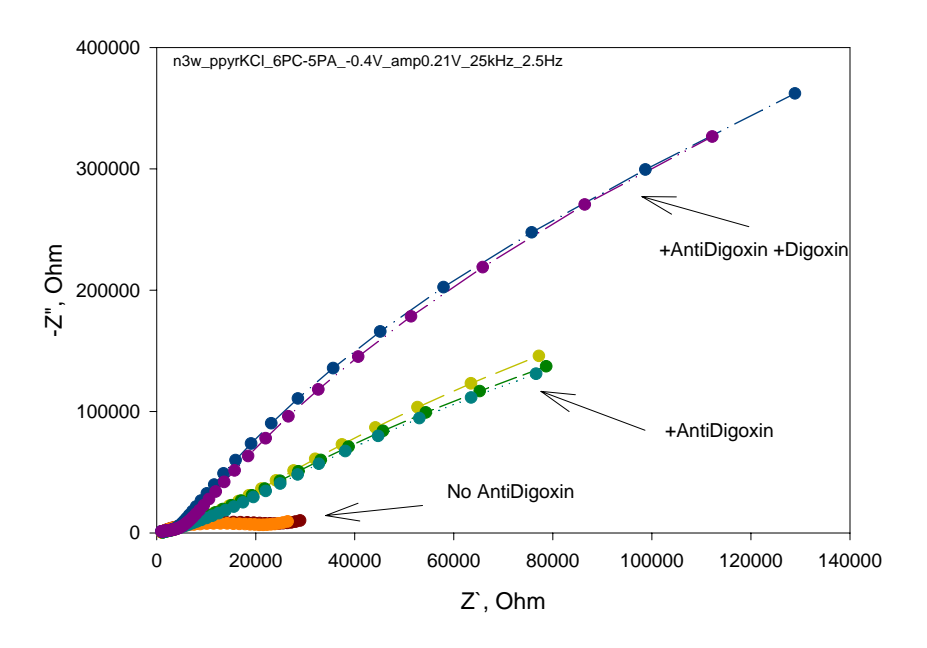


Figure 97. Detection of affinity of digoxin analyte – polypyrrole/Cl base electrode Impedance measurements were performed at -0.4 V vs Ag/AgCl and 0.21 V oscillation amplitude in 0.1 M NaH₂PO₄ solution (pH 8.0). Frequency range was 25 kHz – 2.5 Hz. Polypyrrole was prepared using 0.1 M pyrrole and 0.1 M KCl solution at 800 mV vs Ag/AgCl by passing 1.0 mC charge.

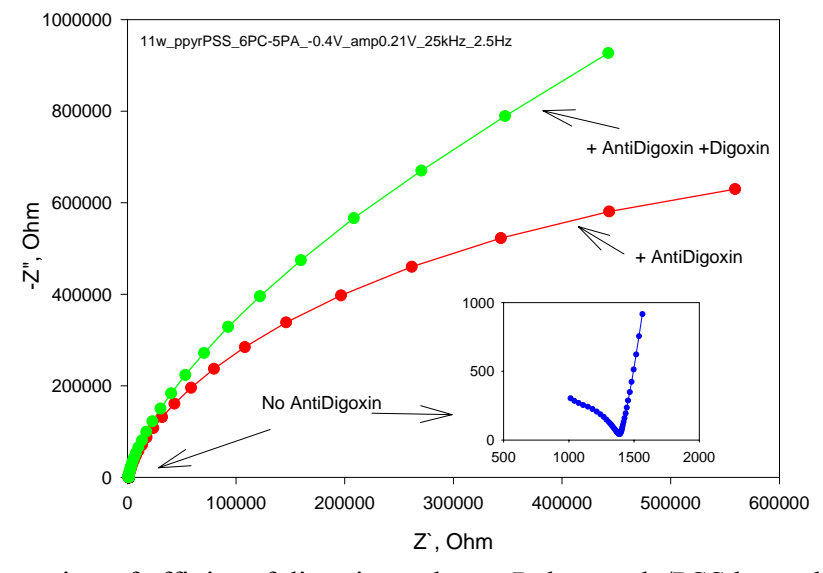


Figure 98. Detection of affinity of digoxin analyte – Polypyrrole/PSS base electrode

Impedance measurements were performed at -0.4 V vs Ag/AgCl and 0.21 V oscillation amplitude in 0.1 M NaH₂PO₄ solution (pH 8.0). Frequency range was 25 kHz - 2.5 Hz. Polypyrrole was prepared using 0.1 M pyrrole and 0.1 M PSS solution at 700 mV vs Ag/AgCl by passing 1.0 mC charge.

The common features of figures 97 and 98 are that the polycation was PDDM and the polyanion was PSS. Layers were prepared by sequential incubation of the electrode with PSS or PDM solution at 0.1 mM (two hours per stage). Anti-digoxin was immobilised by incubation in 10 mg.ml⁻¹ antibody solution overnight. Electrodes were incubated in digoxin solution (1 µM) for 3 hours before measurement.

	A .: 1: :	4 1.	A .: 1: ·	A .: 1: ·	A 1 · ·	A 1 · ·
	Anti-digoxin	Anti-digoxin	Anti-digoxin	Anti-digoxin	Anti-digoxin co-	Antı-dıgoxın co-
	immobilized	immobilized	immobilized	immobilized	polymerised	polymerised
	non-covalently	non-covalently	non-covalently	non-covalently	with	with
Type of	onto	onto	onto	onto	Polypyrrole/KCl	Polypyrrole/PSS
Sensor	Polypyrrole/KCl	Polypyrrole/PSS	Polypyrrole/KCl	Polypyrrole/PSS		
			Polyelectrolyte 5	Polyelectrolyte 5		
			layers	layers		
Impedance	negative	negative	positive	positive	negative	negative
5 14		_	*	*		_

Table 4. Impedimetric detection of digoxin by anti-digoxin polypyrrole gold electrodes.

Chemical modification of the antibody for more efficient entrapment

When polypyrrole or other conducting polymers are formed they incorporate counterions into their structure to balance the charge. Usually these are anions, e.g. chloride or polystyrene sulphonate in our case.

Where the antibody becomes the counterion it is thought that increasing the electro-negativity or anion-like nature of the antibody by chemical derivatisation an effect in the amount and possibly the orientation might occur on polymer deposition. Partner 1 investigated the modification of bovine IgG using pyromelletic anhydride to introduce extra carboxyl functionality into the protein structure. This increased the negative charge and should have influenced the production of immunosensors by polymer entrapment.

The isoelectric point (pI) of a molecule such as an amino acid, peptide or protein is the pH at which it has a net charge of zero. IgG has an approximate pI value of 7.3 +/-1.2. By adding carboxylic groups to IgG molecules, it is possible to increase their negative charge, thus making them adsorb to positively charged surfaces. Non-immune bovine IgG (1 mg/ml⁻²) was dissolved in phosphate buffer solution (100 mM, pH 7). Benzol-1,2,4,5-bBenzenetetracarboxylic dianhydride (pyromellitic dianhydride) was then added to the solution (final conc = 1 mM) and left to react on ice. Samples were then removed at time intervals and the reaction stopped by the addition of glycine. The isoelectric point was then determined by isoelectric focusing. In isoelectric focusing (IEF), the molecules in question are placed on a gel with a stable pH gradient along its length. Since the pH of the surrounding medium determines the charge on the molecules, that charge will change as the molecules migrate through the pH gradient. When each molecule reaches a pH equal to its pI, it will be electrically neutral and will no longer migrate in the electric field. Thus, every molecule subjected to IEF will move to a pH equal to its pI, so by looking at the pH at which a molecule stops, the pI can be measured.

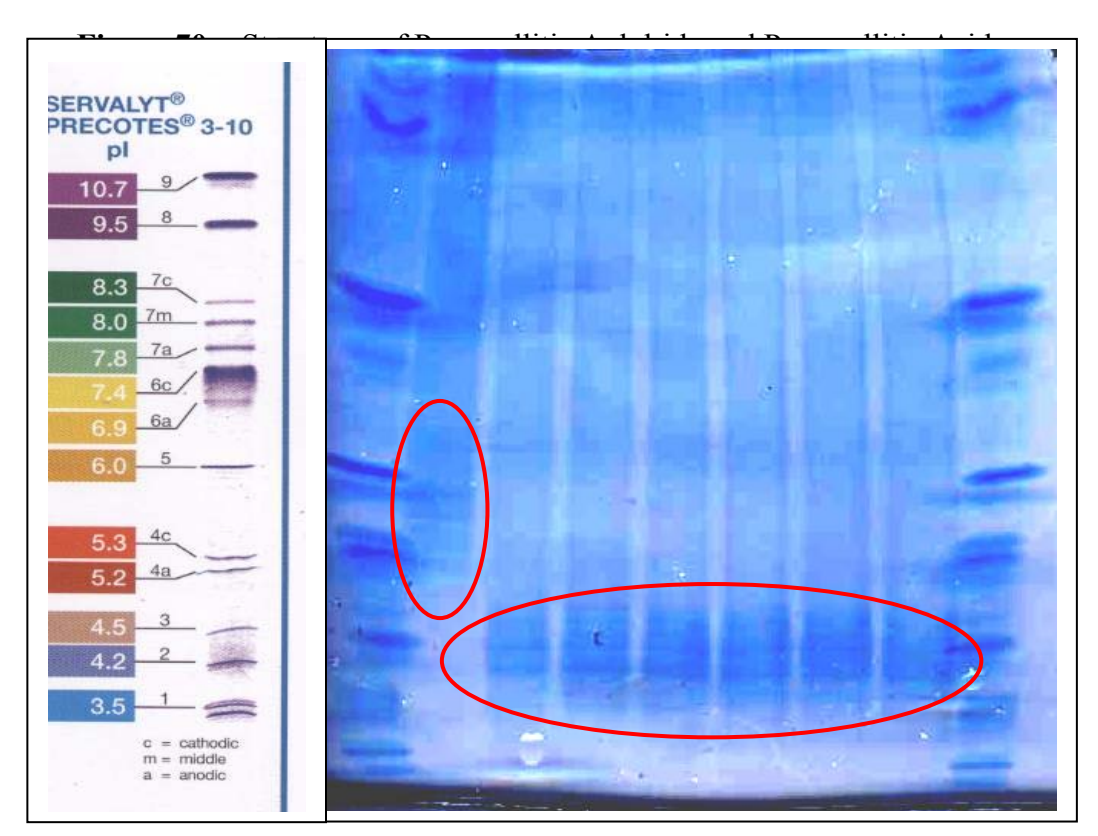


Figure 99: Isoelectric focusing resolving gel containing protein markers (lanes 1 and 10) and IgG treated using pyromylletic anhydride following 0 sec (untreated control, lane 2), 45 sec (lane 3), 1 min (lane 4), 2 min (lane 5), 3 min (lane 6), 5 min (lane 7) and 10 min (lane 8) A key corresponding to the protein markers has been added for reference.

Results appeared to indicate that a shift in IgG pI had occurred within 45 seconds of the addition of pyromellitic acid, as the untreated control (lane 2) appeared to have a higher pI (\sim pH 6 \pm 0.5) than that observed in lanes 3-8 (pH 4.5 \pm 0.3), which had been treated. Further experiments involving less quantities of pyromellitic acid were performed in order to try and control the extent of carboxylation and consequent pI. Furthermore, the binding characteristics of modified antibodies was then be assessed using [125 I] in order to determine whether the modification had inactivated the IgG.

Attempts were then made to incorporate the treated IgG into immunosensors to ascertain if increasing the electronegativity had any effect on the antibody loading.

Inclusion of Ferrocenyl Derivatives for More Efficient Amperometric Signal Generation

Incorporating ferrocenyl containing pyrroles as a co-polymerised matrix for antibody immobilisation and signal enhancement were been carried out at the initial stages by partner 3 (figures 100,101)

The indications were that using just ferrocenyl pyrrole co-polymerised with a phthalimide pyrrole gave a matrix which was too sterically hindered for efficient antibody immobilisation, adding a carboxyl pyrrole as a spacer produced a much more open matrix (figure 102) and enhancements in the amperometric signal on CV were apparent (figure 103).

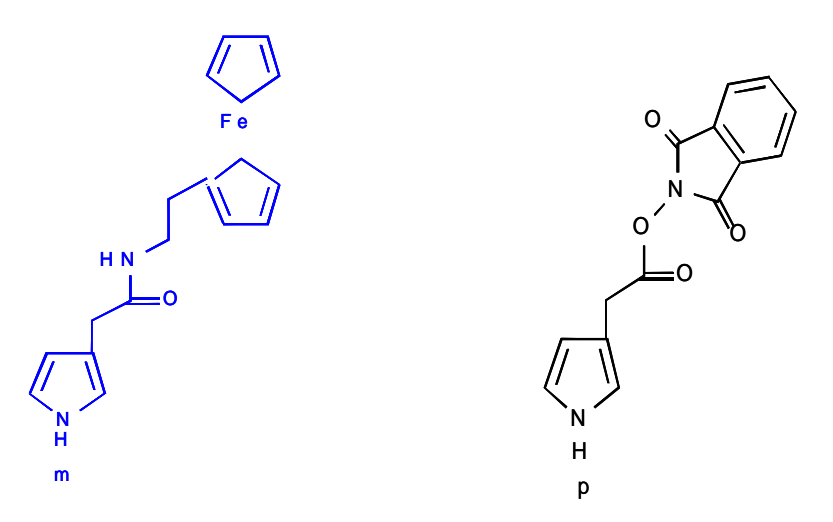


Figure 100. Ferrocenyl Pyrrole and Phthalimide Pyrrole

Figure 101. Initial Immobilisation Matrix Incorporating Ferrocene Groups.

Figure 102. Modified Immobilisation Matrix Incorporating Ferrocene Groups and Spacer.

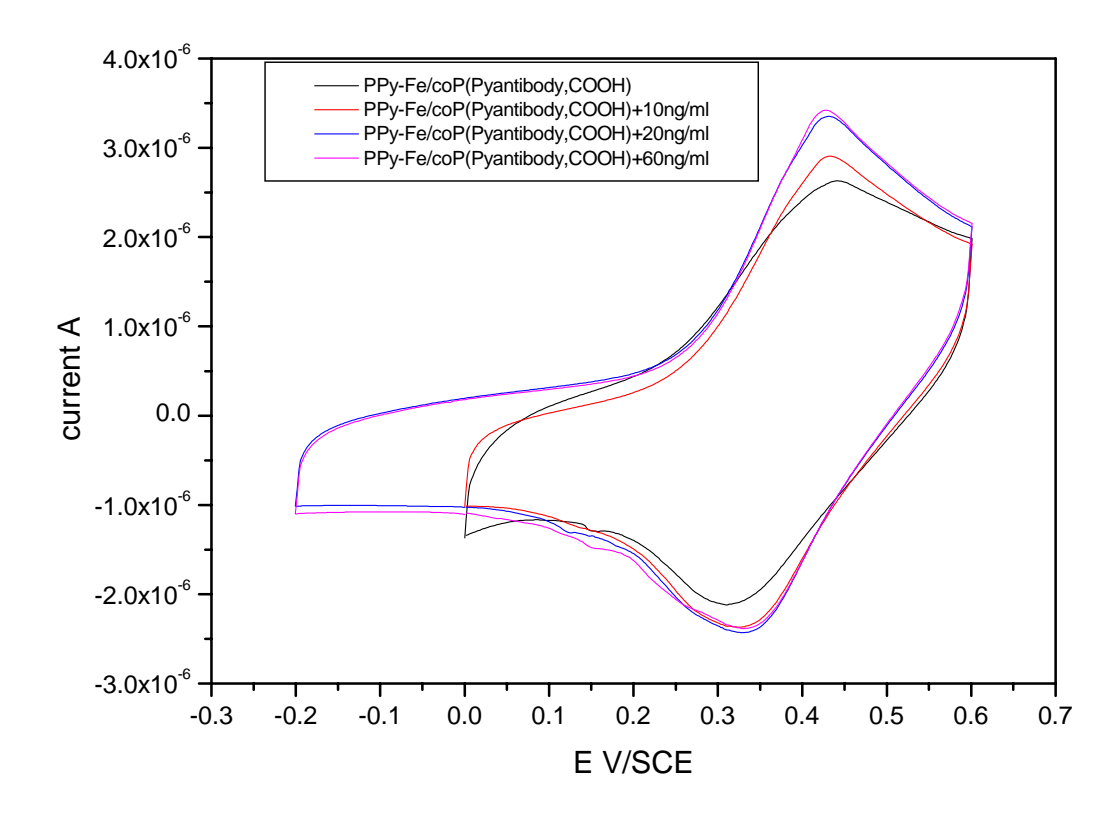


Figure 103. CV of Ferrocenyl Film with anti-IgG plus 10, 20 and 60ng.ml⁻¹ IgG antigen.

Two further immobilisation protocols were devised based on selective chemical derivitisation of conducting polymer surfaces. Such methods are more controllable than simple antibody entrapment.

Partner 1 produced films of polypyrrole using a polyacrylic acid counterion to give numerous carboxylic acid groups available for derivatisation. The reaction scheme is shown in figure 104

Figure 104. Covalent attachment of antibody (R-NH₂) to polyacrylic acid counterion in an electroactive polypyrrole film.

In this case the response of the sensors produced was obtained with the antibody covalently linked to the counterion used which was in intimate contact with the electroactive surface. This had not been attempted before and it was not known if the antibody – antigen binding reaction could be measured. Using the new test-bed electronics and anti-haemoglobin as the selective antibody, the surface was interrogated in the absence of analyte, in the presence of a large concentration of BSA ("control analyte") and then with progressively larger amounts of haemoglobin from 5 nM to 500 nM. The results are shown in Figure 105 overleaf.

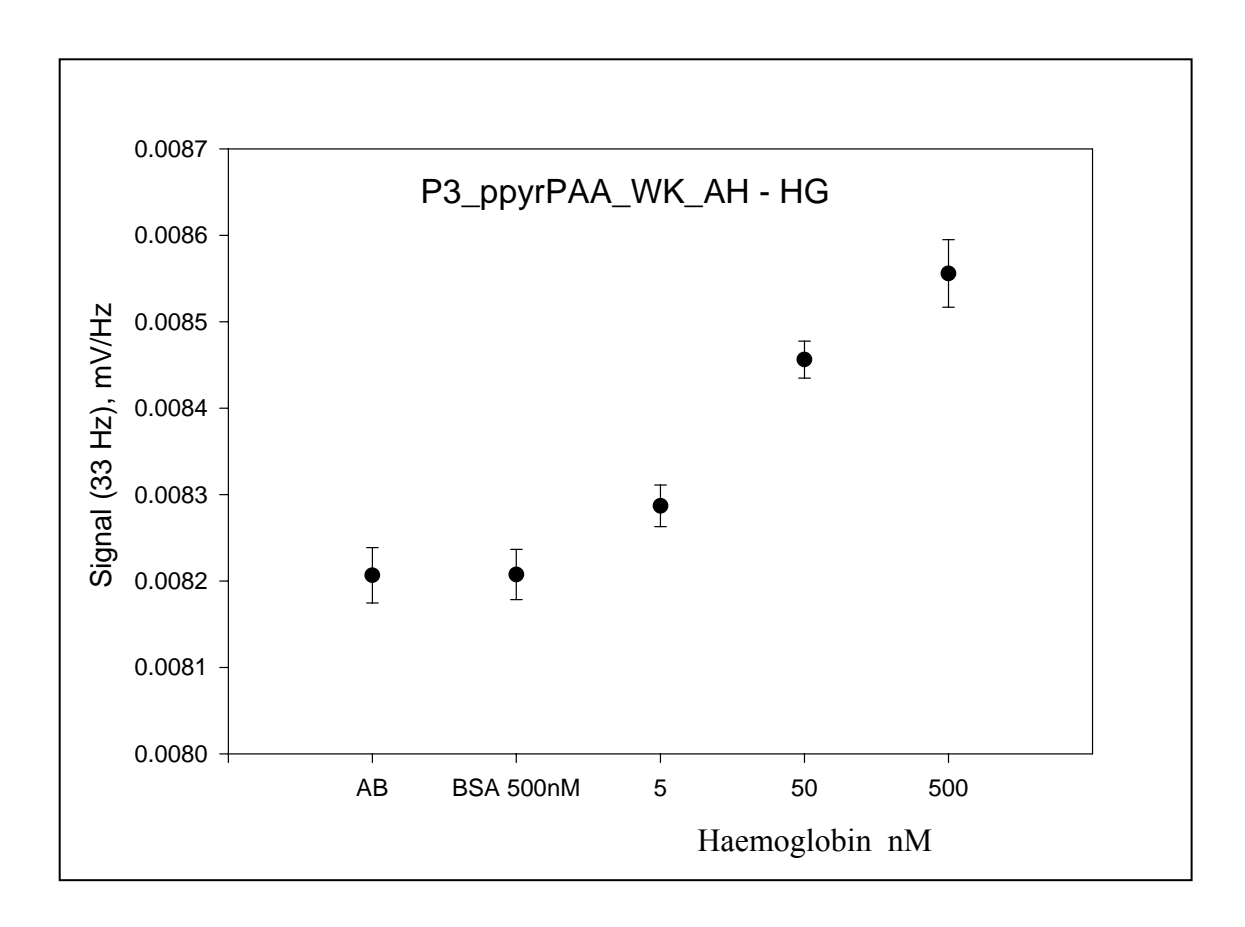


Figure 105. Selective response of an anti-haemoglobin – polypyrrole - polyacrylic acid immunosensor to BSA and haemoglobin. It can clearly be seen that the immobilisation protocol gave responsive immunosensors with good selectivity.

To test the method for PSA as the selective analyte the anti-haemoglobin was replaced with anti-PSA. The results are below in Figure 106.

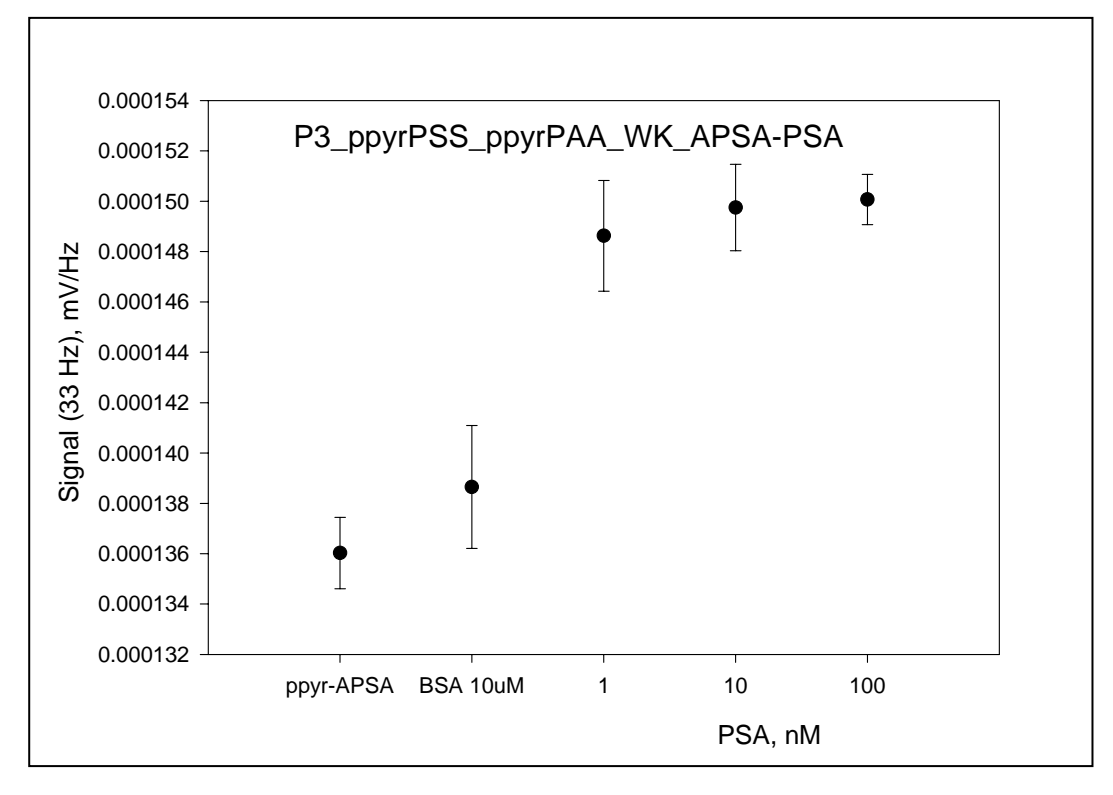


Figure 106. Selective response of an anti-psa – polypyrrole - polyacrylic acid immunosensor to BSA and PSA. In this case the immobilisation protocol gave responsive immunosensors with some non-specific response but the response to PSA was much more sensitive.

Partner 2, working with Partner 1 prepared a combination immobilisation method based on biotin immobilisation of an antibody onto a biotinylated polyaniline matrix. An amino biotinylation agent (BAC-SulfoNHS) was employed to first derivatise the polyaniline matrix and separately derivatise the antibody (anti-fluoroquinoline), (figure 107). The immunosensor was constructed by adding neutravidin to the biotinylated polyaniline than adding the biotinylated anti-PSA, when the nanostructure formed spontaneously by self-assembly (figure 108).

Figure 107. BAC-SulfoNHS Reaction with Antibody to give a Biotinylated Antibody.

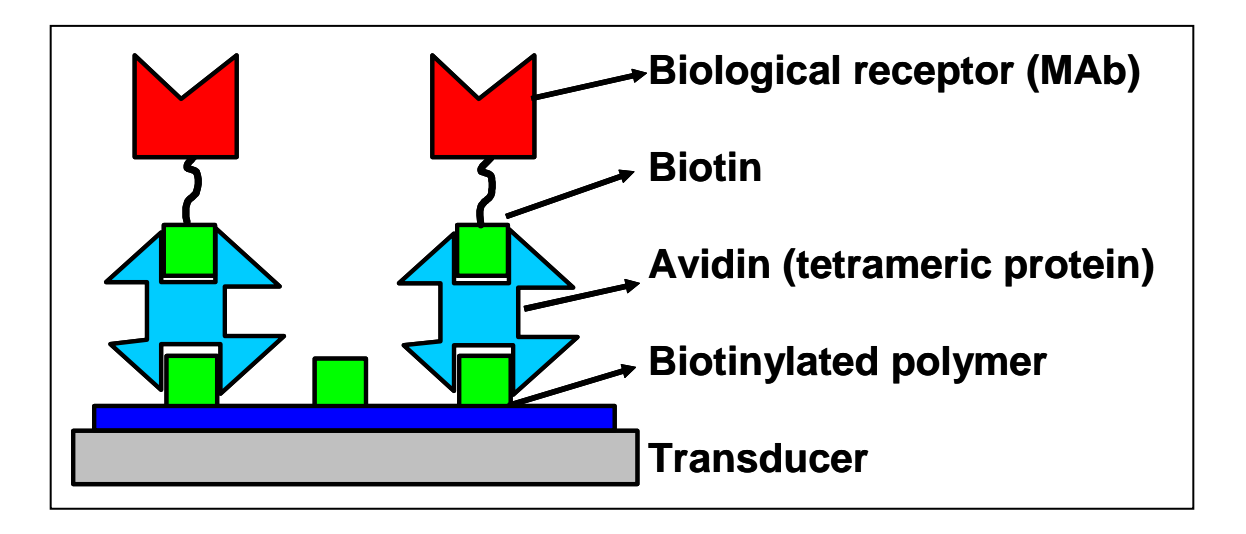


Figure 108. Cartoon representing self-assembly of biotinylated antibody onto neutravidin activated biotinylated polyaniline nanastructured matrix to form an immunosensor.

The self – assembly was originally followed by monitoring mass changes using the QCM instrument which quite clearly showed that sequential addition of neutravidin, antibody and analyte gave clear mass changes, showing sequential binding to be occurring.

Using the anti-fluoroquinoline antibody supplied by Partner 6, an anti-fluoroquinoline immunosensor was produced by the biotinylation route. The anti-fluoroquinoline antibody was not pure as it was supplied in the presence of other proteins as an anti-serum.

The results of the anti-fluoroquinoline immunosensor when interrogated with the pulse waveform used in the anti-PSA experiments gave very low results (figure 109 overleaf). This was thought to be due to the immobilisation of many different proteins contained in the antiserum. The anti-fluoroquinoline required further purification before being used to produce immunosensors.

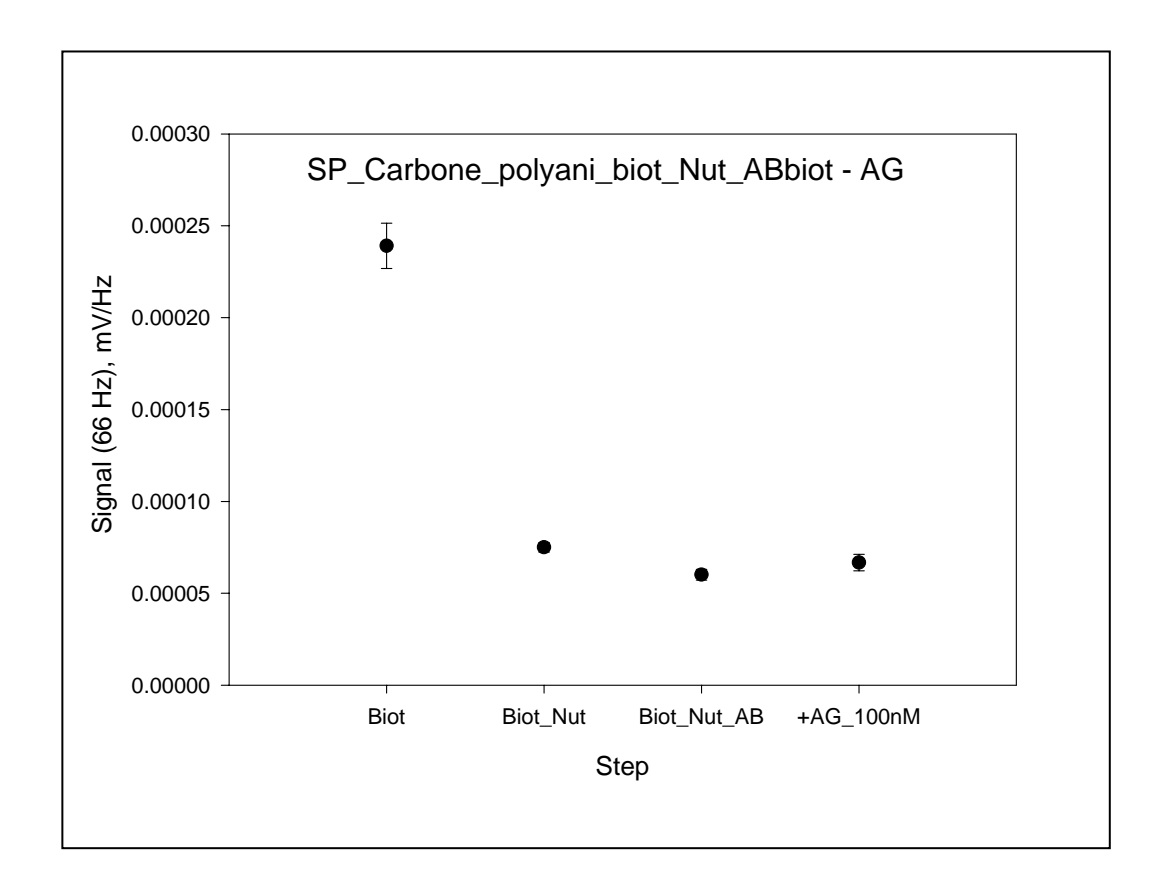
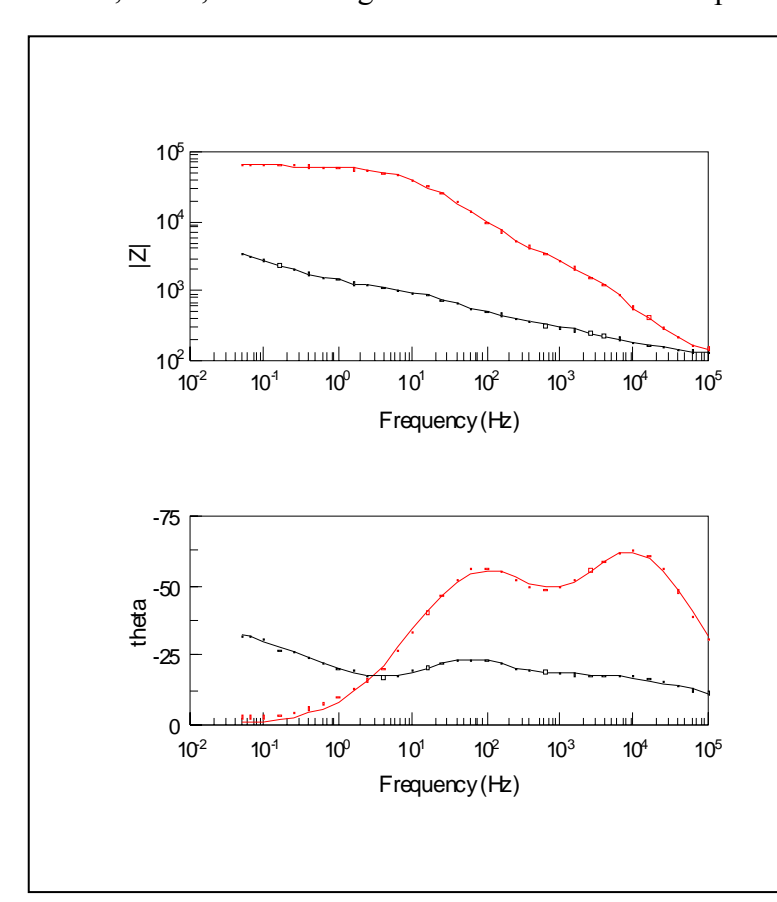


Figure 109. Sequential electrochemical pulsed waveform interrogation of a biotinylated polyaniline matrix first point, with added neutravidin second point, added biotinylated anti-fluorquinoline third point and finally ciprofloxazine as analyte fourth point. Clear differences occur on neutravidin binding, with small changes on the subsequent additions. A small increase is apparent on adding 100nM ciproxazine.

Exploration of self-assembled monolayers (SAMS) as a potential immunosensor matrix.

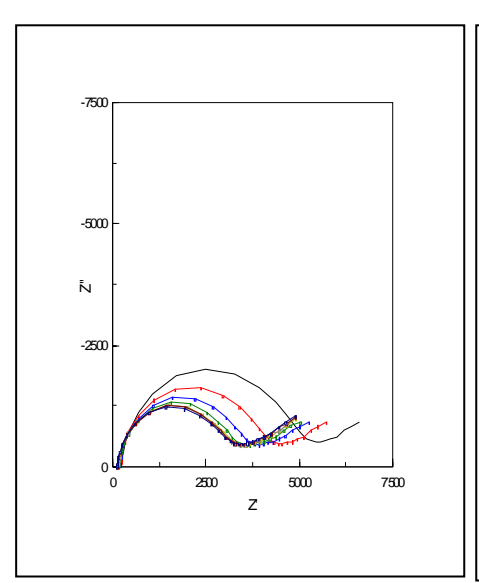
Grafting of SAMs functionalised with activated ester (NHP,NHS) was performed and characterised by XPS, FTIR, Contact angle and Electrochemical Impedance Spectroscopy by Partner 3. Grafting was first



carried out on gold microelectrodes provided by Tyndall. Two configurations were provided A (with a 100 µm gold track) and B (with a 10 µm gold track) as presented in figure 31. In the case of configuration A, there are two contributions in the impedance spectra as shown(figure 110).

It appears that for Electrochemical Impedance Spectroscopy, configuration B was more convenient than configuration A. The grafting was performed by keeping gold microelectrodes in contact with 1 mM of NHP thiol in dioxane solvent for 1 h

Figure 110. Bode diagram of microelectrode (configuration A) in PBS with 5mM of $Fe(CN)_6^{3-/4}$ at formal potential. Black curve :wihout thiol SAM, Red curve: with thiol SAM (figure 111).



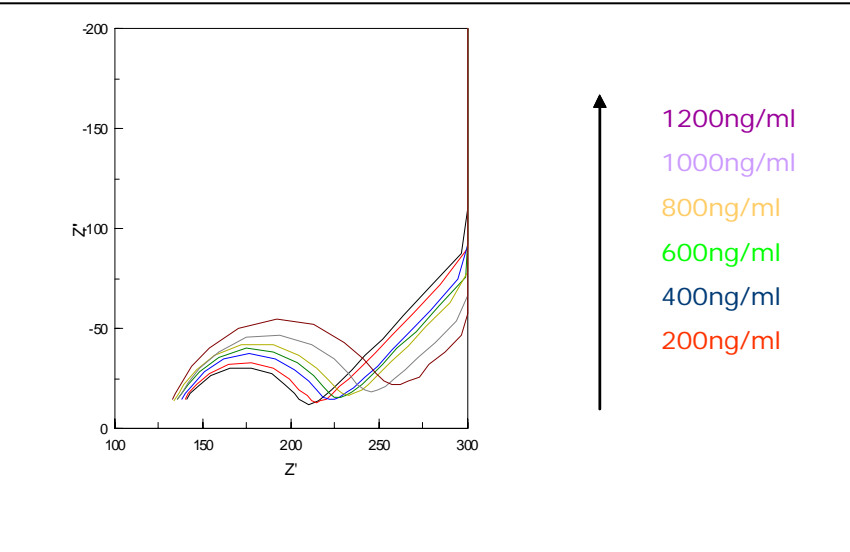


Figure 111. Stability of the NHP thiolSAMs layer in PBS with 5mM $Fe(CN)_6^{3-/4}$ at formal potential

Figure 112. Nyquist diagram of the interaction biotin-avidin in PBS 5mM $Fe(CN)_6^{3-/4-}$ at formal potential

Biotin-NH₂ was then coupled with the activated ester group. The time of reaction was 8h in 0.2mg/ml of biotin-NH₂ in DMSO (since biotin is not soluble in buffer or other organic solvent). The choice of biotin was done because it is a small molecule and it has a good affinity for avidin. Interaction of avidin wih the immobilised biotin layer was monitored by Electrochemical Impedance Spectroscopy. The Nyquist diagram is presented above in figure 112 is for different concentrations of avidin. The feasibility of the SAM based affinity biosensor using Electrochemical Impedance Spectroscopy was shown by the concentration dependent changes occuring.

SAMS Interrogated using Test Bed Electronics.

Partner 1 also explored SAMS as potential route of immobilisation. This was done to check if the test bed electronics used in pulse waveform mode would give a measurable signal.

The main idea for such production was formulated relating to the cross-linking of antibodies onto SAMS.

Mercaptohexadecanoic acid (MHDA) was chosen as a suitable alkanethiol component, due to its relatively long carbon chain backbone (16-C), that enables the formation of a rapid and stable SAM on gold surfaces via thiol-Au bonding. The lipid component was 1,2-dioleoyl-sn-glycero-3-{[n(5-amino-1-carboxypentyl)iminodiacetic acid]succinyl} nickel salt (DOGS- Ni-NTA) which provides the chelation of histidine tagged antibodies by the nitriloacetic Acid – nickle end group.

The NTA-Ni chelating immobilisation technique was identified as a gentle and relatively easy method of achieving SAM functionalisation and antibody ligation. This method circumvents the use of organic solvents, such as those used in NHS/carbodiimide coupling, which may damage the SAM.

The formation of SAMs and histidine tagged anti-atrazine fragment (Fab from partner 4) followed by atrazine binding was investigated using a the test bed electronics in pulse waveform mode to give a power spectrum analysis (Figures 113,114 overleaf). Power spectrum data obtained suggested the successful deposition of mixed monolayers comprising MHDA and a Ni-NTA-phospholipid on gold surfaces had been achieved, however binding of antiatrazine and atrazine is not very obvious on this figure. In order to do this process more clearly the differential power spectrum was proposed. This spectrum obviously demonstrates NTA-SAM formation, binding of antiatrazine, atrazine and removal of components from NTA-SAM with imidazole (figure 115). Note also that this is the first time Fab fragments have been demonstrated to work under pulse waveform interrogation, which is a significant advance in the project.

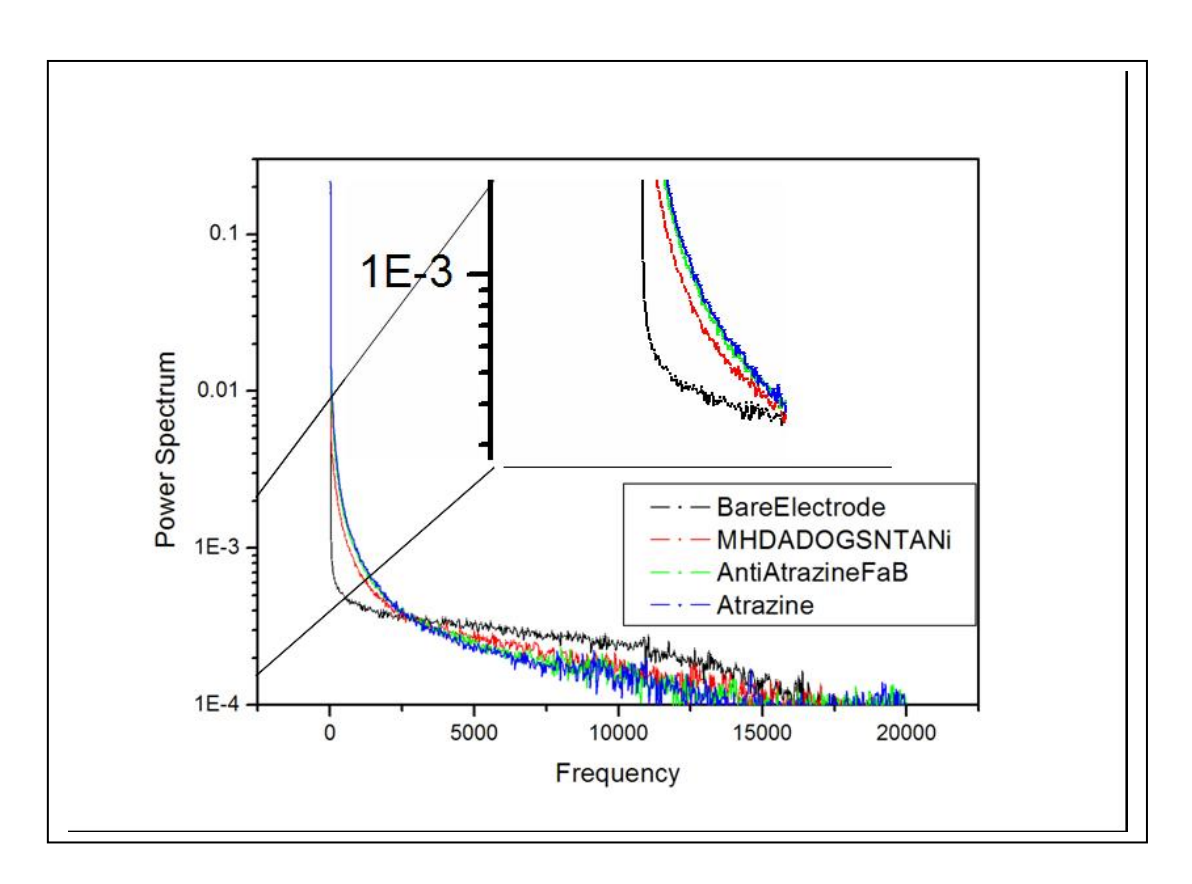


Figure 113. Power spectrum analysis of SAMS gold electrode. Results from successive layers as the structure is built up with thiol and lipid components (MHDA-DOGS-NTANi), with histidine tagged antibody Fab fragment added (Anti-atrazine) and with analyte (atrazine). The responses are difficult to see however it is clear that there are responses being recorded which may be amplified (see figure 115 overleaf).

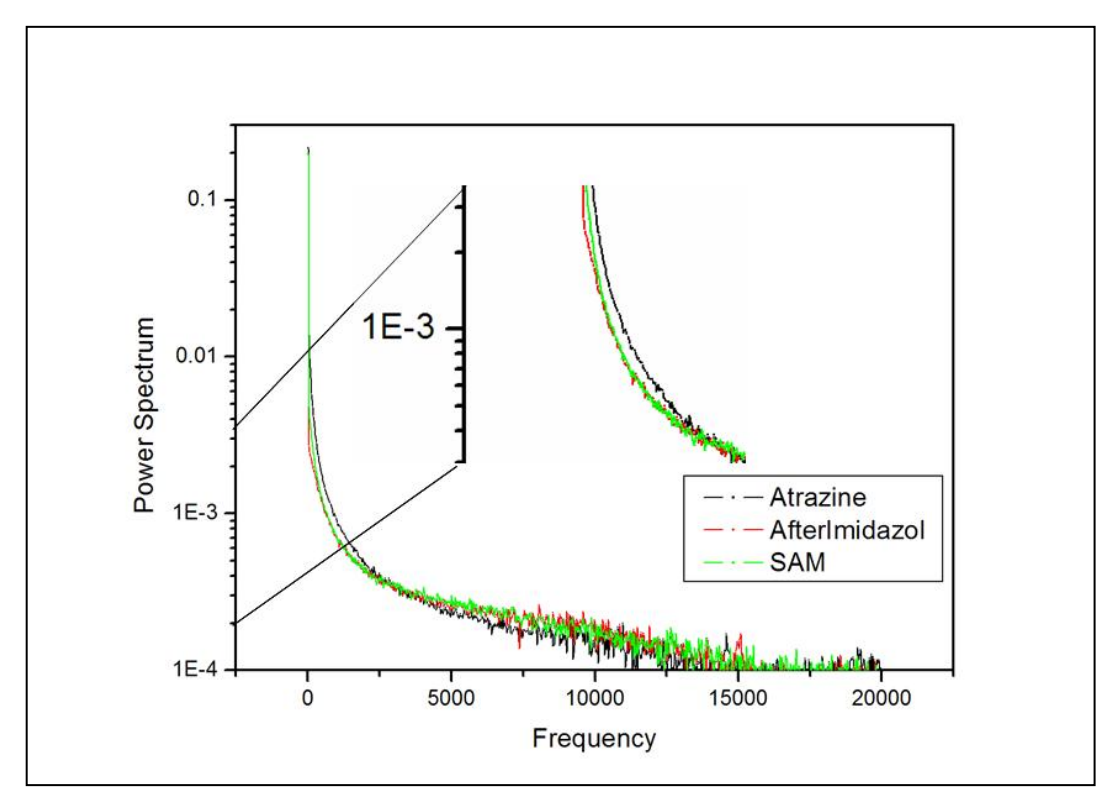


Figure 114. Power spectrum analysis of SAMS gold electrode as the bound antibody is stripped off the surface using imidazole. Imidazole is a competitive chelator for nickel and effectively displaces histidine tagged proteins from NTA surfaces. The responses, again small, show removal of the anti-atrazine.

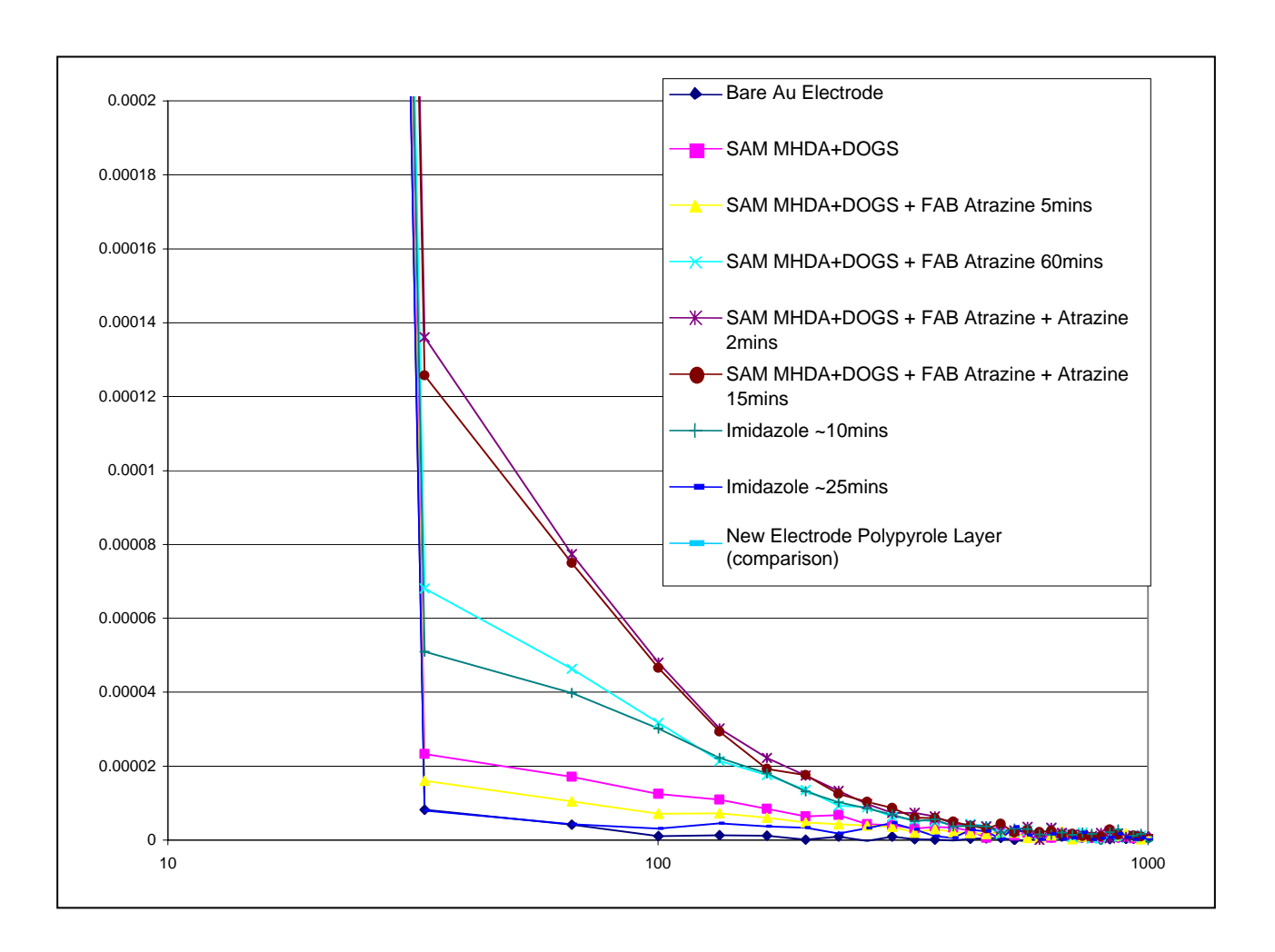


Figure 115. Differential power spectrum of the results shown in figures 113, 114. Taking the first differential from the results effectively amplified the sensor responses to be more visually evident. Here it can be clearly seen the rise in the signal as successive layers are added with the bare electrode being right at the bottom, addition of the SAM and lipid chelator in pink, addition of the histidine tagged anti-atrazine Fab fragment lowers the signal initially after 5 minutes in yellow, then the signal increases as the Fab is immobilised over 1 hour, light blue. Adding atrazine increases the signal after 2 minutes, purple top line which then decreases slightly, probably due to an equilibrium being set up over 15 minutes. Adding imidazole then begins to strip off the histidine tagged Fab after 10 minutes, dark green line in middle and back to baseline by 25 minutes, dark blue at bottom.

This result was extremely significant, as it had the potential to allow a commercialisation route that navigated through all patent areas, being entirely new in the mode of sensor interrogation. It also had the advantage of being very rapid as the manufacture of such sensor devices at the molecular level would proceed by simply dipping the gold sensor devices into the required solutions of reagents when they self-assemble into defined nano-structures. The histidine immobilisation method is generically applicable to any histidine tagged protein.

The pulse interrogation of polypyrrole layers using anti-haemoglobin has also been carried out to a limited extent and initial results are shown in WP7, after the pulsed amperometric interrogation results on page 85. This interrogation technique was more fully explored in the final year of the project.

Immobilisation of Fab fragments onto magnetic particles.

Partner 3 explored a new immobilisation strategy involving magnetic particles, shown below in figure 116. This was was developed and applied for the detection of atrazine as a first example. Streptavidin coated magnetic particles were dispersed in solvent and fixed as a functional monolayer to the standard gold electrodes through the use of a magnetic field placed under the electrode body. Due to the high binding affinity of streptavidin/ biotin, antibody biotinyl-Fab fragment K47 was immobilized onto this magnetic monolayer.

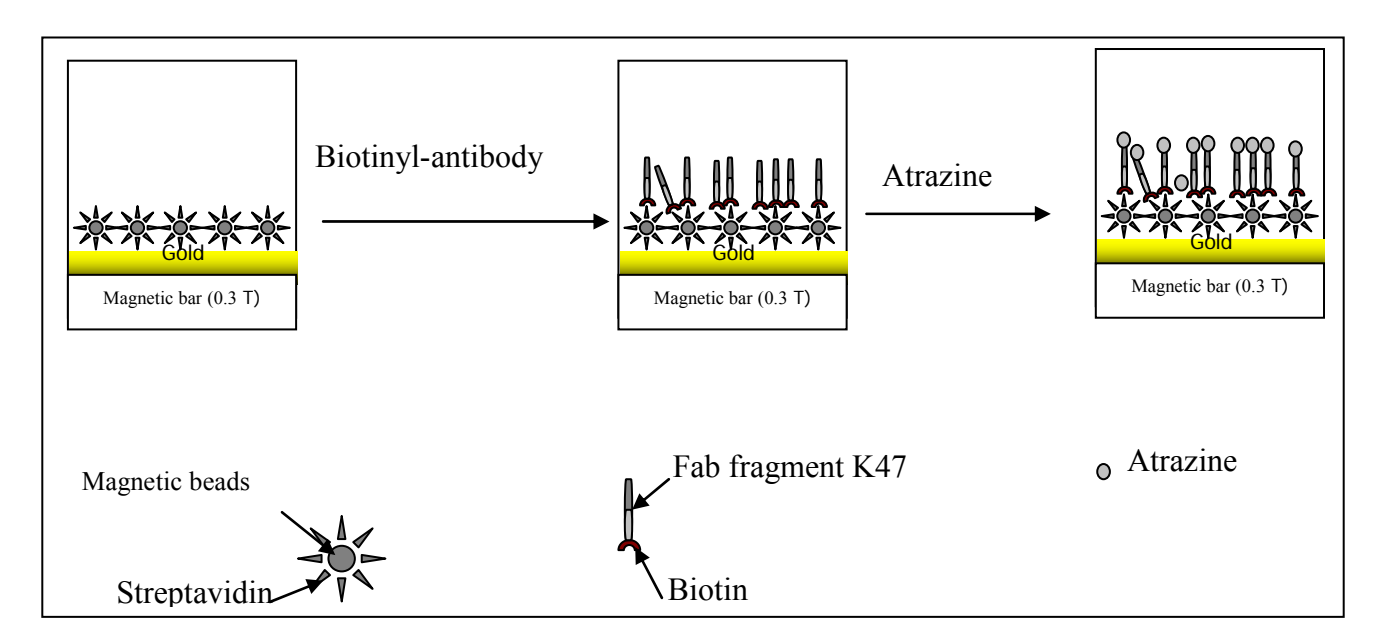


Figure 116. Sequential immobilisation of anti-atrazine Fab fragment onto magnetic streptavidin beads.

Complex impedance plots of the successive build up of the sensing layer magnetic beads/ Au electrode, biotinyl-Fab fragment K47 antibody/ magnetic beads/ Au electrode and after a 600 ng/ml of atrazine injection in cell are shown below in figure 117.

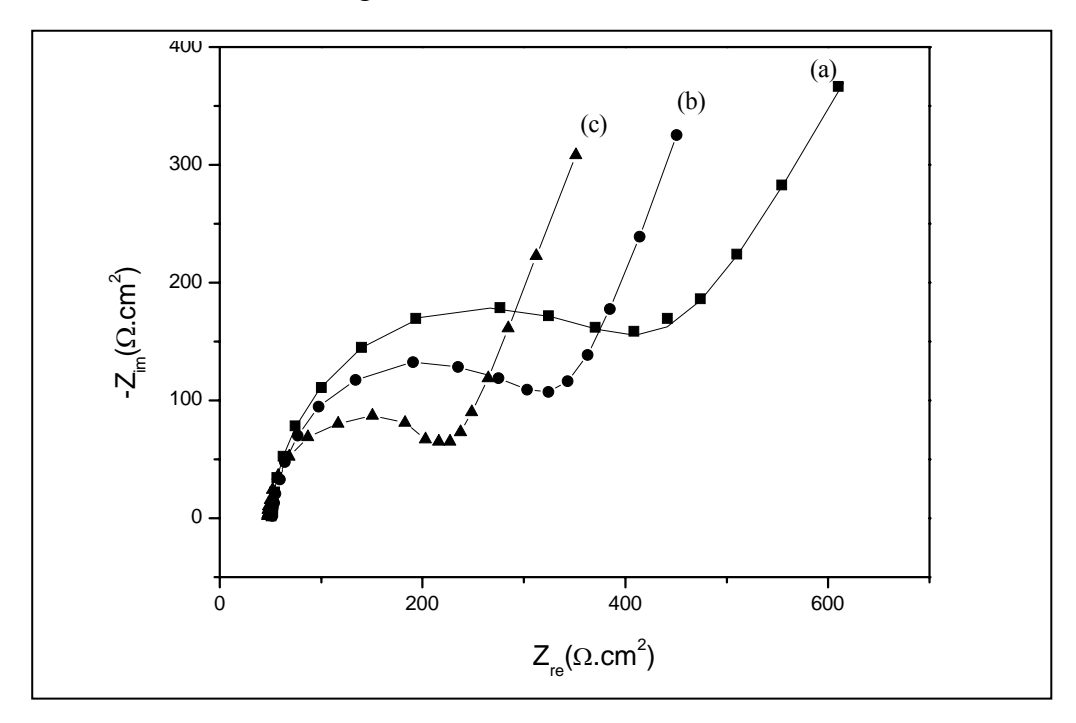


Figure 117. Nyquist diagram (Z_r vs. Z_i) for the non-faradic impedance measurements corresponding to: (a) magnetic beads/ Au-electrode; (b) Fab fragment K47 antibody / magnetic beads/ Au-electrode; (c) 600 ng.ml⁻¹ atrazine/ Fab fragment K47 antibody / magnetic beads/ Au-electrode

In order to obtain a calibration data set, the values of electron transfer resistance differences ΔRet versus the added atrazine concentrations were plotted in figure 118. The change of electron transfer resistance was calculated according the equation:

$$\Delta Rm = Ret(Ab) - Ret(Ab-Ag)$$

Where Ret(Ab) is the value of electron transfer resistance after antibody immobilization on the electrode and Ret(Ab-Ag) is the value after addition of antigen, atazine. As can be seen in figure 118, the plot was linear for high concentrations of atrazine and then reached saturation. A linear relationship between the Δ Ret values and the concentration of atrazine was established in the range from 50 to 500 ng.ml⁻¹.

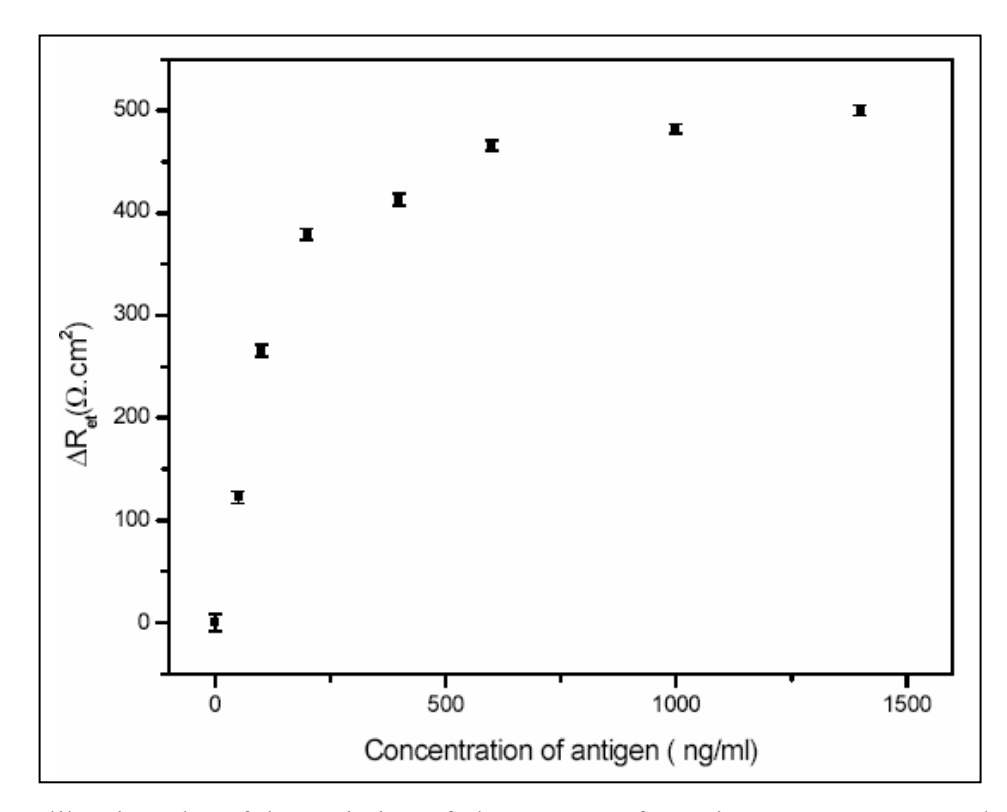


Figure 118. Calibration plot of the variation of electron transfer resistance Δ Ret versus the concentration of antigen (atrazine).

The usefulness of this immobilisation technique is likely to rest in the 'in situ' production of labeless immunosensors in microfluidic devices, possibly for high throughput screening of drugs or expressed proteins in combinatorial experiments or genetic markers in medical diagnosis.

Synthetic receptors

Investigations were done with the aim of selecting synthetic receptors having the potential to act as antibodies mimics. Synthetic receptors like crown ethers or calixarenes, in combination with a suitable electrochemical trancher hold promise for selective recognition and determination of the non oxidizable amino acids.

a) Synthetic receptors on Si/SiO₂/Si₃N₄ transducers

The following compounds were synthesised (figure 119)

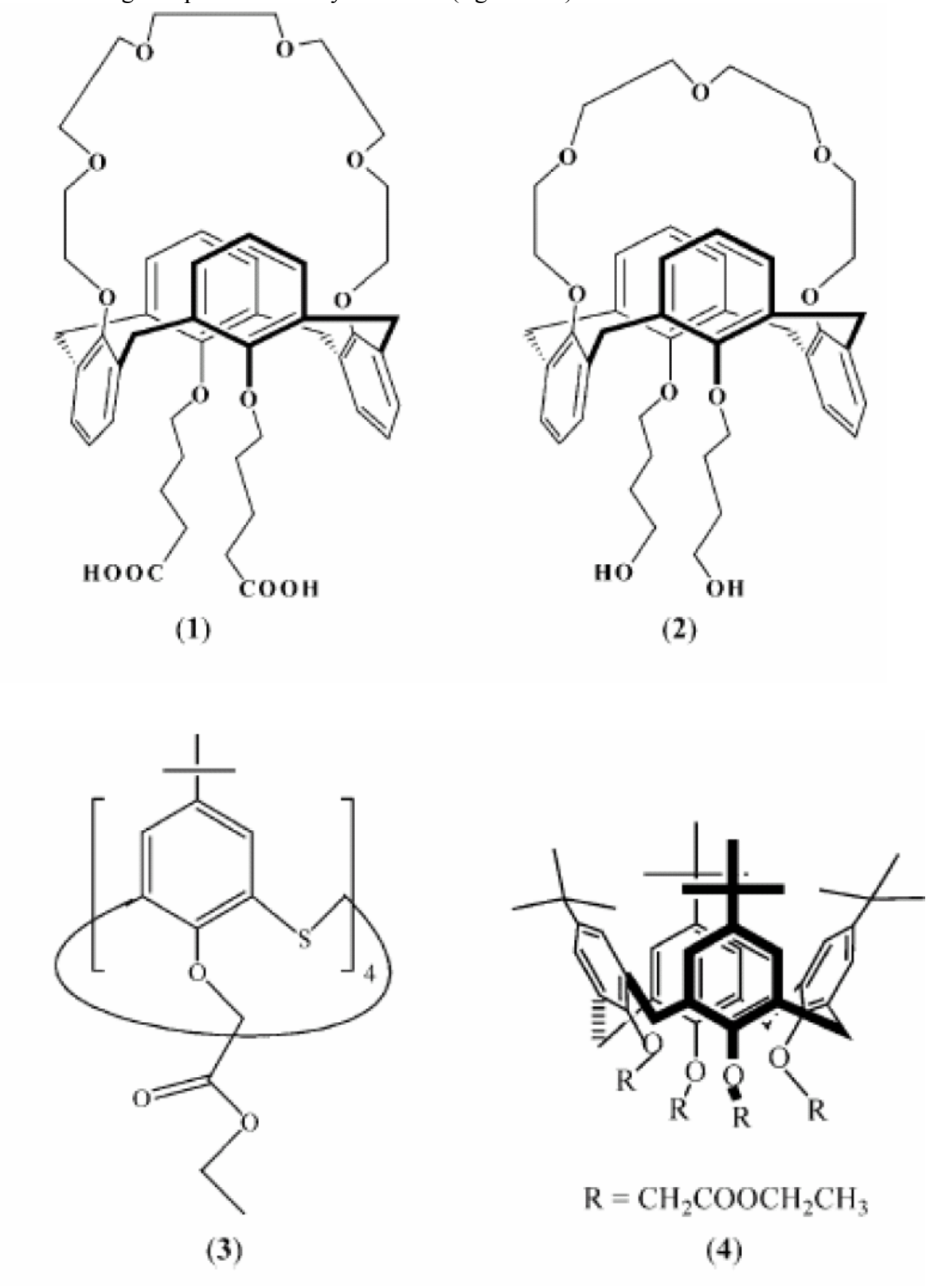


Figure 119. Calixerene type synthetic receptors. <u>Compound 1</u>, 1,3-(diethyl-5-oxavaleric acid)-calix[4]arene-crown-6; <u>compound 2</u>, 1,3-(di-4-oxabutanol)-calix[4]arene-crown-6; <u>compound 3</u>, tetraethyl *p-tert*-butylthiacalix[4]arene tetraacetate; <u>compound 4</u>, tetraethyl *p-tert*-butylthiacalix[4]arene tetraacetate.

The sensors were fabricated by immobilizing calixarene derivatives on Si/SiO₂/Si₃N₄ transducers. The measurements were made in sulphuric acid media of ca. pH 1 and in physiological buffer of pH 7.4. The

different calixarene derivatives showed varying sensitivities to the amino acids ranging from 8 to 137 mV/decade.

Responses obtained for some representative amino acids and albumin, on such functionalised transducers, are summarized in the following table showing biosensing potentialities for these synthetic receptors.

Amino acids	Sensor 1 in H ₂ SO ₄ Slope (mV/decade) Linear range (M)	Sensor 2 in H ₂ SO ₄ Slope (mV/decade) Linear range (M)	Sensor 3 in PBS Slope (mV/decade) Linear range (M)	Sensor 3 in H ₂ SO ₄ Slope (mV/decade) Linear range (M)	Sensor 4 in H ₂ SO ₄ Slope (mV/decade) Linear range (M)
Glycine	$11.9 (\pm 2)$ $1.7 \times 10^{-2} - 1.3 \times 10^{-4}$	$13.8 (\pm 3)$ $1.5 \times 10^{-2} - 2.7 \times 10^{-4}$	$20.3 \\ 2.1 \times 10^{-2} - 2.6 \times 10^{-4}$	35.8 (±1) $1.5 \times 10^{-2} - 3.6 \times 10^{-4}$	$32.9 (\pm 1)$ $1.8 \times 10^{-2} - 3.6 \times 10^{-4}$
Lysine	nss	$9.3 (\pm 2)$ $1.8 \times 10^{-2} - 1.3 \times 10^{-4}$	$27.5 (\pm 2)$ $3.7 \times 10^{-2} - 1.8 \times 10^{-4}$	$43.2 (\pm 2)$ $1.5 \times 10^{-2} - 1.7 \times 10^{-4}$	$45.7 (\pm 3)$ $1.3 \times 10^{-2} - 1.4 \times 10^{-4}$
Proline	nss	$12.9 (\pm 2)$ $2.1 \times 10^{-2} - 5.1 \times 10^{-4}$	19.8 $1.7 \times 10^{-2} - 2.6 \times 10^{-4}$	22.3 (±2) $1.7 \times 10^{-2} - 1.4 \times 10^{-4}$	$21.3 (\pm 2)$ $1.7 \times 10^{-2} - 1.4 \times 10^{-4}$
Histidine	nss	$12.8 (\pm 2)$ $2.5 \times 10^{-2} - 2.7 \times 10^{-4}$	$24.8 (\pm 1)$ $1.5 \times 10^{-2} - 7.8 \times 10^{-5}$	33.8 (± 2) 1.8 \times 10 ⁻² – 1.4 \times 10 ⁻⁵	$31.8 (\pm 3)$ $1.8 \times 10^{-2} - 1.4 \times 10^{-5}$
Asparagine	7.7 (±2) $1.5 \times 10^{-2} - 6.8 \times 10^{-4}$	$10.8 (\pm 2)$ $1.3 \times 10^{-2} - 1.4 \times 10^{-4}$	17.0 $7.7 \times 10^{-2} - 2.3 \times 10^{-5}$	50.5 (±1)	$48.3 (\pm 1)$ $1.3 \times 10^{-2} - 1.4 \times 10^{-3}$
Aspartic acid	$4.8 (\pm 2)$ $5.6 \times 10^{-3} - 6.4 \times 10^{-5}$	5.2 (±1) 5.1 × 10^{-3} - 9.4 × 10^{-5}	137.6 (±3) 7.7 × 10^{-2} - 6.3 × 10^{-5}	$38.4 (\pm 2)$ $5.5 \times 10^{-3} - 5.4 \times 10^{-5}$	$32.4 (\pm 2)$ $5.9 \times 10^{-3} - 5.4 \times 10^{-3}$
Glutamine	7.9 (\pm 2) 1.5 × 10 ⁻² – 2.3 × 10 ⁻⁴	8.9 (±3)	17.1 (\pm 2) 8.8 × 10 ⁻² - 4.6 × 10 ⁻⁵	53.2 (±2)	$51.4 (\pm 2)$ $1.4 \times 10^{-2} - 1.6 \times 10^{-3}$
Glutamic acid	$6.9 (\pm 2)$	9.6 (±2) $1.2 \times 10^{-3} - 1.0 \times 10^{-5}$	127.8 (±3) $9.3 \times 10^{-3} - 3.4 \times 10^{-5}$	$41.7 (\pm 3)$ $4.1 \times 10^{-3} - 5.5 \times 10^{-5}$	$41.5 (\pm 2)$ $4.2 \times 10^{-3} - 5.5 \times 10^{-5}$
Albumin	nss	nss	$103.2 (\pm 3)$ $2.2 \times 10^{-3} - 3.4 \times 10^{-7}$	11.6 (±2)	$10.6 (\pm 2) 2.2 \times 10^{-3} - 2.1 \times 10^{-7}$

b) Synthetic receptors on gold electrodes (in cooperation with partner 2)

The potential complex formation between some calix[4] arene based molecules (figure 120) and some amino acids, including arginine and lysine, was also studied using faradic electrochemical impedance spectroscopy (EIS).

Figure 120. claix[4] arene dreivatives used as synthetic receptors for impedimetric amino acid biosensors.

Calix[4]arene–amino-acid complex formation was tested under two pH conditions. Cyclic voltammetry was used to determine the electrochemical properties of the different layers immobilized on gold electrode surfaces. The electrodes were initially functionalized using cysteamine and then used as a substrate for calix[4]arene immobilization. Impedance spectroscopy permits the study of the electrical

properties of the different layers and also allows for the detection of amino-acids binding to calix[4]arene. Cyclic voltammetry and FTIR proved that calixarenewas assembled at the thiol functionalized gold surface. SEM showed a crystalline organisation; a dendritic structure in the case of the calixarene modified by the carboxylic acid groups (calix 1) and the calixarene with sulphonated long chain (calix 3). The benzyl modified calixarene (calix 2) showed a cubic structure organisation. Faradic impedance spectroscopy allowed f the amino-acid—calixarene interaction to be followed. Calix 1 presented the highest sensitivity to arginine and lysine and allowed 10^{-3} of arginine and 6. 10^{-3} M lysine to be detected (figure 121).

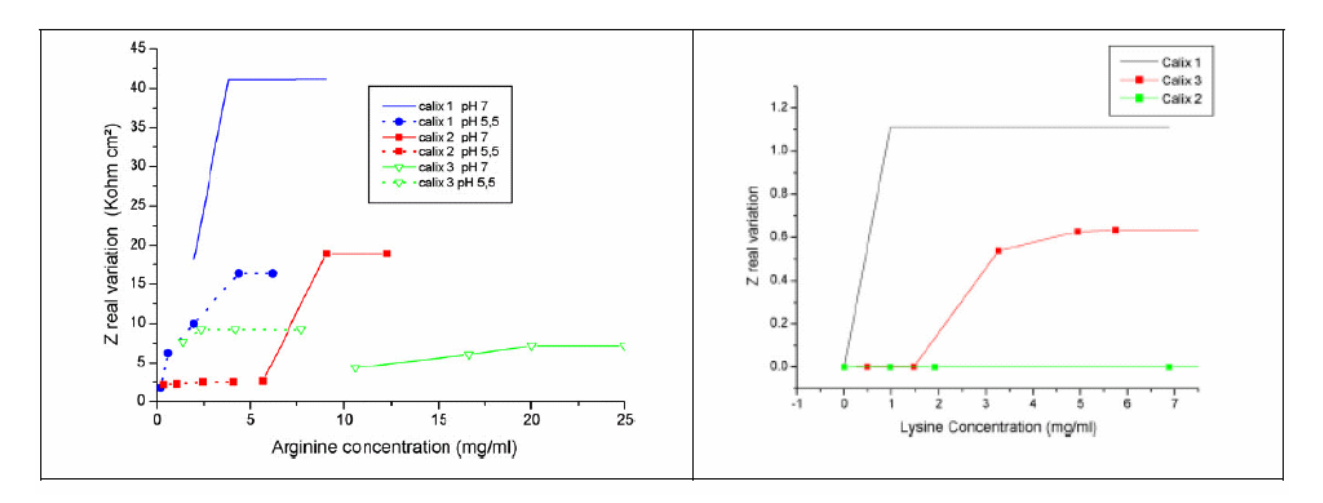


Figure 121. Faradaic impedimetric detection of arginine and lysine using calx[4]arene based based biosensors

Ciprofloxacin immunodetection in cooperation with partners 8, 5, 6.

Impedance spectroscopy approaches combined with the biosensor technology have been used for the determination of trace amounts of ciprofloxacin (figure 122). The sensor electrode was based on the immobilization of anti-ciprofloxacin antibodies by chemical binding onto an poly(pyrrole-NHS) film (figure 123) electrogenerated on a solid gold substrate.

$$\begin{array}{c} & & & & \\ & & & \\ & & & \\ & & & \\ & & & \\ & & & \\ & & & \\ & & & \\ & & & \\ & & & \\ & & & \\ & & & \\ & & & \\ & & & \\ & & \\ & & & \\ & \\ & & \\ & & \\ & & \\ & & \\ & & \\ & & \\ & & \\ & & \\ & & \\ & & \\ & & \\ & & \\ & & \\ & &$$

Figure 122. Ciprofloxacin

Figure 123. Pyrrole-NHS

Electropolymerization of pyrrole-NHS, antibody grafting and ciprofloxacin immunoreaction were characterized by cyclic voltammetry (CV) in the presence of $[Fe(CN)_6]^{3-/4-}$ as a redox system as well as by SEM and AFM imaging. The resulting biopolymer coating was applied to the determination of ciprofloxacin, the immunoreaction triggering directly a signal via impedance spectroscopy measurements that allows the detection of the antigen target, namely ciprofloxacin (range between 100 ng.ml⁻¹ down to 10 pg.ml⁻¹) - (figures 124,125).

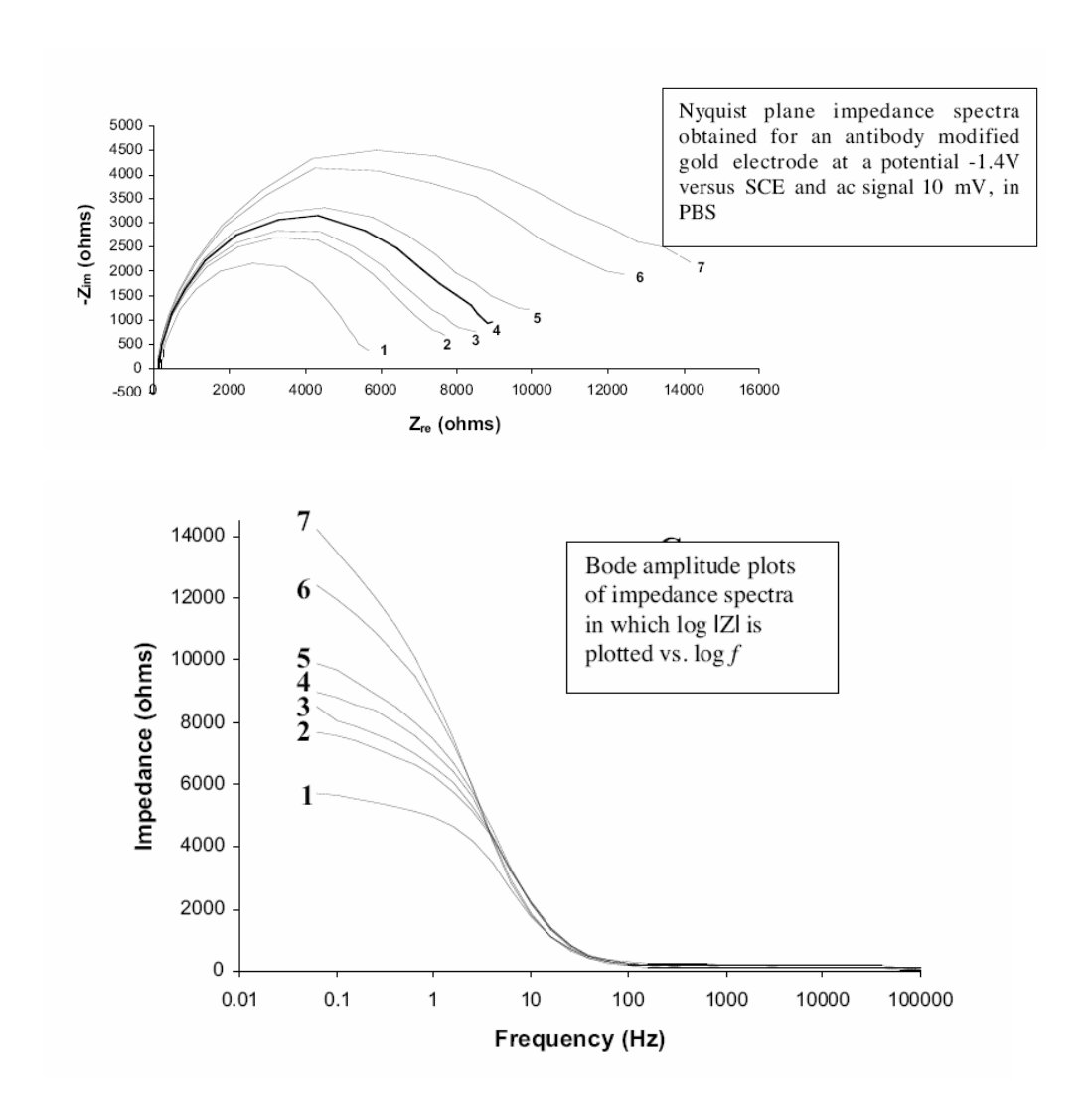


Figure 124. (1)- poly(pyrrole-NHS) electrodeposited on gold, (2)-antibodies deposited onto poly(pyrrole-NHS) electrodeposited on gold, (3)-10 pg/ml ciprofloxacin deposited onto antibodies polypyrrolic-NHS films (CAP), (4)-100 pg/ml CAP, (5) 2 ng/ml CAP, (6) 100 ng/ml CAP, (7) 1 μg/ml CAP.

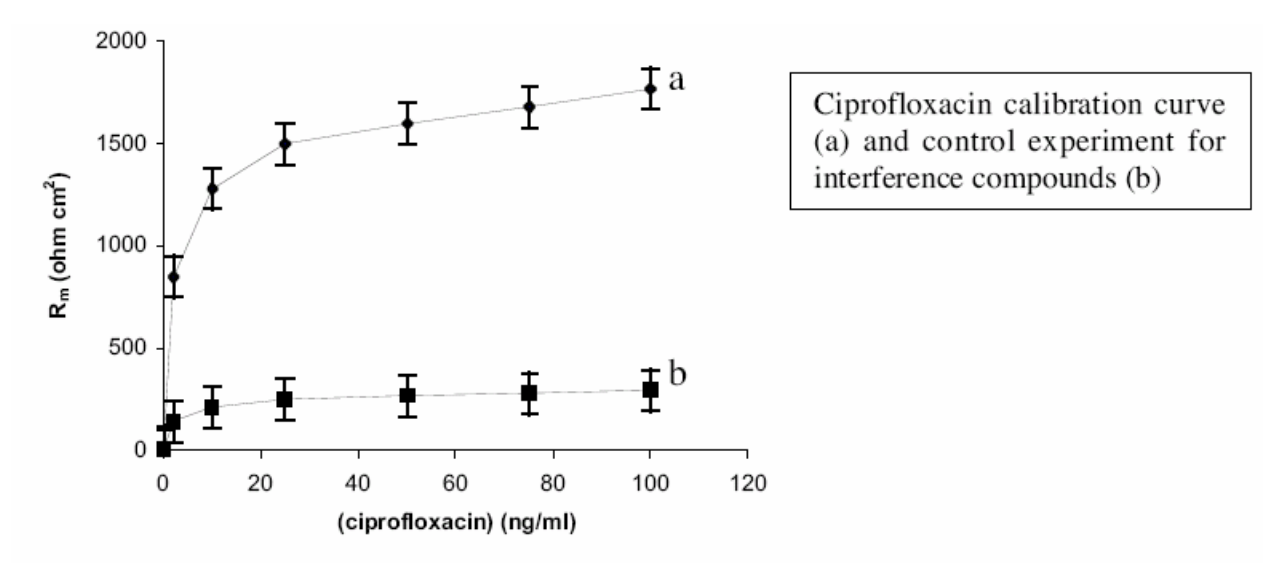
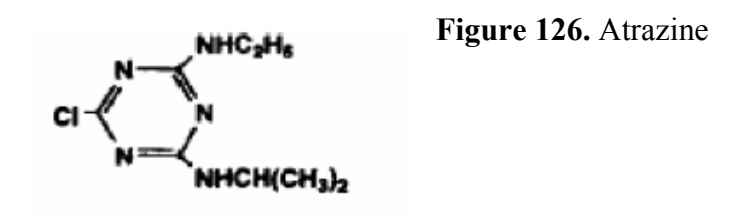


Figure 125. Ciprofloxacin calibration curve for poly(pyrrole-NHS) based immunosensor.

b) Atrazine detection in cooperation with partners 8, 5, 4.



This herbicide (figure 126) constituted a model target for ELISHA project. The polyhistidine tagged Fab anti-atrazine was immobilized on an electrogenerated polypyrrole NTA film, through copper ion coupling according the scheme below (figure 127).

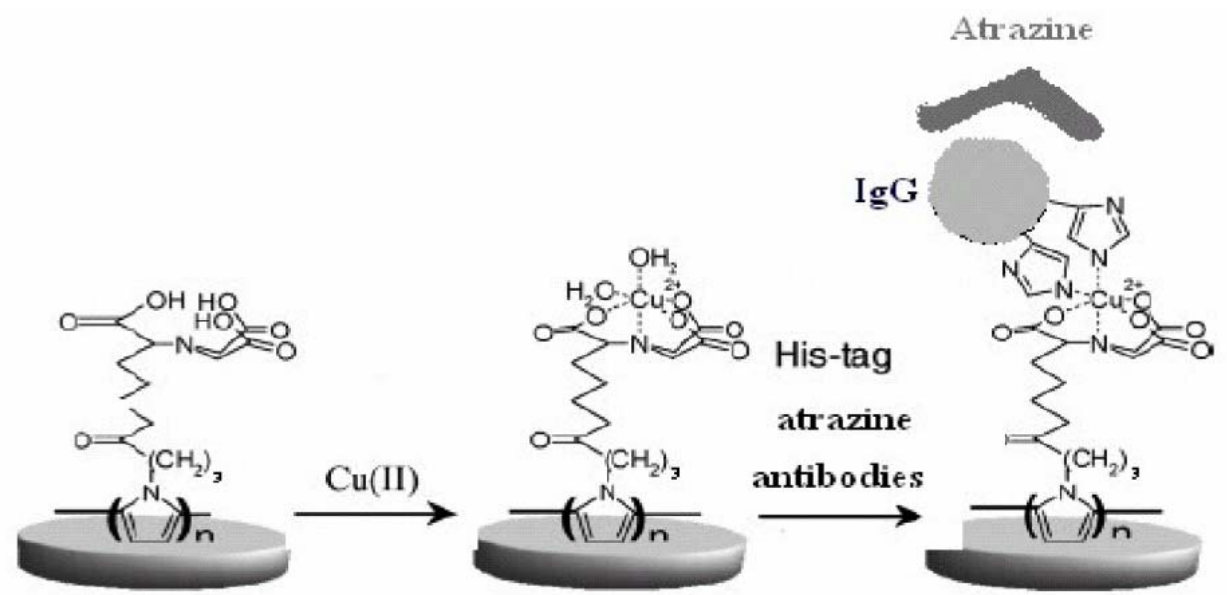


Figure 127. Immobilisation scheme for tethering of anti-atrazine Fab via Cu²⁺NTA chelating groups on the polypyrrole NTA surface.

The different steps of the immobilization process were monitored through cyclic voltametry (figure 128).

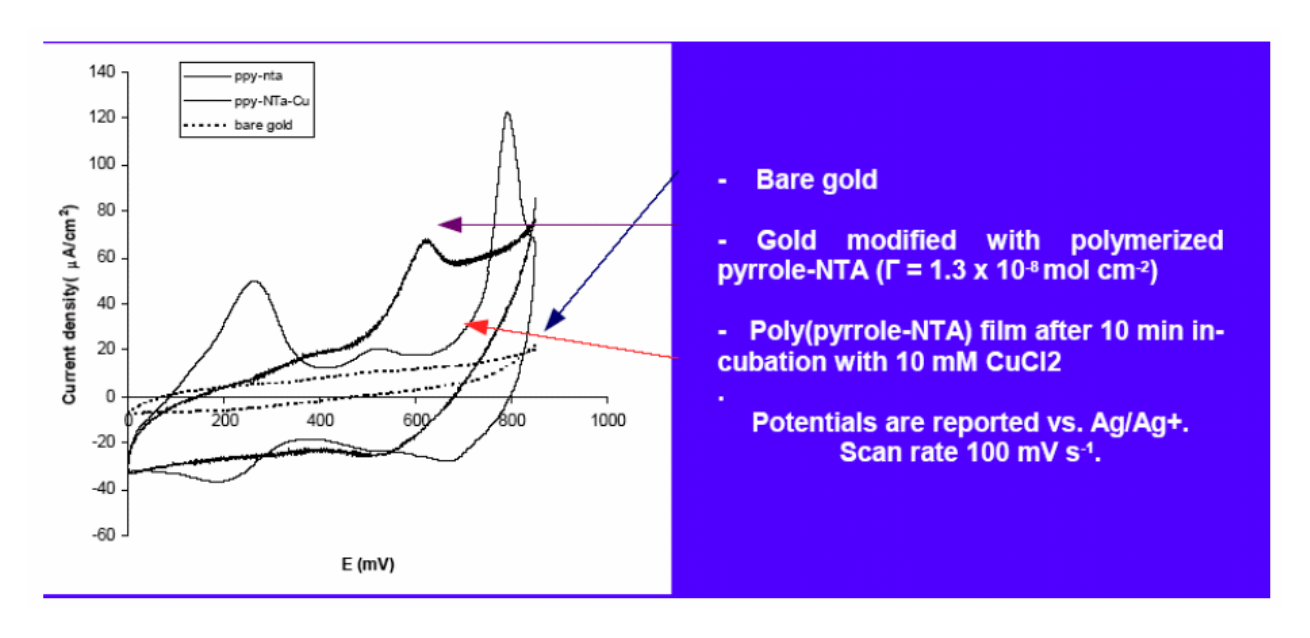


Figure 128. Monitoring of anti atrazine fab attachment by CV.

A typical calibration curve is given on figure 129 (below).

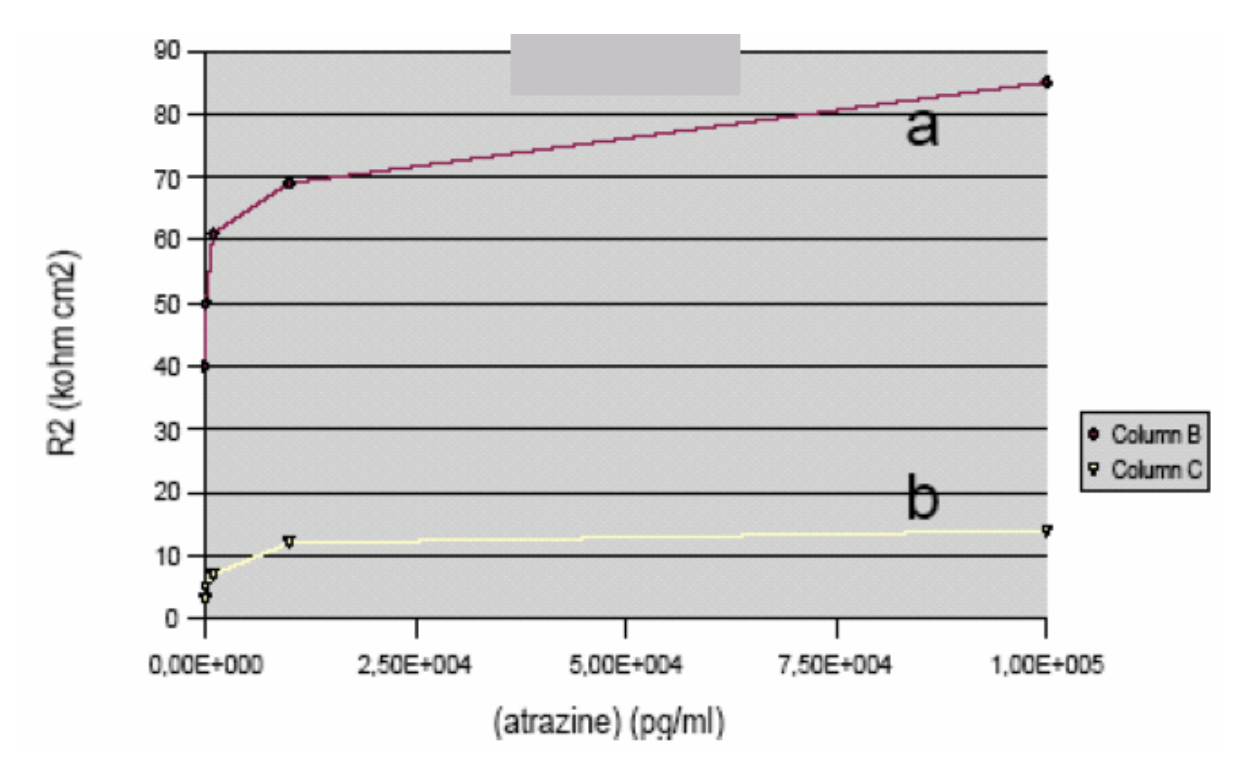


Figure 129. a) Calibration curve for atrazine b) Control curve for interfering compound atraton

Quite low detection limits could be reached for the detection of atrazine, up to 10 pg.ml^{-1} , over a concentration range from 10 pg.ml^{-1} to 100 ng.ml^{-1} (RSD for 4 immunosensors = 3.2%). Such analytical characteristics are quite competitive with other classical atrazine detection methods ($0.01 \mu g.L^{-1}$ for chromatography or ELISA, $0.01 \mu g.L^{-1}$ for piezoelectric competitive immunosensors).

Second ciprofloxacin biosensor using carbon microarrays and sulpho-nhs-biotin immobilisation

The experimental procedure described above was repeated using purified and concentrated anticiprofloxacin. The concentration of immobilised polyclonal and monoclonal antibodies on the sensor surface was 1 mg.ml⁻¹. Figures 130 and 131 are the mean Nyquist and Bode plots from three replicate sensors with immobilised anti-ciprofloxacin when exposed to different concentrations of the antigen. Note that impedance in these figures is presented in ohm.cm⁻² as opposed to Kohm.cm⁻² in previous sections. Impedance of these newly fabricated sensors, containing purified monoclonal antibody, was dramatically lower than the previously sensors previously reported containing non-purified anticiprofloxacin. Additionally, while impedance was previously found to increase upon exposure to increasing concentrations of antigen, in this instance impedance lowered.

Previous work (A. Barton personal communication) showed that the binding event for different antigen/antibody pairs may increase or decrease the impedance of the system, while the current work confirms this. It is argued here that this is the result of two competing processes; non-specific adsorption (non-purified antibody) leads to increases in impedance-especially in regards with the capacitive component of the system (**Z**"). Specific antigen/antibody binding leads to a lowering of impedance.

Additionally, upon the antibody/antigen binding event hydrogen bonds are formed which stabilise this interaction while the binding specificity between the two biomolecules is affected by some weak interactions such as van der Waals and electrostatic forces alongside hydrophobic interactions. Such events may also affect impedimetric responses (impedance increase or decrease) among different antibody antigen pairs. The reasons underlying these two events cannot as yet be answered with certainty. However, if the Nyquist and Bode plots (figures 130,131 overleaf) are compared the with those obtained

for ciprofloxacin on (figure 124) using a different surface and different immobilisation chemistry, the shape and response look remarkably similar indicating the signal generation is also similar.

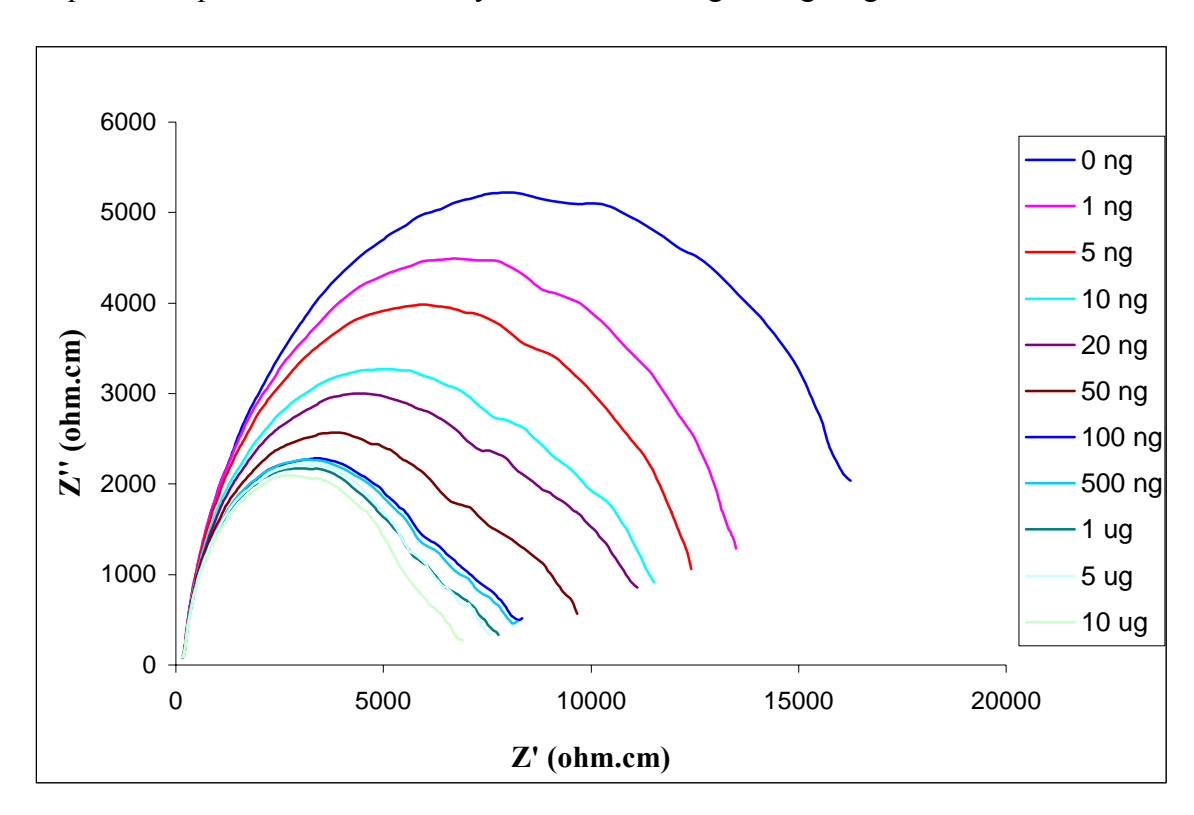


Figure 130: Z' v Z'' - Nyquist plot showing faradaic component against capacitive component for polyaniline doped with anti-ciprofloxacin on carbon electrodes (3 replicates) after exposure to various concentrations of ciprofloxacin (in redox couple).

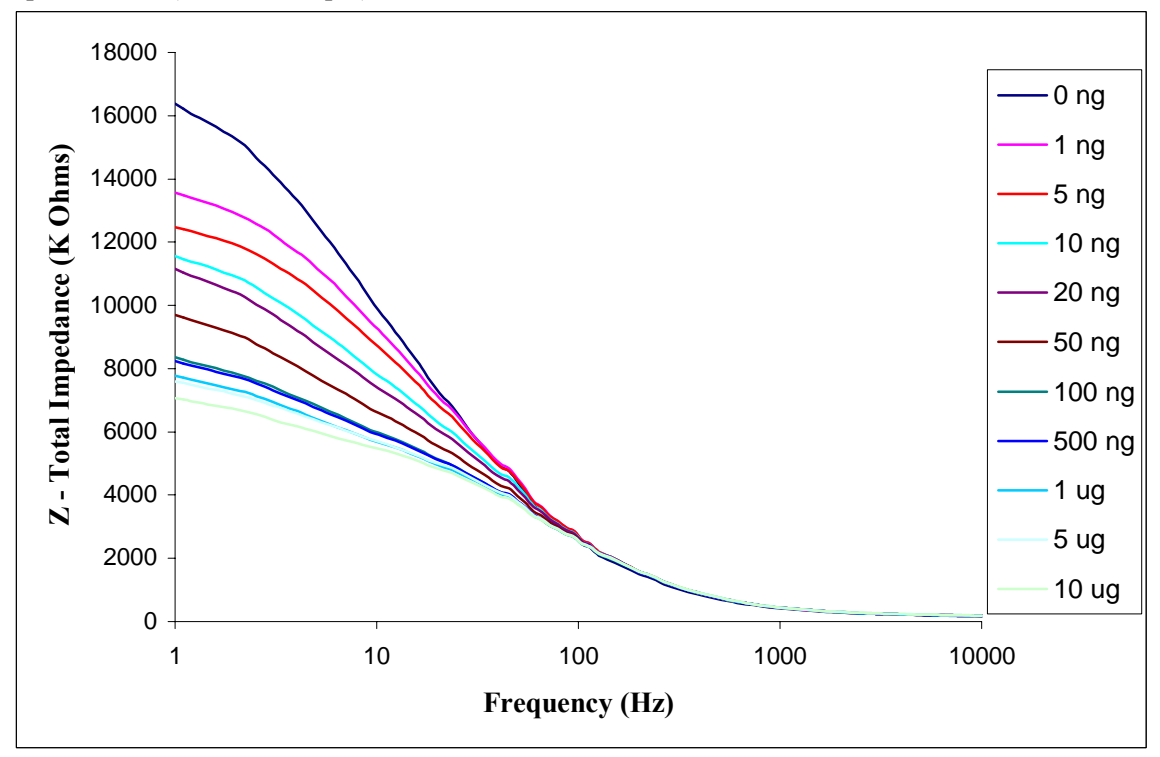


Figure 131: Bode plot-total impedance vs frequency. Total impedance response for polyaniline doped with anticiprofloxacin on carbon electrodes (3 replicates) after exposure to various concentrations of ciprofloxacin (in redox).

It should be noted that while the observed impedance changes may be positive or negative, the percent impedance change from baseline values were always positive, hence sensors containing different antibody antigen pairs may be compared.

Figures 132 to 135 respectively depict the percent impedance change from baseline, calibration profile for anti-ciprofloxacin (figure 133) and nonspecific IgG (figure 134) doped polyaniline sensors exposed to purified ciprofloxacin and finally the corrected (specific response minus non-specific response) calibration profile for the produced sensors (figure 135).

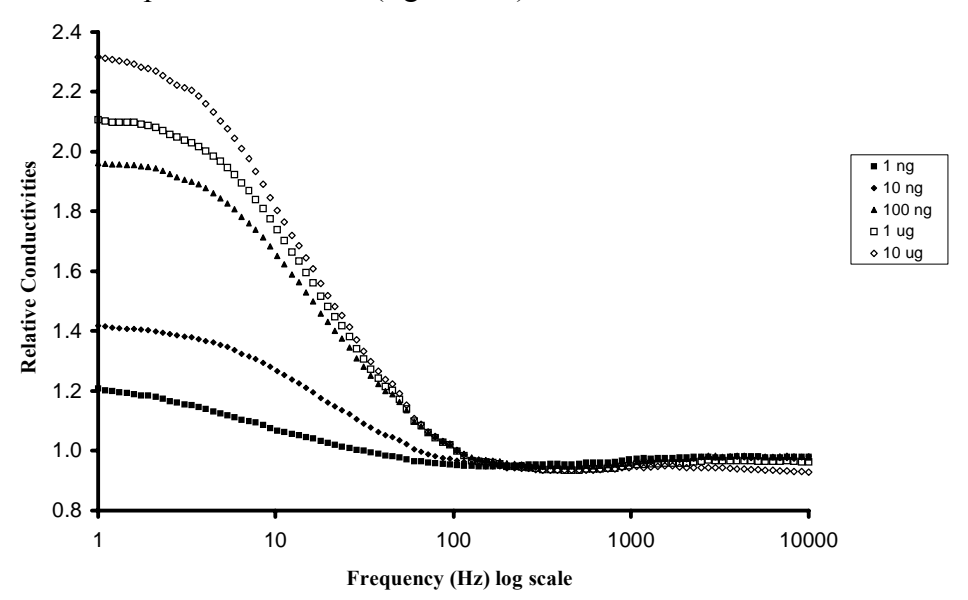


Figure 132 Relative conductivities of ciprofloxacin immunosensors after exposure to ciprofloxacin.

Figure 135 shows the percentage decrease in Z' across a range of antigen concentrations. As can be seen, there is a steady decrease in impedance as antigen concentration increases up to a concentration of about 100 ng ml^{-1} , above which concentration there is a tend towards a plateau, possibly indicating saturation of the specific binding sites. It is possible that any further changes in impedance beyond this level could simply be due to non-specific interactions. Between a concentration range of 1-100 ng ml⁻¹, there is a near linear correlation of the impedance change with the \log_{10} of concentration (R^2 =0.96).

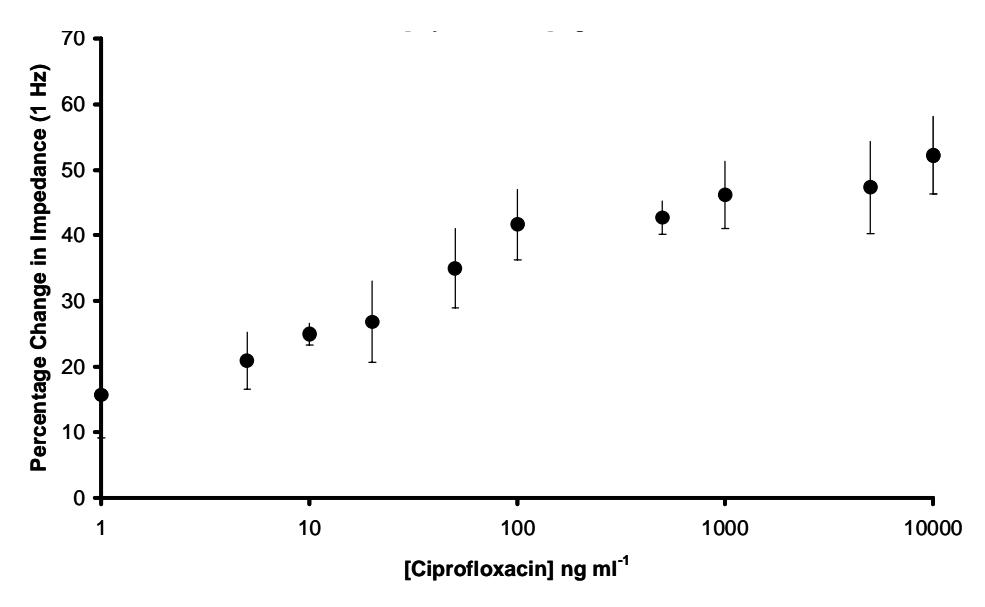


Figure 133: Calibration profile of percentage specific impedance response against ciprofloxacin concentration for carbon electrodes at 1Hz (in redox couple) coated with polyaniline doped with anti-ciprofloxacin.

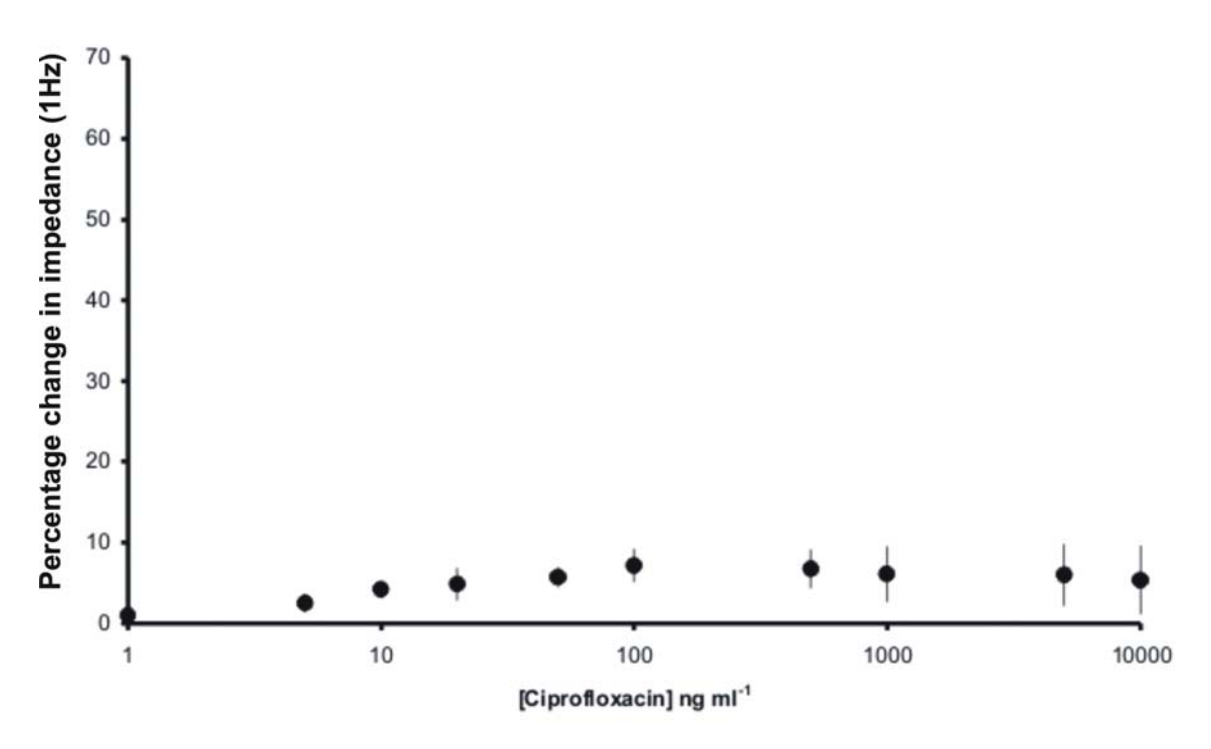


Figure 134 : Calibration profile of percentage <u>non-specific</u> impedance response against ciprofloxacin concentration for carbon electrodes at 1Hz (in redox couple) coated with polyaniline doped with non specific antibody.

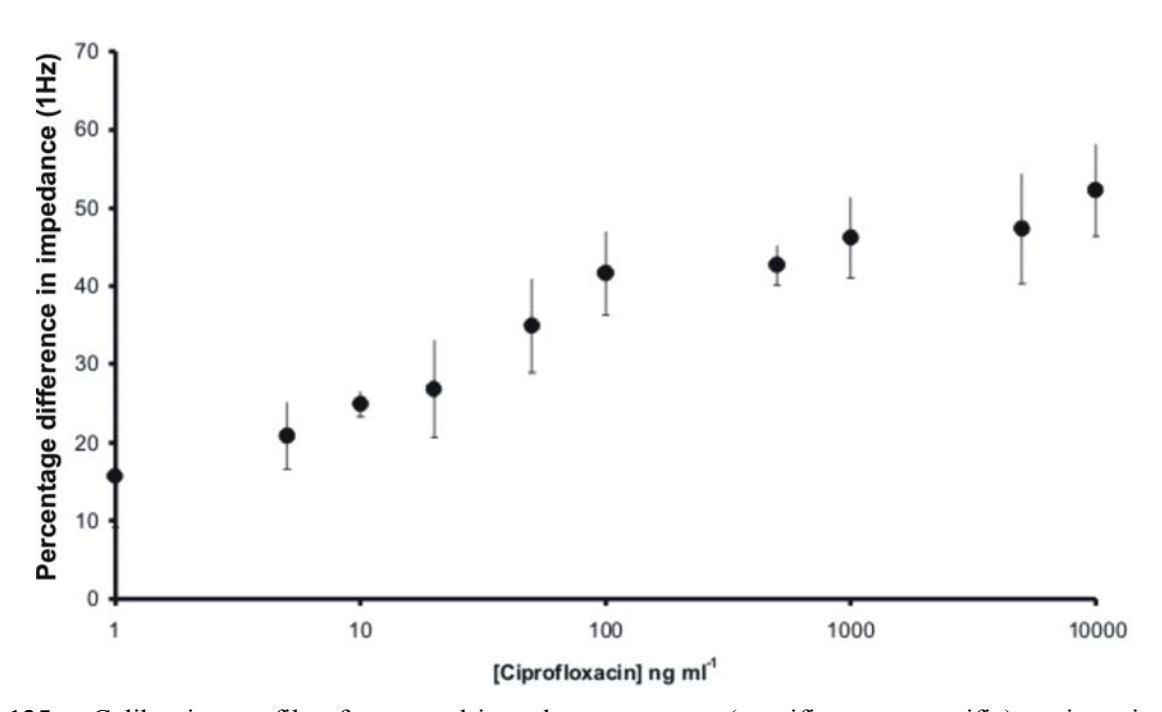


Figure 135 : Calibration profile of corrected impedance response (specific - non-specific) against ciprofloxacin concentration for carbon electrodes at 1Hz (in redox couple) coated with polyaniline doped with specific or non specific antibody.

In conclusion, we have demonstrated the construction of an immunosensor for the antibiotic ciprofloxacin using a combination of screen-printed electrodes coated with conducting polyaniline and an immobilised polyclonal antibody. Interrogation of the electrodes by AC impedance demonstrated the detection of the antigen.

Workpackage number:

W6. Sensor Address Systems and Interrogation Electronics

Objectives. To design and evaluate novel interrogation techniques for extraction and de-convolution of signals generated from the affinity sensors. To develop purpose designed electronics for integration into 1) test bed evaluation rigs and 2) the laboratory prototype sensor system. To iteratively feed back into W3, W4, W5 and W7 to optimise and develop sensors, interfaces and electronics for immunosensors.

Project Timeline		1 2 3 4 5 6 7 8 9 10 11 12 13 14 15 16 17 18 19 20 21 22 23 24 25 26 27 28 29 30 31 32 33 34 35 36
Workpackage 6.	Sensor Electronics	
Task 6.1	Test Beds	
Task 6.2	Prototype	

For Uniscan Instruments the ELISHA project encompasses the design of physical, electronic and software interfaces to perform a variety of Electrochemical and Pulsed-Waveform interrogation techniques. A connector has been designed so that these techniques can be applied to single, double and interdigitated electrodes. The first prototype PCB has been designed and populated with components, and a number of simulation tests have been performed using a programmable Potentiostat PG580 for proof of principle.

Figure 136 below shows an illustration of the progress in these fields over the last six months in the first year.

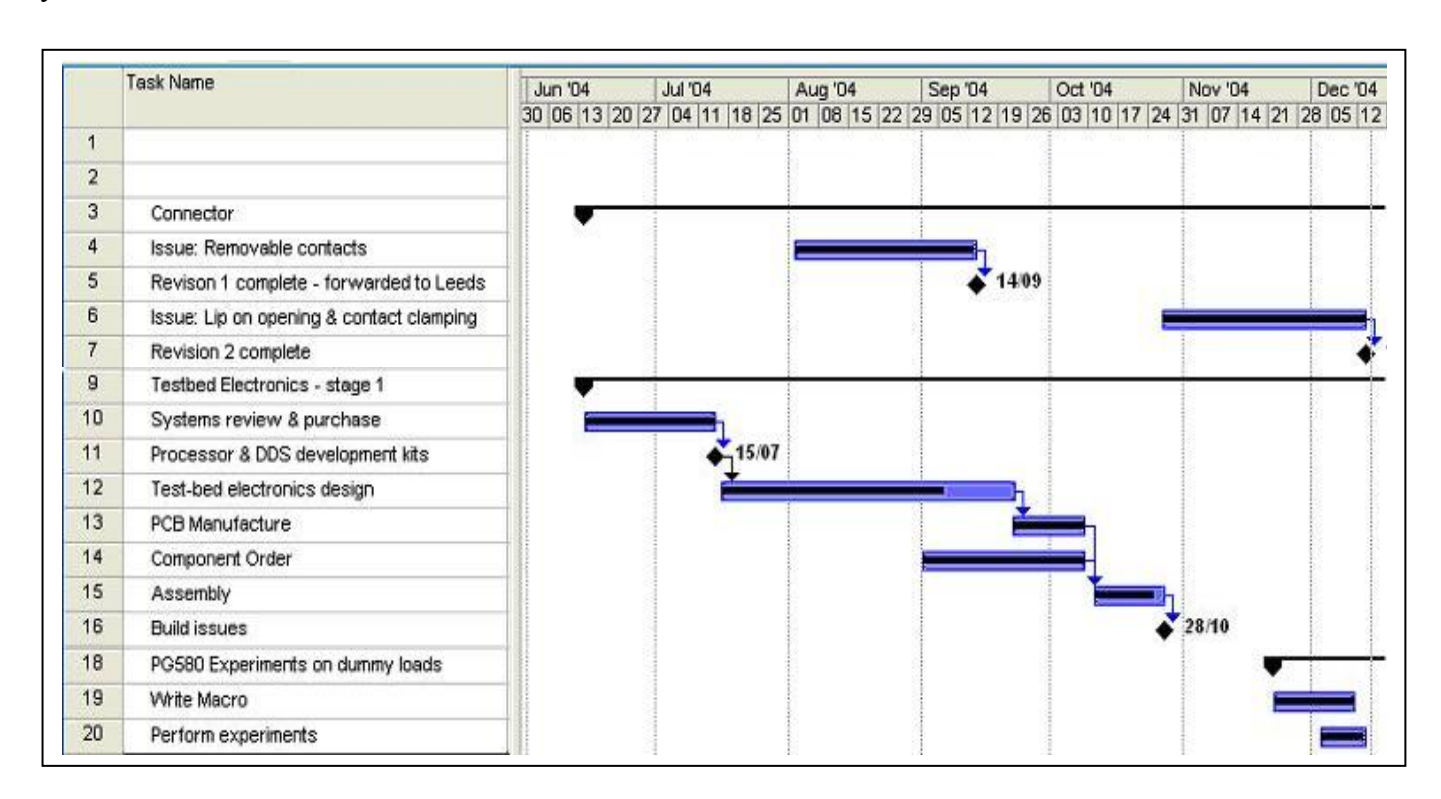


Figure 136. Illustrating the areas of work and the current progress towards end of first year.

The connector has undergone two revisions to allow the unit to have removable contacts so that the user may replace failing contacts, and also to remove issues resulting from the manufacturing process. This was presented and accepted at the 12 month meeting; an order of 100 off was placed at the time. The design of the double connector is shown in Figure 137 (overleaf).

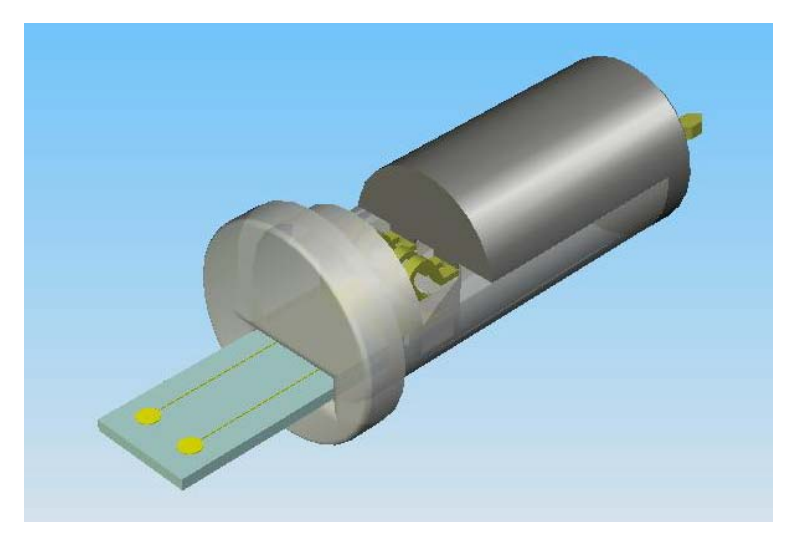


Figure 137. Connector for double and interdigitated electrodes. The design inserts into a 10mm tube for ease of manipulation.

Production of the electronics started after a review of possible methods to apply the techniques. In review it was obvious that flexibility was one of the most essential features and lead quickly to the choice of an embedded microprocessor design. An AMD design was selected due to its speed and simple interface logic, and has resulted in the design of the peripherals board / microprocessor system as shown in Figure 138. This combination provided Uniscan the ability to develop the embedded control software to run experiments as dictated by the PC based control software. The system is designed to run initial diagnostic tests on onboard memory and runs a boot program. Program development was underway by month 13.



Figure 138. Microprocessor and peripherals board.

Uniscan Instruments planned to implement a version of the UiEChem Electrochemistry package, so that the package can communicate with the ELISHA electronics system. UiEChem has provided a Windows™ graphical user interface to display data as required. To ascertain the methods required to produce Pulsed-Waveform spectra, UiEChem has been programmed to control a programmable Potentiostat PG580 such that resonance spectra are acquired from a dummy load. A sample from the results is shown in figure 139. These techniques can further expanded to the higher specifications of the ELISHA electronics.

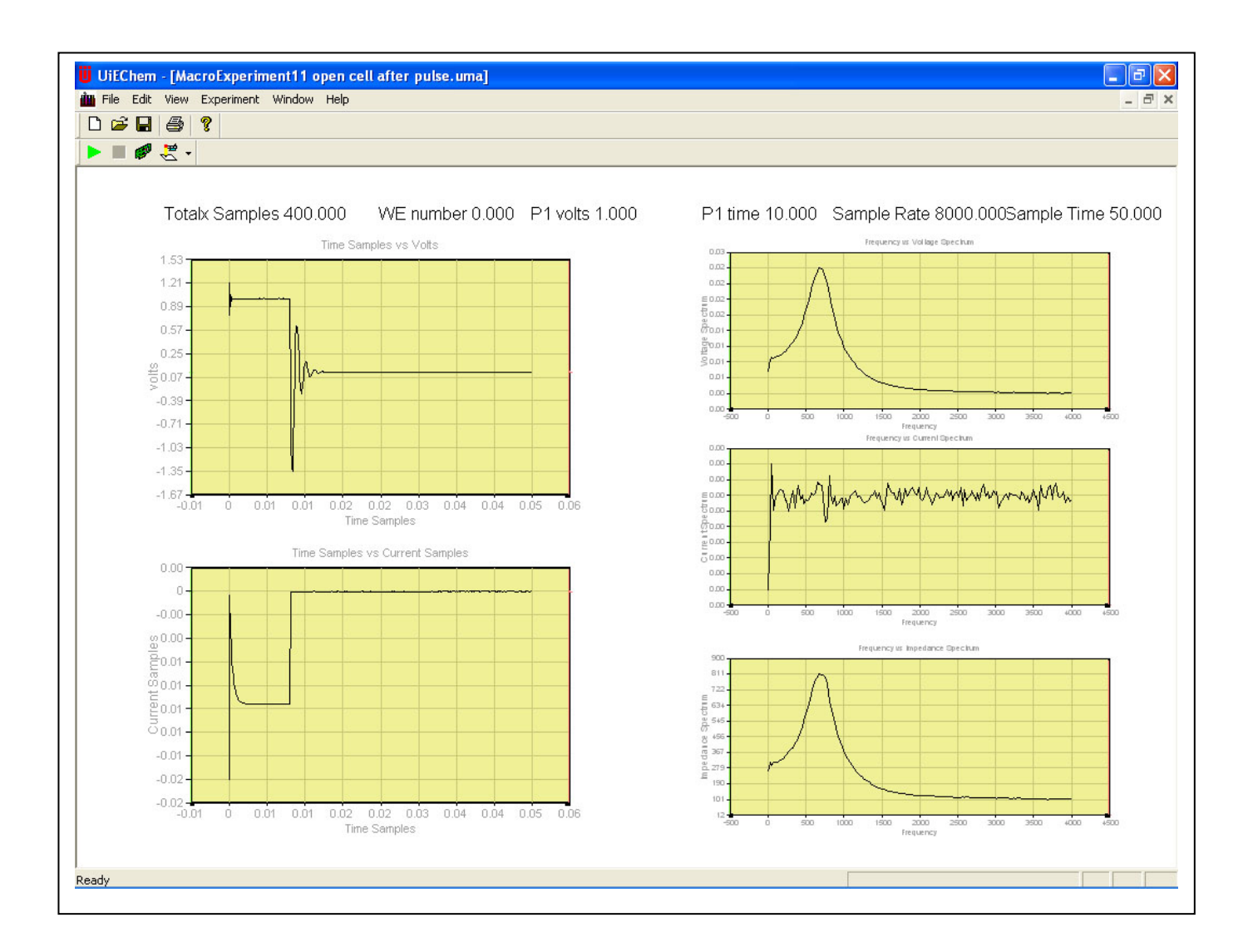


Figure 139. A resonance in voltage and its Fourier transform as a step is applied to a resistive/capacitive/inductive dummy cell.

A significant part of the work that remained was to produce the first prototype by month 18. This included the iterative cycle that encompassed the electronics design and embedded control software. This was in its infancy in month 13 and it was expected that a number of PCB revisions would take place before a working prototype was presented. At the time of the 12 month report, the project was on target to meet the month 18 milestone.

A meeting of the electrochemists and engineers was found necessary to clearly define the specifications of the design of the test bed equipment. This took place on the 9th March 2005 and formed the basis of the construction of the initial test rig completed and demonstrated by the mid-term meeting.

Sensor Test Rig Design Specifications:

This section specifies the functional requirements for the instrumentation developed for the ELISHA project final outcome. As per the ELISHA engineering-electrochemist meeting of the 9th March 2005, the original specification (v1.00) detailed on 12th March 2003 was added to and refined in terms of the final required operating parameters, as detailed below:

Requirements

The specific requirements for the final outcome are listed here:-

- 1. Connection to the ELISHA electrochemical electrodes.
- 2. Connect to the electrochemical cell with two Working Electrodes (WE), one Reference Electrode (RE) and one Counter Electrode (CE).
- 3. The instrumentation will consist of an electronics enclosure connected to a Windows based PC running the control and analysis software.
- 4. Measure the electrochemical impedance of the electrodes in electrolyte using the single sine methodology, with the following parameter ranges:-
 - 4.1. Impedance range 10hm to 1M0hm.
 - 4.2. Frequency range 0.01Hz to 100KHz. (1MHz desirable).
 - 4.3. Electrochemical Cell Modulation range 0.1mV to 1V.
- 5. Measure the electrochemical pulse response of the electrodes in electrolyte using the following techniques: Pulse Waveform Spectroscopy (PWS), Pulsed Potential-Step Voltammetry (PPS) and Pulsed Amperometric Detection (PAD) with the following parameter ranges:-
 - 5.1. Pulse widths to satisfy a frequency range up to 50KHz
 - 5.2. PPS and PWS amplitude variations in the range 1mV to 1V, bipolar.
 - 5.3. PAD amplitude ranges up to 10mA.
 - 5.4. Data Acquisition, 100KHz, 16bits, 100,000 Points.
 - 5.5. Frequency analysis, Discrete Fourier Transform (DFT).
- 6. The system software will provide the following features:-
 - 6.1. Experiment parameter configuration.
 - 6.2. Communications with the system hardware.
 - 6.3. Experiment execution.
 - 6.4. Display of experimental data in graphical and table formats.
 - 6.5. File management of experimental data for storage and retrieval.
 - 6.6. Export of the data in standard ASCII format for use in third party applications.
 - 6.7. Export of the data via the Windows clipboard for use in third party applications.

2.3. Additions from specification v1.00.

During the Engineers-Electrochemists' design meeting held at the University of Leeds on the Wednesday 9th March 2005, it was noted that the ELISHA electronics would be required to measure two independent WE simultaneously. This was noted and added to the design document. The functional parameters for the four types of experiments were discussed and the modifications to specification made accordingly.

Test-bed Instrument:

The following pictures (figures 140 to 142) show the initial test-bed instrument that Uniscan Instruments developed for the ELISHA project. Also shown is the Windows based control interface that controls this ELISHA test-bed.

Electronics



Figure 140. Front of test-bed unit showing "ELISHA v1.00" electronics.



Figure 141. Rear of ELISHA electronics with serial communications port for connection to PC and power supply connections.

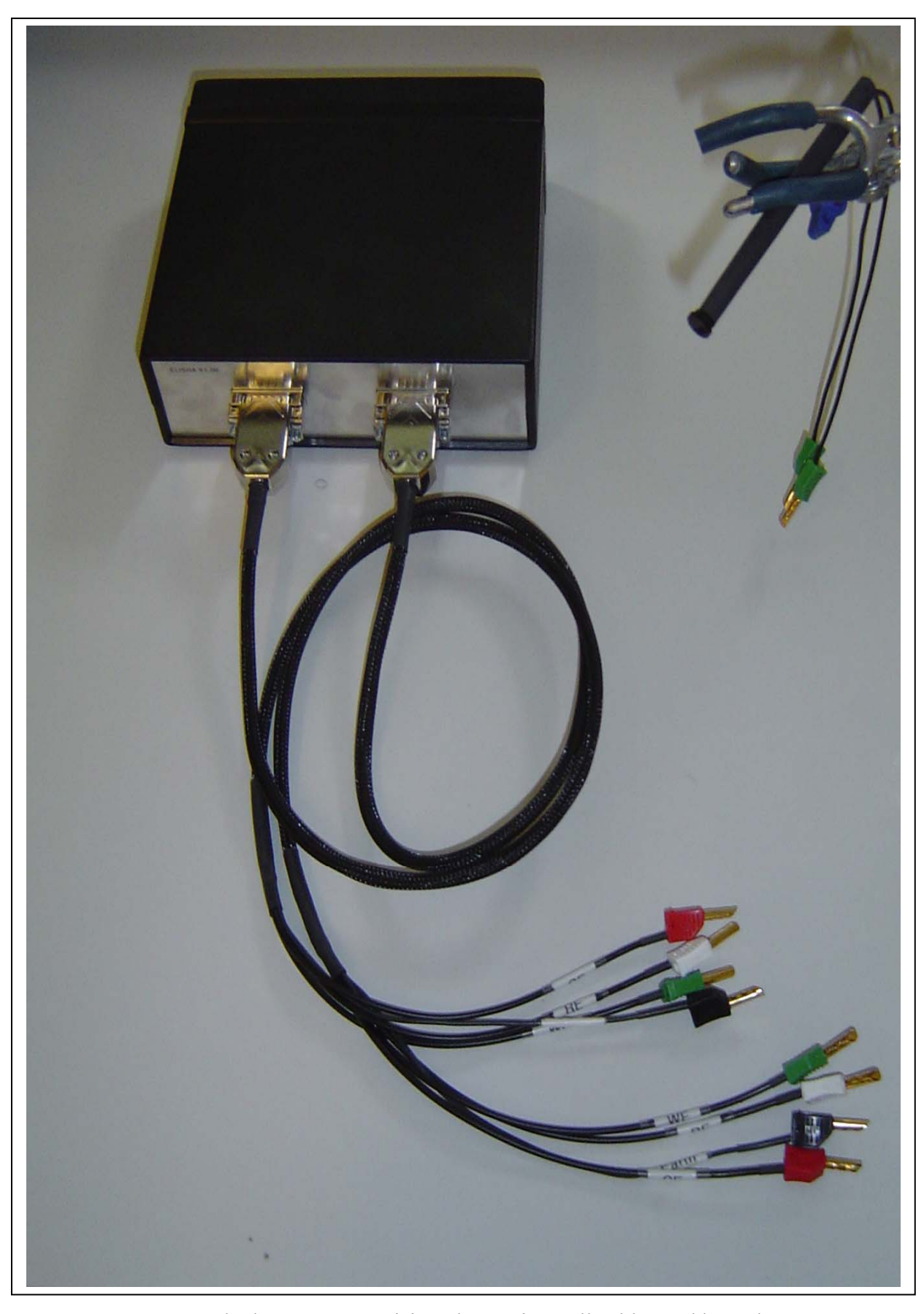


Figure 142. Test-bed system comprising electronics, cell cables and bespoke connectors

Software Interface.

Displayed in the following section are pictures of the ELISHA Windows software (figures 143, 144). This is the main control mechanism by which users define the experiment parameters and display the results.



Figure 143. Overall ELISHA Windows control interface

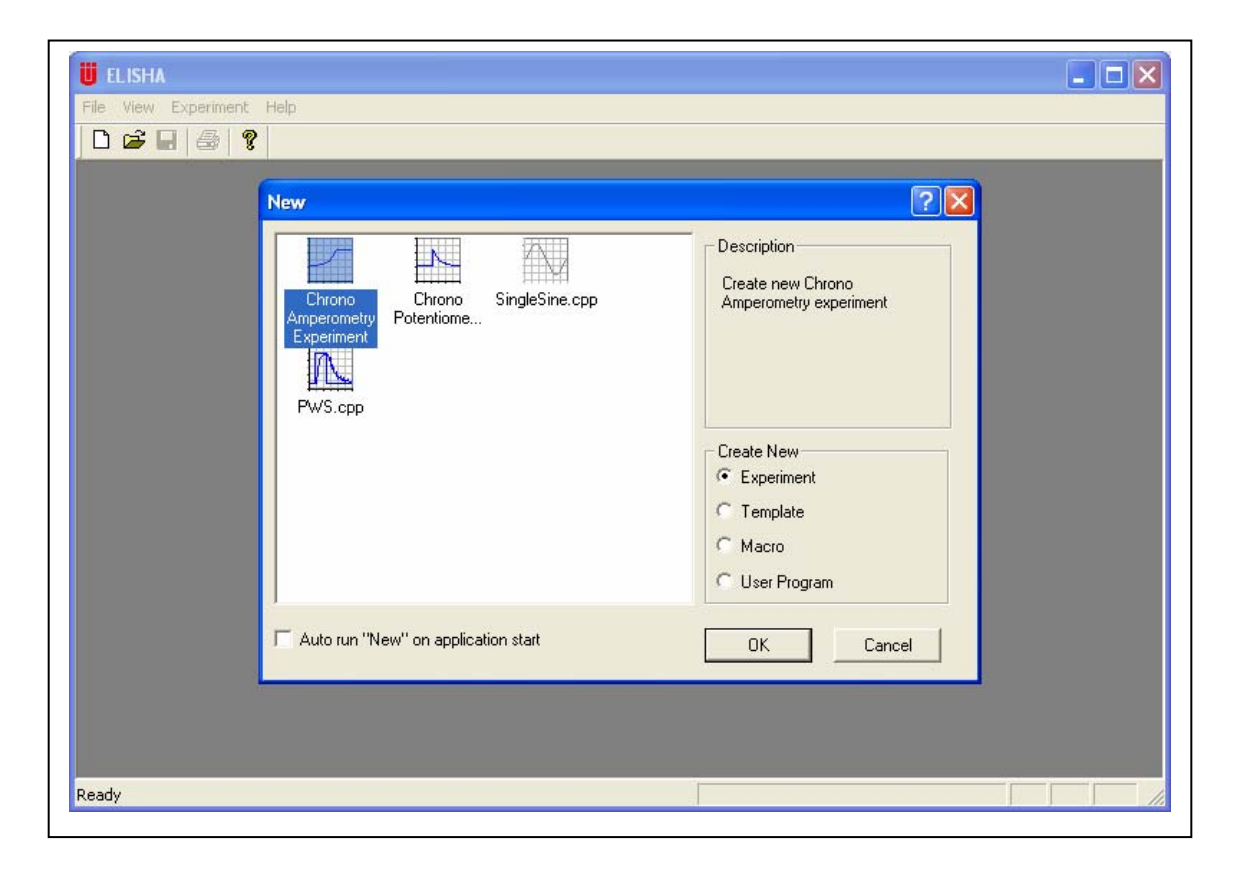


Figure 144. New Experiment selection box showing the four main experiment types that were used in the ELISHA project.

Review of Progress to Mid-Term:

With reference to the original specifications defined under the design specification for the test bed, the following was achieved by mid-term:

The bespoke ELISHA connector (item 1) for use with the electrodes that was used in the ELISHA project was completed and accepted by the ELISHA partners. A majority of orders have been received from those partners that requested a batch of connectors and Uniscan proceeded with fabrication when all orders were received, delivering connectors to the partners in good order.

Items 2 and 3 of the specification were met with the test-bed unit. However, the addition of an extra WE as requested at the 9th March 2005 meeting between Uniscan Engineers and ELISHA electrochemists was not fully implemented by mid-term. As a measure to satisfy this additional requirement, two multiplexed WE were supplied in the test-bed unit to emulate the dual WE final requirement.

Item 4 of the design specification was incomplete by mid-term (impedance measuring capabilities), however this was not detrimental to the project as all electrochemist partners have their own impedance rigs available and the pulsed techniques were considered to have a higher priority of implementation for this reason.

The pulsed techniques comprise PWS, PPS voltammetry and PAD as described in item 5 of the specifications. All three techniques were implemented with the ability to specify pulse-widths between tens of microseconds and seconds.

The experiments available to users allow for variable amplitude and duration with pulse amplitudes ranging from 1mV to 2volts. Similarly, data acquisition is currently possible at 16bit resolution and 80KHz, with the number of points limited to 128K samples. Finally, the system incorporates the FFT technique to complete the requirements of the PWS technique.

Item 6 defines the functionality of the Windows based software. Here, all items have been addressed giving the user control over the experiments, configurations, execution, data display and export.

Mid-Term Summary,

Uniscan completed a significant proportion of the requirements outlined in the specification by mid-term as required. The test-bed performs PPS, PAD and PWS experiments.

As a test bed it satisfied the requirements of D18 and formed the basis of the final prototype due at the end of month 36.

At the mid-term stage, the test-bed electronics and the controlling software were not yet fully tested and contained minor errors, which were dealt with as they were identified, working with the respective partners.

Further development of the test-bed unit was scheduled up to month 30, however it was decided to go directly to the laboratory prototype as the first test-rig was quite successful, negating the need of a second iteration of the test-rig electronics.

Bespoke connectors were supplied to all partners who requested them from Uniscan. The general functionality allows connection to both single (P3, P10), and dual (P4, P5) electrodes. In total, 95 connectors were supplied, comprising housing, lid and gold-plated contacts.

The ELISHA test bed electronics and control suite PC software underwent substantial work to ensure its stability, user friendliness and suitability to the requirements given by the ELISHA project management board and associated scientists. With the test bed constructed, there are seven specific experiments that a user can access in the general fields of Pulse Waveform Spectroscopy, Pulsed Amperometric Detection and Pulsed Potential Step Voltammetry. The techniques and example results were discussed separately.

The first prototype system was delivered to the University of Leeds on the 16th November 2005. A number of experiments were performed at the University to demonstrate the equipment's operation and the viability of the techniques to detect binding events on a sensor surface. Different responses were recorded from various electrode configurations including:

- bared gold electrode
- self-assembled monolayer (SAM) coated electrode
- SAM coated electrode + antibody fragment FAB Atrazine
- SAM coated electrode + antibody fragment FAB Atrazine + Atrazine
- Removal of above products with Imidazole.

These results are shown and discussed in WP5, pages 64 - 66.

A number of other tests were also performed including the ability to detect polypyrole binding with antihaemoglobin and haemoglobin, and also the repeatability of the measurements, described in WP7, page 81.

Feedback has been collected from the University of Leeds on the functionality and usability of this first prototype system. In particular, the main items that were noted are:

- Good Response.
- Reproducible.
- Quick.
- FFT Data was very useful.
- Differential of Data function would be useful.
- Automatic File Naming and Saving would be useful.
- For long Measurements, throw away data function would be useful.

It was reported that the differentiated data is particularly useful. This functionality has been obtained by the use of Microsoft Excel. Uniscan have addressed the ability to throw away inconsequential data during extended measurement periods; the last item on the list. All other comments seem positive.

Software Configuration of Prototype Electronics:

Figures 145 - 147 (overleaf) show the user interfaces of the test bed electronics including the configuration box for the three main types of experimental interrogation;

Pulsed Potential Step Voltammetry (PPS Voltammetry), Pulsed Amperometric Detection (PAD) Pulse Waveform Spectroscopy (PWS).

Of these the last one seems to be the most important and most useful technique.

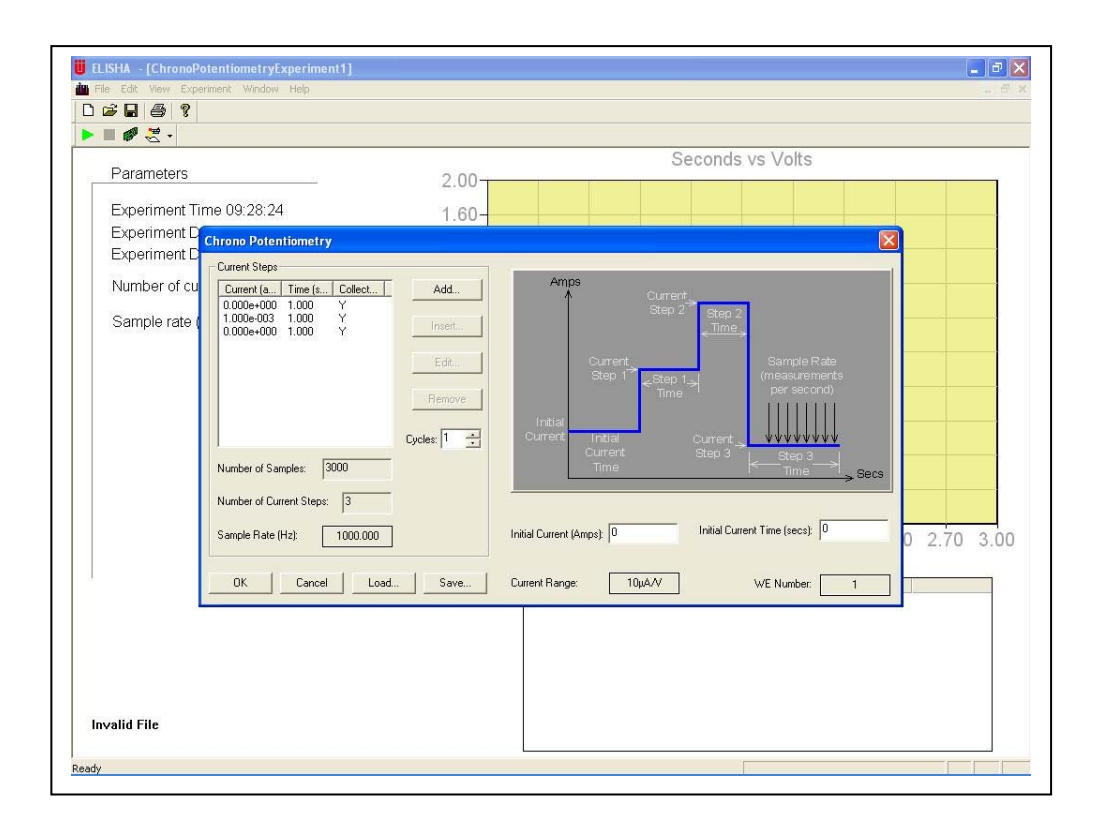


Figure 145. An example of the main interface for a Chronopotentiometry (PADs) experiment. In the top level configuration dialog box, it is possible to add current steps, acquisition rates, whether or not to acquire data, the instrument current range and working electrode being addressed.

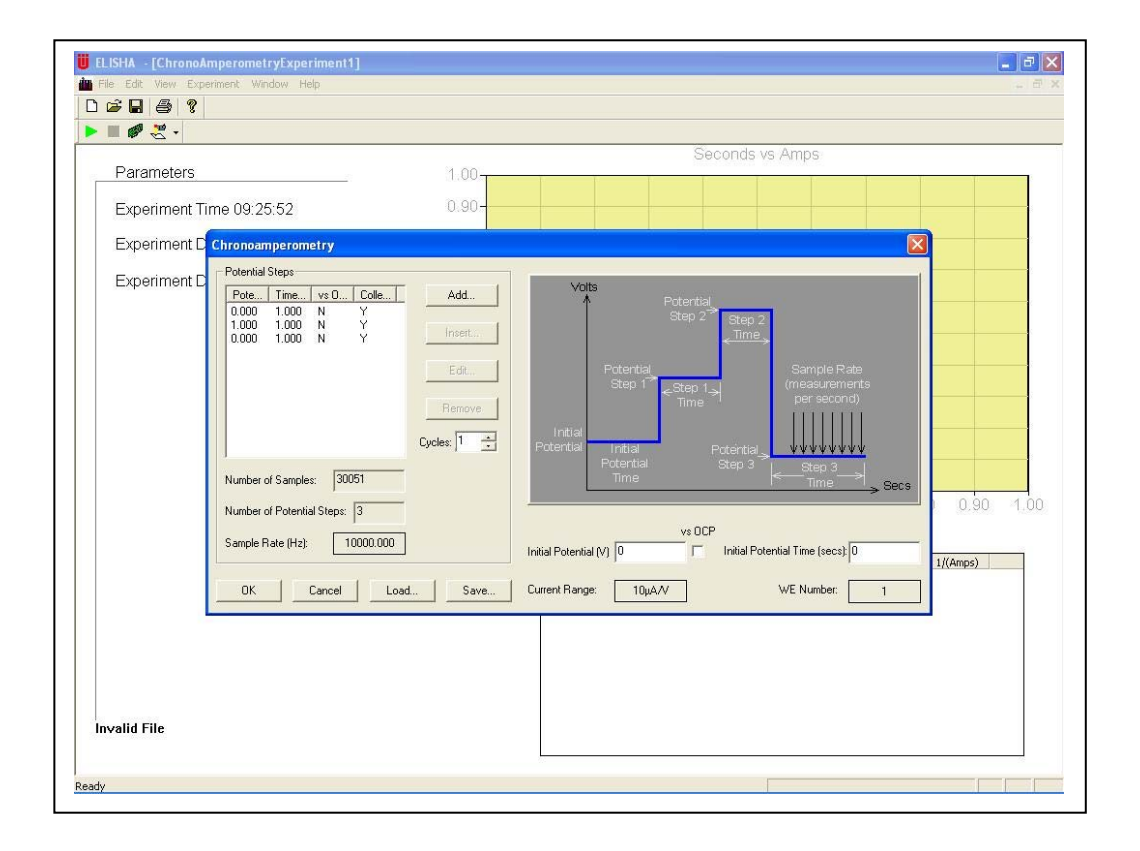


Figure 146. A similar configuration screen is used for the Chronoamperometry (PPS) experiment as for the PADs screen using similar controls to dictate the voltages applied to a sample.

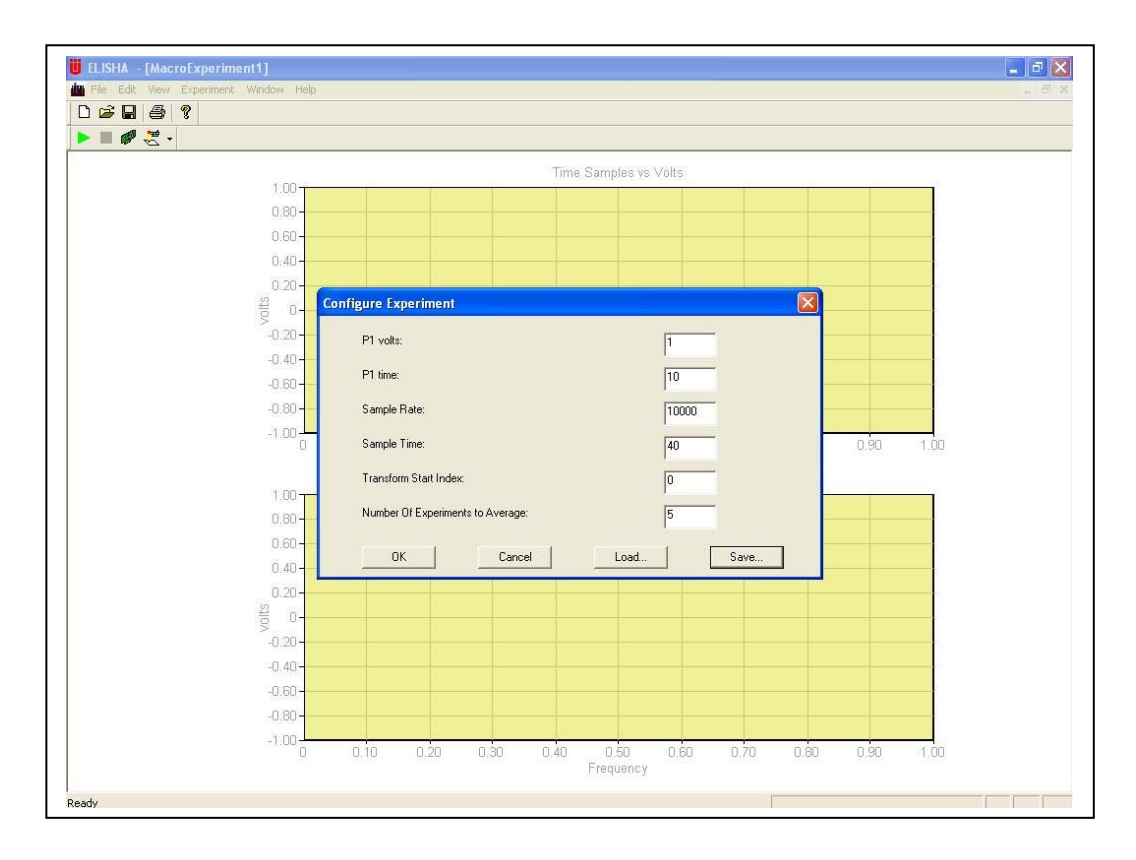


Figure 147. The PWS screen shows the user the time domain and the Fourier transformed data. Here, a user defines the pulse width and voltage, the acquisition time and the window from which data is taken for the Fourier transform. Finally, it is possible to repeat and average the results by stating how many experiments should be performed.

An example of the PWS raw data output is shown below, Figure 148. This is from the experiments described on pages 64 – 66 using SAM anti-atrazine immunosensors.

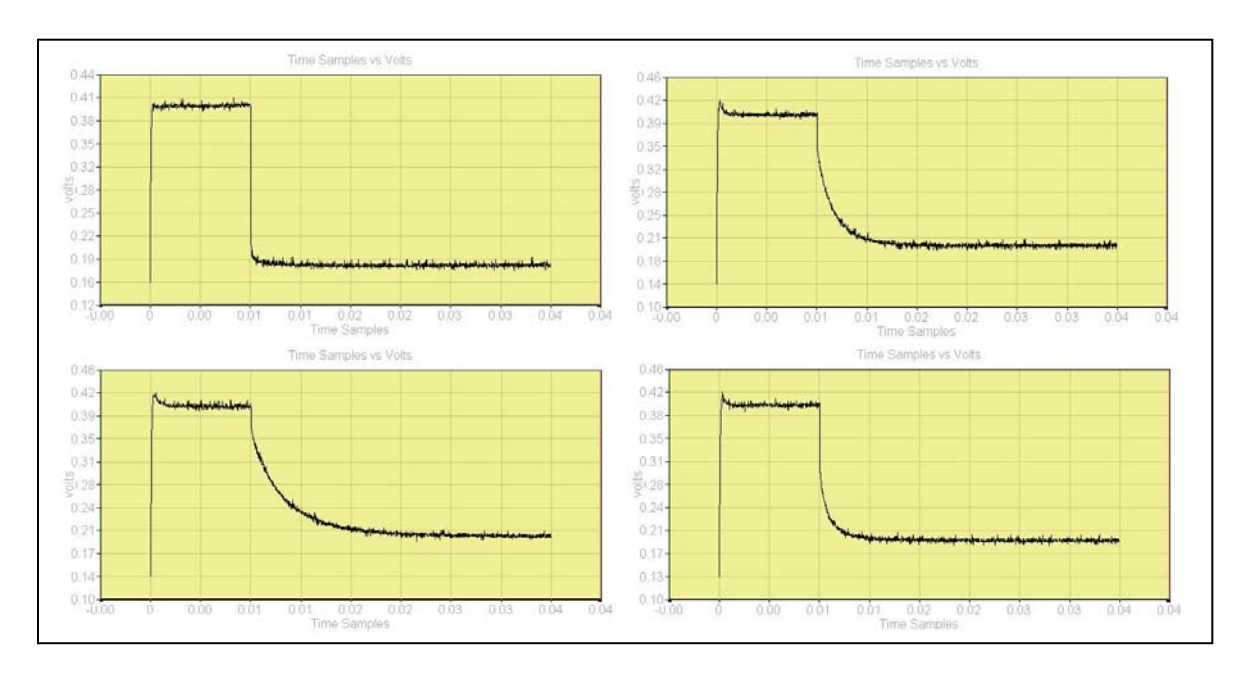


Figure 148. Example time Domain Traces of 1) Top Left: Bare Gold Sensor, 2) Top Right: SAM with antibody fragment, 3) Bottom Left: Binding to atrazine, 4) Bottom Right: Removal of antibody by imidazol.

Laboratory Prototype Electronics (Second Prototype):

The testing of the first DC test rig prototype was ongoing after delivery and was used mainly by partner 1.

The design of the lab prototype was in progress from mid-term and combined the functionality of the first DC test rig with the more familiar AC impedance technique. The design engineering process was expected to provide the main PCB ready for assembly by March/April 2006 and this proved the case. Assembly, testing and revising of the equipment then took place leading up to the next deliverable of D19 (August 2006).

Figure 149 below shows the functional schematic for the front-end interface that will be used to acquire the data for PPS, PADs, PWS, and impedance techniques. The majority of work in the latter 18 months was focused on this area of electronics as the control and data acquisition systems have been established on the whole.

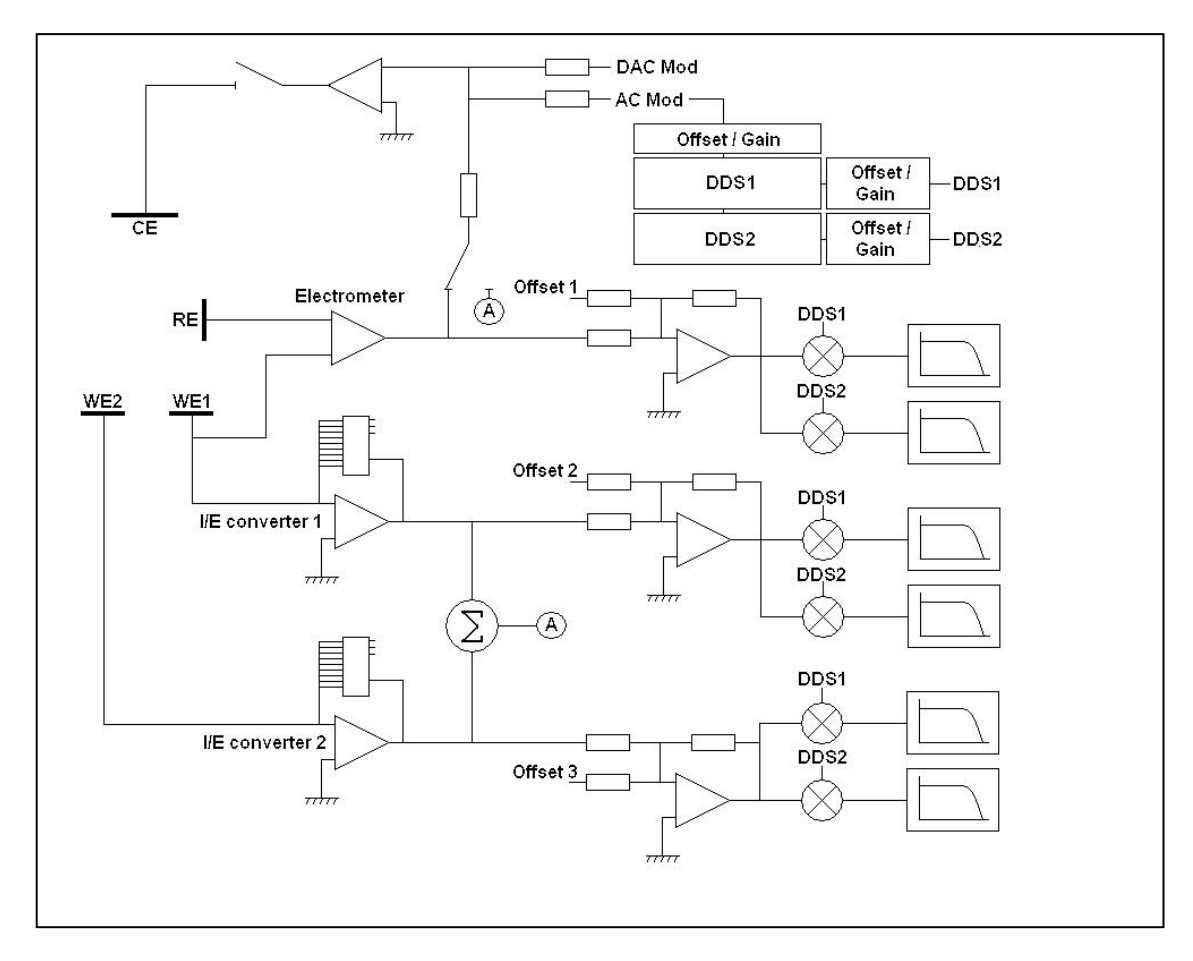


Figure 149. The dual WE designed provides connection to the electrochemical cell and gives simultaneous monitoring and acquisition of the reference and currents through both active and baseline sensors. The ability to apply pulsed and DC currents/potentials is applied through the DAC mod input taken from the control electronics. Similarly, it is possible to apply AC modulation through the AC Mod input, and determine the magnitude and phase response of RE, WE1 and WE2 by the demodulation circuitry.

The following have been added to the general functionality of the 1st prototype.

- Simultaneous Dual Working Electrode acquisition.
- USB interface to PC.
- Additional Experiments available (CA, CP, CV, DFV, LV, NPV, SWV, OCP) on single WE.
- Main experiment macros (PPSV, PADs, PWS) converted to operate with dual WEs.

- Raw data from dual working electrodes available in tablature format.
- No stop-reconfigure to re-run experiments. Waveforms and timing are now precise.
- Automatic baseline (background) subtraction performed before graphing.
- Help files available for the Windows application and the PPSV, PADs and PWS macros.
- Easier and more intuitive experiment configuration.
- High accuracy data acquisition trigger/synchronisation.
- Polarising/Depolarising double pulse experiments for the dual WE techniques.
- Two acquisition points definable for the PPSV and PAD, giving four raw data streams.
- User feedback incorporated, e.g. multi-run experiments, throw-away data, etc.

The instrument does not include single-sine impedance capabilities as originally intended. The single-sine impedance technology was demonstrated as a Frequency Response Analyser component form at the 2006 Cranfield meeting; however, although this section of the electronics showed good response for a 'standard' dummy cell, its operation was limited in terms of its bandwidth and its susceptibility to noise and drift when measuring small signals. Revision of the printed circuit board to reduce these effects is taking place, however, it was not possible to bring this part of the electronics up to the desired specification and meet the instrument handover at the 2007 Grenoble meeting. The options available were discussed with Tim Gibson and Paul Millner and attention was focused on the pulsed techniques, thereby giving access to the most interesting techniques so that they could be continued to be investigated. This allowed the laboratory prototype instrument to be handed over at the January 2007 meeting.

The laboratory prototype (second prototype) is discussed in WP9, p156.

Workpackage number:

W7. Signal Generation and Non-Specific Binding Optimisation.

Objectives. To determine the origin of signal generation in the immunosensors fabricated and relate this to the matrix used and the method of immobilisation. To determine the parameters defining non-specific signal generation and to reduce the non-specific effects by a number of experimental means.

Project Timeline	1 2 3 4 5 6 7 8 9 10 11 12 13 14 15 16 17 18 19 20 21 22 23 24 25 26 27 28 29 30 31 32 33 34 35 36
Workpackage 7. Signal Generation	

The improvement of signal generation was an area investigated immediately since this was intimately connected with the immobilisation strategies in W5. This was important for investigations into the actual origin of the signal being recorded in this workpackage.

The original technique of immobilising the antibodies into growing polypyrrole films was the starting point of the work. Co-polymerisation of an existing anti-digoxin antibody as a model into a polypyrrole layer showed clear increases according to the amount of electric charge passed through the electrode during polypyrrole formation (figure, however the quality of the polypyrrole film prepared from solution of pyrrole-antibody was lower compared to pyrrole-Cl system. This agreed with the original observations on which the project was based.

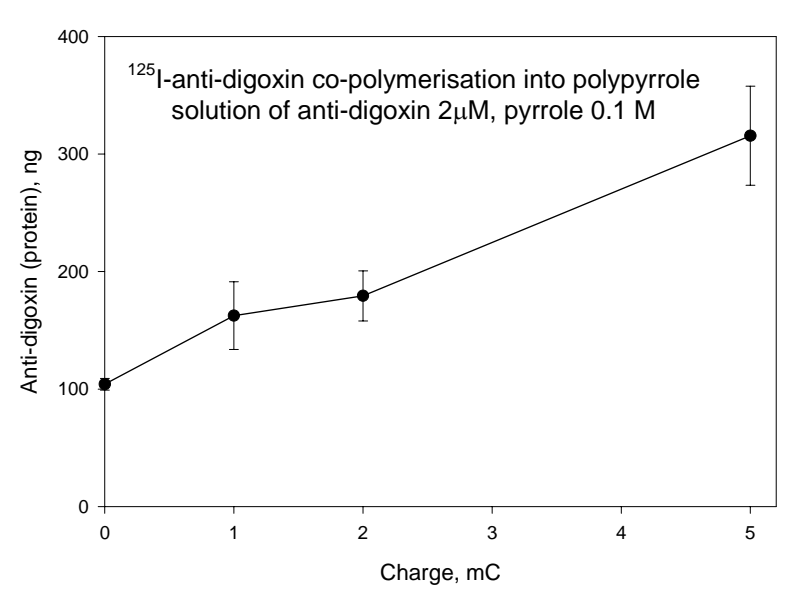


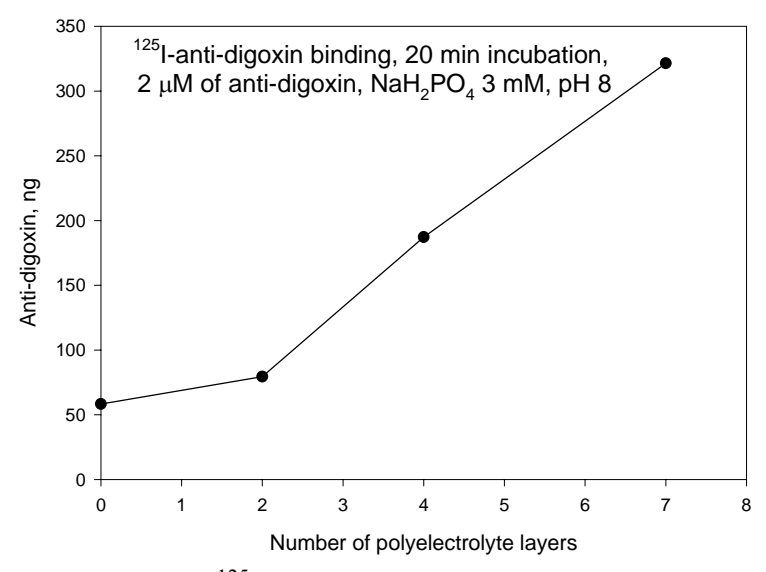
Figure 150. Dependence of [¹²⁵I]-antidigoxin amount co-polymerized into polypyrrole from solution of antidigoxin 2mM, pyrrole 0.1 M on charge passed through electrode.

It was noticed from past experience in the immobilisation strategies that using polyelectrolytes to form a non-covalent electrostatic layer, sensors could be made more sensitive to the respective analyte being measured and less susceptible to non-specific interference. Checking this technique with the polypyrrole – antibody model gave some interesting results in the immobilisation technique using the respective polyelectrolytes shown below (figure 151).

$$\begin{bmatrix} -CH_2 - CH - \\ \\ SO_3 - Na^{\dagger} \end{bmatrix}_n$$

Figure 151. Polystyrene Sulphonate Poly(diallyldimethylammonium) chloride PDDM

To increase the capacity of polypyrrole for antibody electrostatic non-covalent immobilization, polyelectrolyte multilayers were prepared on the polypyrrole surface (figure 152 and scheme depicted on page 55, WP4).



[¹²⁵I]-anti-digoxin binding, 30 min incubation in 2 mM of anti-digoxin, NaH₂PO₄, 3 mM, pH 8. Polyelectrolyte layers made by incubation of the electrode in solutions of polyanion and polycation respectively. First incubation was made with polyanion. Each layer consists of both polyanion and polycation.

Figure 152. [125]-anti-digoxin electrostatic non-covalent immobilization onto the polypyrrole-gold electrodes was increased by polyelectrolytes depending on number of polyanion-polycation layers.

Pulsed Amperometric Interrogation.

Some original work was done many years ago with pulsed amperometric interrogation of antibody sensors which indicated changes can be seen on antibody antigen binding. Using the new sensors fabricated, an initial series of experiments have been attempted to see what the effect of pulsing the surface would be. These experiments were thought of as forerunners of the planned experiments using the new ELISHA interrogation electronics, as pulsing was done using the AutoLab analyzer in Partner 1's laboratory. Polyelectrolyte loaded sensors described on page 42-43 and above were used for the experiments, with a pulsing frequency of -0.2V for 1 second followed by +0.6V for one second over a 30 minute timescale Transient currents were measured each 0.005 second. Both anti-digoxin (0.1 mg.ml⁻¹) and digoxin solution (1uM) were passed over the electrode in sequence to first immobilise the antibody by electrostatic adsorption and then follow the antigen response. The graphs shown (figures 153 - 156) indicate distinct changes in the amplitude of the transient currents measured.

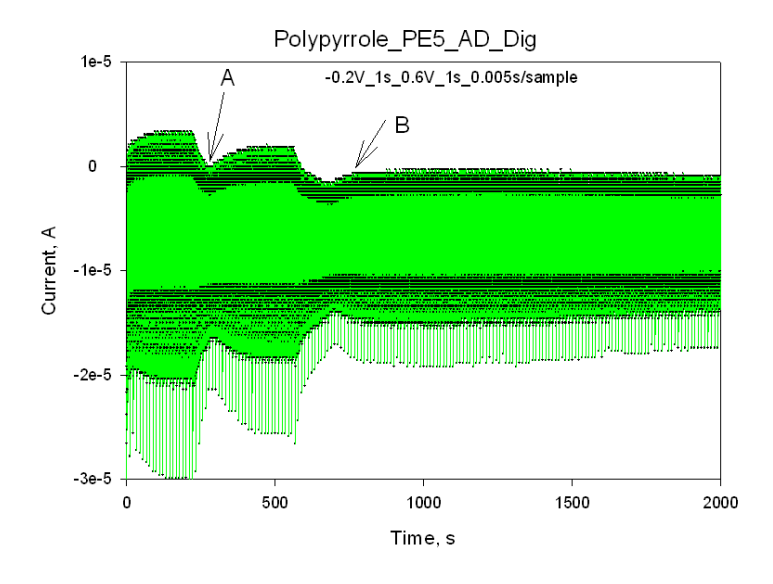


Figure 153. Pulsed detection of antibody loading and antigen binding

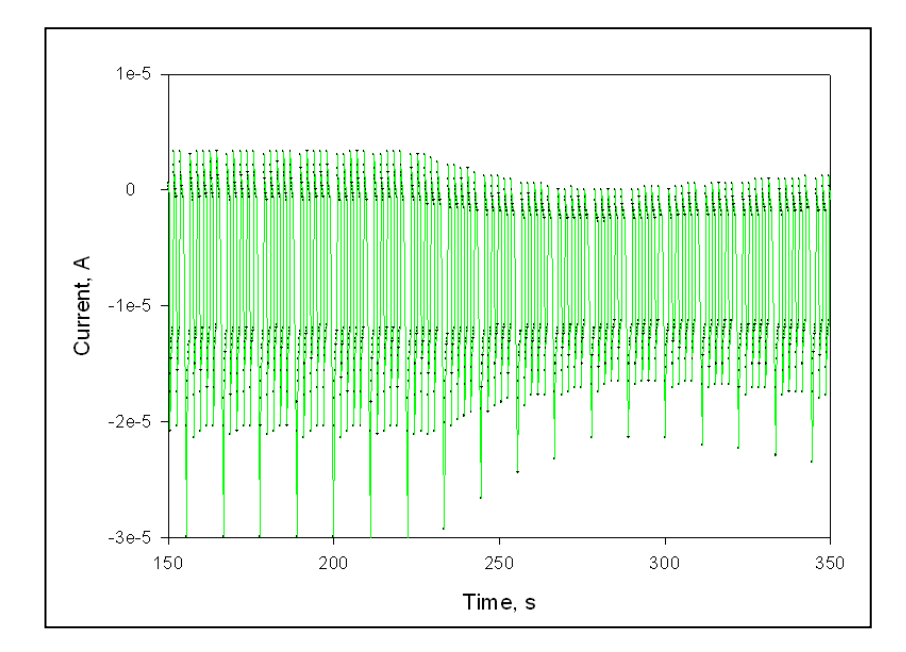


Figure 154. Expanded view of pulsed amperometric result between 150 and 350 seconds. This shows the changes in amplitude when antidigoxin is added to the polyelectrolyte layered sensor. It can be clearly seen a reduction in current transient occurs.

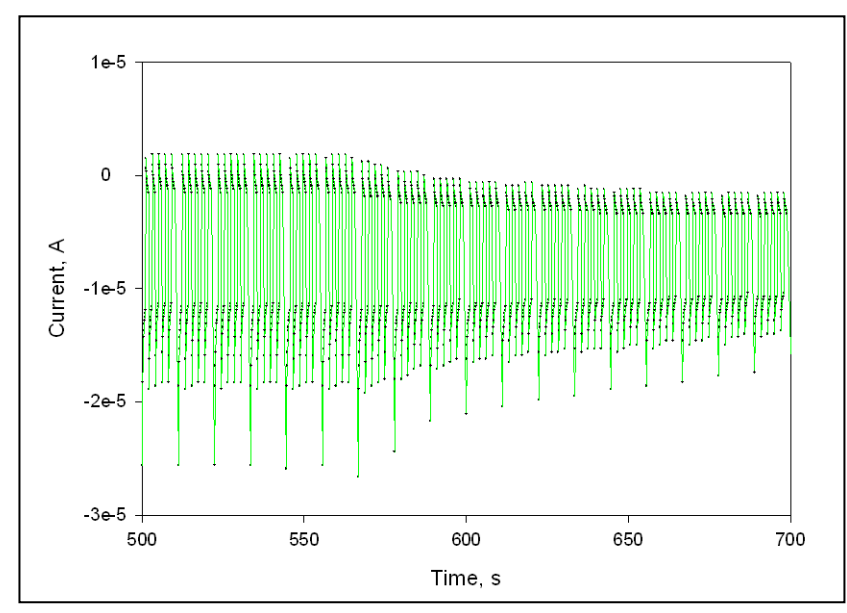


Figure 155. Expanded view of pulsed amperometric result between 500 and 700 seconds. This shows the changes in amplitude when digoxin is added to the antibody loaded polyelectrolyte layered sensor. It can be clearly seen a second reduction in current transient occurs indicating binding of the antigen to the antibody.

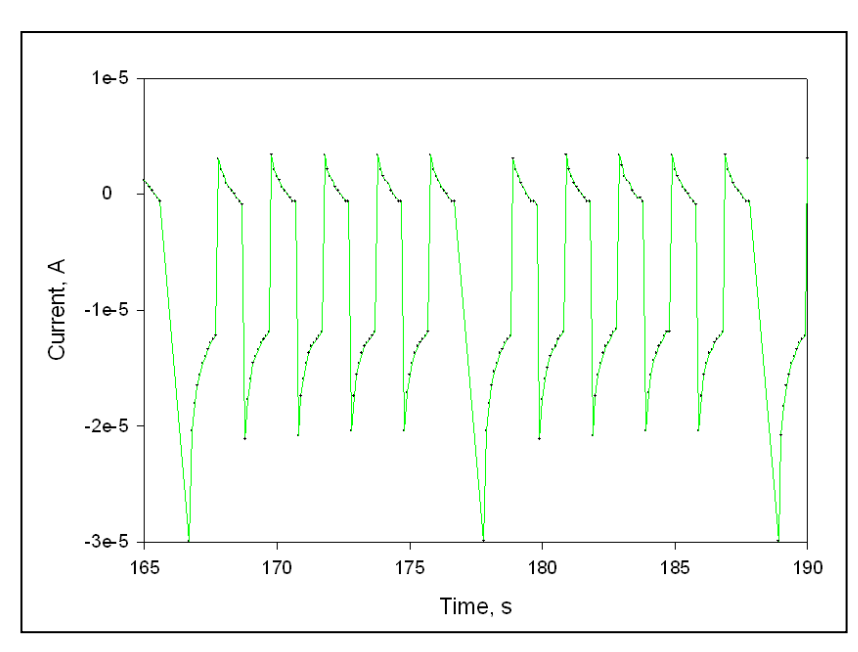


Figure 156. Further expanded view of pulsed amperometric result between 165 and 190 seconds. To show the shape of the current transient. The pause between pulses every group of 5 is an artefact introduced by the interrogation system and this should be removed when the ELISHA test bed electronics become available. **See figures 157 and 158 overleaf.**

Pulse Interrogation of Polypyrrole Matrices using the First Prototype Electronics.

Following on from the successful results of SAM immobilised anti-atrazine Fab using the first prototype electronics in WP5, page 65-66, the pulse interrogation technique was attempted with anti-haemoglobin-polypyrrole sensors. The results are shown below in Figures 157 and 158.

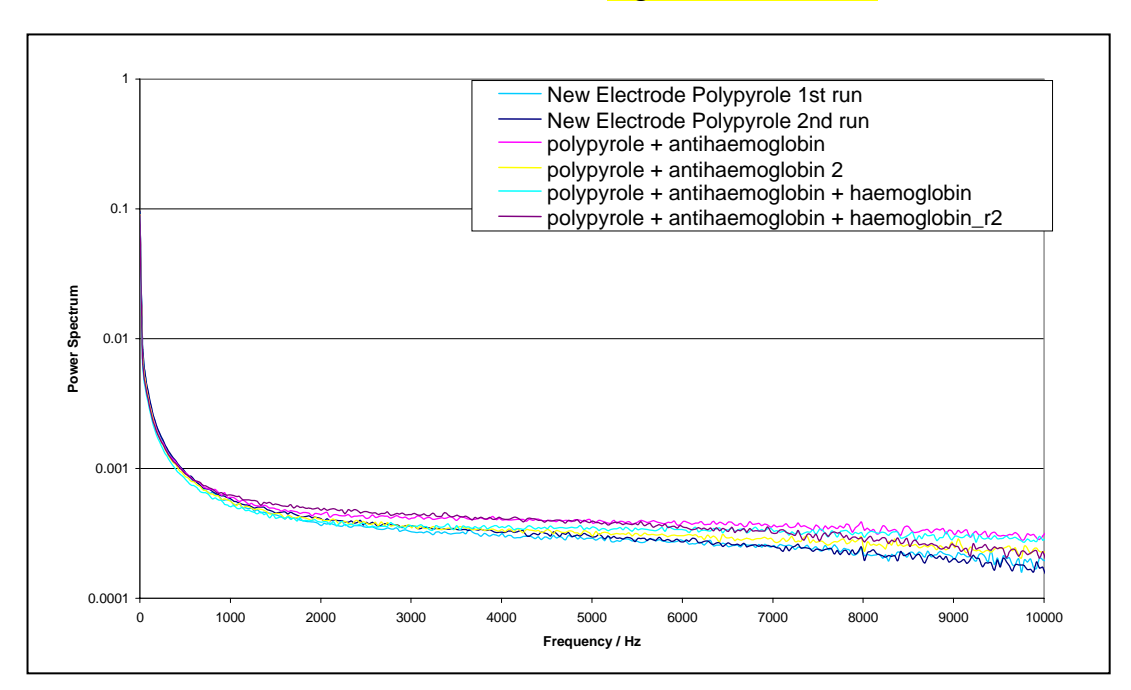


Figure 157. Pulse interrogation of polypyrrole-anti-haemoglobin sensors produced by non-covalent binding of the antibody to the polypyrrole surface. The results are small and difficult to see but they are significant. The differential power spectrum is shown below.

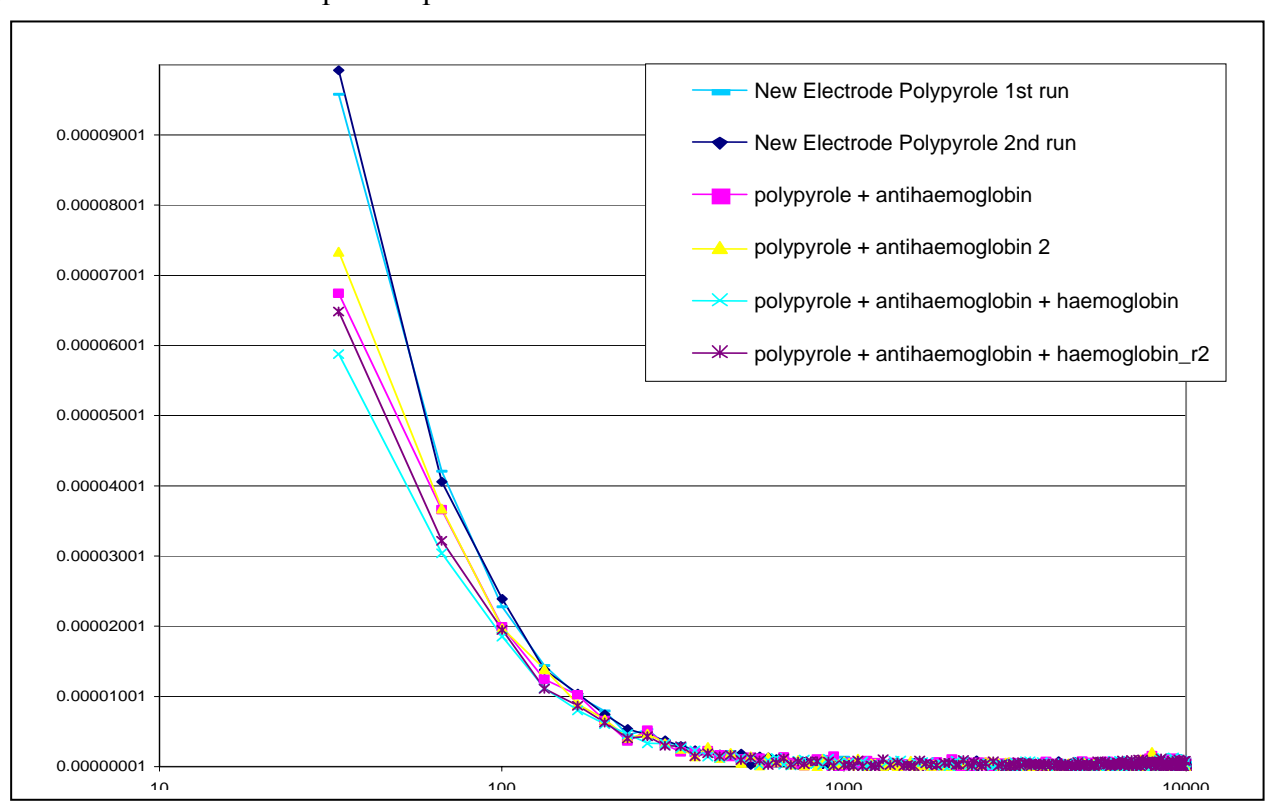


Figure 158. Differetial power spectrum for polypyrrole –anti-haemoglobin. The responses are small but can be seen, indicating that the pulse interrogation works using antibody loaded conducting polymer layers.

The first prototype electronics showed that the pulsed interrogation of antibody sensors is potentially a good route for generating discriminant signals.

The technique appears not to be destructive to the normal polypyrrol layers unlike the traditional electrochemical methods. This is thought to be due to the polarisation time being very short, 10 milliseconds rather than a few minutes.

Signal Generation Observations from ssDNA – copolypyrrole matrices.

Based on the electropolymerised matrices and ssDNA studies being done by Partner 3, some insights into the signal generation have been observed. The functionalisation of polypyrrole by the ss-DNA probe has been controlled by a) infra-red measurements and b) cyclic voltammetry. It is the CV work that has given some details as to the generation of the signals.

a)IR measurements

The amino-substituted oligonucleotide, ssDNA, was grafted on the copolymer by a direct chemical substitution of the easy leaving group, N-hydroxyphtalimide, by the terminal amino groups. This reaction was followed by FT-IR spectroscopy (Figure 159) which showed the disappearance of the bands associated with pyrrolidinedione at 1820 cm-1 and 1786 cm-1 with the concomitant appearance of a new band at 1715 cm-1 characteristic an amide function which confirms the formation of amide bond formed between the activated polypyrrole and the amino groups of ss-DNA. The appearance of an intense band at 1590 cm-1 may be associated with the carbonyl groups of the ODN bases, and the bands at 695 cm-1 and 790 cm-1 may be associated with the phosphodiester bond of ODN.

The time necessary for the reaction to be complete was determined both by the measurement of Open Circuit Potential monitored during reaction and FT-IR measurement and was evaluated to less than two hours.

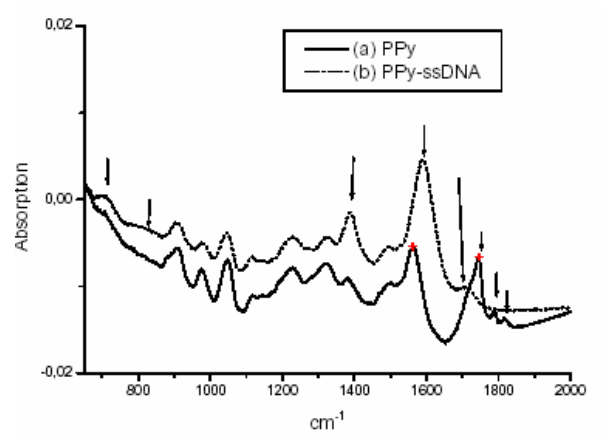
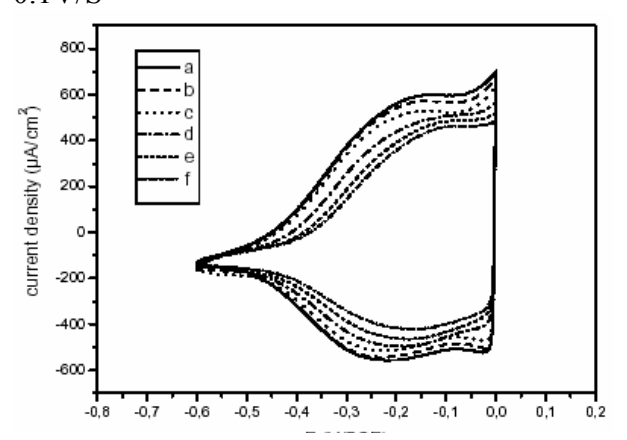


Figure 159: FTIR spectra of a polypyrrole film deposed on a gold electrode a) poly(PyCOOH, PyNHP), b) poly(PyCOOH, Py-ss-DNA)

Figure 160: Electrochemical voltammograms of modified electrode Poly(PyCOOH, Py-ss-DNA), after hybridization with its complementary target in phosphate buffer solutions pH 7 containing 137 mM NaCl and 2.7 mM KCl and DNA target a): 0 nmoles, b): non complementary ODN, c-f): complementary DNA of 0.5 nmoles/ml (c), 1.5 nmoles/ml (d) 3.5 nmoles/ml (e) and 5.5 nmoles/ml (f). Scan rate 0.1V/S



b) Cyclic voltammetry

The modified electrode was electrochemically characterized in phosphate buffer at pH 7, and the voltammogram shows reversible redox signal with an oxidation peak at -0.2 V/SCE associated with the oxidation of the polypyrrole backbone. These low oxidation potential values, together with the symmetry

of the redox wave, confirmed the high electroactivity of the ODN substituted polypyrrole film in aqueous medium. The modified electrode was incubated with both with a non-complementary target and complementary target. When incubated in the presence of the non complementary oligonucleotide the electrochemical response of the modified electrode remained unchanged. On the other hand, incubation with the complementary DNA target with various concentration between 0.5 to 5.5 nmole/ml leads to a significant modification of the voltammograms (Figures 159 and 160 - previous page). Indeed it appears that hybridisation reaction induces a decrease in the current density together with a shift of the oxidation wave to a more positive potential.

Similar results have already been described as a result of the recognition process in conjugated polyheterocycles when functionalised with other recognition centres such as cation complexing crown ethers or enzyme-inhibiting peptide. The increase of oxidation potential can be attributed to the hindering of conformational modifications in the conjugated polymer backbone during its oxidation. In its neutral aromatic state the polymer chain is more flexible and hence the pendant groups are more mobile, whereas it adopts a rigid quinoid structure upon oxidation. Any increase in the bulkiness and stiffness of the pendant groups following the recognition process, induces a higher energetic constraint on the planarization of the polymer backbone, and hence an increase in its oxidation potential. The decrease in current may be due to the modified surface blocking the penetration of counterions.

Such insights into the changes in oxidation potentials and decreases in currents may be directly comparable to the efficient monitoring of other affinity reactions, including antibody binding of antigens.

Partner 1 has demonstrated that polyaniline films respond to electronic stimulation by changing mass due to ion movement. This has been done just for polyaniline in the absence of antibody at this stage, however in the future antibody loaded films will be investigated. It is very clear that the redox state of the polyaniline influences the ion content. Also as the films age the selectivity between cations and anions is reversed, figures 160-162

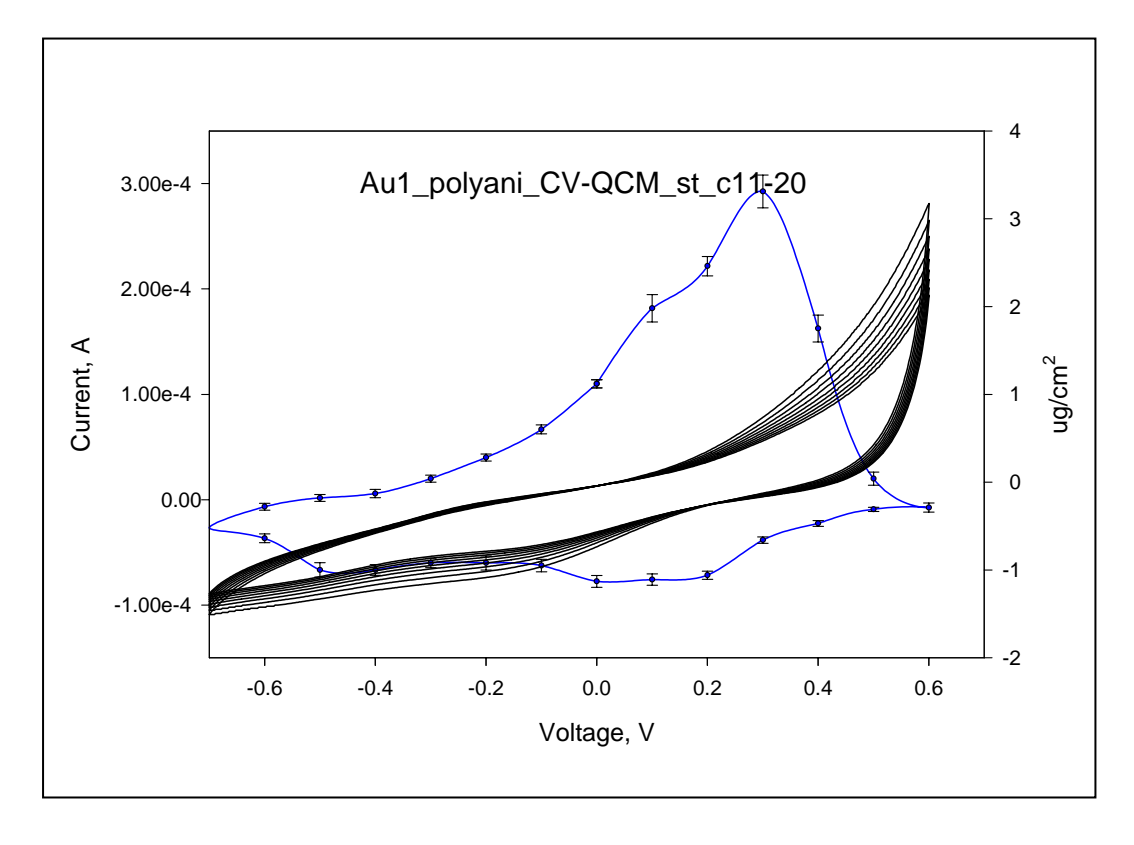


Figure 160. Cyclic voltammogram (cycles 11-20) of polyaniline superimposed with mass change in $\mu g.cm^2$ due to <u>anions</u> moving in and out of the polyaniline matrix. CV was done between -0.7V to +0.6V in 0.5M KCl. Polyaniline was deposited from 0.2M aniline sulphate solution in the presence of 0.3M KCl.

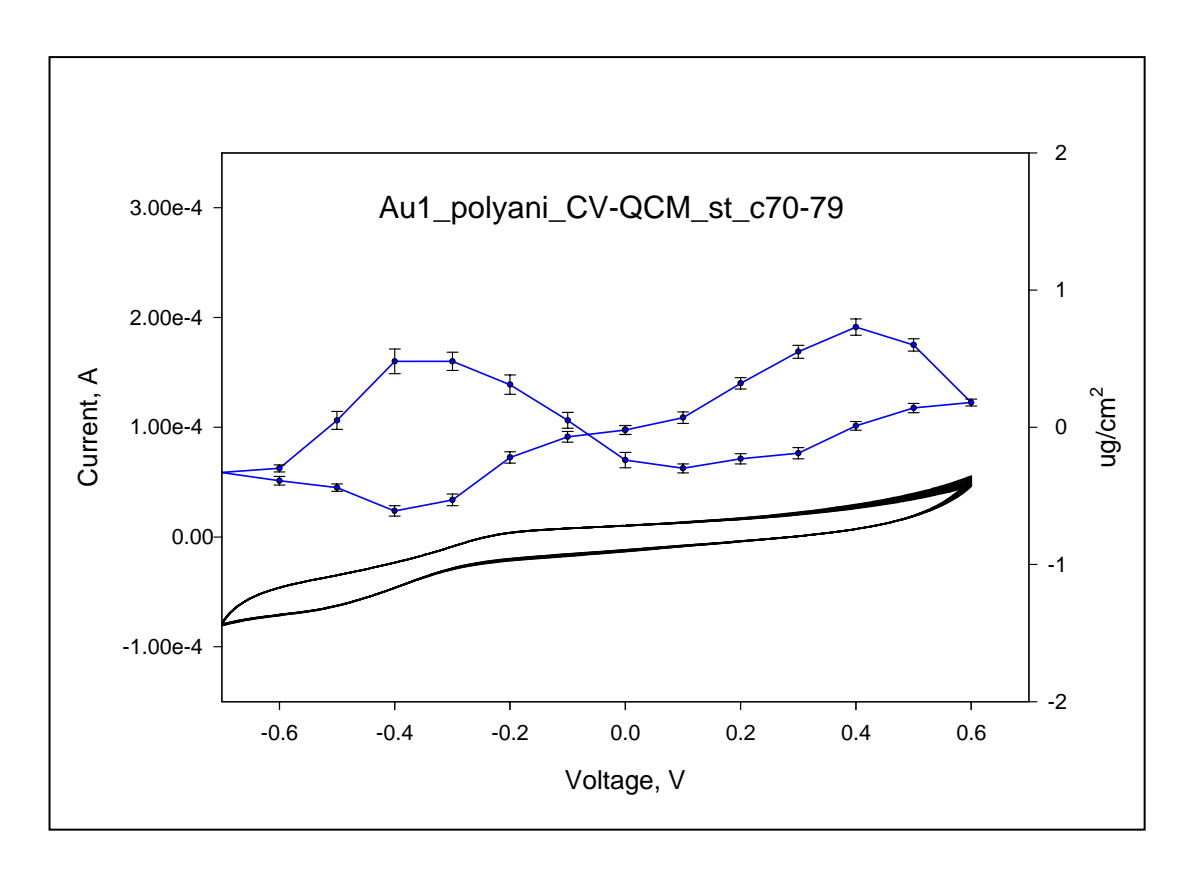


Figure 161. Cyclic voltammogram (cycles 70 - 79) of polyaniline superimposed with mass change in $\mu g.cm^2$ due to **anions and cations** moving in and out of the polyaniline matrix. CV was done between -0.7V to +0.6V in 0.5M KCl. Polyaniline was deposited from 0.2M aniline sulphate solution in the presence of 0.3M KCl.

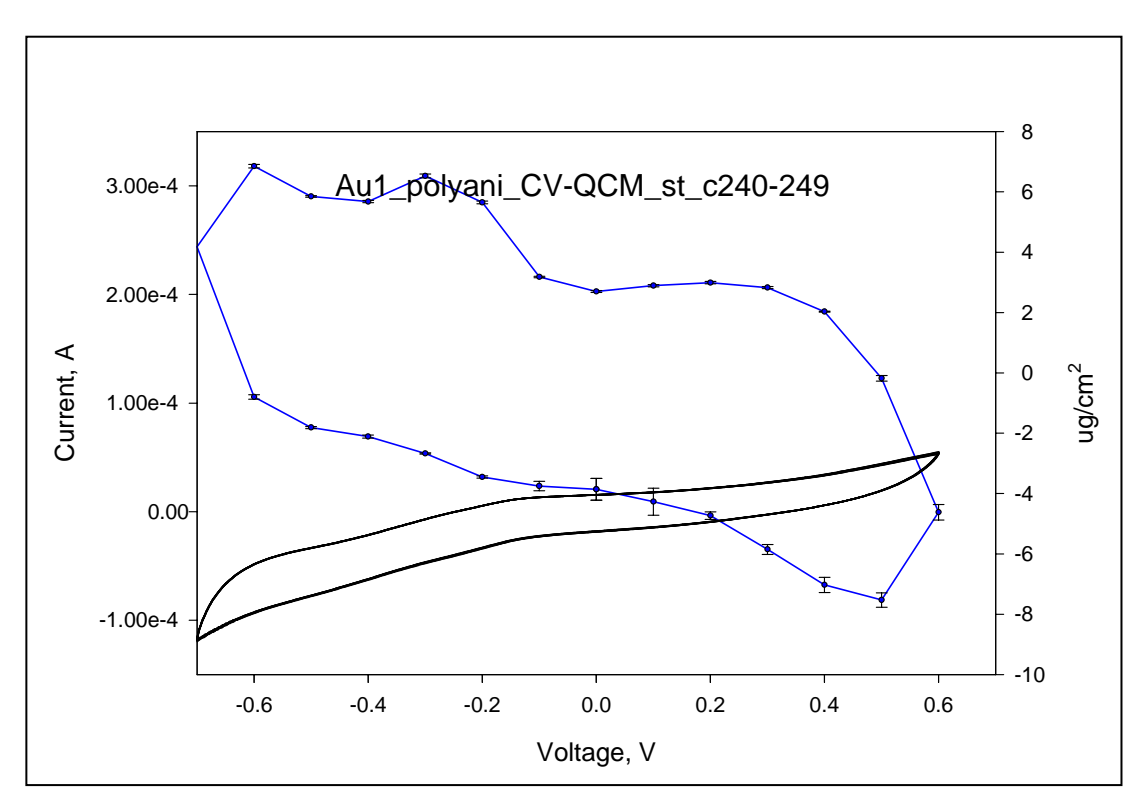


Figure 162. Cyclic voltammogram (cycles 240 - 249) of polyaniline superimposed with mass change in $\mu g.cm^2$ due to <u>cations</u> moving in and out of the polyaniline matrix. CV was done between -0.7V to +0.6V in 0.5M KCl. Polyaniline was deposited from 0.2M aniline sulphate solution in the presence of 0.3M KCl.

It has also been found that changing the anion and cation used influences the mass change observed, this is a direct check on the actual ion movement in terms of the differing molecular masses. Further work in this area was done using antibody loaded films to test if antigen binding influences ion movement. If so a possible mechanism of signal generation could be shown to occur.

Partner 2 has been investigating non-specific binding and the elimination of this by treating antibody loaded polyaniline films using standard immunoassay blocking agents such as albumins, particularly bovine serum albumin (BSA). The construction of the films was by a new process using polyaniline deposited by 15 CV sweeps onto carbon micro-electrodes as before, then reacted with N-hydroxysuccinamide – biotin conjugate, washed and reacted with neutravidin, then biotinylated antibody is loaded onto the captured neutravidin. BSA is then added to block the surface of the immunosensor.

In the process the subtraction of control results using a non-specific IgG loaded film has definitively proven the validity of the ELISHA sensors, giving a specific signal for the added antigen alone which in this case was PSA. Calibration curves for PSA between 0.1ng.ml⁻¹ up to 1000ng.ml⁻¹ have been produced using a plot of total impedance (Z) vs PSA concentration. Comparisons with a non-selective antibody (Non-specific Anti-IgG) and Anti-PSA clearly shows a specific PSA concentration response, figures 163 and 164. Subtraction of the non-specific responses gives a specific calibration curve for PSA, figure 165.

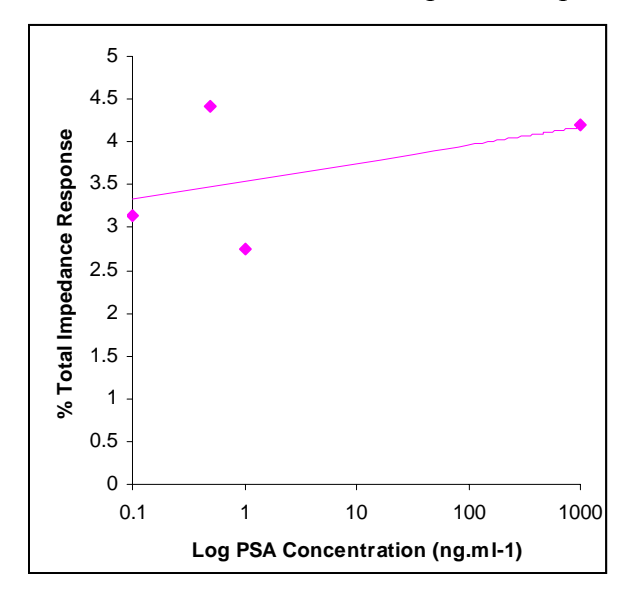
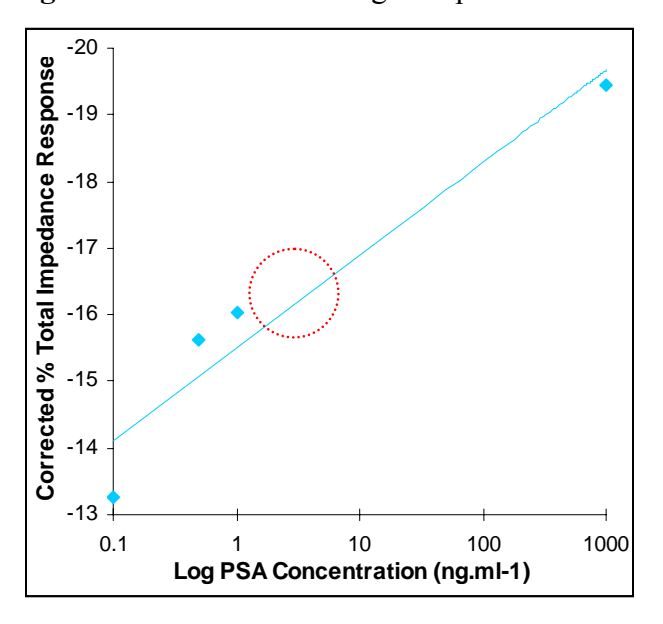


Figure 163. Control Anti IgG response to PSA



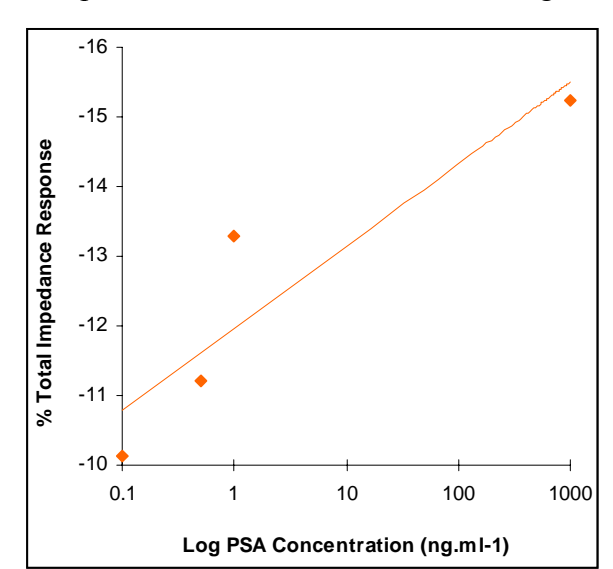
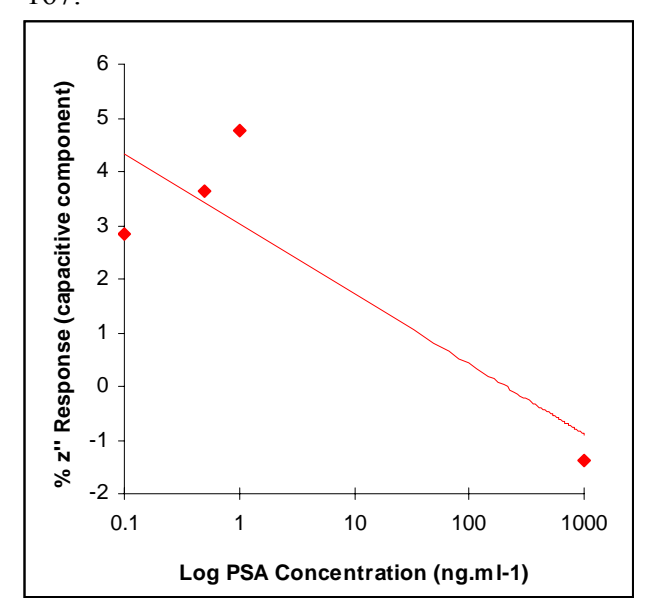


Figure 164. Selective Anti-PSA response to PSA.

Figure 165. Specific corrected calibration curve for PSA, by subtraction of non-specific % total impedance response from specific anti-PSA response.

Important clinical levels for PSA in blood are indicated by the red circle.

Taking the total impedance responses and sub-dividing them into their capacitive and faradaic components z''and z' respectively, clearly indicates that the faradaic component is the one recording the antibody – antigen binding event. The capacitive component is blocked out by the BSA added to remove non-specific binding. The figures are normalised by plotting a % change over baseline, figures 166 and 167.



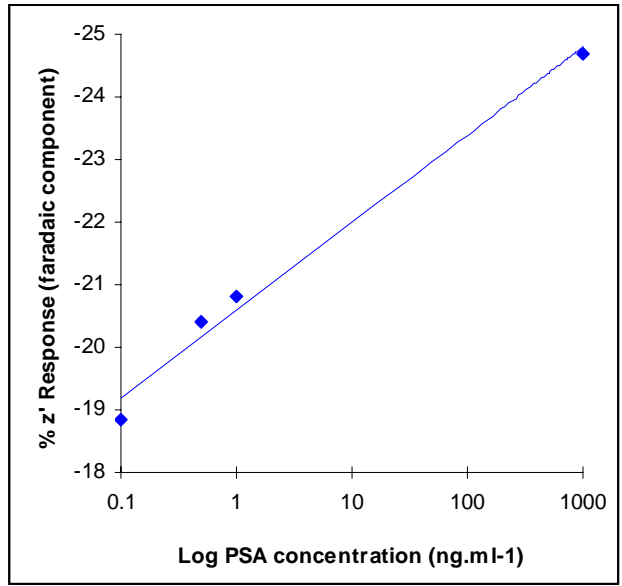


Figure 166. Anti-PSA Immunosensor z'' (capacitive component) response.

Figure 167. Anti-PSA Immunosensor z' (faradaic component) response.

Further to this a % plot of the faradaic component z' of the Anti-PSA, BSA blocked immunosensor gives a PSA concentration curve just on the transient bulk current changes occurring in the sensor matrix, figure 168. This definitively proved the ELISHA concept of labeless immunosensors and these early results demonstrated substantial removal of non-specific binding and signal response generation. These results also validated the workpackage outcome and elevated the project to the next level of experimentation for the final year.

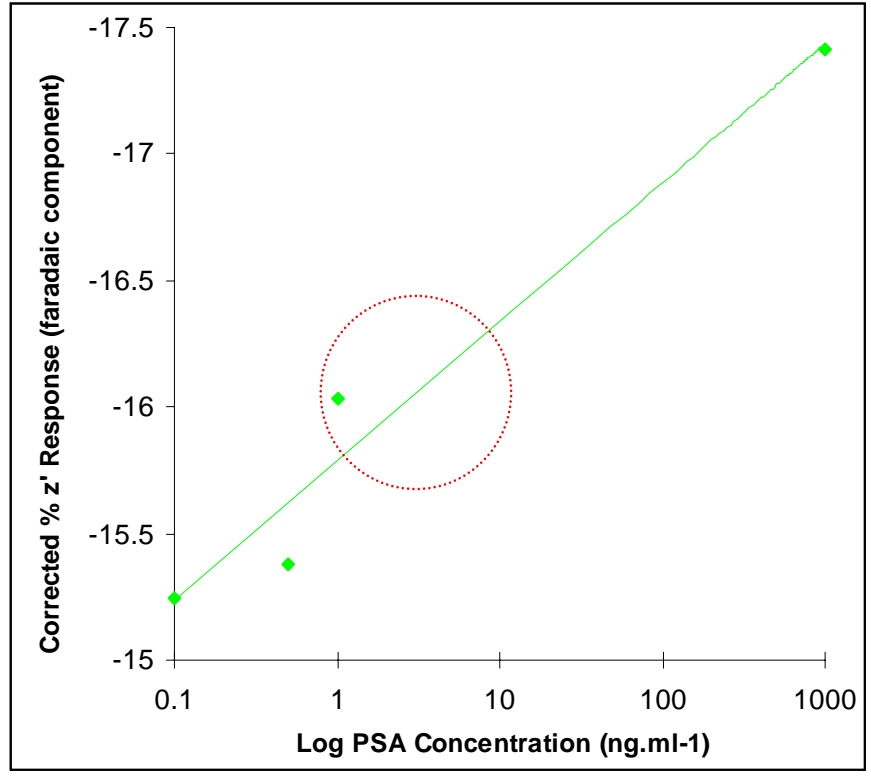


Figure 168. Corrected z' (faradaic response) of Anti-PSA immunosensor to different concentrations of PSA. Red circle indicates clinical levels.

Further Improvements to Sensor Performance using Blocked Microarray Electrodes.

Non-specific interactions could potentially interfere with immunosensor performance. This was addressed in the project by utilisation of a second sensor containing either no antibodies - or alternatively a non-specific antibody. This was the main aim of the sensor development for the final year of the project and to be able to effectively demonstrate proof of principle with many analytes.

Identical sets of immunosensors were fabricated utilising 1) specific anti-fluoroquinoline and 2) a non-specific IgG antibody in place of the specific ciprofloxacin antibody.

Figure 169 a shows the percentage decrease in z' across a range of antigen concentrations. As can be seen, there is a steady decrease in impedance as antigen concentration increases up to a concentration of about 100 ng.ml^{-1} , above which concentration there is a tend towards a plateau, possibly indicating saturation of the specific binding sites. It is possible that any further changes in impedance beyond this level could simply be due to non-specific interactions. Between a concentration range of 1-100 ng ml⁻¹, there is a near linear correlation of the impedance change with the \log_{10} of concentration (R^2 =0.96).

Results for the non-specific electrodes were obtained in exactly the same way as the specific ones and the calibration plot is shown (Figure 169 b). As can be seen, there is a much lower response for the non-specific antibody, showing that although there are non-specific interactions, between the ranges of 1-100 ng.ml⁻¹, they comprise a minor component of the detected response.

Figure 169 c shows the subtracted responses (a-6) and again this demonstrates linearity between the response and the \log_{10} of ciprofloxacin concentration between 1-100 ng.ml⁻¹ (R²=0.96).

In each case the measurement sequence was as follows:

- a) Incubate respective specific or non-specific sensors with antigen for 30 minutes to 1 hour to allow complete antibody antigen binding to take place.
- b) Wash briefly with distilled water.
- c) Immerse in a phosphate buffered saline containing 5mM Ferrocyanide / Ferricyanide redox couple and measure the impedance vs a silver/silver chloride reference and platinum counter electrode.

The presence of redox couple was found advantageous as it stabilised the electrochemistry of the system.

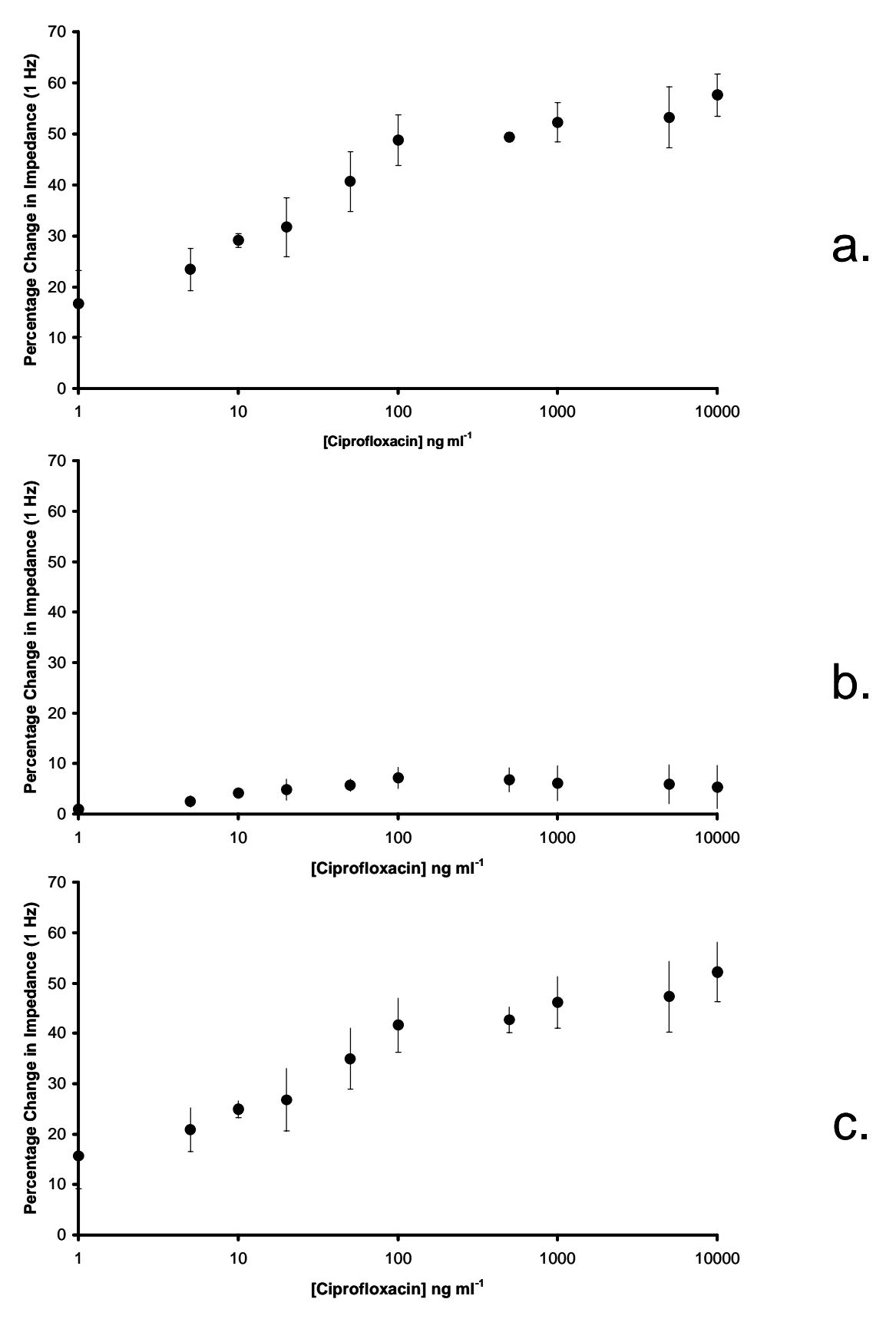


Figure 169 a-c: Calibration profile of % impedance response against ciprofloxacin concentration for carbon electrodes at 1Hz (in redox couple) coated with polyaniline doped with (a) anti-ciprofloxacin (b) IgG (c) corrected calibration curves (curve a – curve b)

Immunosensors for digoxin.

Digoxin (Figure 170) is a purified cardiac glycoside extracted from the foxglove plant and is widely used in the treatment of various heart conditions, namely atrial fibrillation, atrial flutter and congestive heart failure that cannot be controlled by other medication. There are a variety of adverse effects associated with its use, including loss of appetite, nausea, vomiting, diarrhoea, blurred vision, confusion, drowsiness, dizziness, nightmares, agitation, and/or depression. These effects are concentration dependant and do not usually occur at levels below 0.8 ng ml⁻¹ (Rossi 2006). Effective plasma levels are fairly well defined, 1-2.6 nmol l⁻¹ (equivalent to 0.8-2.1 ng ml⁻¹). Higher concentrations can have very severe effects, Charles Cullen is a former nurse who is the most prolific serial killer in New Jersey history and in December 2003 admitted to killing as many as 40 patients with overdoses of heart medication - usually digoxin during the 16 years he worked at ten hospitals in New Jersey and Pennsylvania. When digoxin is given as a drug therefore, either orally or intravenously, care must be taken not to drift out of the therapeutic range.

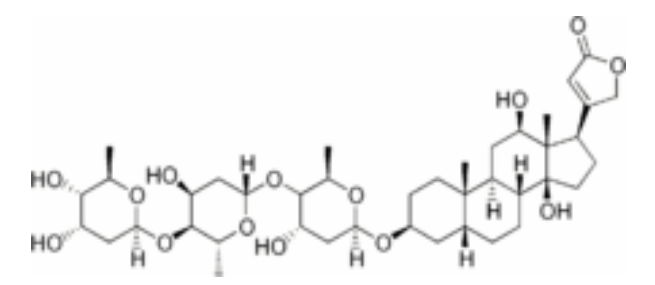


Figure 170: Structure of digoxin.

The method for construction of the immunosensors was basically identical to that utilised for ciprofloxacin. Anti-digoxin was obtained from Sigma and biotinylated as before, along with an IgG control. Sensors were fabricated in triplicate utilising purified anti-digoxin at 0.3 mg/ml to fabricate the specific sensors and polyclonal IgG at 0.3 mg/ml to fabricate the control sensors. The sensors were then exposed to concentrations corresponding to the therapeutic range of digoxin.

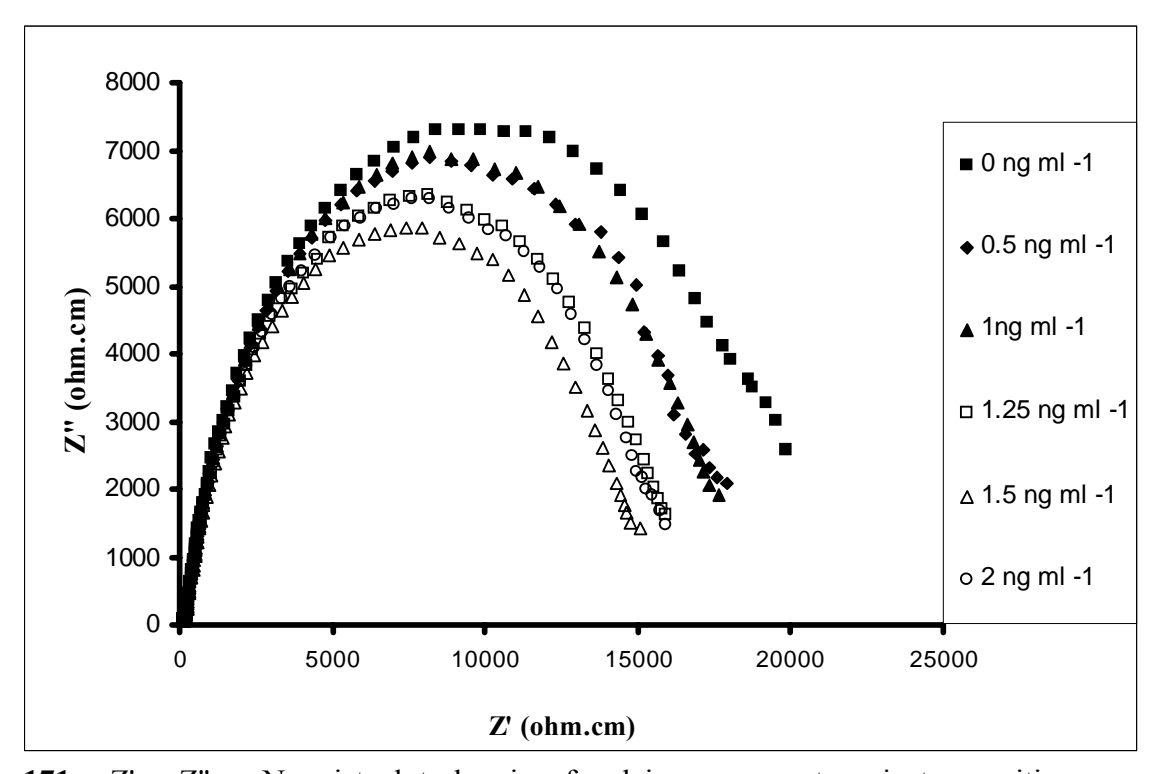


Figure 171 : Z' v Z" - Nyquist plot showing faradaic component against capacitive component for polyaniline doped with anti-digoxin on carbon electrodes (3 replicates) after exposure to various concentrations of digoxin (in redox couple).

AC impedance was used to interrogate the sensors as before and similar behaviour was found as shown for ciprofloxacin. Presence of the antigen caused a drop in impedance as shown by the Nyquist plots (Figure 171). From the Nyquist it again became obvious that the greatest changes in impedance occured at 1 Hz. Figure 171a shows the calibration profile for anti-digoxin modified sensors. Non-specific binding has also been measured within the same concentration range (figure 171b) and a corrected (specific minus non-specific) calibration profile is shown overleaf in figure 171c. Although a trend is visible, electrode-to-electrode variability and the fact that digoxin solubility in water is very poor led to large error bars.

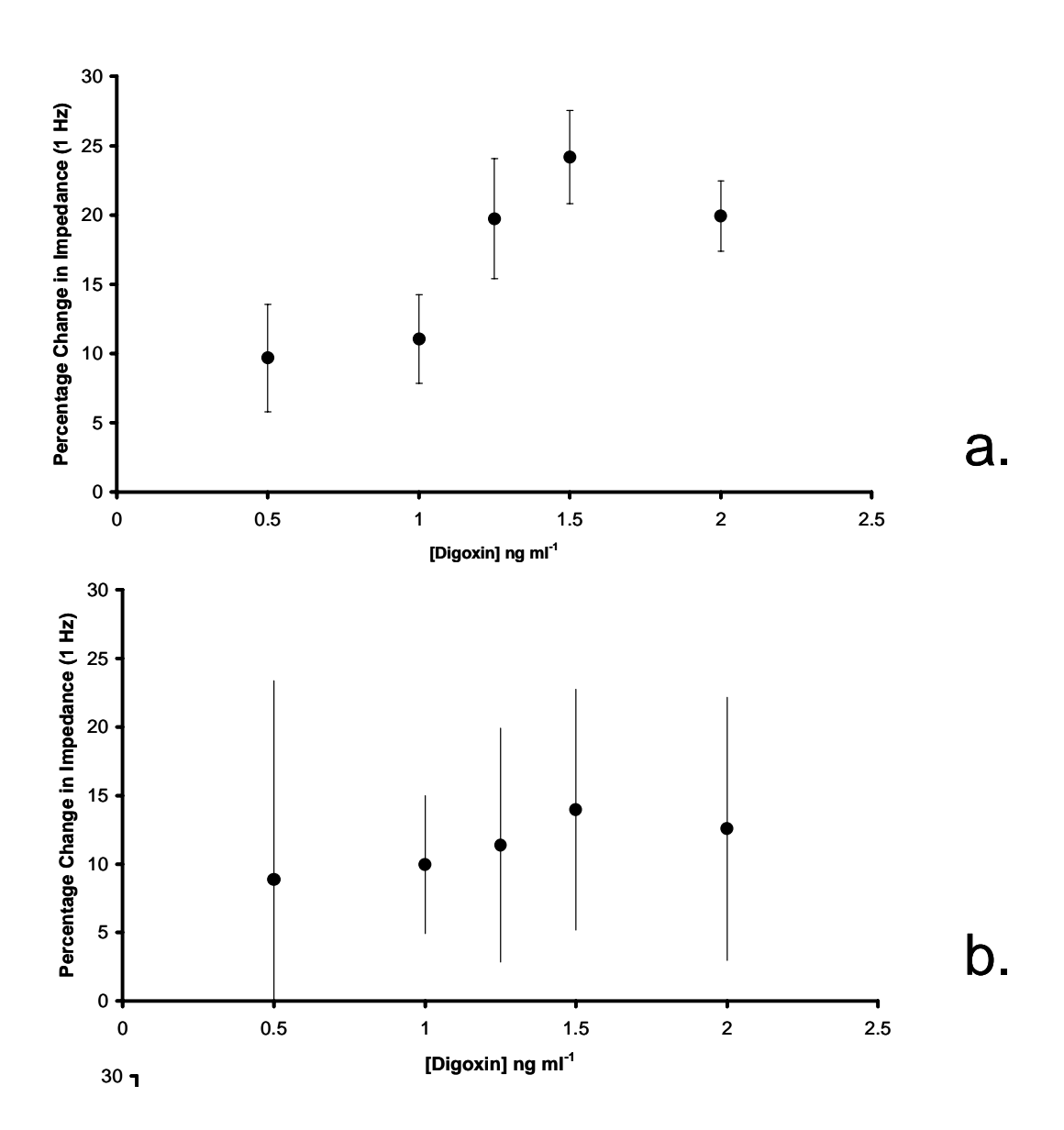


Figure 172: Calibration profile of % impedance response against digoxin concentration for carbon electrodes at 1Hz (in redox couple) coated with polyaniline doped with (a) anti-digoxin and (b) IgG

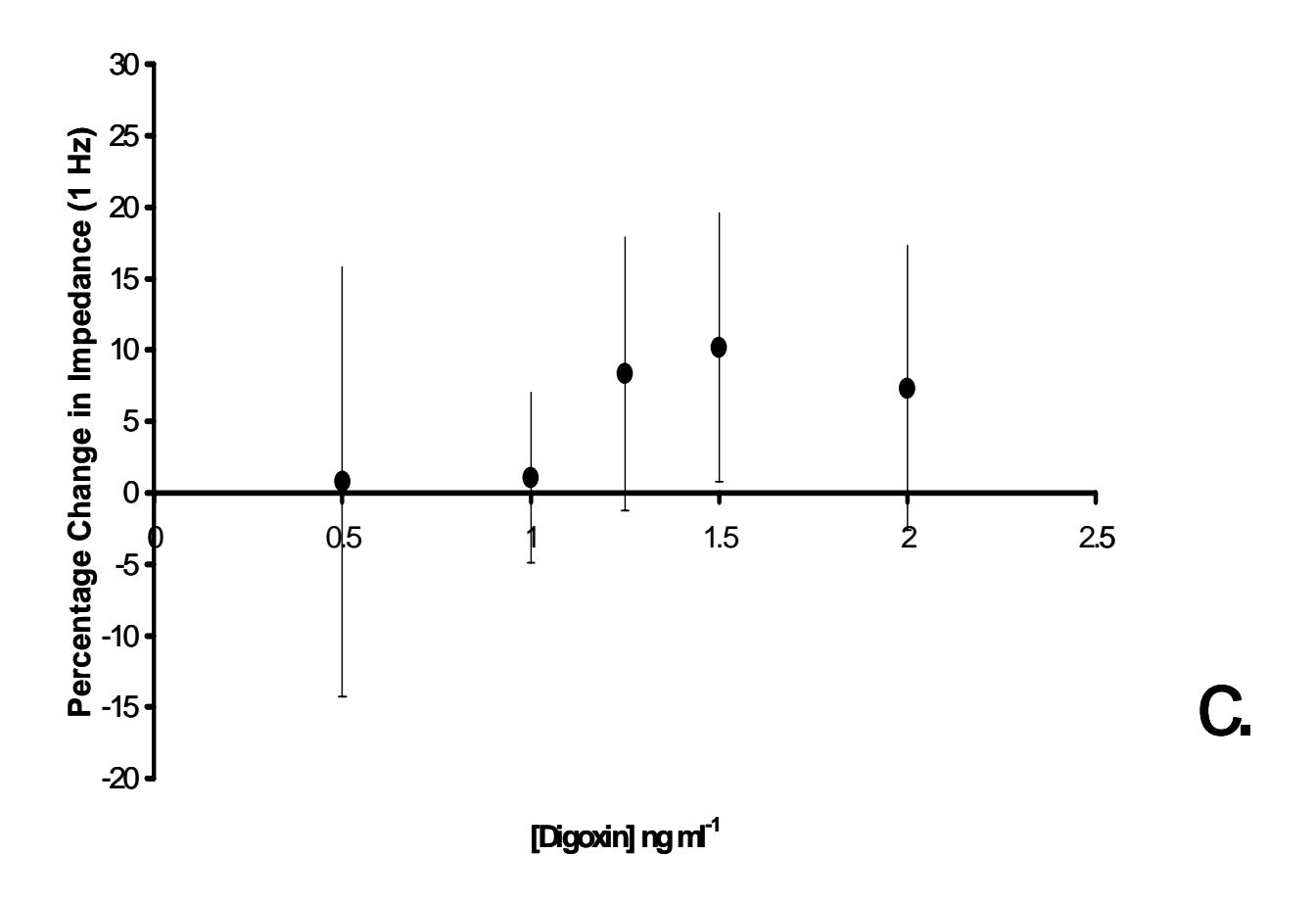


Figure 171 continued: Corrected calibration profile of % impedance response against digoxin concentration for carbon electrodes at 1Hz (in redox couple) coated with polyaniline doped with (a) anti-digoxin (b) IgG. The corrected calibration curve was obtained by subtracting curve b from curve a from the previous page.

Immunosensors for myelin basic protein (MBP).

Myelin basic protein (MBP) is a protein believed to be important in the process of myelination of nerves in the central nervous system. A demyelinating disease is any disease of the nervous system in which the myelin sheath of neurons is damaged. This impairs the conduction of signals in the affected nerves, causing impairment in sensation, movement, cognition, or other functions depending on which nerves are involved.

Multiple Sclerosis is an example of a demyelinating disease.

The presence of antibodies against myelin proteins such as MBP can be a predictor of multiple sclerosis [Berger *et al* 2003]. L Myelin basic protein levels between 4 and 8 ng.ml⁻¹ in cerobospinal fluid may indicate a chronic breakdown of myelin, or recovery from an acute episode. If the myelin basic protein levels are greater than 9 ng.ml⁻¹, active demyelination is occurring. Normally there should be less than 4 ng.ml⁻¹ of myelin basic protein in the cerebral spinal fluid.

Experimentally, myelin basic protein antibody (Sigma monoclonal anti-MBP from rat, M9434) was biotinylated then immobilised at the surface of screen-printed carbon electrodes using avidin-biotin interactions. Exposure of the resultant immunosensors to MBP (Sigma) caused reproducible increases in impedance (Figure 172).

This immunosensor reacts in an opposite manner to the previous hapten sensitive examples, indicating a different mode of signal generation. MBP has a molecular weight c20 kDa unlike the smaller ciprofloxacin and digoxin species and the postulation of passivating or rigidifying the sensor surface given previously (page xxx) with the concomitant hindrance of ion exchange at the surface of the polymer layer seems likely.

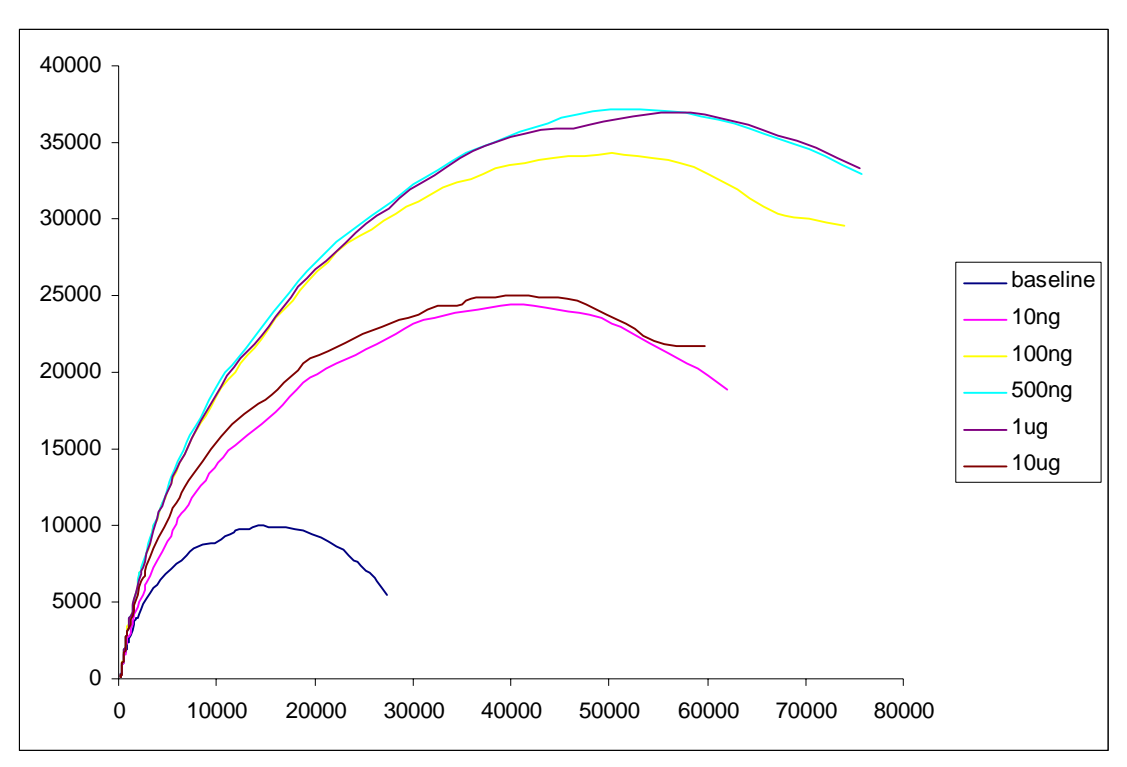


Figure 172. Z' v Z" - Nyquist plot showing faradaic component against capacitive component for polyaniline doped with anti-MBP on carbon electrodes (3 replicates) after exposure to various concentrations of MBP (in redox couple).

Calibration of MBP Immunosensors.

Measurements to show concentration dependant calibration curves using several electrodes per concentration point are given overleaf.

Figure 173a shows the change in z' with increasing MBP concentrations between 0-15 ng ml⁻¹. There is a clear semi-logarithmic correlation between impedance of the immunosensors and concentration of antigen.

Non-specific binding has also been measured within the same concentration range (figure 173b) and a corrected (specific minus non-specific) calibration profile is shown in figure 173c.

Higher levels have also been measured and saturation shown to between 100 and 500 ng ml⁻¹.

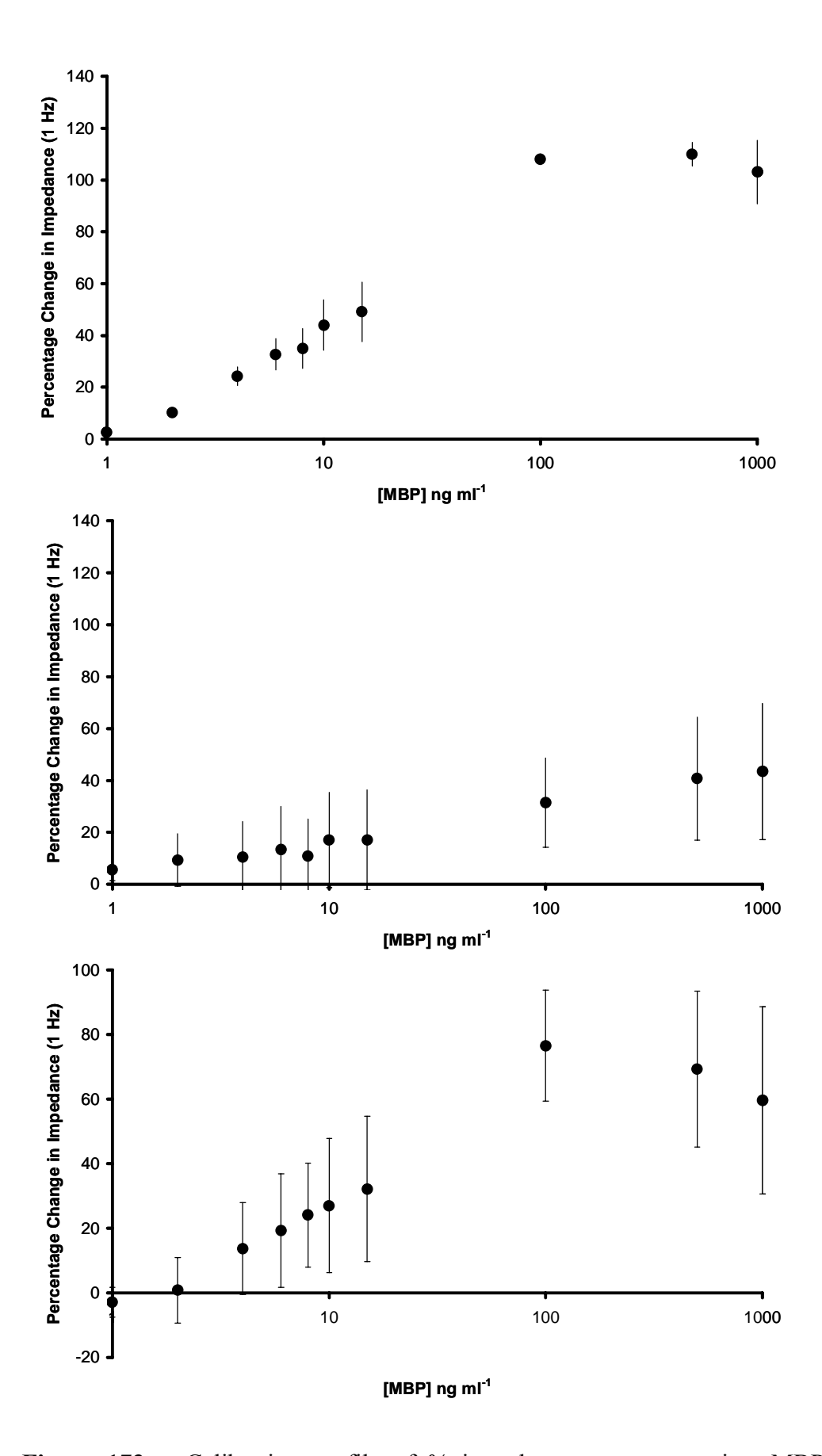


Figure 173.: Calibration profile of % impedance response against MBP concentration for carbon electrodes at 1Hz (in redox couple) coated with polyaniline doped with (a) anti-MBP (b) IgG (c) corrected calibration curves (curve a – curve b).

Objectives. To characterise and determine the performance characteristics of a range of affinity sensors in terms of reproducibility, stability and analytical performance. To evaluate a range of prototype sensor systems towards a number of differing targets in terms of lower limits of detection, selectivity and possible interference effects. To compare analytical performance with standard detection and quantification methods, e.g. ELISA.

Project Timeline		1 2 3 4 5 6 7 8 9 10 11 12 13 14 15 16 17 18 19 20 21 22 23 24 25 26 27 28 29 30 31 32 33 34 35 36
Workpackage 8.	Evaluation/Processing	
Task 8.1	Signal Processing	
Task 8.2	Sample Analysis	

The approach was to specify an electric equivalent circuit, to provide an understanding of the physicochemical processes taking place on the sensor surface. These included quantitative evaluation of a reaction kinetics which were required information for instrumentation development and optimisation. In addition, possible new ideas for instrumentation design and data processing were also developed.

The modelling approach was based on nonlinear complex impedance fitting procedures and presented an ascending step-by-step algorithm, which included

- starting from a crude sensor equivalent circuit (SEC) with two parameters
- more accurate specification of the SEC in each next step by introducing an additional element with initial parameters for optimisation procedure taken from the previous step
- using a target function based on different metrics and comparison of results to one another
- control of the approximation accuracy against the precision of the experimental data.

The developed approach was applied for specification of the equivalent circuits for polypyrrole on graphite sensor. Results of the fitting procedure with evaluation of approximation errors in different metrics are shown in Table 8, where a different metric was used to estimate the circuit parameter dispersion.

Metric	circ	Rs	Wk	C nF	Rc	Rw	De	eL	eLs
L	rw	786.11	10.072	-	-	-	370.89	1.011	0.239
Ls	rw	883.02	5.4577	-	-	-	155.18	1.193	0.147
D	rw	873.33	5.3721	-	-	-	154.53	1.201	0.148
L	(r-c) w	-	525.81	31388.3	1132.14	-	156.6	0.327	0.115
Ls	(r-c) w	-	558.4	37502.1	1194.33	-	112.11	0.346	0.095
D	(r-c) w	-	478.82	39353.2	1241.73	-	105.65	0.373	0.101
L	r-((r-c) w)	557.93	107.93	31851.6	682.515	-	102.79	0.173	0.066
Ls	r-((r-c) w)	548.54	93.411	35610.2	741.719	-	79.681	0.206	0.055
D	r-((r-c) w)	600.87	71.474	36146.9	724.107	-	77.193	0.238	0.058
L	r-((r-w) c)	658.31	4.339	87.0327	-	350.545	131.79	0.214	0.084
Ls	r-((r-w) c)	677.38	4.7007	86.4383	-	306.153	124.33	0.232	0.08
D	r-((r-w) c)	652.87	4.9735	72.0478	-	287.163	120.33	0.272	0.085

Best fit experimental data provided two four-parametric equivalent circuits (R-(Rc-C)||W) and R-(C||(Rw-W)) but for both of them the approximation accuracy was still far from experimental accuracy. In order to improve the approximation it was suggested that some physical aspects could be taken into account.

Further development of the approach for specification of the sensor electric equivalent circuit was done. This provided: 1) understanding of chemical processes taking place on the sensor surface including

quantitative evaluation of a reaction kinetics; 2) required information for instrumentation development and 3) optimisation and possible new ideas for instrumentation design and data processing. The main efforts were concentrated on improving the approximation accuracy in the low frequency region. In this process, the structure of the biosensors under development was taken into account more carefully. At this stage of the project, the biosensors were mainly based on the use of conductive porous polymer films (e.g. polypyrrole), for which more complex distributed equivalent circuits than the classical Randle's circuit were applied. Three different distributed equivalent circuits and the serial and parallel connection of the equivalent circuits for planar interfaces as the other options were considered for the sensor equivalent circuit determination. For all these cases algorithms and dedicated software for their parameters definition were developed.

The developed approach was applied for specification of the equivalent circuits for a polypyrrole (on Au electrode) on silicon sensor. Results of the fitting procedure with evaluation of approximation errors in an L-metric, which as was previously shown is the most appropriate to the electrode type of sensors, by the example of one of experimental data sets are shown in Table 9. For comparison, approximation results obtained for traditional Randle's equivalent circuit (r-((r-w)||c) - circuit) are also given in this Table.

Table 9. Model Fitting of Experimental Data Set.

circ	Rw	W	C,nFRs	α/Rw2	W2	β/C2,uFD	d	ds	L	Ls
r-((r-w) c)	2324.48	3 14567.:	50 64.20 494.37	0.50	-	- 38145	.360.2	93 0.75	70.63	70.374
r-((r-wa) c)	3315.68	3 14057.:	5671.33536.38	0.761	-	- 12301	.85 0.1	380.24	3 0.24	10.138
r-((r-wcota) c)	2920.12	2 3613.4	45 69.69 522.36	-	11.59	1.00 5808.0	5180.1	010.15	3 0.15	10.101
r-((r-wacota) c)	2814.26	5316.2	20 70.45 515.69	0.723	7.63	9 0.536 1908.8	371 0.0	790.14	0 0.13	90.077
r-((r-w) c)- (r-w) c)	3247.61	3813.:	56 70.23 536.14	47270.42	39080.7	8 89.285 5138.2	245 0.1	270.19	20.18	70.127
r-((r-wa) (r-w) c)	4846.93	19484.	60 69.01 533.70	8925.88	48628.9	0.932 4963	.670.1	270.18	5 0.18	40.129

As one can see all improved equivalent circuits gave a better approximation accuracy than the Randle's circuit.

Best fit experimental data provided a seven-parametric equivalent circuit ((r-(r-wcota)||C, model with constant phase element (CPE) restricted diffusion whose complex impedance <math>Z is described by equation

$$Z(\text{Rs},\text{Rw},\text{W},\text{W2},\alpha,\beta,\vec{f}) = \text{Rs} + \frac{\frac{1}{1j \cdot 2 \cdot \pi \cdot f \cdot C \cdot 10^{-12}} \cdot \left[\text{Rw} + \text{W} \cdot \frac{\left(1j \cdot 2 \cdot \pi \cdot f\right)^{\alpha} \cdot \sqrt{1j \cdot \frac{\beta}{f}} + \left(\text{W2} \cdot \coth\left(\sqrt{1j \cdot \frac{f}{\beta}}\right)\right)}{\text{W2} \cdot \sqrt{1j \cdot \frac{f}{\beta}} + \left[\left(1j \cdot 2 \cdot \pi \cdot f\right)^{\alpha} \cdot \coth\left(\sqrt{1j \cdot \frac{f}{\beta}}\right)\right]} \right]}{\frac{1}{1j \cdot 2 \cdot \pi \cdot f \cdot C \cdot 10^{-12}} + \left[\text{Rw} + \text{W} \cdot \frac{\left(1j \cdot 2 \cdot \pi \cdot f\right)^{\alpha} \cdot \sqrt{1j \cdot \frac{\beta}{f}} + \left(\text{W2} \cdot \coth\left(\sqrt{1j \cdot \frac{f}{\beta}}\right)\right)}{\text{W2} \cdot \sqrt{1j \cdot \frac{f}{\beta}} + \left[\left(1j \cdot 2 \cdot \pi \cdot f\right)^{\alpha} \cdot \coth\left(\sqrt{1j \cdot \frac{f}{\beta}}\right)\right]} \right]}$$
(1)

In this equation: α is the exponent of the low frequency CPE; β is a characteristic frequency that depends on the species chemical diffusion coefficient D and the thickness of the film L ($\beta=D/L^2$), W2 is related to the CPE's prefactor.

This equivalent circuit provided for a satisfactory approximation accuracy in the investigated frequency region as shown in the figure 174 in rectangular system of coordinates (real and imaginary parts of impedance) in absolute (left) and logarithmic (right) scales.

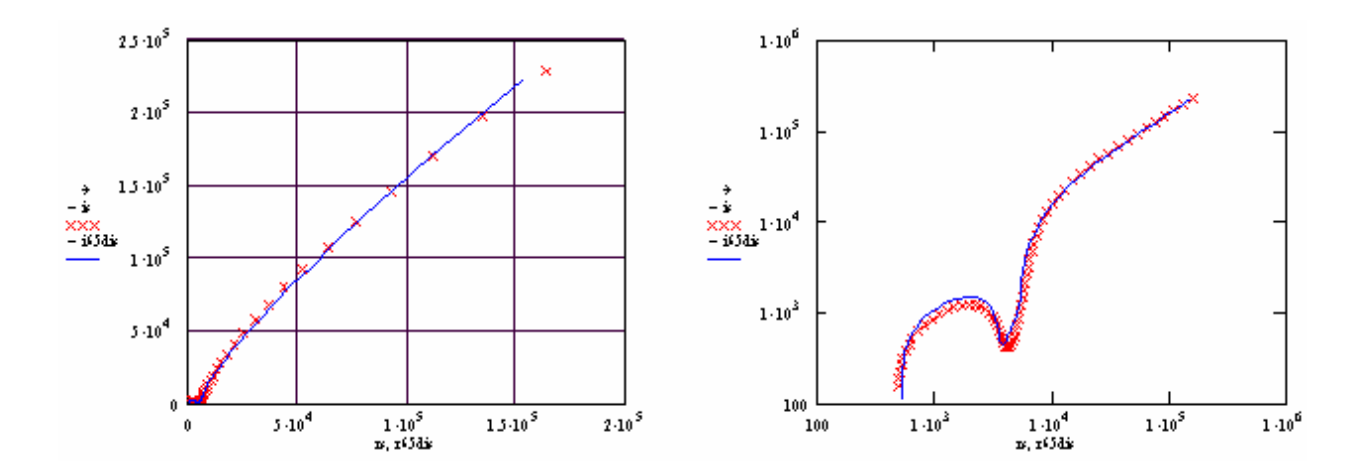
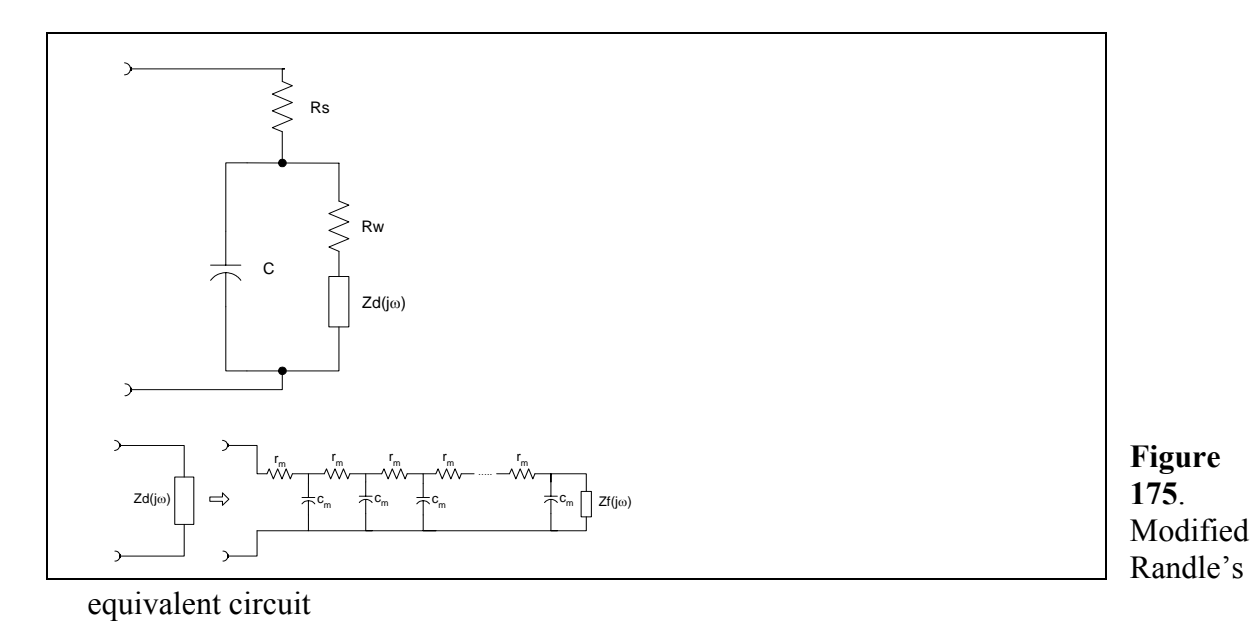


Figure 174. Comparison of experimental (rs,is) and calculated (i65dis, r65dis) impedance data in rectangular system of coordinate (real, imaginary parts) in absolute (left) and logarithmic (right) scales.

The developed approach with distributed equivalent circuits was applied for inspection of a polypyrrole on Au/silicon transducer, which was subjected to degradation by means of a series of cyclic voltammetry sweeps.

In the period between the mid-term and the 24 month report the the following development of the approach for specification of the sensor electric equivalent circuit was performed. It was found that the most suitable equivalent circuit, which met the requirements of the tasks under investigation, was a modified Randle's equivalent circuit shown in figure 175(left circuit). Its difference from the classical Randle's circuit is the presentation of the diffusion impedance $Zd(j\omega)$ in the form of input impedance of the distributed RC-line with complex valued load impedance (see figure 175, right) taking into account porosity of the polypyrrole film and its bonding to the electrode surface.



In this case the diffusion impedance could be presenting by equation (2)

$$Z_{d} = Wo \frac{1 + \frac{Zf(jw)}{Wo} \sqrt{\frac{jw}{w_{d}}} \coth \overset{\mathcal{E}}{\underbrace{\underbrace{\sqrt{\frac{jw}{\ddot{o}}}}}} \frac{\ddot{o}}{\frac{\dot{\dot{c}}}{\ddot{o}}}}{\frac{Zf(jw)}{Wo} \frac{jw}{w_{d}} + \sqrt{\frac{jw}{w_{d}}} \coth \overset{\mathcal{E}}{\underbrace{\sqrt{\frac{jw}{\ddot{o}}}}} \frac{\ddot{o}}{\frac{\dot{\dot{c}}}{\dot{c}}}}{\frac{\dot{\dot{c}}}{\ddot{o}}}}$$
(2)

In this equation Wo=L(dE/dc)/(qSD) is a characteristic impedance where L is the film width, dE/dc is a concentration derivative of applied overvoltage E, S is the sensor area, D is a diffusion coefficient and q is the elementary charge; $\omega_d=D/L^2$ is a characteristic frequency of the distributed line; $Z_f(jw)$ is a frequency dependent line load impedance. Line load impedance $Zf(j\omega)$ is related to boundary conditions for electro active species at the end of the diffusion zone on the electrode surface. The general case of this impedance is $Zf(j\omega) = 1/[1/\rho + Q(j\omega)^n]$ where 0 < n < 1 and Q is a constant with the dimensions Fs^{n-1} . The larger value of ρ and 1/Q, the better bonding of polypyrrole film to the electrode surface.

To specify parameters of the equivalent circuit the fitting algorithm based on nonlinear complex valued optimization procedure was developed. Its distinctive features used target functions based on different metrics (absolute, relative, semi-logarithmic and logarithmic metrics) that secures finding the global optimization minimum.

The developed approach was applied to a study of silicon-gold polypyrrole biosensor degradation provoked by applying a sequence of cyclic voltammetry treatments in the potential range -0.7V to +0.6V with scan rate of 50 mv.s⁻¹. After each 20 cycles of CV the biosensor impedance was measured and parameters of the equivalent circuit for each step of CV treatment were specified. Results of the fitting in logarithmic metric obtained by software developed for the batch mode data processing are shown in Figure 176 (fitting and experimental results for imaginary vs. real part of impedance dependencies) and in Figure 177 (frequency dependences of approximation and experimental errors). As one can see the fitting was quite good for all data proving the validity of the used equivalent circuit.

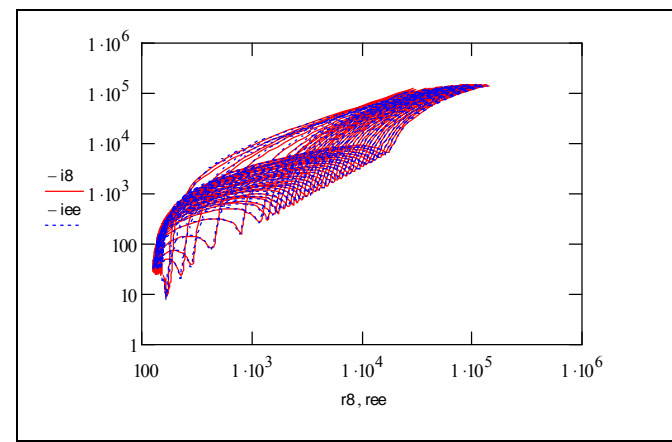


Figure 176. Fitting (solid) and experimental (dash) results for imaginary vs. real part of impedance dependencies for different number of CV treatments

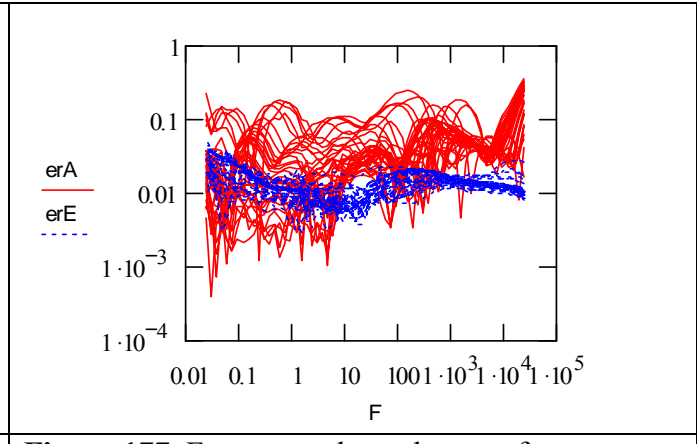
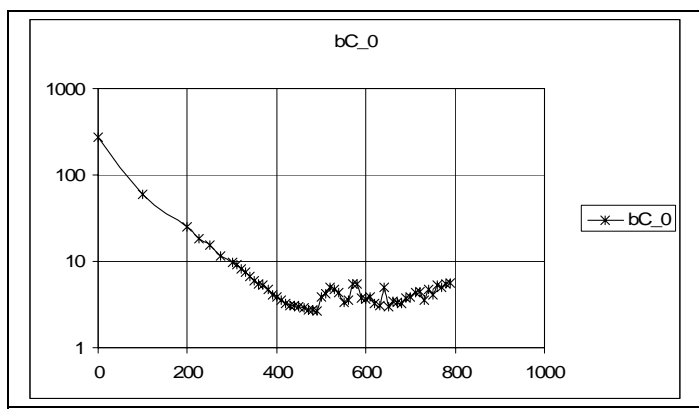
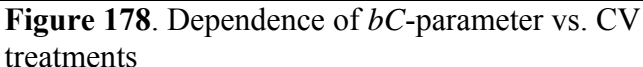


Figure 177. Frequency dependences of approximation (solid) and experimental (dash) errors for different number of CV treatments

Considerating the dependencies of the parameters within equivalent circuits versus a number of CV treatments revealed that degradation provoked by CV treatment took effect mostly on fd, Rw, Wo and parameters of the load line impedance bC=1/Q and $bR=\rho$. If the number of CV treatments increased, Rw and Wo increased; bC and bR decreased; the characteristic frequency fd took the minimum value of around 500 CV cycles. Examples of bC- and bR- dependencies versus number CV are shown overleaf in Figure 178 and Figure 179 correspondingly.





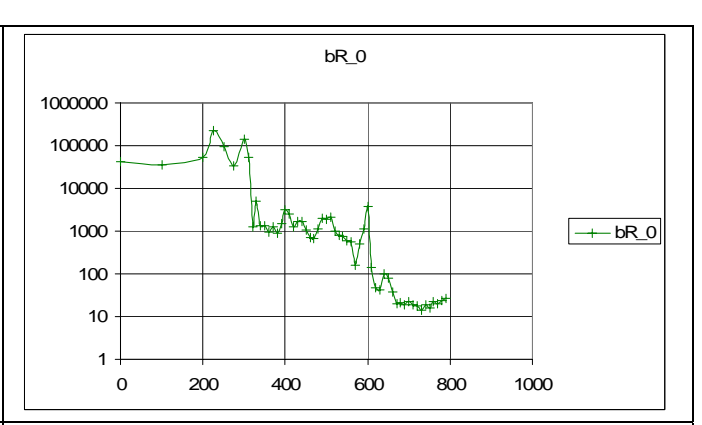


Figure 179. Dependence of *bR*-parameter vs. CV treatments

Also, the equivalent circuit approach was applied for study of the biosensor stabilisation by mercaptohexadecanoic acid treatment. In this process the above procedure of finding parameters of the equivalent circuit after applying cyclic voltammetry treatments was carried out on polypyrrole biosensors subjected to a mercaptohexadecanoic acid treatment for 1 and 24 hours. It was found that the treatment affected mostly the fd, W and parameters of the load line impedance, bC and bR. Stabilisation became apparent by increasing line load impedance component (see Figure 180 and Figure 181) and more stable dependence fd versus the number of CV treatments.

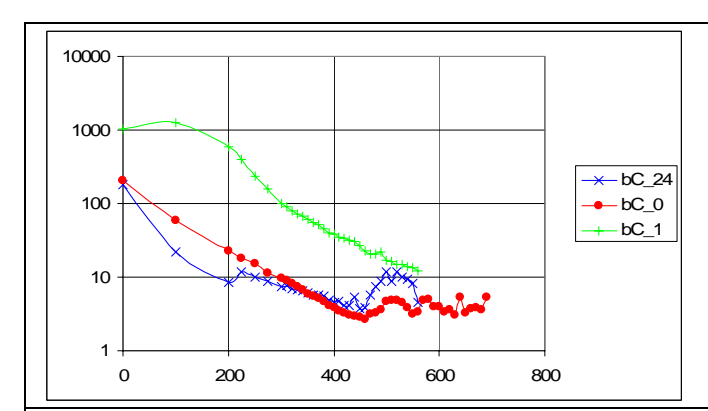


Figure 180. Dependence of *bC*-parameter vs. CV treatments before (_0) and after mercaptohexadecanoic acid treatment.

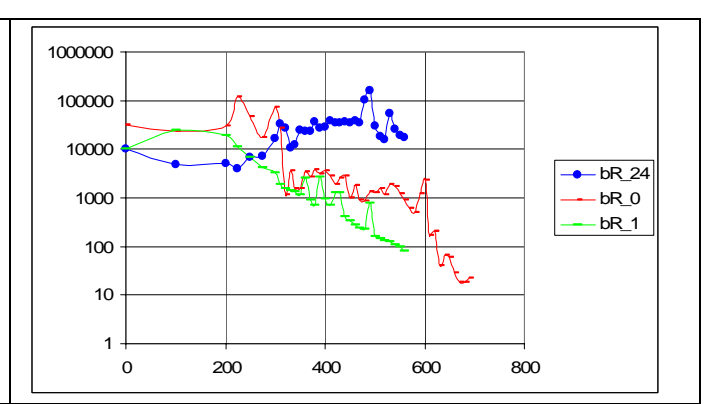


Figure 181. Dependence of *bR*-parameter vs. CV treatments (_0) and after mercaptohexa-decanoic acid treatment.

Further Study of polypyrrole transducer degradation

In further studies the process of transducer degradation during measurements or storage was investigation was investigated by means of complex impedance spectrum analysis and subsequent specification of the sensor equivalent circuit after application to the sensor a number of cyclic voltammetry (CV) sweeps resulting in sensor degradation up to the point of the polymer film peeling.

Typical experimental data for sensor degradation for different number of CV sweeps (25 sweeps for each impedance measurement step) as Bode (direct frequency dependences) and Nyquist plots are shown in figure 182 and figure 183 respectively. Nyquist plots are presented in absolute and logarithmic scales that allow obtaining a full picture of the sensor response. The upper plots in each figure show data for all sweeps (from 0 and up to 50*25=1250); the lower plots show data for selected number of sweeps (2*25=50, 20*25=500, 40*25=100 and 48*25=1200).

There was a clear difference between sensor responses for different CV treatment steps. Degradation of the sensor resulted in an increase inimpedance. The main changes appeared in the low and medium frequency regions and changes in real part of impedance are the most significant.

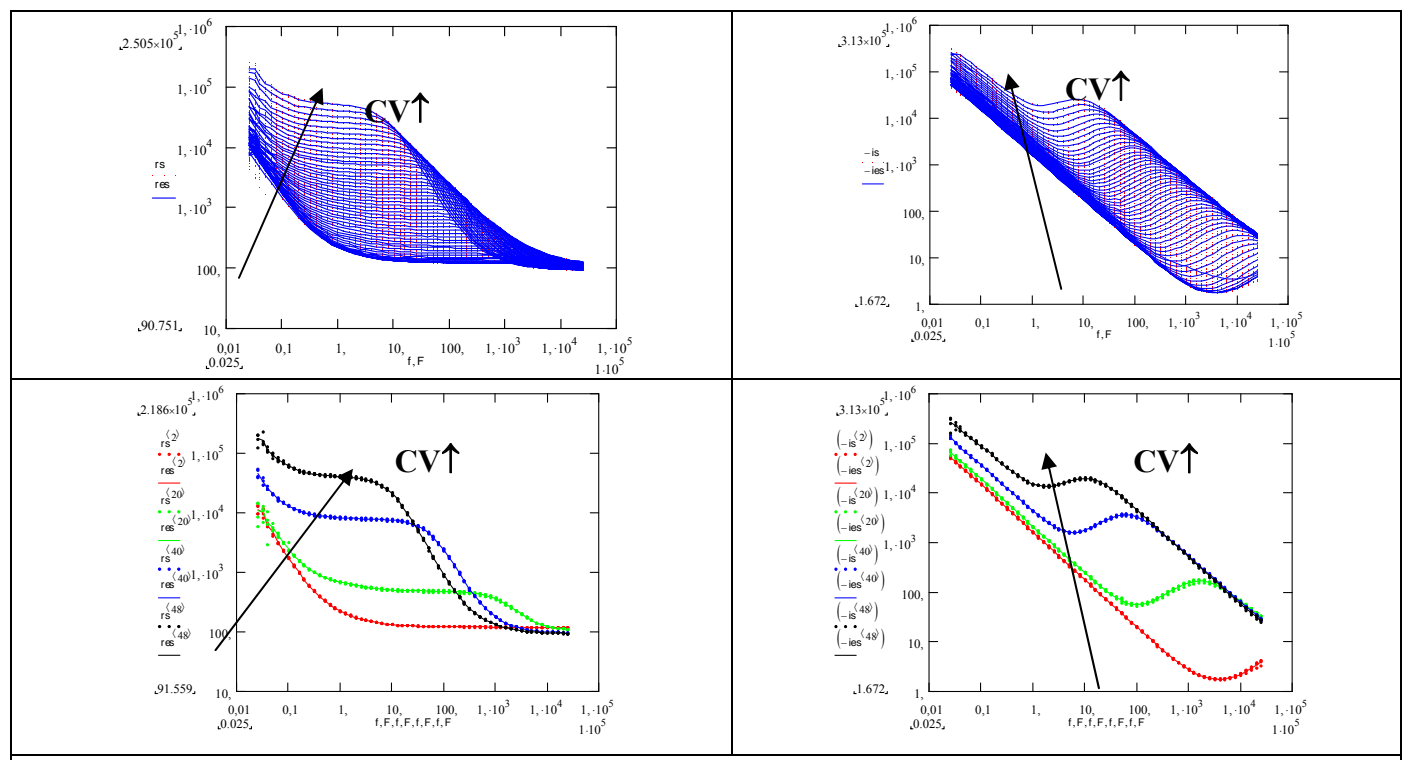


Figure 182. Dependencies of real (left) and imaginary (right) parts of the transducer impedance after application of increasing numbers of CV treatment steps

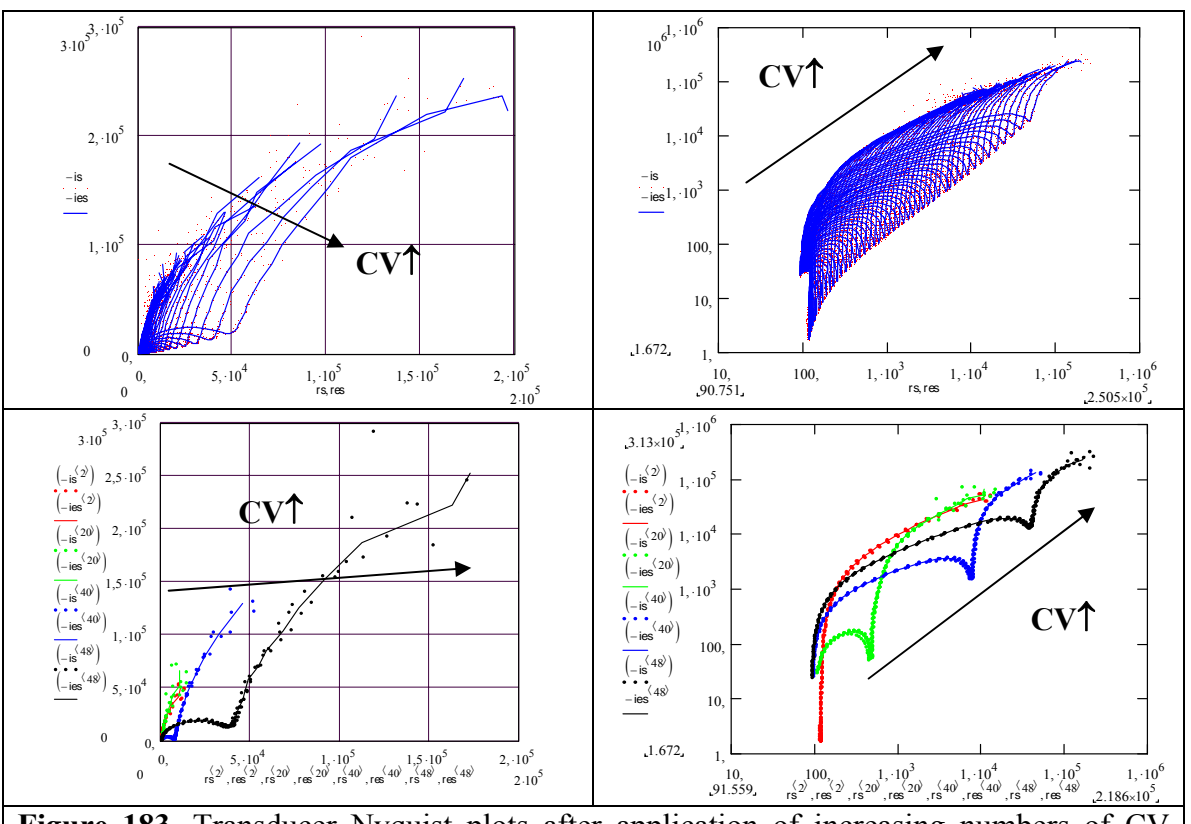


Figure 183. Transducer Nyquist plots after application of increasing numbers of CV treatment steps

In Nyquist plots the sensor degradation became apparent through an increase of impedance coordinate values and emergence of the break on the dependencies. This break is better observed in a logarithmic scale and it moves from the origin to the right upper corner of the plot.

Dependence of the real part of the beak position is shown in figure 184.

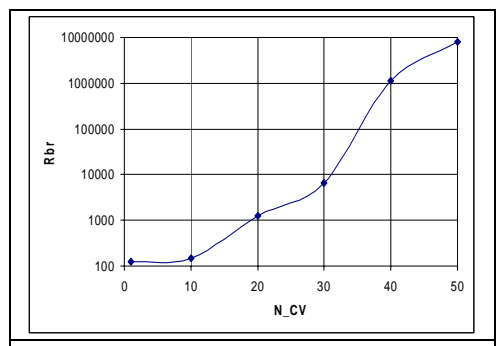


Figure 184. Real part of the break position vs. step of CV treatment.

The most useful parameter for the practical use of transducer performance relates to its capacitive behavior. To reflect this a local sensor static capacitance accordingly equation was introduced.

$$Cs(f) = -\frac{1}{\text{Im} \left[Z(f) \right] \cdot 2\pi f}$$
 (Equation 8.1)

Dependencies of the sensor static capacitance vs. frequency after application of different numbers of CV sweeps calculated from the data presented in figure 182 are shown in figure 185. The upper plots in each figure show data for all sweeps (from 0 and up to 50*25=1250); the lower plots show data for selected number of sweeps (2*25=50, 20*25=500, 40*25=100 and 48*25=1200). The left plots shows static capacitance in absolute and the right plots – in logarithmic scales.

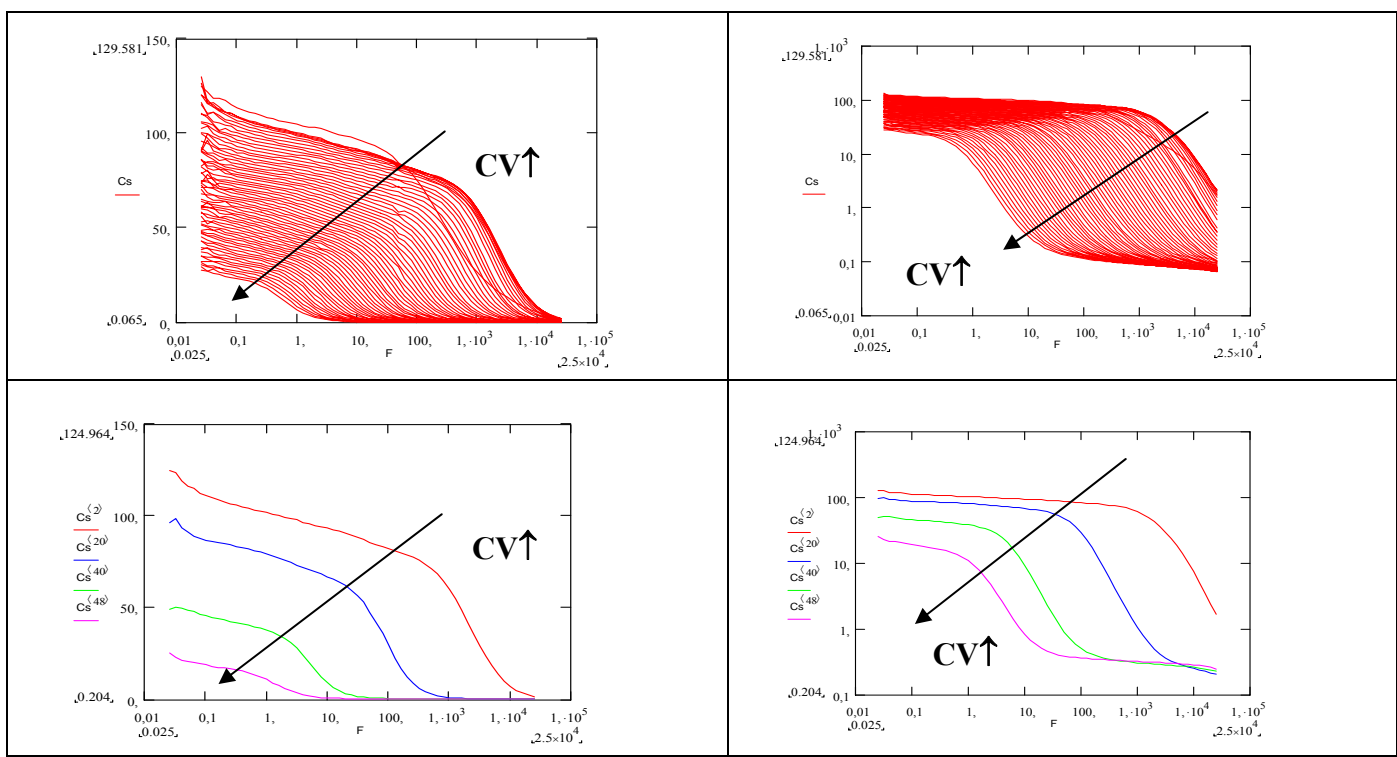


Figure 185. Dependence of the static sensor capacitance after application different numbers of CV treatment steps.

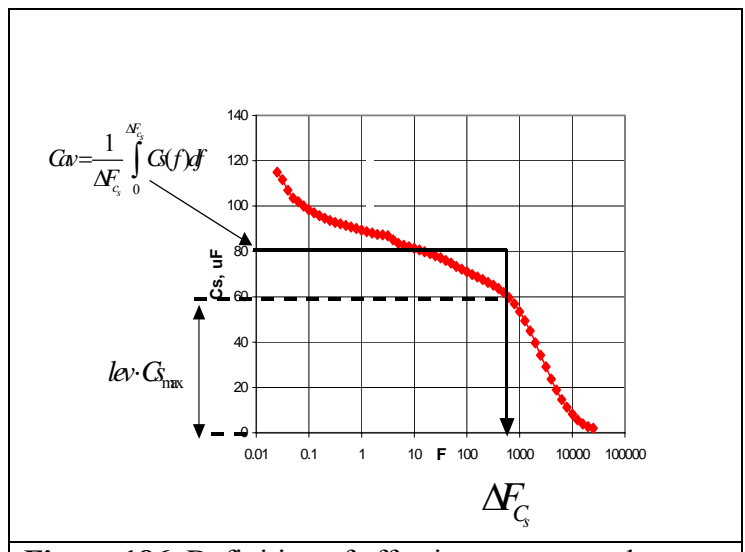
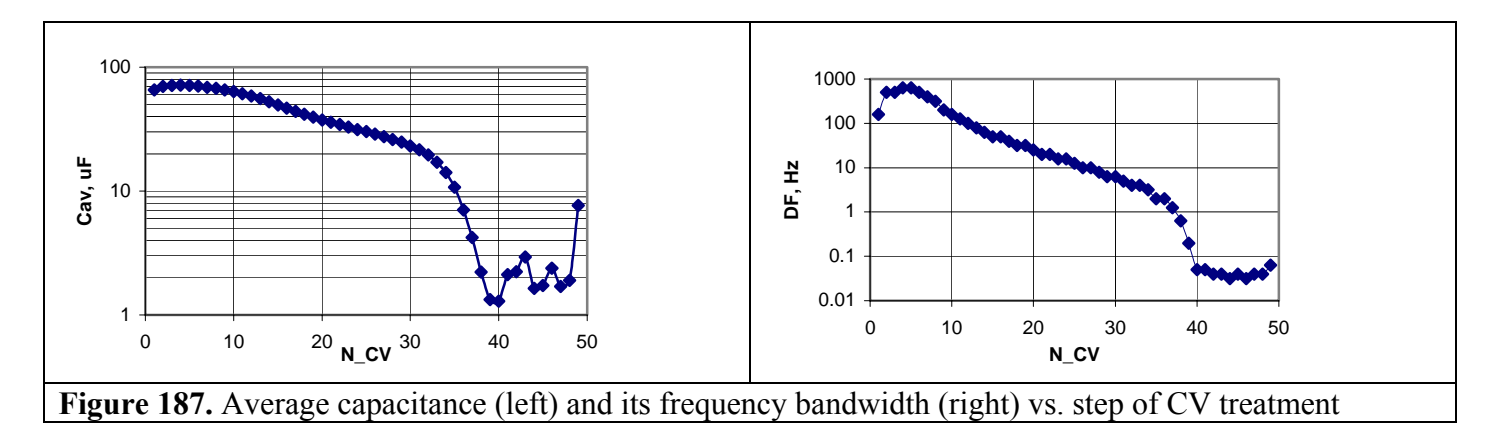


Figure 186. Definition of effective average and frequency band of the static sensor capacitance.

The value of the static capacitance significantly depended on frequency. The maximum values are located in the low frequency region; the minimum values - in the high frequency region and a rapid change from large to the small capacitance value happens in middle frequency region. With transducer degradation the maximum of capacitance and the frequency bandwidth occurs where the static capacitance is about its maximum values decrease (see right plots of the figure 136). Thus an effective frequency bandwidth and average of the static capacitance could be suggested as integrated parameters for characterization of the sensor degradation. The process of finding an effective frequency band and average static capacitance is illustrated by figure 186.

Dependences of the average capacitance and its frequency bandwidth in logarithmic scale vs. step of CV treatment are shown in figure 187.



As can be seen these sensor parameters gradually degraded up to 36*25=900 CV sweeps and after that degradation increased dramatically.

Silicon-gold polypyrrole sensor performance spread

Silicon-gold polypyrrole sensor performance spread can be evaluated by figures 188 - 192 where Nyquist absolute and logarithmic plots, dependencies of real, imaginary and static capacitance vs. frequency are shown for selected number of sweeps (2*25=50, 20*25=500, 40*25=100 and 48*25=1200) for 4 sensors.

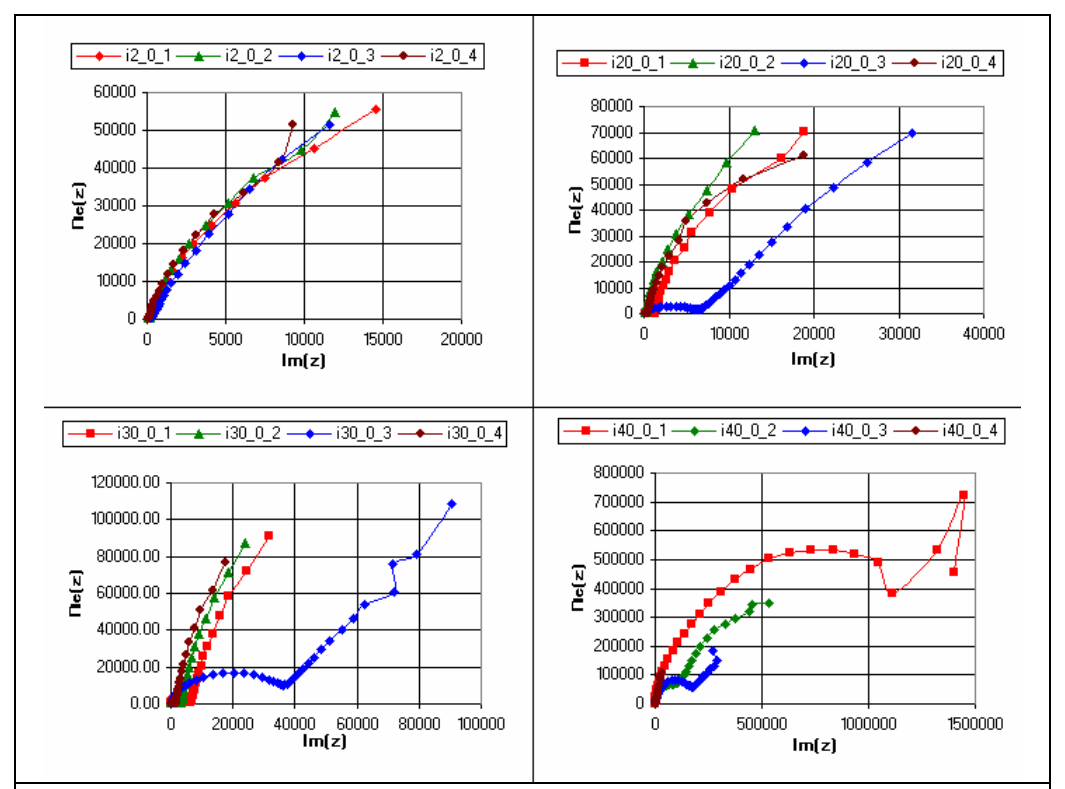


Figure 188. Nyquist absolute plots for 4 sensors after application different numbers of CV treatment steps

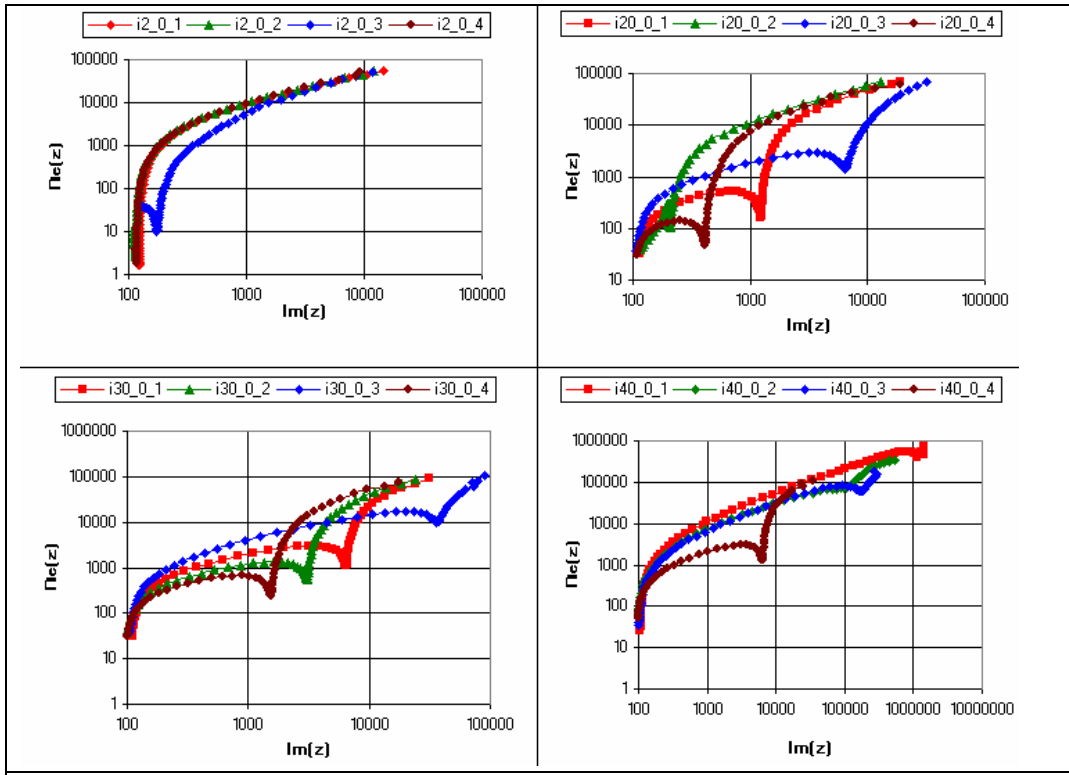


Figure 189. Nyquist logarithmic plots for 4 sensors after application different numbers of CV treatment steps

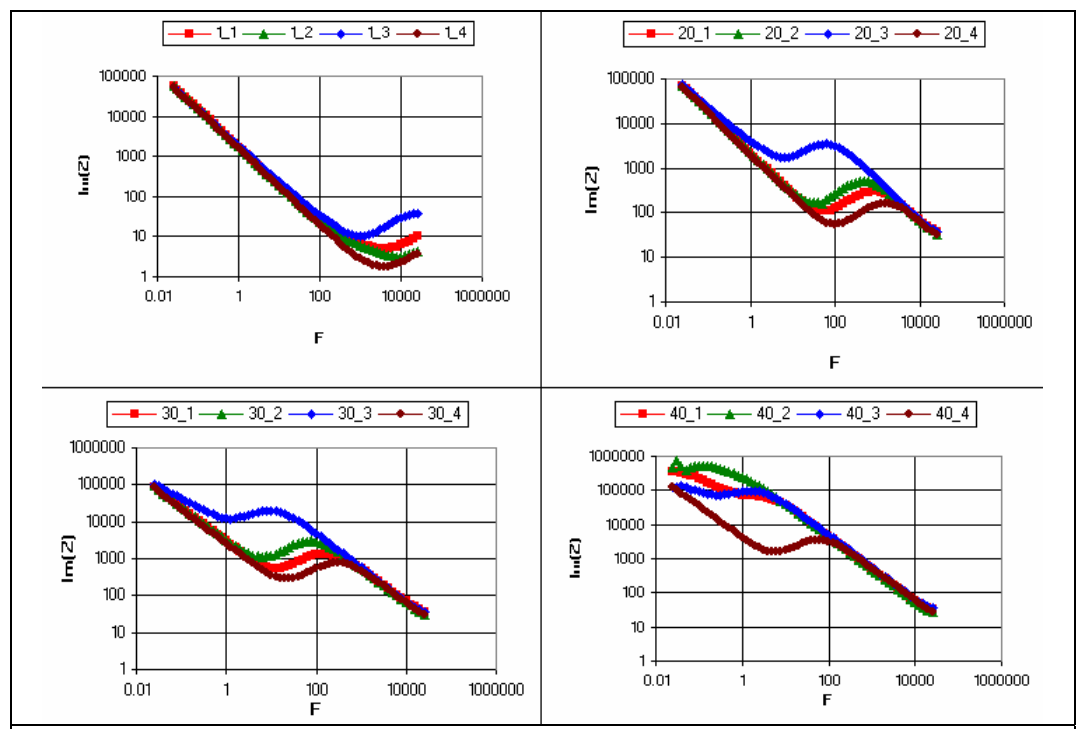


Figure 190. Dependencies Im(Z) vs. frequency for 4 sensors after application different numbers of CV treatment steps

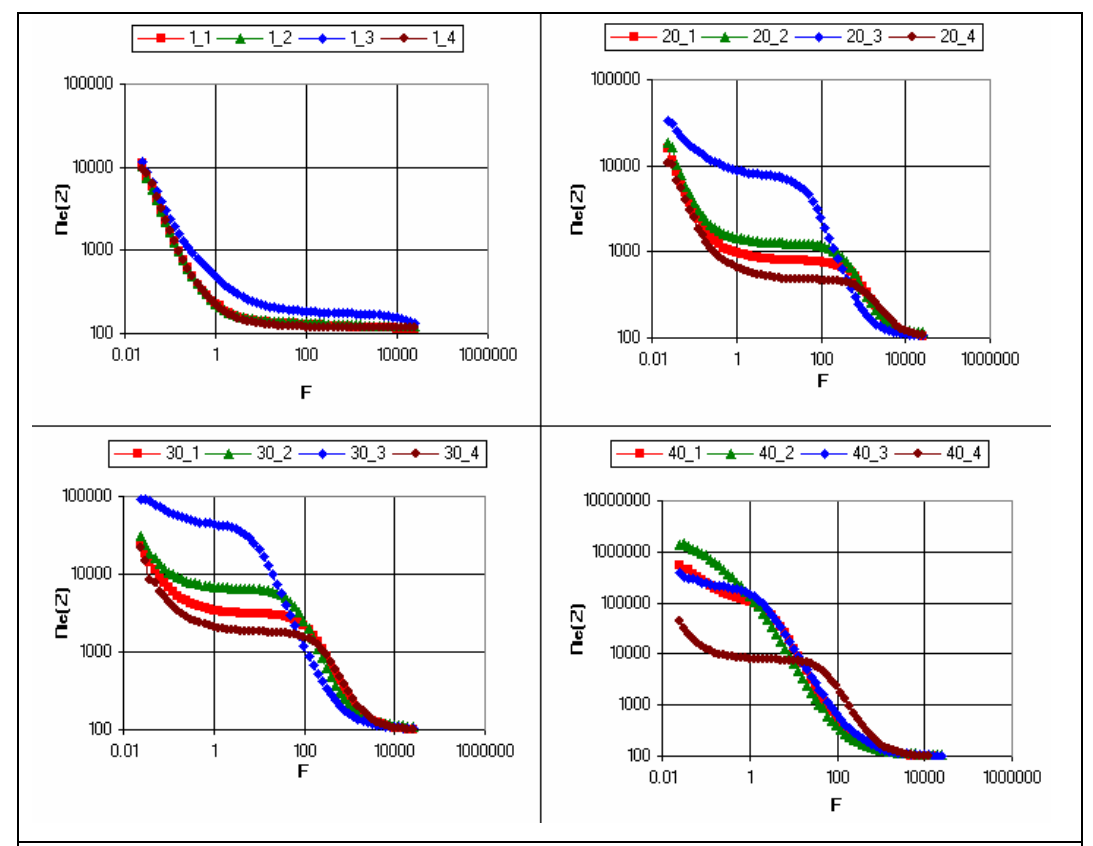


Figure 191. Dependencies Re(Z) vs. frequency for 4 sensors after application different numbers of CV treatment steps

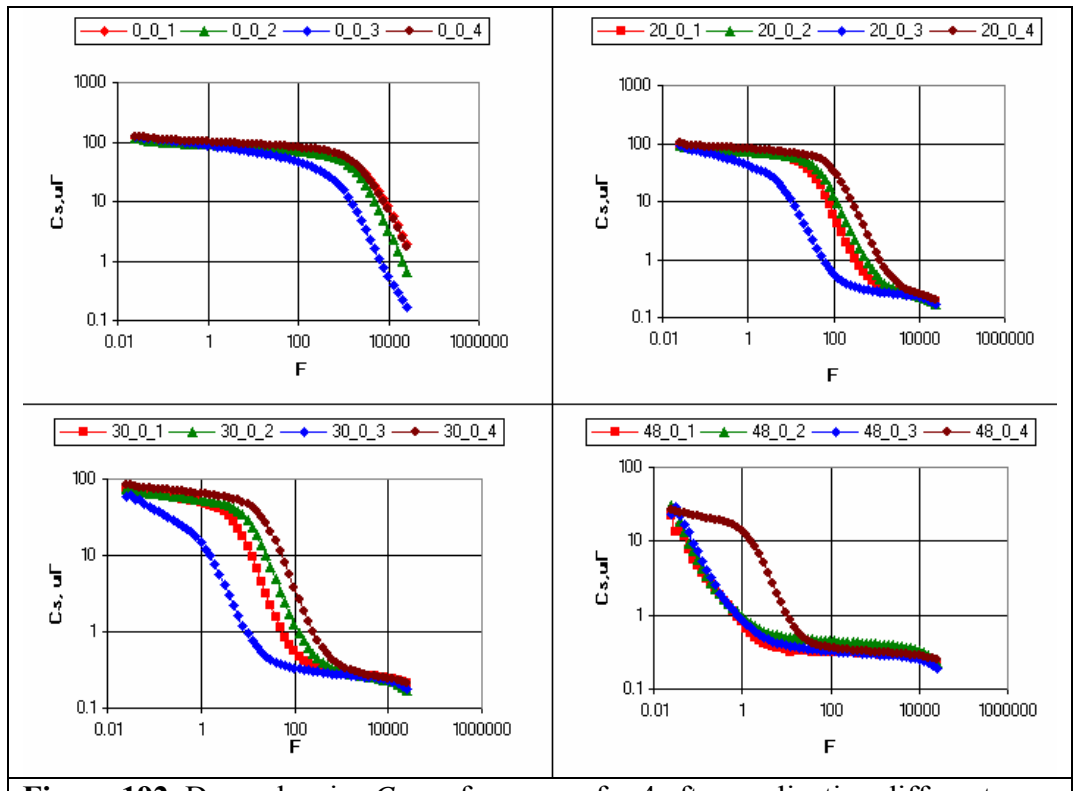


Figure 192. Dependencies *Cs* vs. frequency for 4 after application different numbers of CV treatment steps

As can be seen from these figures, each transducer performed differently. This difference grews when the number of CV treatments increased. Impact of CV treatment on the sensor performance was irregular and individual for each sensor. This final conclusion was confirmed by data withn figure 193 and figure 194 where dependencies of integrated parameters Cs_{av} , ΔF_{Cs} and R_{br} vs. number of CV treatment steps are shown.

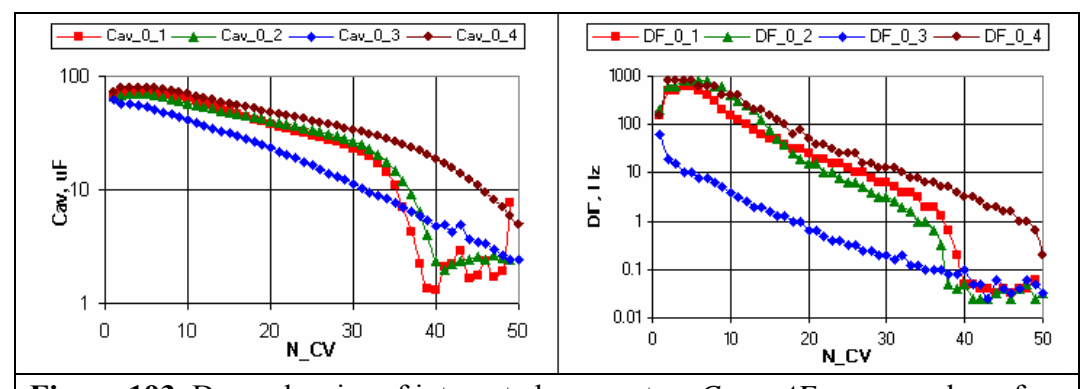


Figure 193. Dependencies of integrated parameters Cs_{av} , ΔF_{Cs} vs. number of CV treatment steps

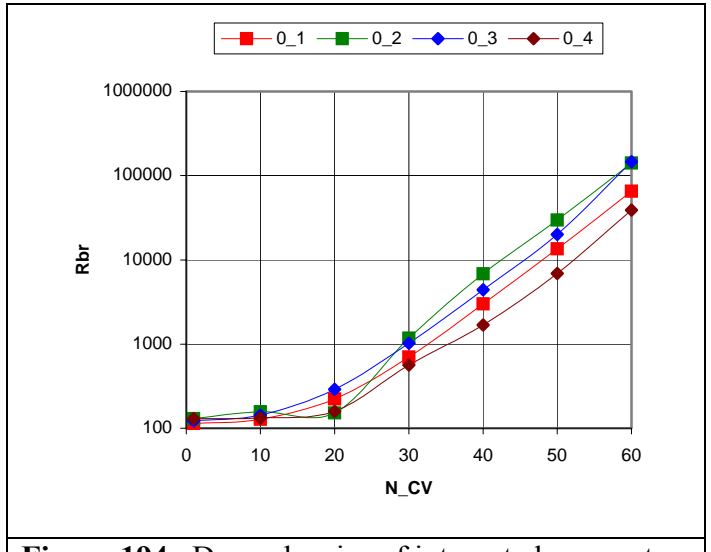


Figure 194. Dependencies of integrated parameters R_{br} vs. number of CV treatment steps

Equivalent electric circuit for the sensor with thick polypyrrole film

Results of polypyrrole sensor degradation can be seen in figure 195 where two microscope images of the sensor before and after application of CV treatment are shown. The transducer structure comprised a thick film with a number of pores sizes; it is likely that the number of these increased when the sensor degraded. Equivalent circuit for this structure needs in further modification in comparison with the equivalent circuit for uniform film considered earlier. In this case, the electrical behavior of the pores cannot be described just by equivalent specific pore capacitance and more complex two-phase model of the sensor cross-section shown in figure 196 was developed. In this model each cross-section is characterized by specific resistance of ionic (ρ_1) and polymer (ρ_2) channels with cross-channel specific interfacial impedance (Z_{HO}). This impedance reflects interfacial behavior of the pores and can be presented by modified Randle's equivalent circuit shown in figure 197.

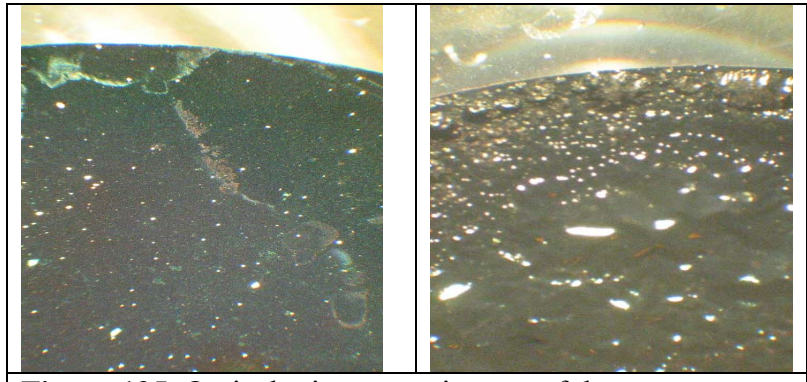


Figure 195. Optical microscope images of the sensor before (left) and after (right) a number of CV treatments.

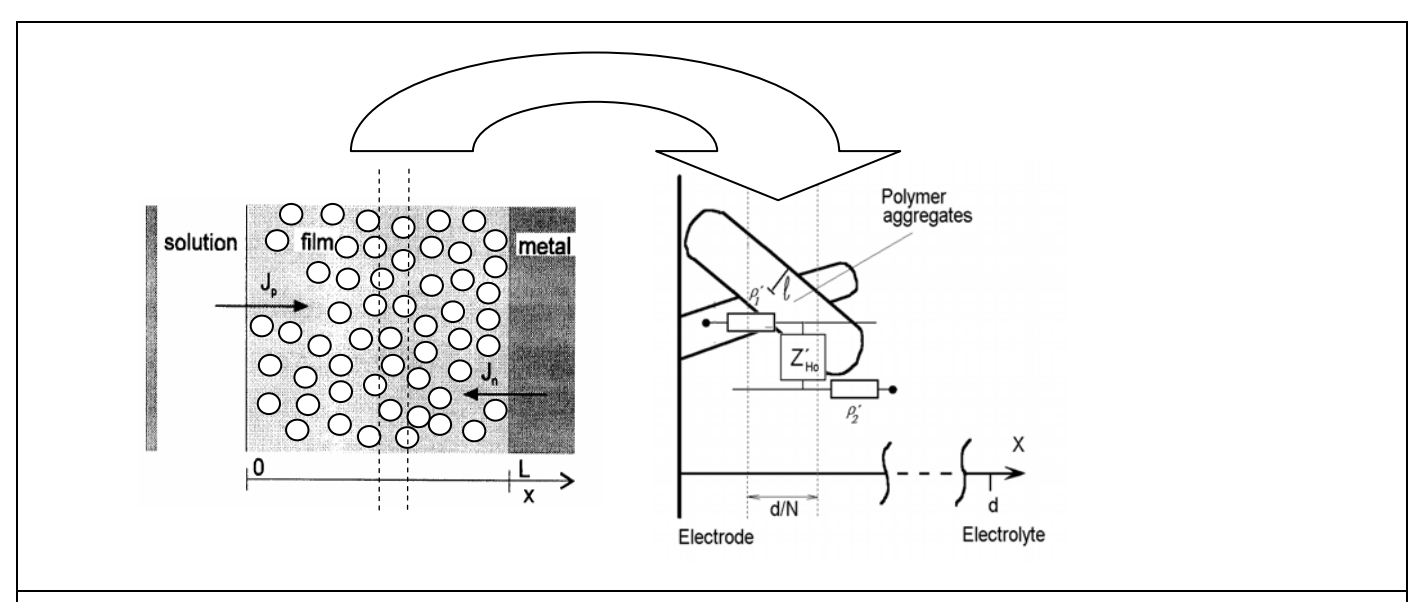
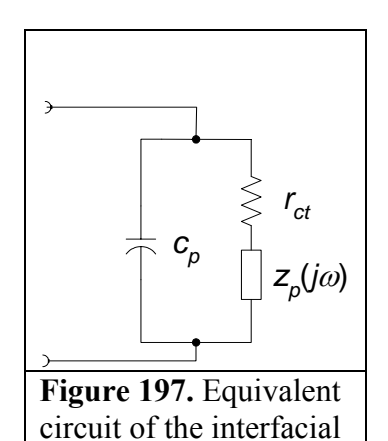


Figure 196. Polypyrrole film sensor with large size of pores and two-phase model of the sensor cross-section



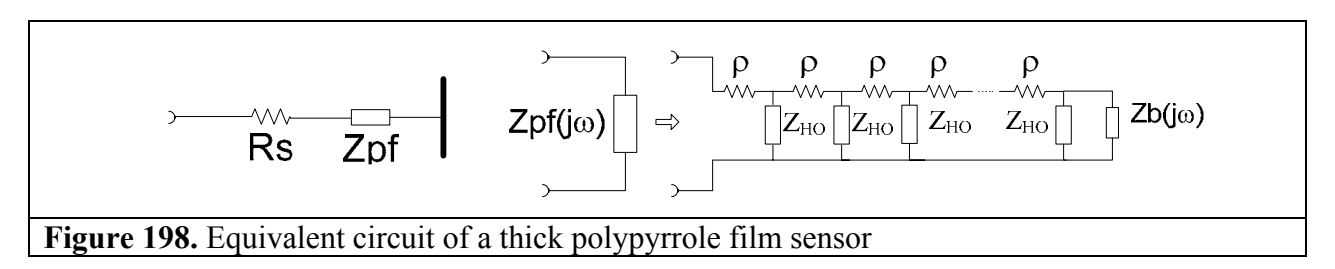
impedance.

In this equivalent circuit c_p is a double layer specific capa-citance, r_{ct} is a charge transfer specific resistance and $z_p(j\omega)$ is a specific diffusion impedance of the pore averaged along the cross-section. After investigation, it wwas discovered that $z_p(j\omega)$ could be described by equation 8.2

$$z_{p}(jw) = w_{p} \frac{\cot \frac{\partial c}{\partial x} j \frac{w}{w_{p}} \frac{\overset{\circ}{\circ}^{a} \overset{\circ}{\circ}}{\overset{\dot{\circ}}{\circ}}}{\underbrace{\frac{\dot{c}}{\dot{c}}}{\dot{c}}}}{\underbrace{\frac{\dot{c}}{\dot{c}}}{\dot{c}}}$$

$$\underbrace{z_{p}(jw) = w_{p}}_{p} \frac{\partial c}{\partial x} \frac{\dot{c}}{\dot{c}}}{\underbrace{\frac{\dot{c}}{\dot{c}}}{w_{p}} \overset{\circ}{\dot{c}}}}$$
(8.2)

where w_p is a pore characteristic impedance; $\omega_p = D/L_p^2$ is a pore characteristic frequency; $0 < \alpha \le 1$ is constant phase coefficient, which can take into account possible abnormal diffusion and specific boundary condition inside the pores (in case of normal diffusion and totally reflecting boundary conditions $\alpha=1$); D is a diffusion coefficient; and L_p is a pore length. If ionic specific resistance ρ_I is significantly larger than polymer specific resistance ρ_2 , the sensor equivalent circuit can be presented by the circuit shown in the figure 198.



Here Rs is a liquid volume resistance and Z_{pf} is a polymer film impedance characterized by equation 8.3

$$Z_{pf} = Zo \frac{1 + \frac{Z_b(jw)}{Zo} \coth(gL_f)}{\frac{Z_b(jw)}{Zo} + \coth(gL_f)}$$
(8.3)

In equation 8.3 $Z_o = \sqrt{Z_{HO}\rho}$ is a film complex characteristic impedance; $\gamma = \sqrt{\rho/Z_{HO}}$ is a film propagation coefficient; L_f is a film thickness; $Z_b(j\omega)$ is a complex boundary impedance related to the concentration boundary conditions of electroactive species in the end of the polymer zone at the metal electrode surface. The general case of this boundary impedance can be described by equation 8.4

$$Zf(j\omega)) = 1/[1/r + Q(j\omega)^n]$$
(8.4)

where r has the dimensions of Ω ; n is non-dimensional CPE constant 0 < n < 1 and Q is a constant with the dimension of Fsⁿ⁻¹.

In order to obtain correct results of the equivalent circuit specification it is very important to understand how parameters of the model influence its response. To gain this the case was analyzed when the complex boundary impedance $Zb(j\omega)$ was significantly larger than the film complex characteristic impedance Z_o (corresponds to reflecting boundary conditions). At this condition equation 8.3 can be rewritten as equation 8.5.

$$Z_{pf} = Zo \coth(gL_f) = R \frac{1}{\sqrt{\frac{1}{\frac{Z_p}{R} + d_{ct}}}} \coth(\frac{w}{w_L}) + j\frac{w}{w_L} + j\frac{w}{w_$$

where $R = \rho L_f$ is a total ionic resistance of the film, $\omega_L = 1/(C_{dl}R)$ is a film characteristic frequency; C_{dl} is a total double layer capacitance of the film pores; $d_{ct} = R_{ct}/R$ is a ratio of a total film charge transfer resistance $R_{ct} = r_{ct}L_f$; $Z_p = z_pL_f$ is total pore part film impedance. Additionally two limiting cases were analysed.

The first one was the case when ionic specific resistance ρ was significantly less than module of the specific interfacial impedance Z_{HO} (i.e. at the very low frequency region). Thus, the equivalent circuit for Zpf in figure 198 presents a parallel connection of cross-channel specific interfacial impedances (Z_{HO}) forming a film integral pore impedance described by equation 8.6.

$$Zp = R \frac{1}{\frac{1}{\cosh \frac{\partial u}{\partial x} + j \frac{w}{w_L}}} + j \frac{w}{w_L}$$

$$a_p \frac{\partial u}{\partial y} + d_{ct}$$

$$(8.6)$$

where $a_p = W_p/R$ and $W_p = w_p L_f$ is a film pore characteristic impedance.

The second case was the case when the frequency was high and the average cross-section pore acts because of the presence of the double layer pore capacitance. The equivalent circuit for *Zpf* in figure 149 is a *RC*-distributed line with impedance described by equation 8.7.

$$Z_{L} = R \frac{1}{\sqrt{j \frac{w}{w_{L}}}} \coth \frac{\mathcal{E}}{\mathcal{E}} \sqrt{j \frac{w}{w_{L}} \frac{\ddot{o}}{\dot{\overline{\phi}}}}$$
(8.7)

Normalized to R and ω_L frequency dependencies of real and imaginary parts of impedances, these three cases for Rs/R=0.1, $a_p=0.1$, $d_{ct}=0.1$, $\alpha=1$ and three relationships between characteristic frequencies ω_p and ω_L : $\omega_p=10\,\omega_L$ (small size of the pore), $\omega_p=0.1\,\omega_L$ (large size of the pore) and $\omega_p=\omega_L$ are shown in figures 199, 200 and 201 respectively.

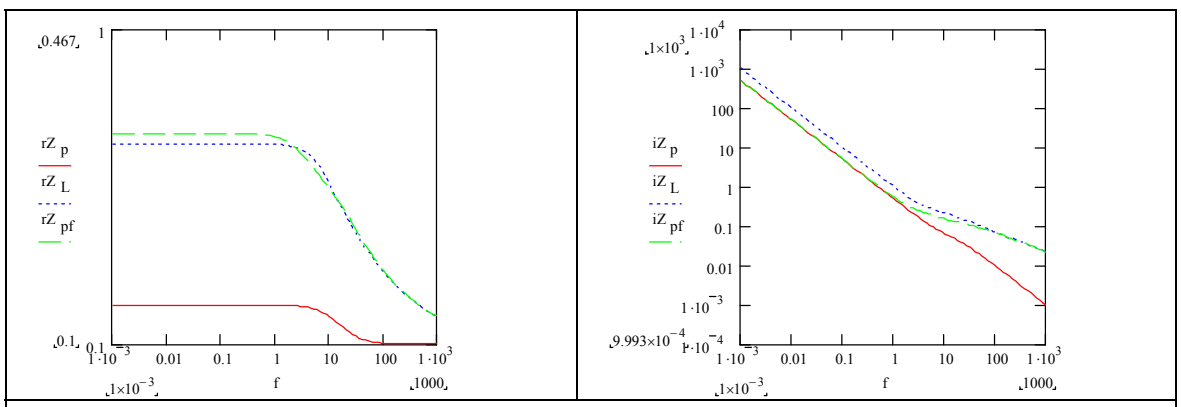
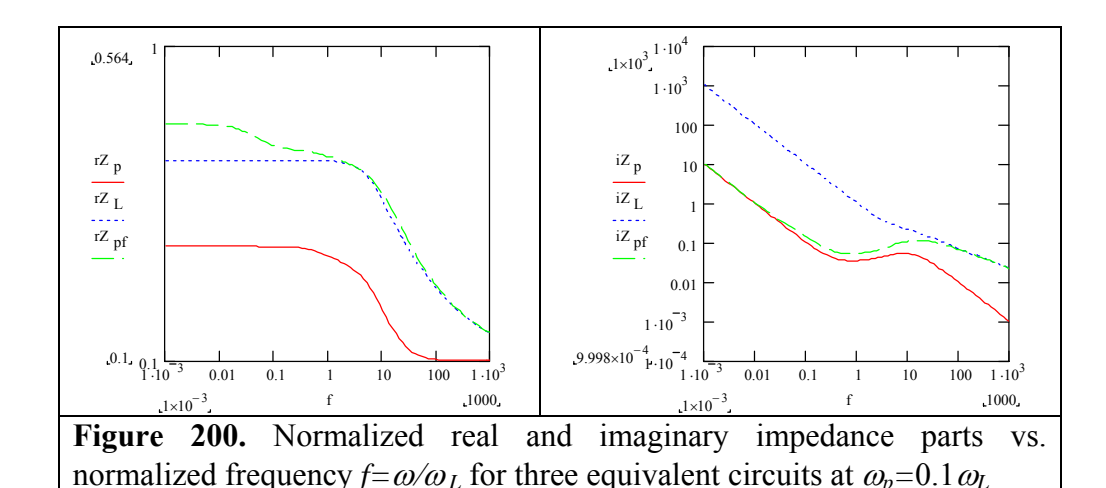


Figure 199. Normalized real and imaginary impedance parts vs. normalized frequency $f=\omega/\omega_L$ for three equivalent circuits at $\omega_p=10\omega_L$



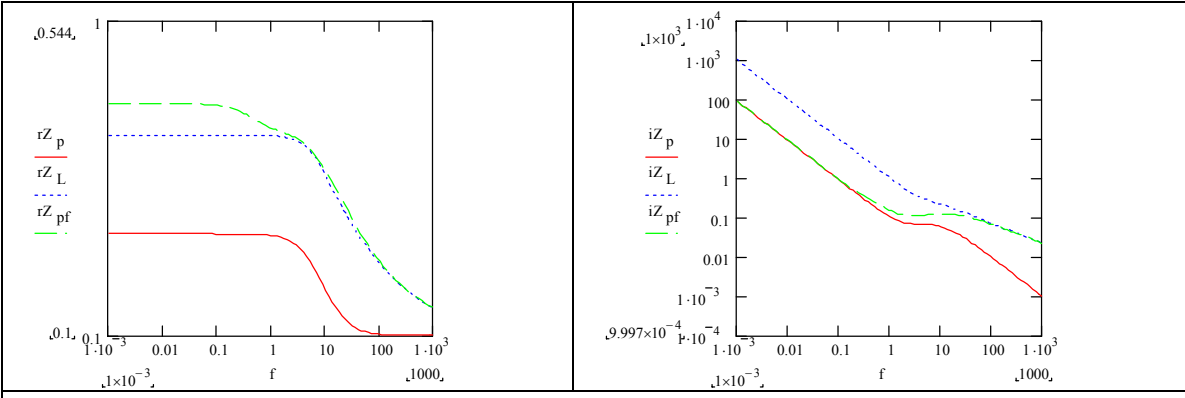


Figure 201. Normalized real and imaginary impedance parts vs. normalized frequency $f = \omega/\omega_L$ for three equivalent circuits at $\omega_p = \omega_L$

Nyquist plots and frequency dependencies of the static capacitances for considered relationships between characteristic frequencies ω_p and ω_L are shown in figure 202 and figure 203 correspondingly

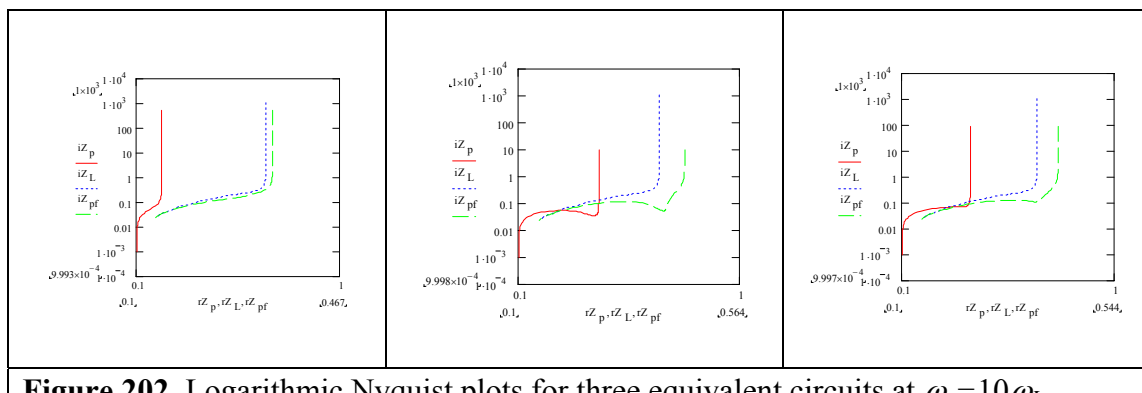


Figure 202. Logarithmic Nyquist plots for three equivalent circuits at $\omega_p = 10 \omega_L$, $\omega_p = 0.1 \omega_L$ and $\omega_p = \omega_L$

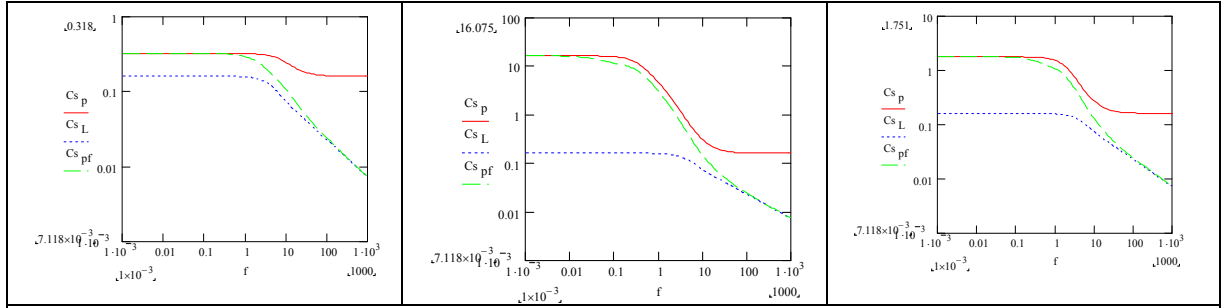


Figure 203. Frequency dependencies of the static capacitance for three equivalent circuits at $\omega_p = 10 \omega_L$, $\omega_p = 0.1 \omega_L$ and $\omega_p = \omega_L$

As can be seen, the frequency dependencies of imaginary part of impedance and static capacitance for Zpf in the low frequency region are defined by the pore impedance Zp and in the high frequency region – by the line impedance Z_L . The capacitance frequency bandwidth is defined by the pore characteristic frequency ω_p .

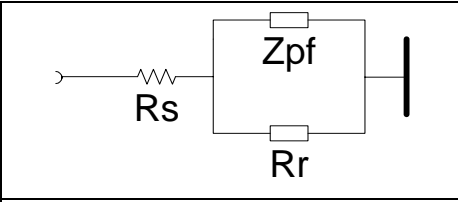


Figure 204. Equivalent circuit of thick polypyrrole film sensor with a film relaxation resistor *Rr*

Although frequency dependences of Zpf looked very similar to experimental ones, the Nyquist plots did not coincide with experimental ones. This is probably because the model does not take into account a possible relaxation process inside the polypyrrole film. To check this the modification of the equivalent circuit (figure 149) was undertaken and a Rr as shown in figure 204 was incorporated into it. Nyquist plots for the modified equivalent circuits at considered relationships between characteristic frequencies ω_p and ω_L are shown in figure 205.

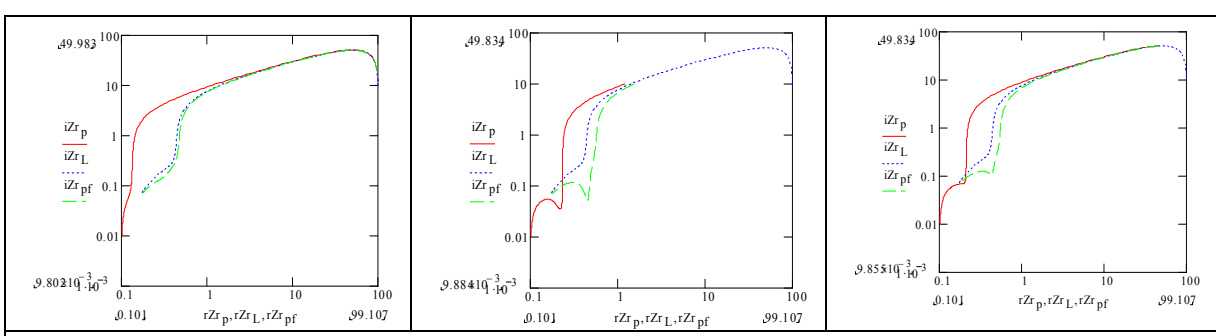


Figure 205. Logarithmic Nyquist plots for three equivalent circuits with a film relaxation resistor Rr=100R at $\omega_p=10\omega_L$, $\omega_p=0.1\omega_L$ and $\omega_p=\omega_L$

As can be seen with this modification, the match between the model and experimental data was much better and the model in figure 204 was selected for the equivalent circuit specification.

Improvement strategy of specification of equivalent circuit

The strategy of specification of equivalent circuit was based on the mean square root fitting of sensor complex impedance measurements. The fitting procedure was performed by minimisation of the average approximation errors determined for absolute D, semi-logarithmic Ls and logarithmic L metrics in the frequency sweep range. These metrics differ in evaluation of a distance between two complex points on the complex plane (experimental Ze and calculated Zc complex impedances) presented in the corresponding system of coordinates. For absolute metric D there is an orthogonal system with real (Re(Z)) and imaginary (Im(Z)) parts of impedance Z as coordinates or a polar system with absolute value |Z| and phase angle θ of impedance Z so the fitting error for each experimental point was calculated as

$$D = \left| Ze - Zc \right| = \sqrt{\left(\operatorname{Re}(Ze) - \operatorname{Re}(Zc) \right)^2 + \left(\operatorname{Im}(Ze) - \operatorname{Im}(Zc) \right)^2}$$
 (8.8)

For logarithmic and semi logarithmic metrics the distance is defined in orthogonal logarithmic (logarithm of real and modulus of imaginary parts of impedance) and polar logarithmic (logarithm of absolute value and phase angle in radian) systems so the fitting error inthis case was

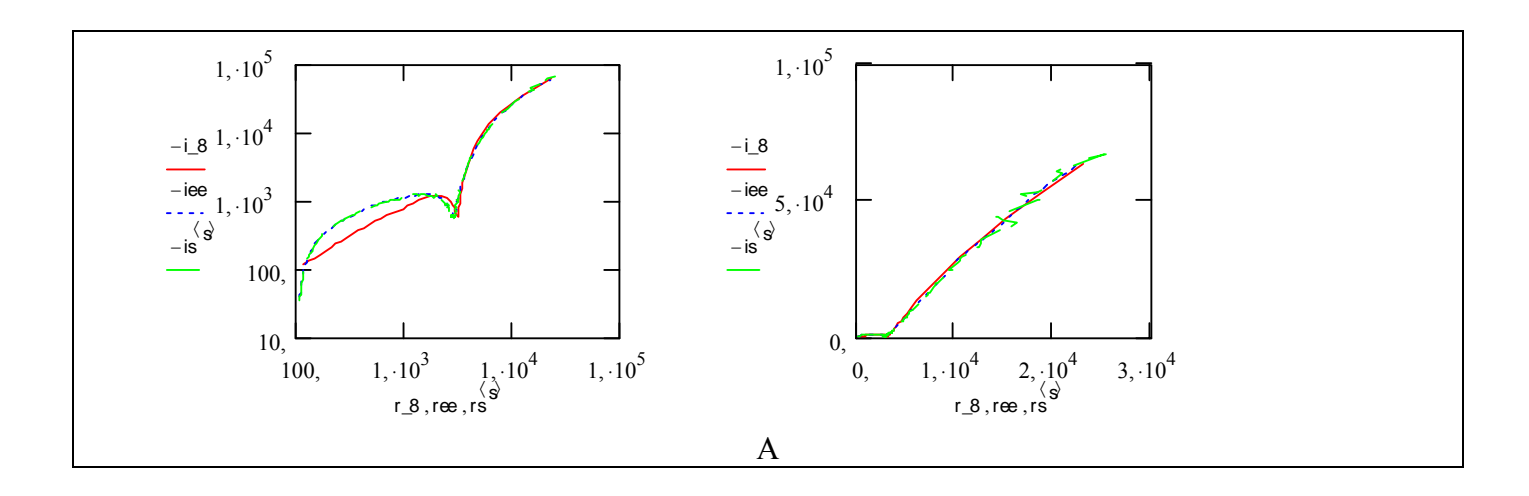
$$L = \sqrt{\left(\ln\left|\operatorname{Re}(Ze)\right| - \ln\left|\operatorname{Re}(Zc)\right|\right)^{2} + \left(\ln\left|\operatorname{Re}(Ze)\right| - \ln\left|\operatorname{Re}(Zc)\right|\right)^{2}}$$
(8.9)

and

$$Ls = \sqrt{\left(\ln\left|Ze\right| - \ln\left|Zc\right|\right)^2 + \left(\theta e - \theta c\right)^2}$$
(8.10)

correspondingly.

It is clear that the best fitting for experimental data presented in some system of coordinates was in case when the metric selected for averaging of the approximation error corresponded to the coordinate system. At the same time this does not guarantee that this fitting is the best in the case when another system of coordinate is used for impedance data presentation. This assertion is illustrated in figure 157a,b where results of the fitting for absolute (figure 206a) and logarithmic (figure 206b) metrics are shown in absolute and logarithmic scales.



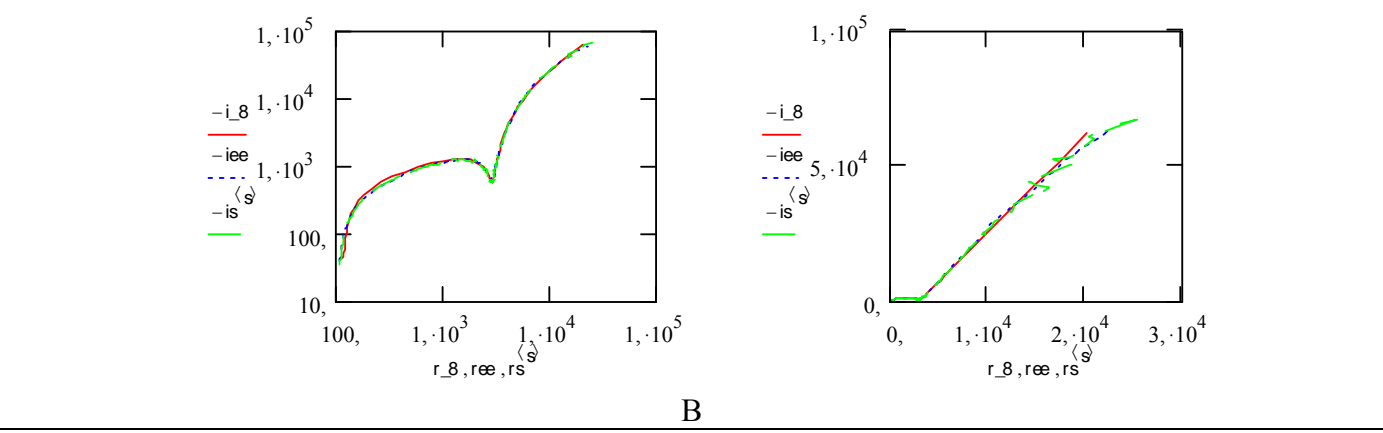


Figure 206. Results of the fitting for absolute (A) and logarithmic (B) metrics presented in logarithmic (left) and absolute (right) coordinate systems.

It is clear that the use of an absolute metric gave a better approximation on an absolute scale and logarithmic metric gave a better approximation on a logarithmic scale. Fitting performance in the system of coordinate incongruous to the selected metric was inferior to the coinciding case. To obtain a compromise in approximation, which provides satisfactory fitting of the experimental data in different systems of coordinate at the same time, the use of mixed metrics was suggested. These mixed metrics are equal to the product of the metrics corresponding to the system of coordinate selected for presentation of experimental data i.e *DL*, *DLs*, *LLs* or *DLLs*. Result of the fitting with use of mixed *DL* metric is shown in Figure 207.

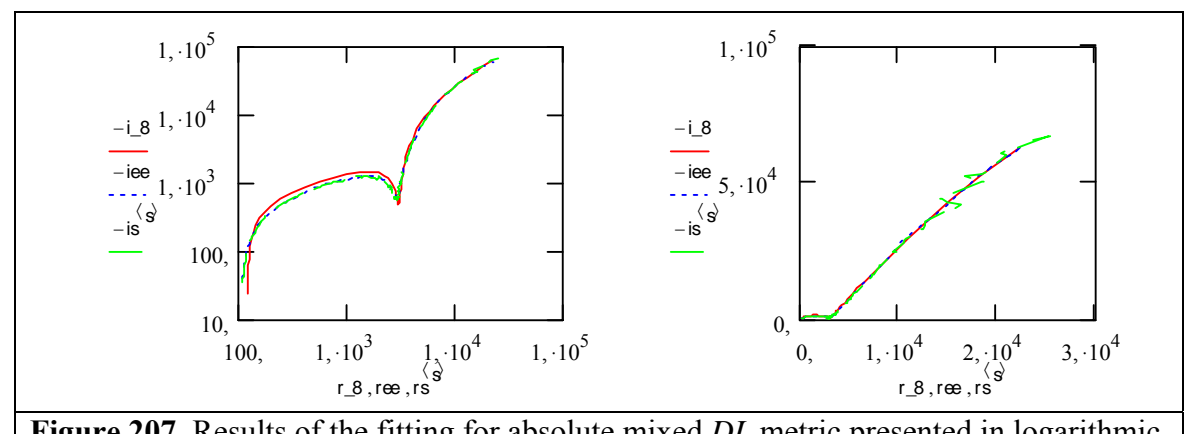


Figure 207. Results of the fitting for absolute mixed *DL* metric presented in logarithmic (left) and absolute (right) coordinate systems.

As one can see the use of this metric provided a good fitting of the impedance data in both logarithmic and absolute scales and mainly this mixed metric was selected for the fitting of the experimental data.

Specification of the equivalent circuit

The improved equivalent circuit and fitting approach based on the use of mixed metrics were applied to experimental data for specification of the circuit parameters. Typical results of the fitting in mixed *DL* metric presented in absolute and logarithmic scales are shown in figure 208 and 209.

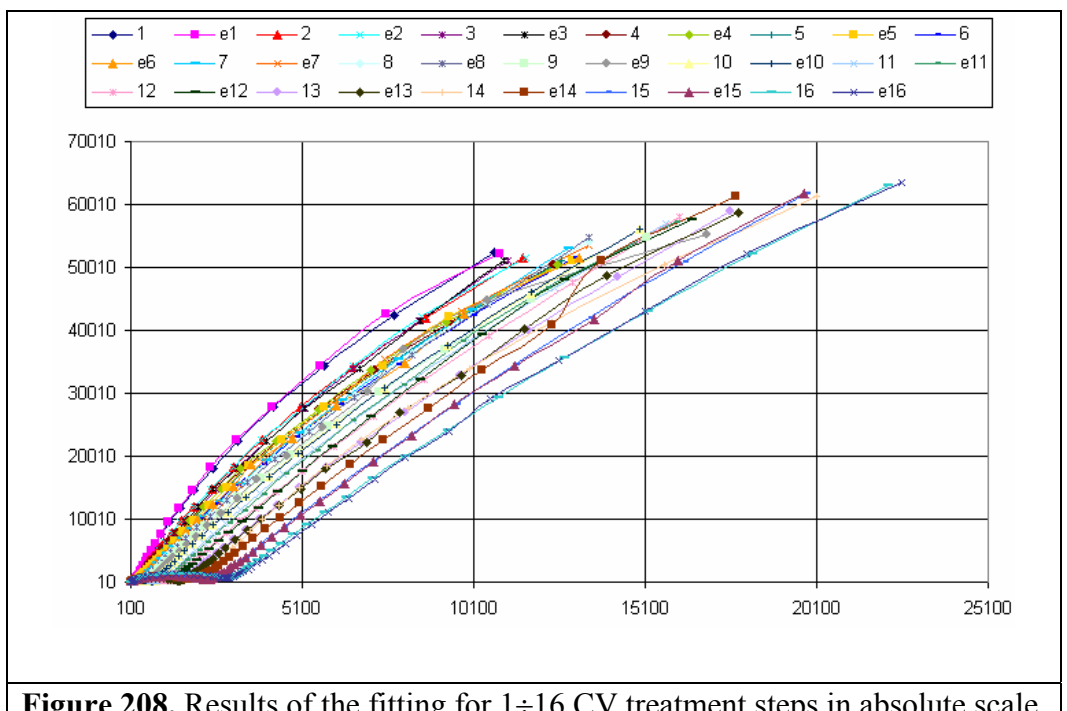


Figure 208. Results of the fitting for 1÷16 CV treatment steps in absolute scale.

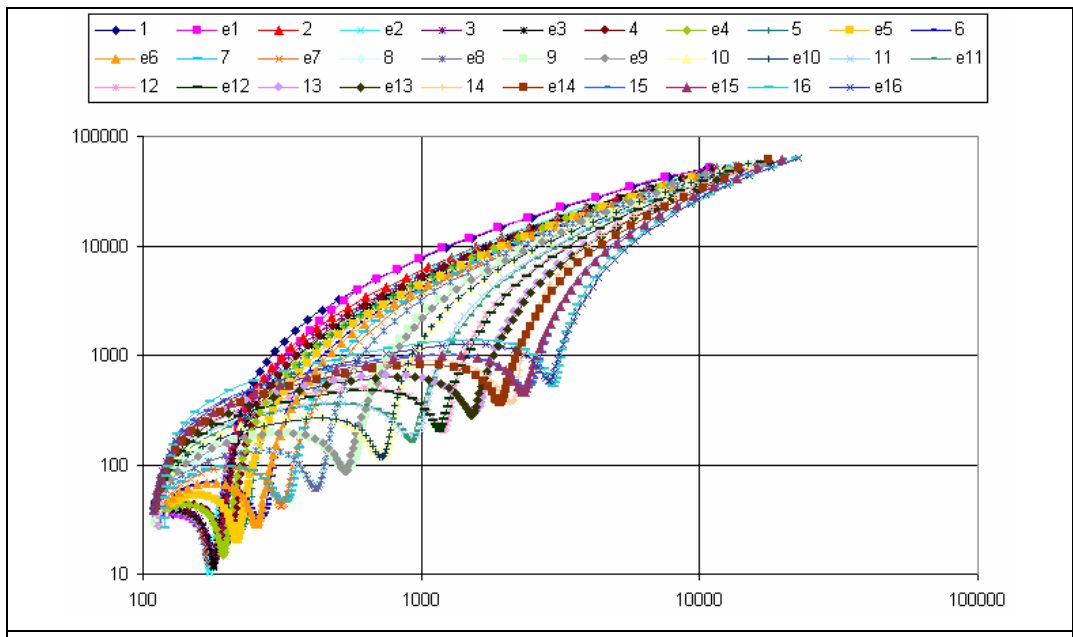
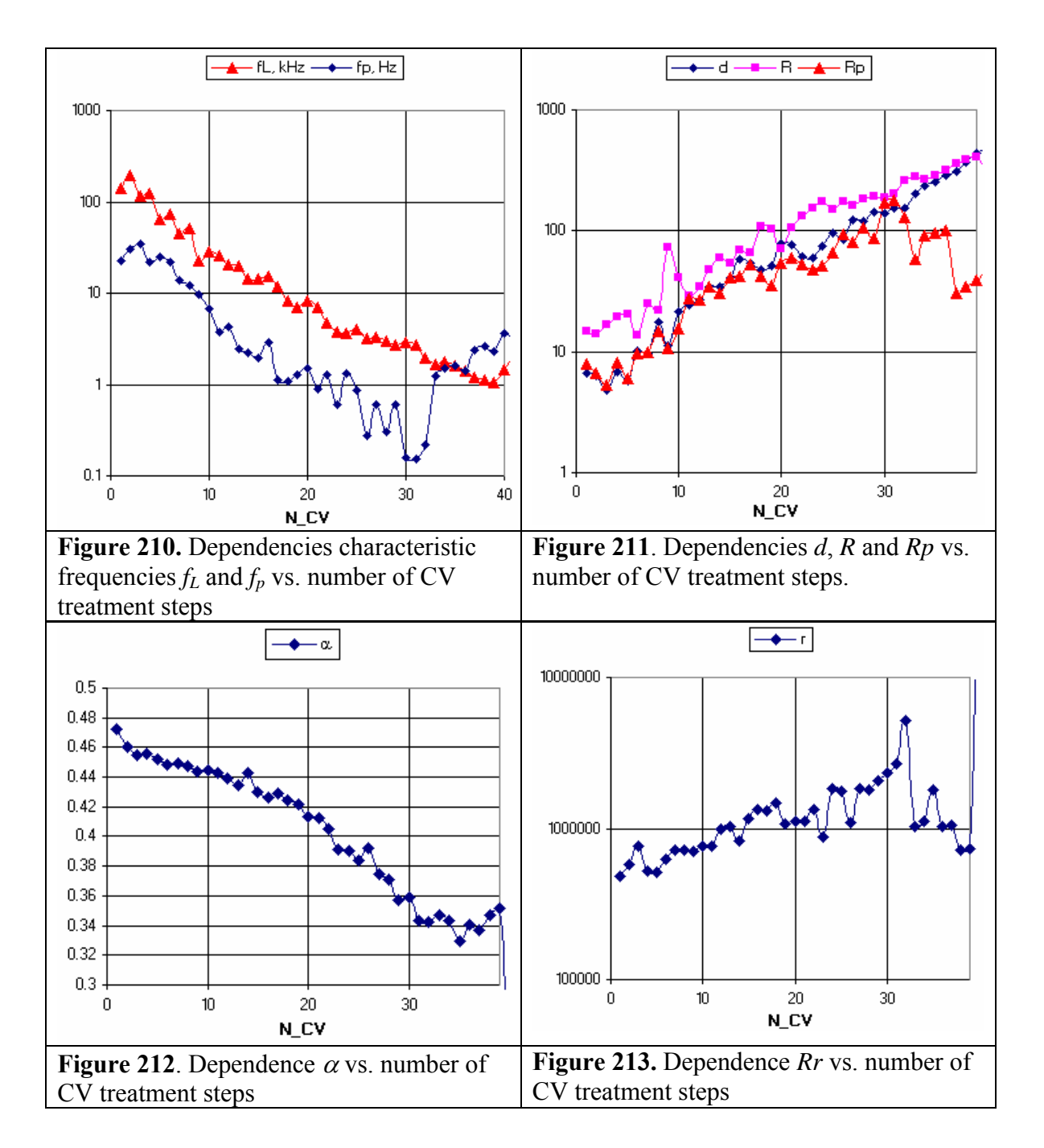


Figure 209. Results of the fitting for 1÷16 CV treatment steps in logarithmic scale.

The fitting is quite good in both system of coordinates. Dependencies of the circuit parameters vs. CV treatment steps are shown in figure 210-213.



It was evident that if the number of CV treatments increased the characteristic frequencies f_L and f_p and constant phase coefficient α decreased whilst d, R, Rp and Rr increased. These changes coincide with figure 195 where photographs of transducers before and after CV treatments are shown. As follows from the photographs, CV treatment resulted in an increase of the pore size. It gave an increase in pore area that accompanied the increase of the pore double layer capacitance, d and Rp. Additionally, according to the definition of the characteristic pore $\omega_p = D/L_p^2$ and film $\omega_L = 1/(C_{dl}R)$ frequencies, both of these parameters decreased if pore size increased. Exactly the same behavior of the circuit parameters could be derived from the circuit specification.

Study of silicon-gold polypyrrole sensor stabilization by mercaptohexadecanoic acid treatment

Results of the sensor impedance spectroscopy (absolute and logarithmic Nyquist plots and static capacitance vs. frequency) after 30 minutes and 2 hours MHDA treatment are shown in figure 214 - 219.

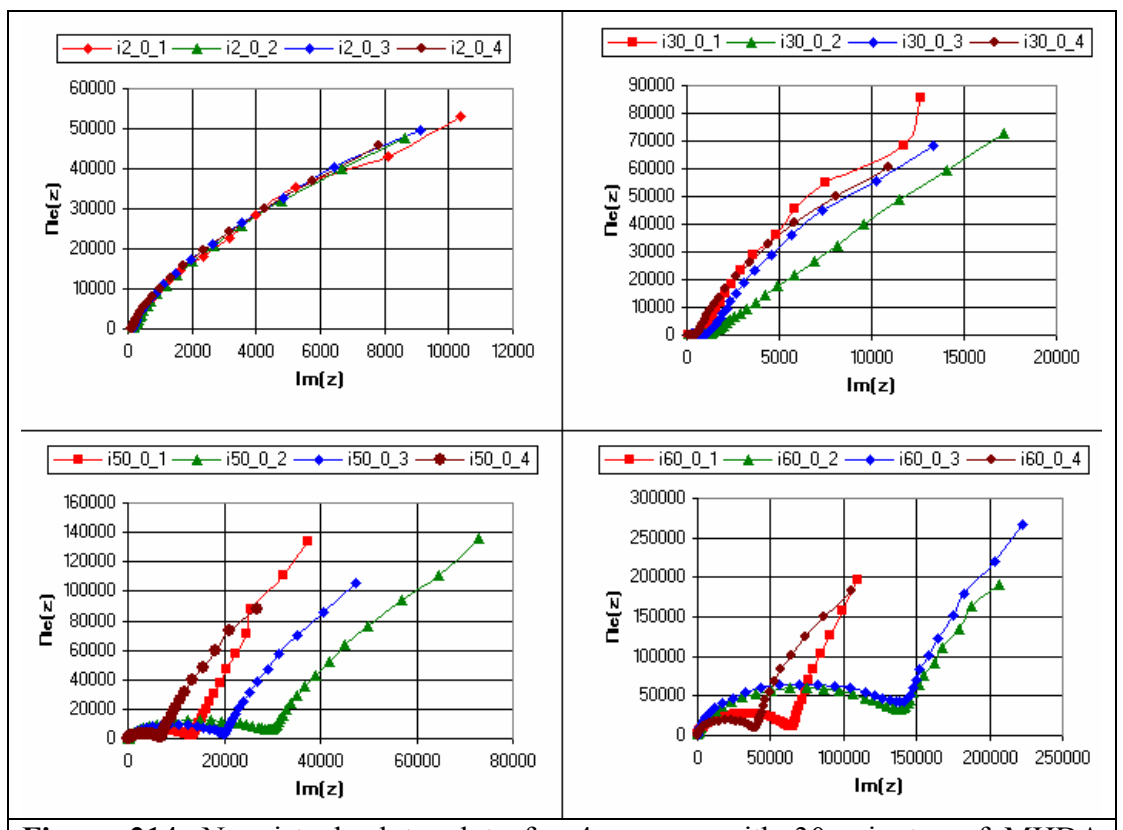


Figure 214. Nyquist absolute plots for 4 sensors with 30 minutes of MHDA treatments after application different numbers of CV treatment steps

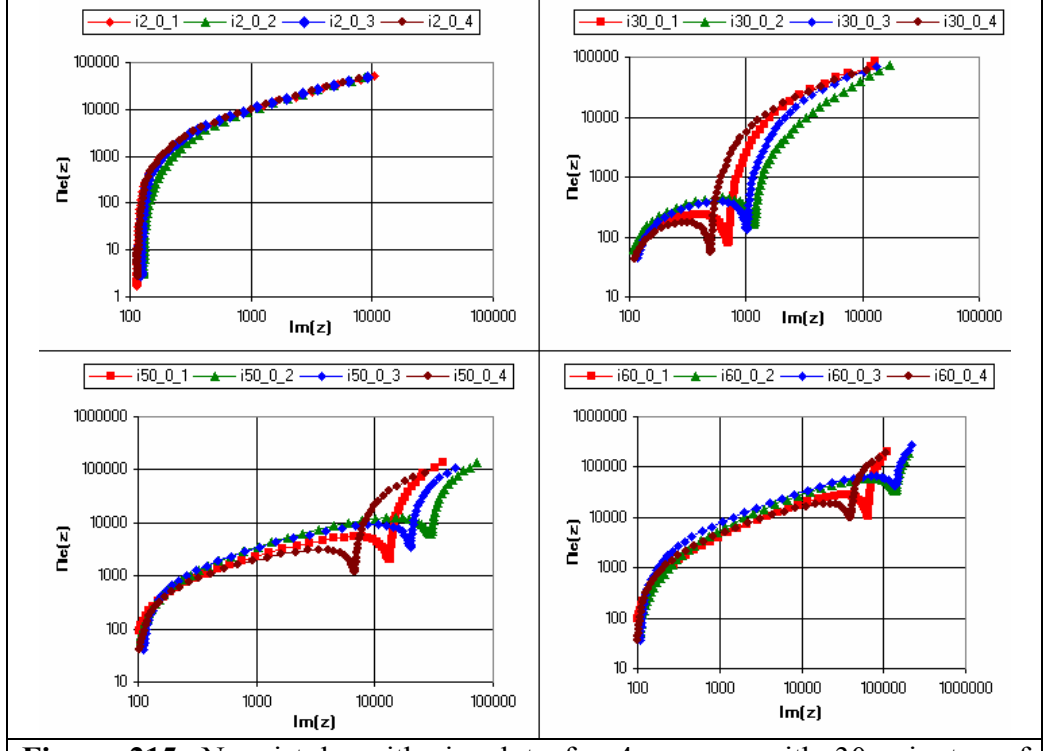


Figure 215. Nyquist logarithmic plots for 4 sensors with 30 minutes of MHDA treatments after application different numbers of CV treatment steps

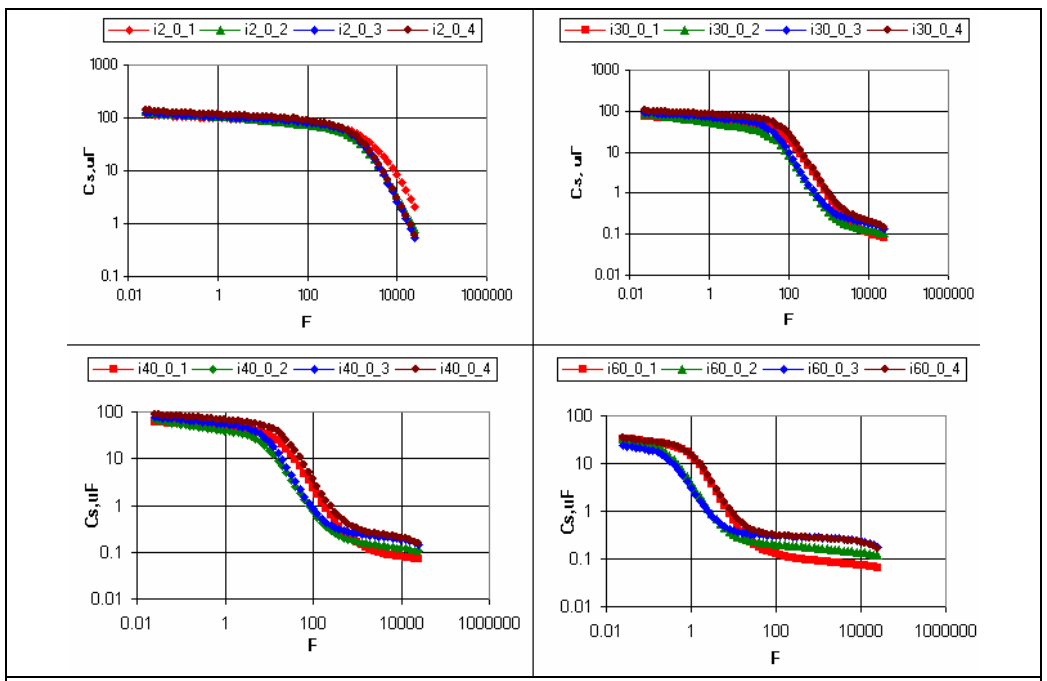


Figure 216. Dependencies *Cs* vs. frequency for 4 sensors with 30 minutes of MHDA treatments after application different numbers of CV treatment steps

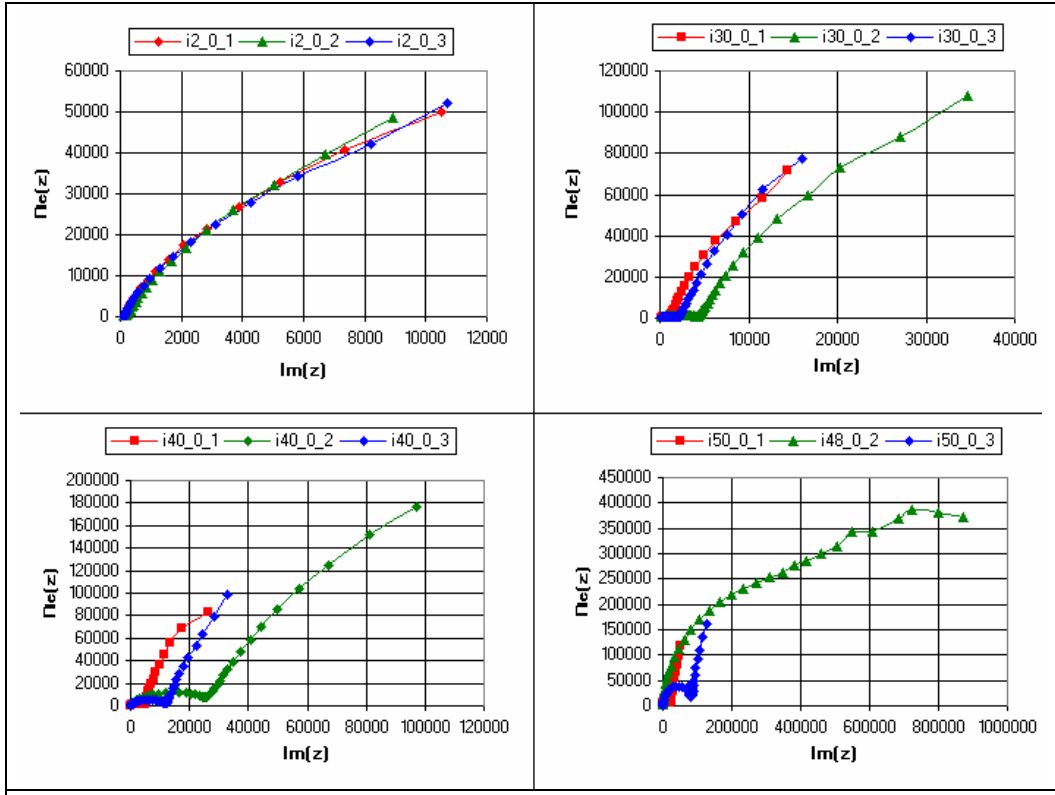


Figure 217. Nyquist absolute plots for 3 sensors with 2 hours of MHDA treatments after application different numbers of CV treatment steps

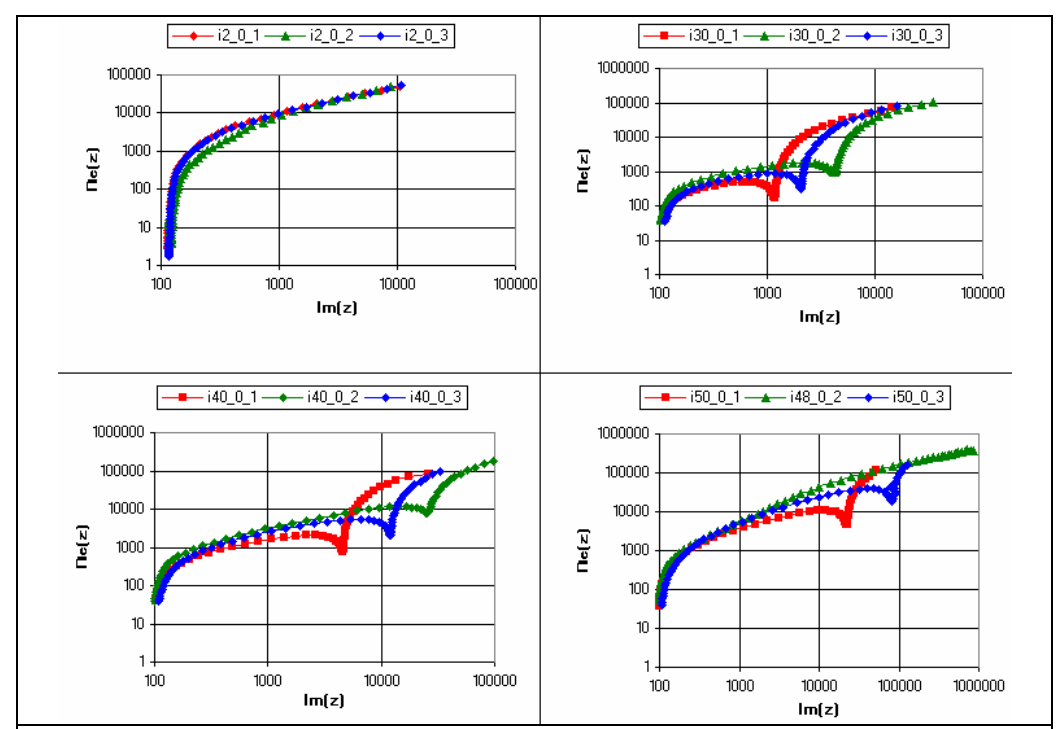


Figure 218. Nyquist logarithmic plots for 3 sensors with 2 hours of MHDA treatments after application different numbers of CV treatment steps

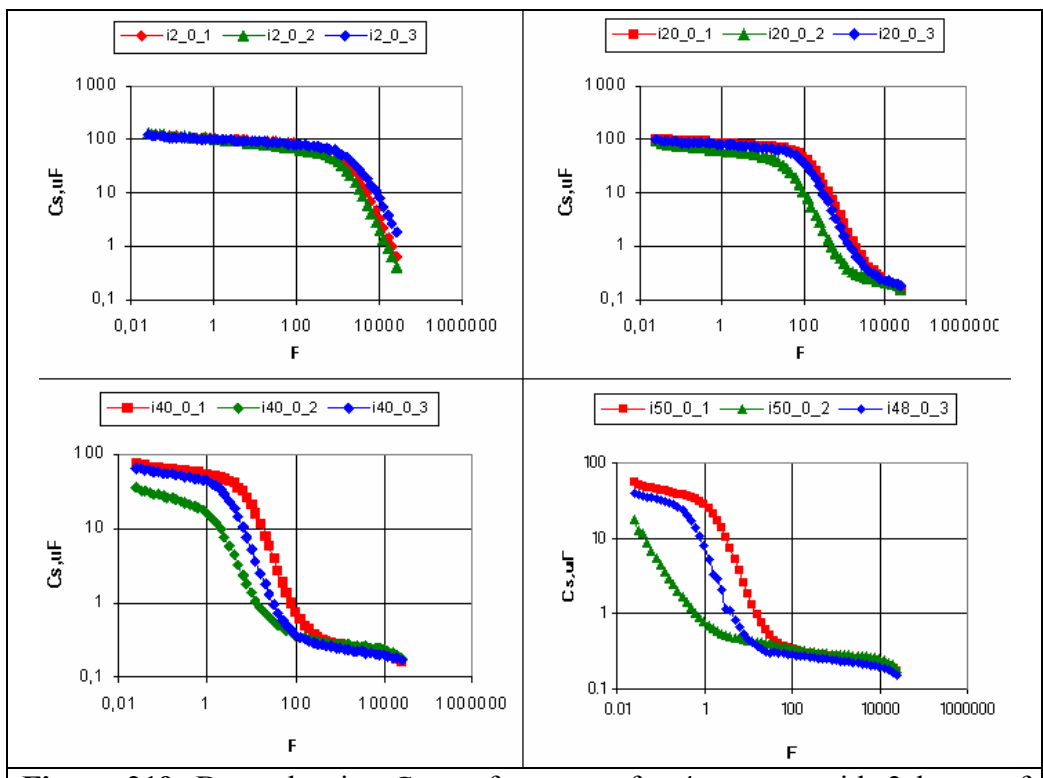


Figure 219. Dependencies *Cs* vs. frequency for 4 sensors with 2 hours of MHDA treatments after application different numbers of CV treatment steps

As one can see the MHDA treatment improved the tranducerr tolerance to degradation and this improvement depended on treatment time. As one can see from figure 220 and figure 221 where dependencies of integrated parameters for estimation of sensor degradation vs. numbers of CV treatment steps are shown 30 minutes MHDA treatment gave better results than 2 hours MHDA treatment. Unfortunately due to a large sensor spread this improvement of the sensor tolerance to degradation could not be evaluated quantitatively.

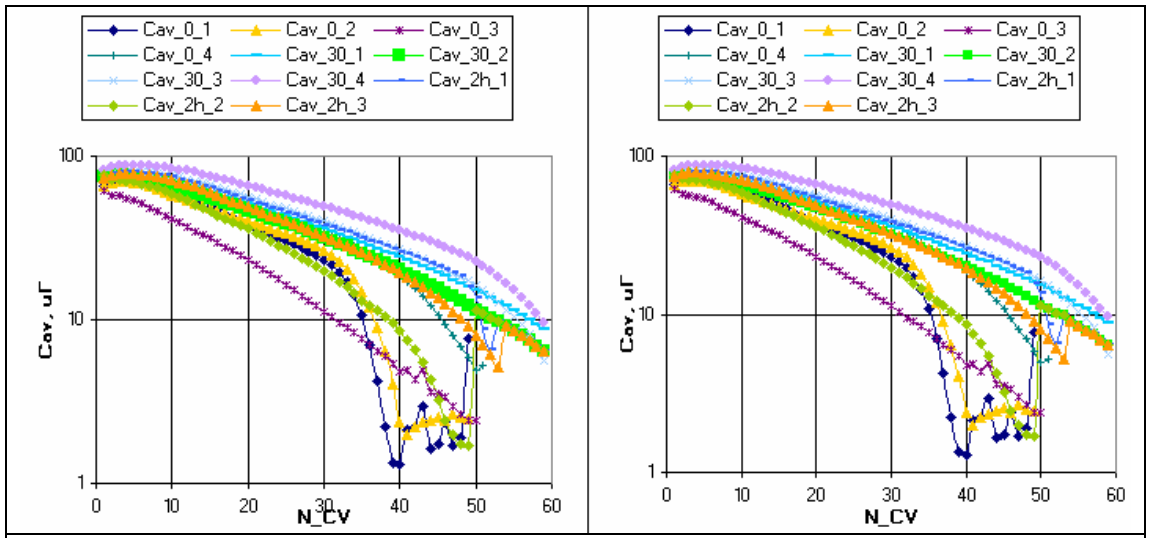


Figure 220. Dependencies of integrated parameters Cav and ΔF_{Cs} vs. numbers of CV treatment steps for all sensors (0, 30 minutes and 2 hours MHDA treatment)

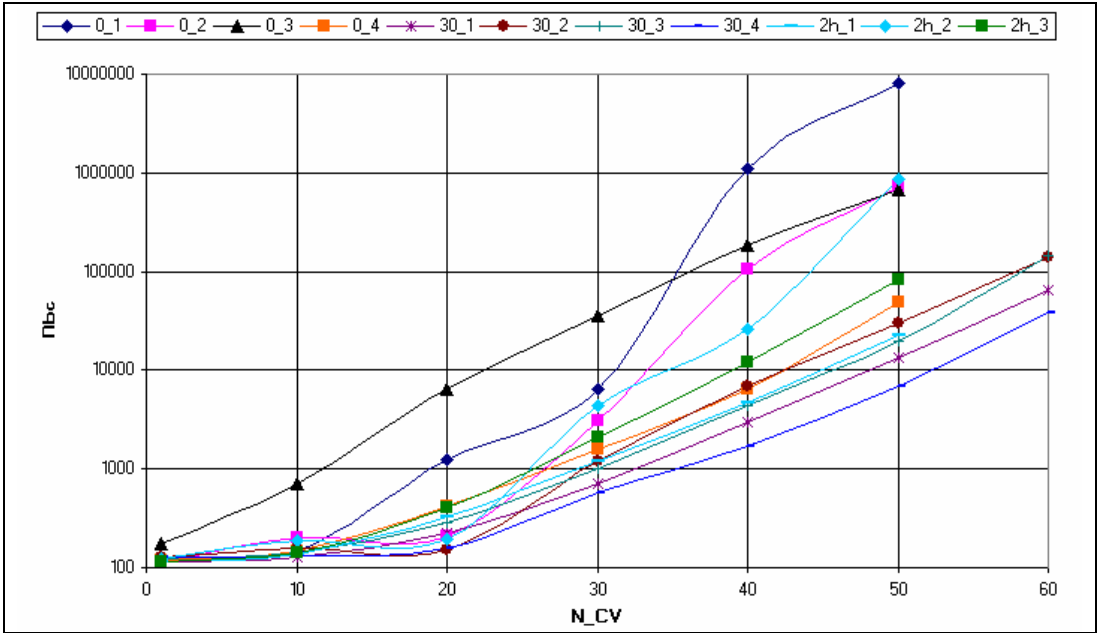


Figure 221. Dependencies of integrated parameters Cav and DF vs. numbers of CV treatment steps for all sensors (0, 30 minutes and 2 hours MHDA treatment)

Conclusions

Investigation of degradation of silicon-gold polypyrrole tranducers was performed by means of complex impedance spectrum analysis after application to the tranducer of a number of cyclic voltammetry (CV) sweeps was performed. Degradation became apparent through increases of real and imaginary impedance components and the emergence of a break in the Nyquist plots. The real part of this break position (R_{bk}), the average static capacitance (Cav) and its effective frequency bandwidth (ΔF) were suggested to be used for characterization of the tranducer degradation. If the tranducer degraded (number of CV treatment steps increased) R_{bk} increased and Cav and ΔF decreased. For different tranducers, the influence of CV treatment on the sensor performance was different. It was irregular and individual for each sensor due to sensor manufacturing spread.

An equivalent circuit for transducer modeling was developed and analyzed. It was based on a two-phase distributed model where a specific cross-section average pore took the place of cross-channel interfacial impedance. To improve fitting accuracy a film relaxation resistor was introduced in the equivalent circuit and the fitting strategy was amended by means of using mixed metrics.

Corresponding software for equivalent circuit parameter specification was developed and was applied to experimental data. If the number of CV treatments increased then characteristic frequencies f_L and f_p and constant phase coefficient α decreased and film and pore parameters d, R, Rp and Rr increased. From the physics of the model these changes relate to an increase in the pore size that coincided with transducer photographs taken before and after CV treatments.

Finally, MHDA treatment could used for improvement of the sensor tolerance to degradation. The efficiency of this treatment depended on a treatment time and experimentally, 30 minutes MHDA treatment provided better results than 2 hours MHDA treatment. Sensor manufacturing spread would need to be decreased and more experimental data analyzed for optimization of the treatment time. Results on the circuit specification and MHDA treatment for sensor stabilization were reported at International Congress on Analytical Sciences, ICAS-2006, 25-30 June, Moscow [1,2]

Objectives.

To develop a laboratory prototype system to prove principle using the nanostructured affinity sensors developed in the project as the detection method.

Project Timeline	1 2 3 4 5 6 7 8 9 10 11 12 13 14 15 16 17 18 19 20 21 22 23 24 25 26 27 28 29 30 31 32 33 34 35 36
Workpackage 9. Laboratory Prototype	

Workpackage 9 started in month 24 with the laboratory prototype being designed and constructed forming the basis of the deliverable.

The test-bed electronics constructed in W6 formed the basis of the prototype and were fed forward from W6 into W9. The circuit diagram for W6 is shown on page 113, figure 149.

The following pictures (figures 222 - 227) show the laboratory prototype instrument that Uniscan Instruments developed for the ELISHA project. Also shown is the Windows based software that controls the ELISHA laboratory prototype.

Laboratory Prototype

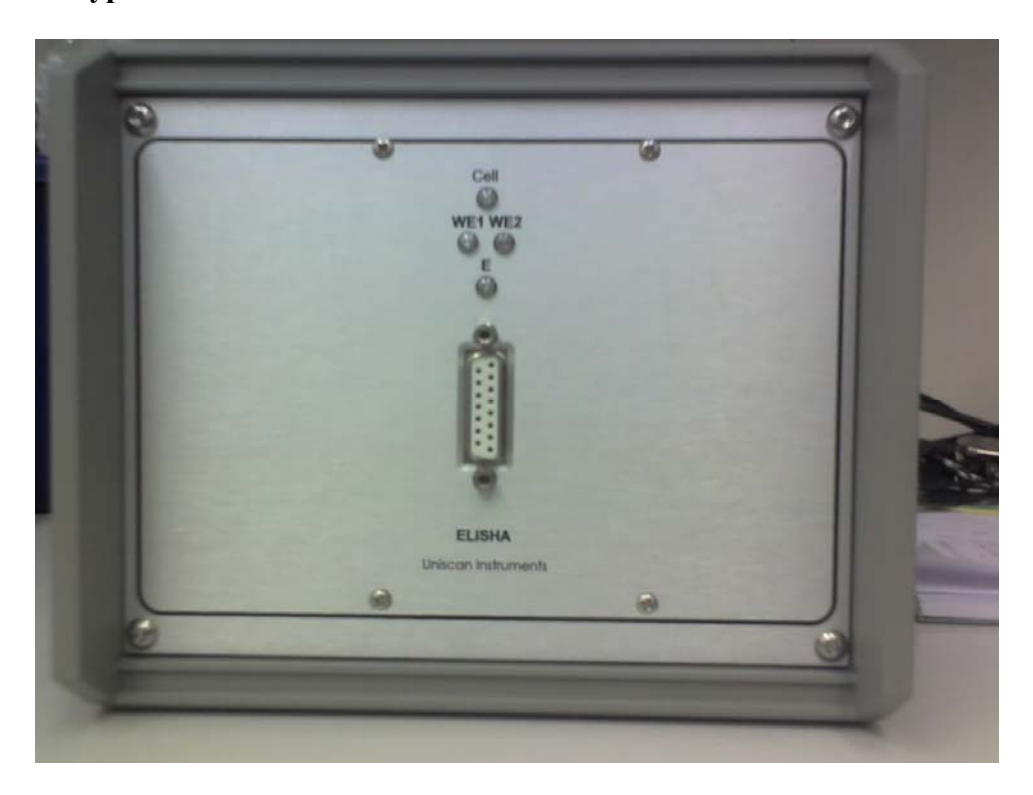


Figure 222. Front of test-bed unit showing "ELISHA v2.00" electronics. There are lights depicting cell status, WE1 and WE2 status and the cell potential E.



Figure 223. Rear of ELISHA electronics with USB communications port for connection to PC, power supply jack and earth stub.



Figure 224. Isometric view of the ELISHA electronics with cell cable attachment.

Software Interface.

Displayed in the following section are pictures of the ELISHA Windows software. This is the main control mechanism by which users define experimental parameters and display the results. The additions to the software were mainly in the support for the two WEs and the easier and more flexible configuration of the experiments. Initial work in the ELISHA project used the Pulsed Amperometric Detection (PAD)

technique. The idea behind PADs is that a sample has a voltage step/pulse applied to a sample and the resulting current is monitored. Typically, prior to performing a PADs experiment, a series of Pulsed Potential Step Voltammetry (PPSV) experiments are performed. These PPSV experiments 'interrogate' the samples' response to different pulse potentials and displays the resulting responses graphically. In this way, the most appropriate potential for use in the PADs experiments could be determined. It is also desirable for the researcher to be able to specify where in the pulse period to start sampling data and for what period. The laboratory prototype allows the definition of two precise periods within the PPSV and PADs experiments over which to acquire data from both WEs. The data from WE2 is then subtracted from the WE1 data for both acquisitions and then displayed graphically. Access to the original raw data is also available should to the scientist if required. Figure 225 and 226 (below) show the general scheme employed to define the PPSV and PADs experiments. The quiet times (denoted by Qn) can be defined as open or closed circuit, the potential (if closed circuit) and the time of the quiet period. The pulses (denoted by Pn) are again defined by time and potential and the acquisition is defined by time parameters only.

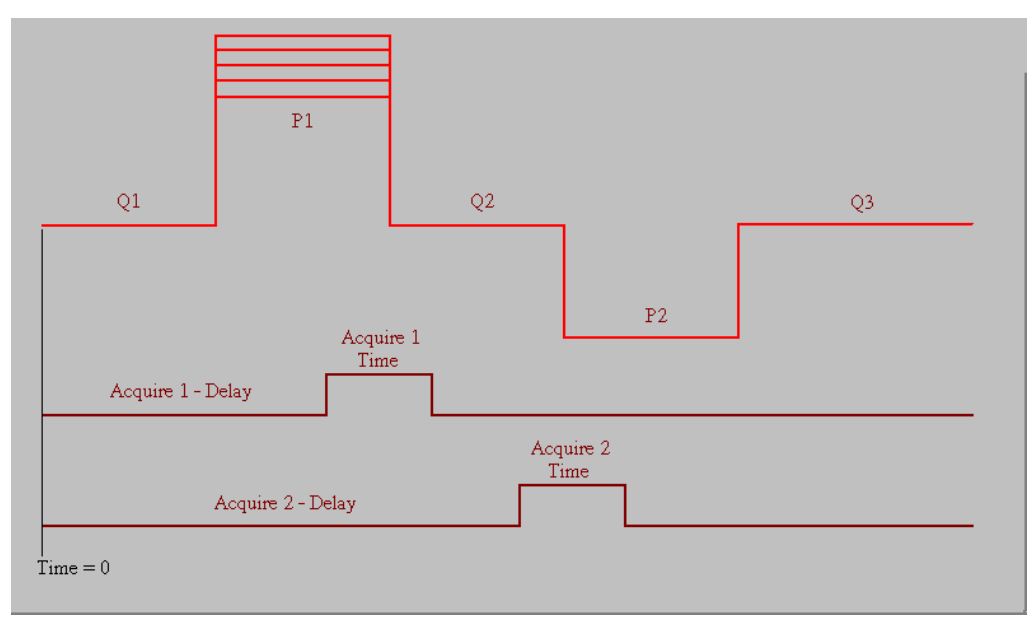


Figure 225. The acquisition scheme employed in PPSV. Quiet-times and polarising/depolarising pulses can be seen in the top trace, and the definition of acquisition times is shown on the bottom two traces.

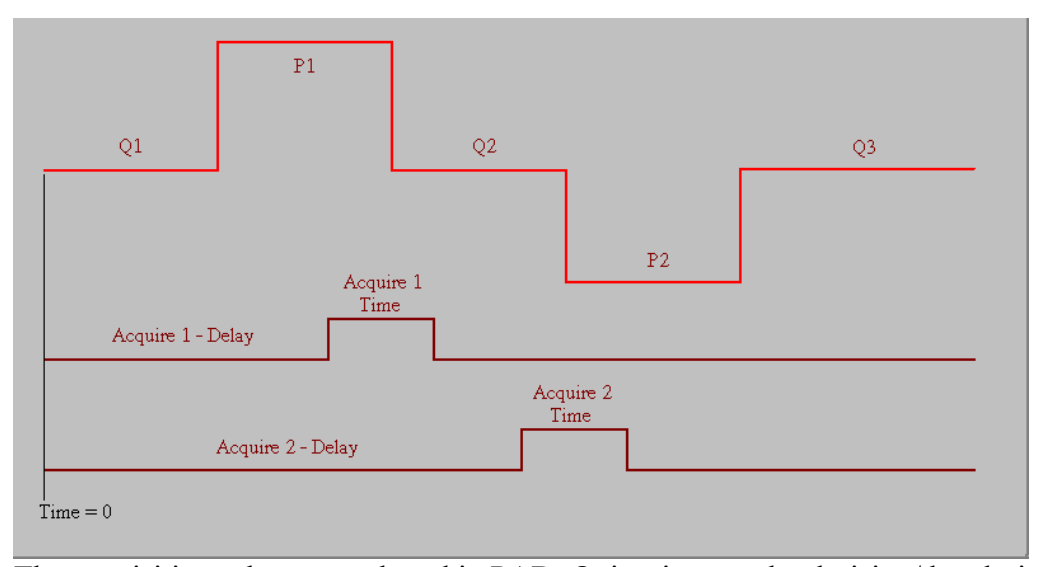


Figure 226. The acquisition scheme employed in PAD. Quiet-times and polarising/depolarising pulses can be seen in the top trace, and the definition of acquisition times is shown on the bottom two traces.

Figure 227 shows the definition of the pulsed waveform spectroscopy configuration. Here the data is acquired and transformed to produce a voltage magnitude spectrum of the sensor response. This experiment is typically a higher-speed experiment than the previous experiments. In particular, the acquisition speed is typically substantially higher. This is essentially due to the charging/decay of sensor potential due to the polarising pulse P1 and the open circuit time coincident with the acquisition time. Typically time-constants between 1 millisecond and 40 milliseconds were seen in work done previously at Leeds with partner 1, which necessitated acquisition times between 2kHz and 500Hz minimum, respectively. The system can currently operate in the PWS mode at acquisition periods of up to 8kHz. Previous work by the ELISHA partners showed that the point of interest was approximately 30Hz and below, which required minimum acquisition periods of 33 ms to extract useful data. As a consequence of this, the decay time and the data down-load speed, there is a trade off between being able to see the decay, provide a transform that shows the point of interest in sufficient detail (~30Hz or less) and the time it takes data to load from the instrument for both WEs.

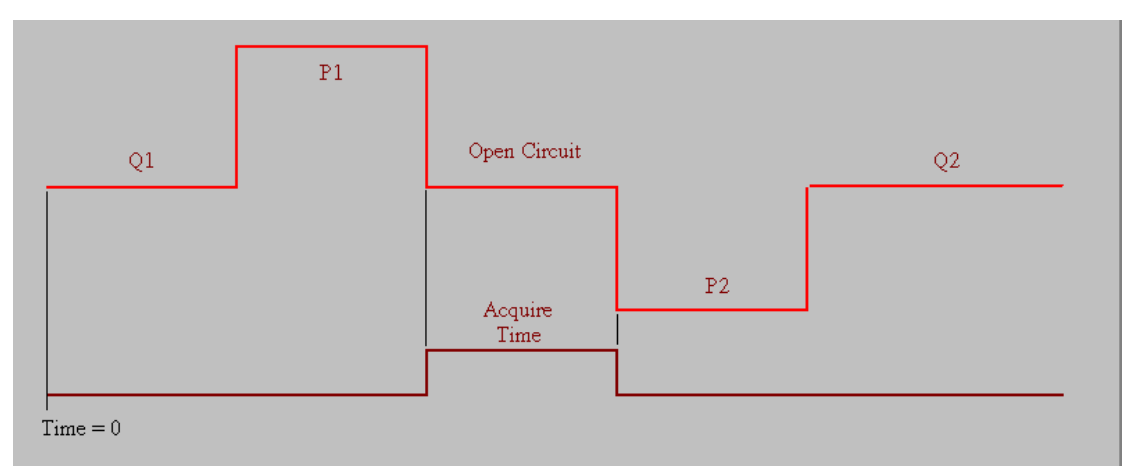


Figure 227 Definition of the sensor interrogation response for the Pulsed Waveform Spectroscopy experiment.

As a point of note, the researcher may not require, for example, certain quiet periods or depolarising pulses as part of their experiment. It is perfectly viable to specify these with zero time forcing them to be excluded from the experiment. It was also intended that either the initial of final quiet periods were used to 'time' the experiment as the scientist desired. For example, setting Q2 in figure 3.2.3 to 60 seconds minus (Q1 + P1 + A1 + P2) time would force the sequence to acquire/repeat on each minute. Each experiment can be set to repeat in this way.

Figures 228 - 230 show the configuration of the PPSV, PADs and PWS experiments, with their associated help files open for reference.

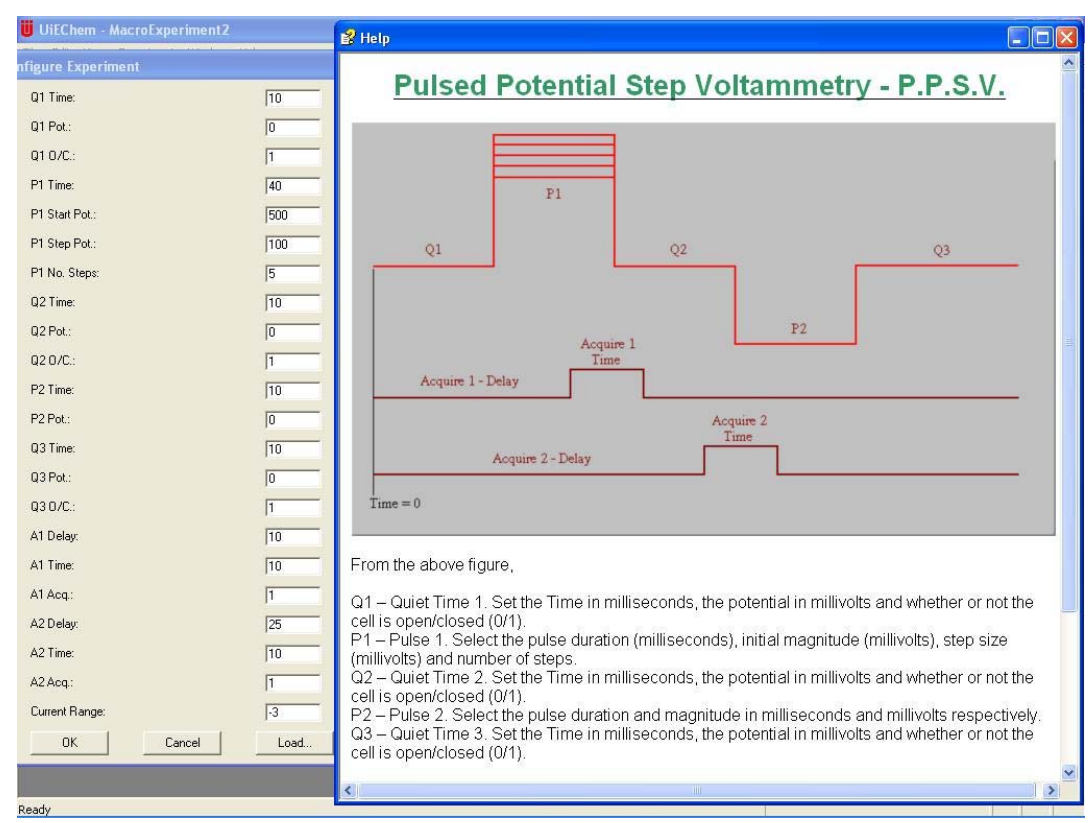


Figure 228. Pulsed Potential Step Voltammetry experiment config and help.

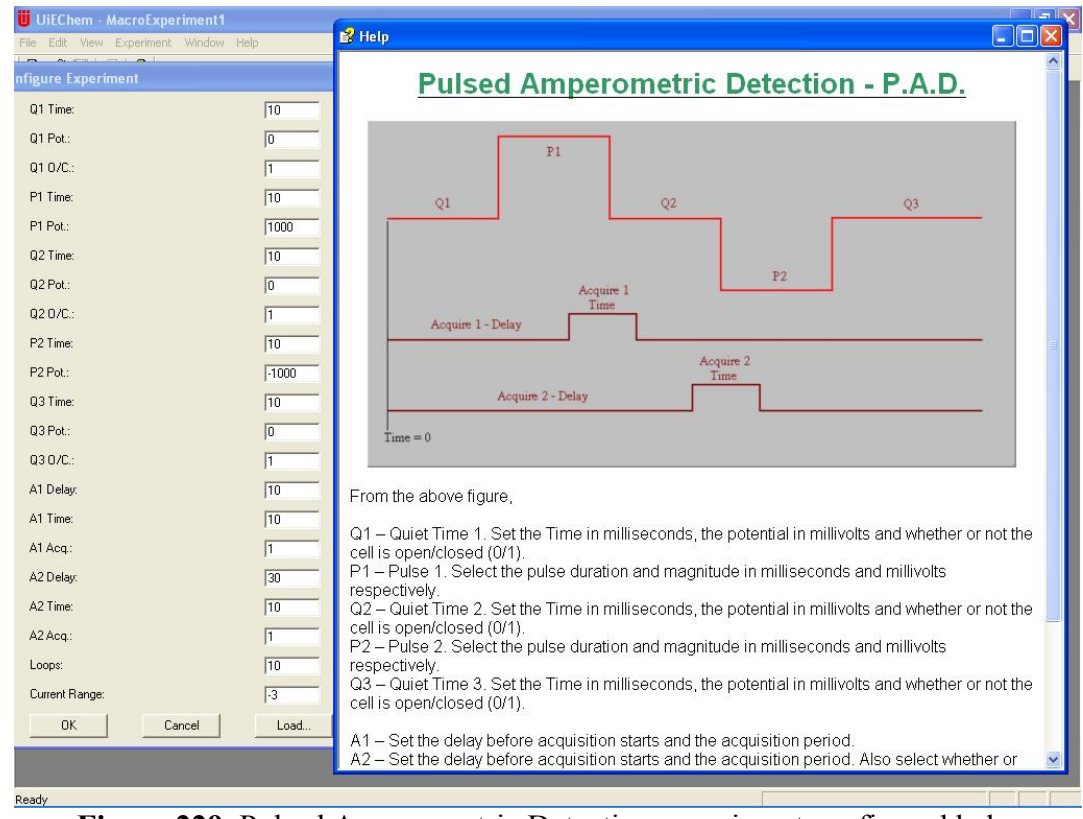


Figure 229. Pulsed Amperometric Detection experiment config and help.

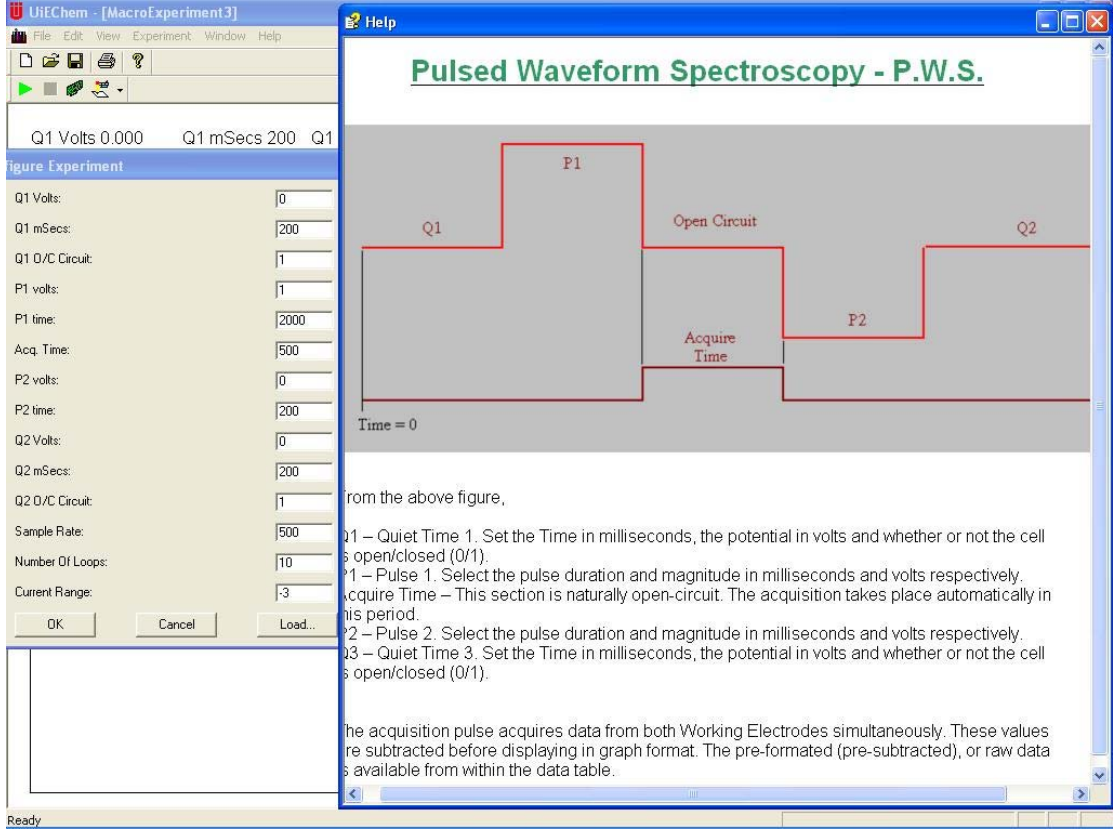


Figure 230. Pulsed Waveform Spectroscopy config and help.

Test Report:

Basic tests were performed to ensure the system performed as expected. Below (figures 231-236) are numerous screen dumps of the system tests performed on various dummy cells. Finally there is a review of the PWS raw data and the resulting subtraction and the %CV variation over a 10-run experiment for dual dummy cells with decaying responses with time constants of 75ms and 150ms.

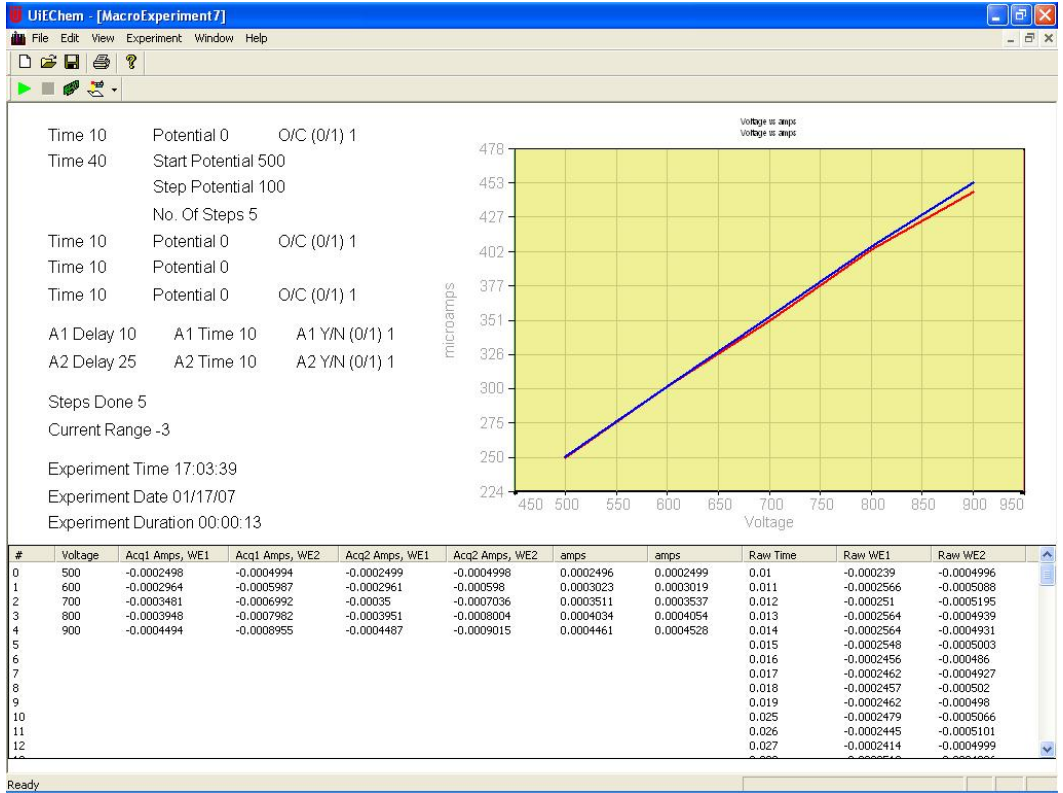


Figure 231 PPSV response to a $1k\Omega$ (WE1) and $2k\Omega$ (WE2) dummy load with potential starting at 500mV, and 5 steps of 100mV.

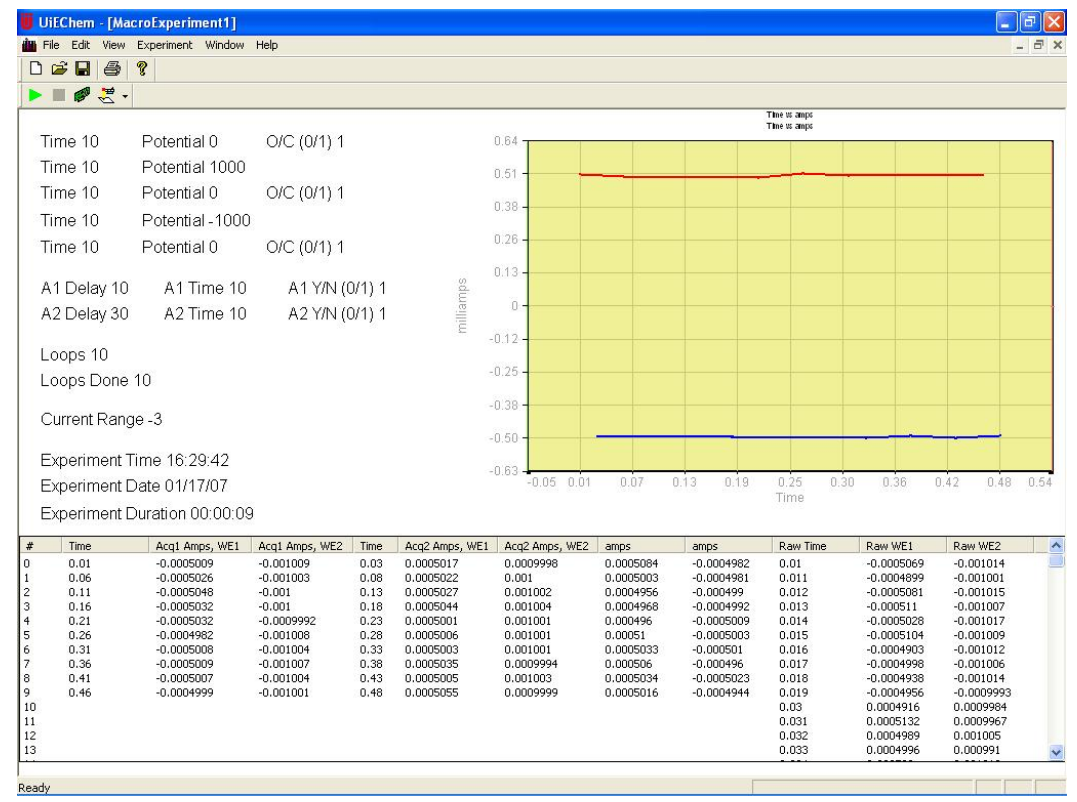


Figure 232. PADs experiment with a $1k\Omega$ (WE1) and $2k\Omega$ (WE2) dummy load.

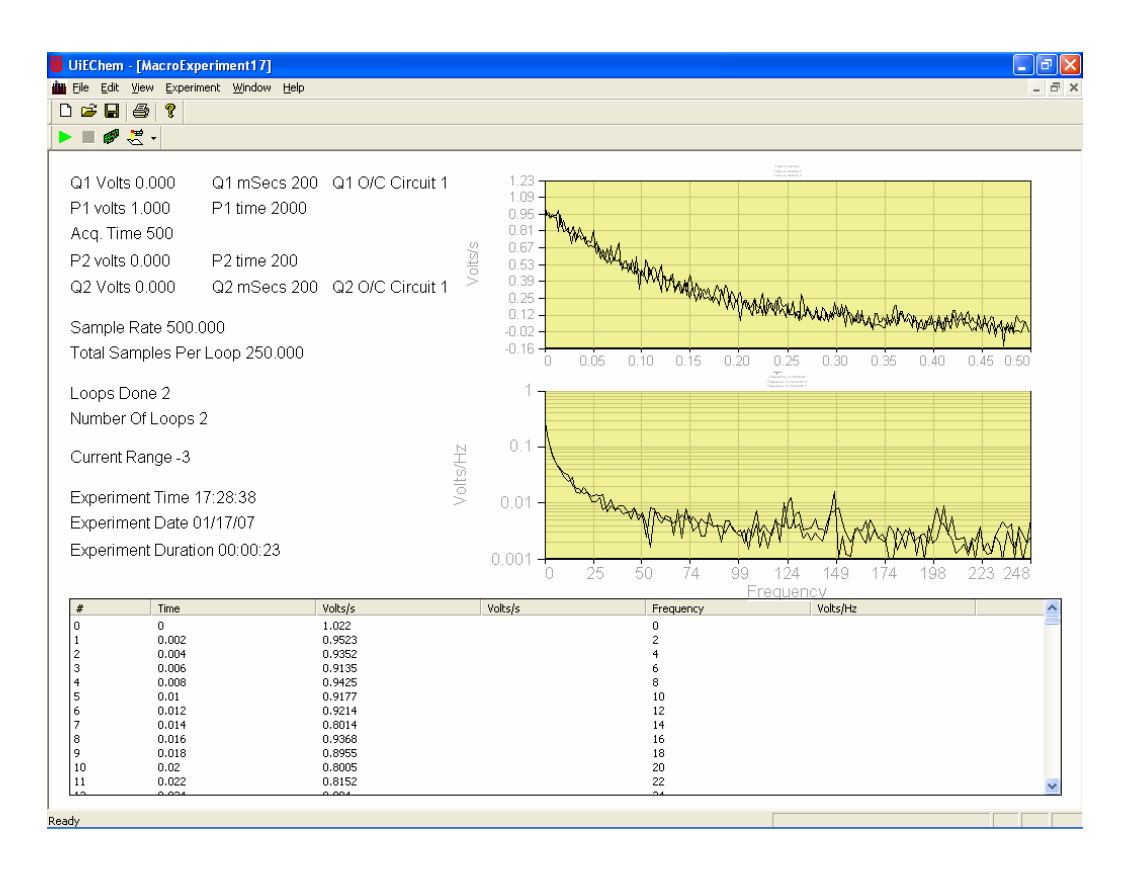


Figure 233. PWS experiment with a 150ms time-constant decaying load on WE1 and a $2k\Omega$ load on WE2.

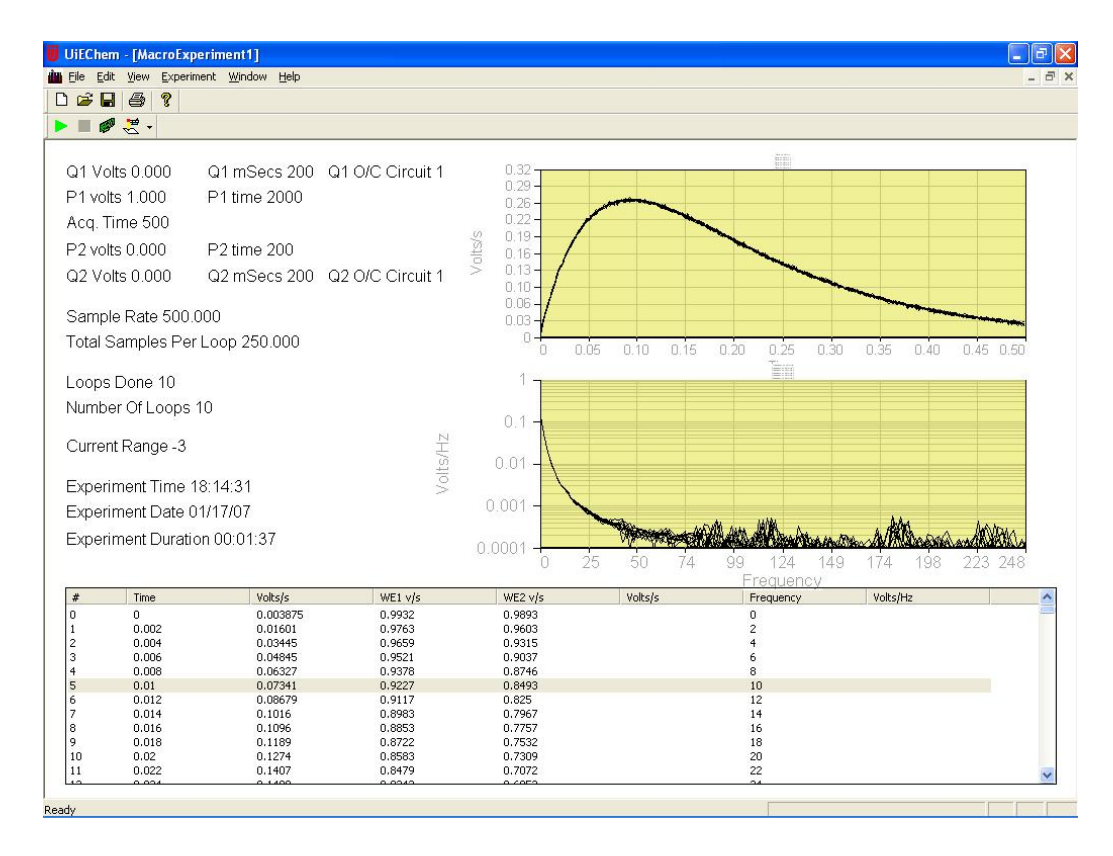


Figure 234. PWS experiment with two decaying loads, time-constants of 75ms and 150ms, auto baseline subtraction and transformation.

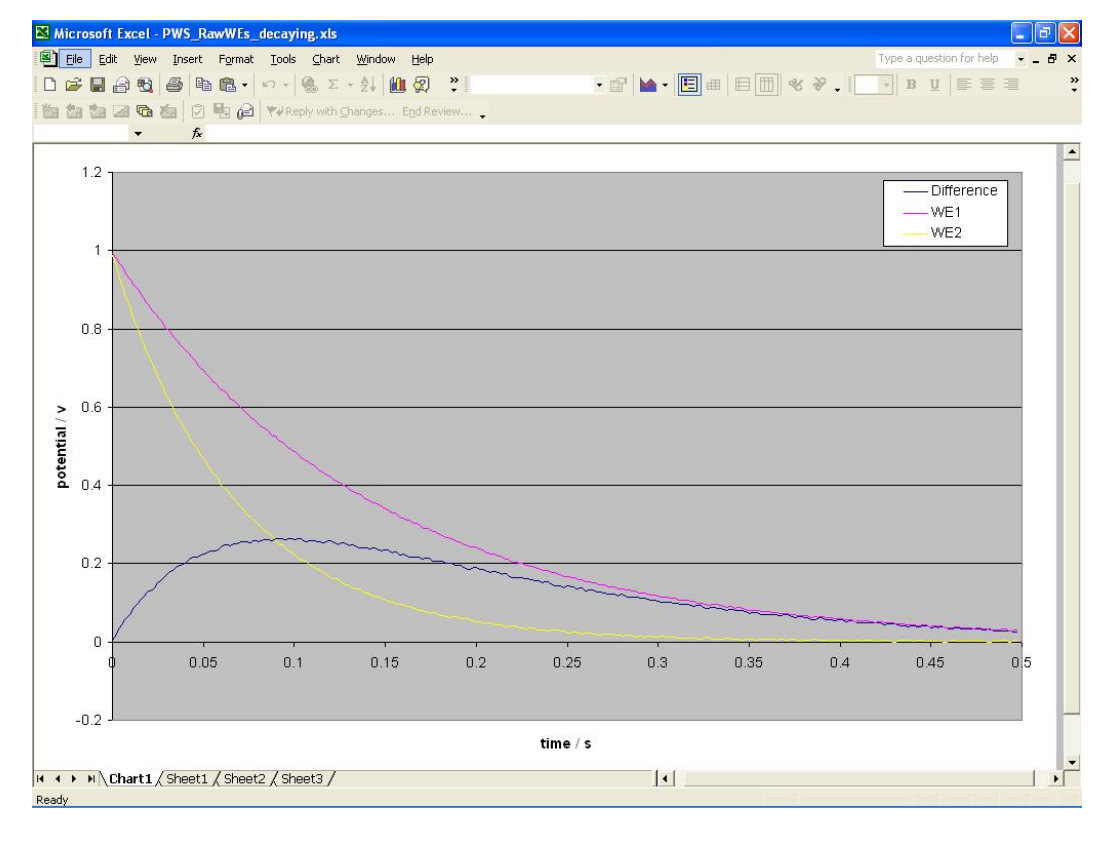


Figure 235. PWS raw data extracted from figure 4.4 first pulse-train. Shown are the responses from WE1, WE2 and the resulting subtraction.

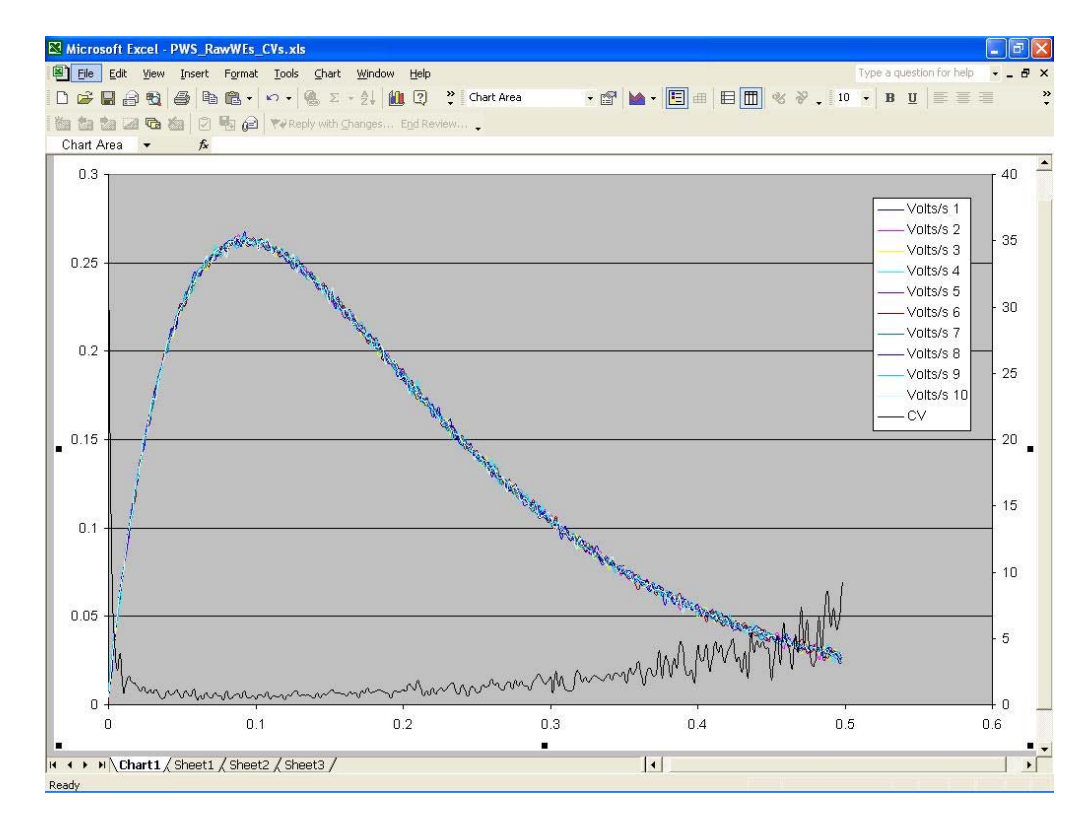


Figure 236. PWS raw data extracted from figure 4.4. The black trace at the bottom of the figure shows he %CV (right hand axis) over 10 runs.

Summary.

The laboratory prototype was completed and handed over at the January 2007 project meeting in Grenoble. The system had evolved substantially from the first prototype, including many new features and upgrades to existing features. It is understood that there is significant commercial interest in the techniques and methods used in ELISHA, and as such additional effort was made to make the electronics compact and professional in appearance. Further feedback will be documented for inclusion in future work, possibly even after project. Finally, the laboratory prototype was tested against known dummy loads and performed as expected. Work also continued on the development of the combined pulsed technique/impedance technique electronics to produce a stable system with high signal to noise ratio that is comparable in performance to existing bench-top equipment.

164

Exploitation and Market Activities that Underpin the Technical Workpackages.

During the first year the IP position, the market information and the potential exploitability of immunosensors has been researched in detail by partner 9. The exploitation potential is contained in the Annex to the report as specified by the reporting guidelines, the IP position and the market information including potential competitors is briefly explained below.

IP Position.

Only one patent has been found that could pose a threat to the eventual commercialisation of immunosensors developed in the project and only if any instrument developed uses impedance spectroscopy as the sensor interrogation technique. The patent is US6300123, Sensor Employing Impedance Measurements. Vadgama Pankaj M and Warriner Keith S R. July 1999.

The successful demonstration of the pulse waveform spectroscopy technique is a significant advance for the exploitation capability and should form the basis of new IP or be kept as a trade secret, with any electronics used commercially encased in tamper proof opaque polymers to prevent reverse engineering.

Market Information and Potential Competing Technologies.

The indications regarding market interest are extremely good provided labeless antibody based sensors can be manufactured that will give the same accuracy, sensitivity and precision as existing enzyme linked immunosorbant assays (ELISA's) and for the same price or less. The results for PSA and other analytes indicates that the sensitivity for ELISHA immunosensors will be at least as good as existing assays and that it is possible to significantly reduce non-specific binding.

The exploitation potential of the project is enormous, as labeless immunosensors that will work in the same manner as the most successful biosensor ever produced (i.e. blood glucose, having a worldwide yearly market turnover of \$5 billion) would make it very simple to test for a huge range of analytes.

Competition in the field of immunosensors is low, with just 4 companies being identified worldwide to date.

- 1) Ambri, Australia;
- 2) Texas instruments Inc, USA;
- 3) Axis-Shield Inc. USA;
- 4) Innovative Bisensor Inc. USA

Only one company (Ambri) makes an electrochemical device based on ion channel amplification, while the rest use optical technology to generate immunosensor signals. The BiaCore technology has not been included in the market competition survey as this is primarily used as a research tool in the development and screening of affinity reagents such as antibodies. It is rare to find a true analytical use of the BiaCore instrument and it is very expensive.

No company known makes simple, low cost electrochemical immunosensor formats at this time, however it is clear that many diagnostics companies are carrying out R&D in this area.

The four potential competitors are listed in Appendix 3.

Acumen Fund

In addition to companies a fund has also been identified that has been formed to develop Low Cost Immunosensor Devices: www.acumenfund.org/Work/HealthTechnology/Immunosensors.asp

The basic tenants of the fund are given below.

Focus on Design

IDEO, the design firm, is beginning to discuss new ways to design the immunosensors to make them more marketable and more user-friendly. The immunosensor project serves as an example of an effective collaboration of non-profit, private and academic institutions resulting in an effective and marketable design to benefit the poor.

The Challenge

Though early detection and intervention of dengue fever is the key to reducing morbidity and mortality, the tests that are currently available are prohibitively expensive for developing country health care systems

The Innovation

Field testing of a portable, point-of-care disease detection device that is capable of detecting major diseases such as dengue fever, HIV, malaria, and measles at one-third the cost of existing technologies so that diagnosis can be made rapidly and accurately in the field.

The Impact

Field trials are underway in Nicaragua to ensure that the poor will receive crucial diagnoses with accuracy and quality, despite their constrained economic resources

The concept and need for low cost immunosensor devices is an important target for many it would seem.

Target Focus.

In a situation where the aim of a commercial development can be taken forward into a very large potential market area, it is crucial to success to focus the commercial effort towards a particular target. In the original project application the model target analytes were chosen for two reasons; 1) having some commercial usefulness and 2) to cover a range of immunoassay types. PSA is a proteins target, i.e. a large molecule target; pesticides and fluoroquinolines antibodies are hapten targets, i.e. small molecule targets and; prion peptides are an interim size.

Commercial usefulness having some part to play, has started to focus the sensor development, but it is important to remain current with industry news and Partner 9 has been looking at the viability of these targets in the light of the eventual implementation of the project results.

One major area of interest in the medical diagnostics industry is the field of biomarkers. These are effectively defined as molecules that are produced as the result of a medical condition such as cancer or an infection, that would not be normally present and which can therefore be detected and quantified to give an early diagnosis leading to early intervention. In cancer patients in particular, the earlier any treatment can begin has a significant effect on patient outcome and survival. Cancer markers are often unusual proteins or peptides that either appear or become elevated in concentration. Many tests rely on immunoassay techniques for detection and antibodies to the different biomarkers are often one of the earliest tools to be produced for diagnostic purposes.

The early detection of cancer would therefore seem to be a very important area and is likely to become a commercial focus for the project. Early diagnosis of infectious diseases have also been communicated to the consortium as a target of great commercial interest.

Biomarkers for Cancer Types.

Prostatic cancer has a new potential biomarker that is reported to be better than PSA.

The press release is included in appendix 4.

Exploitation Appoaches by External Companies.

In December 2005 an approach was made by a diagnostics company to the project manager, asking if it would be possible to have a license to the ELISHA technology to assist them in developing a prospectus towards a placement on the alternative investment market.

This was followed up by the two commercial partners of the consortium as laid down in the consortium agreement and negotiations are underway to explore this possibility. In addition year 3 will be the start of discussions with various other potentially interested established companies to begin to exploit the technology further.

Section 3. Consortium Management.

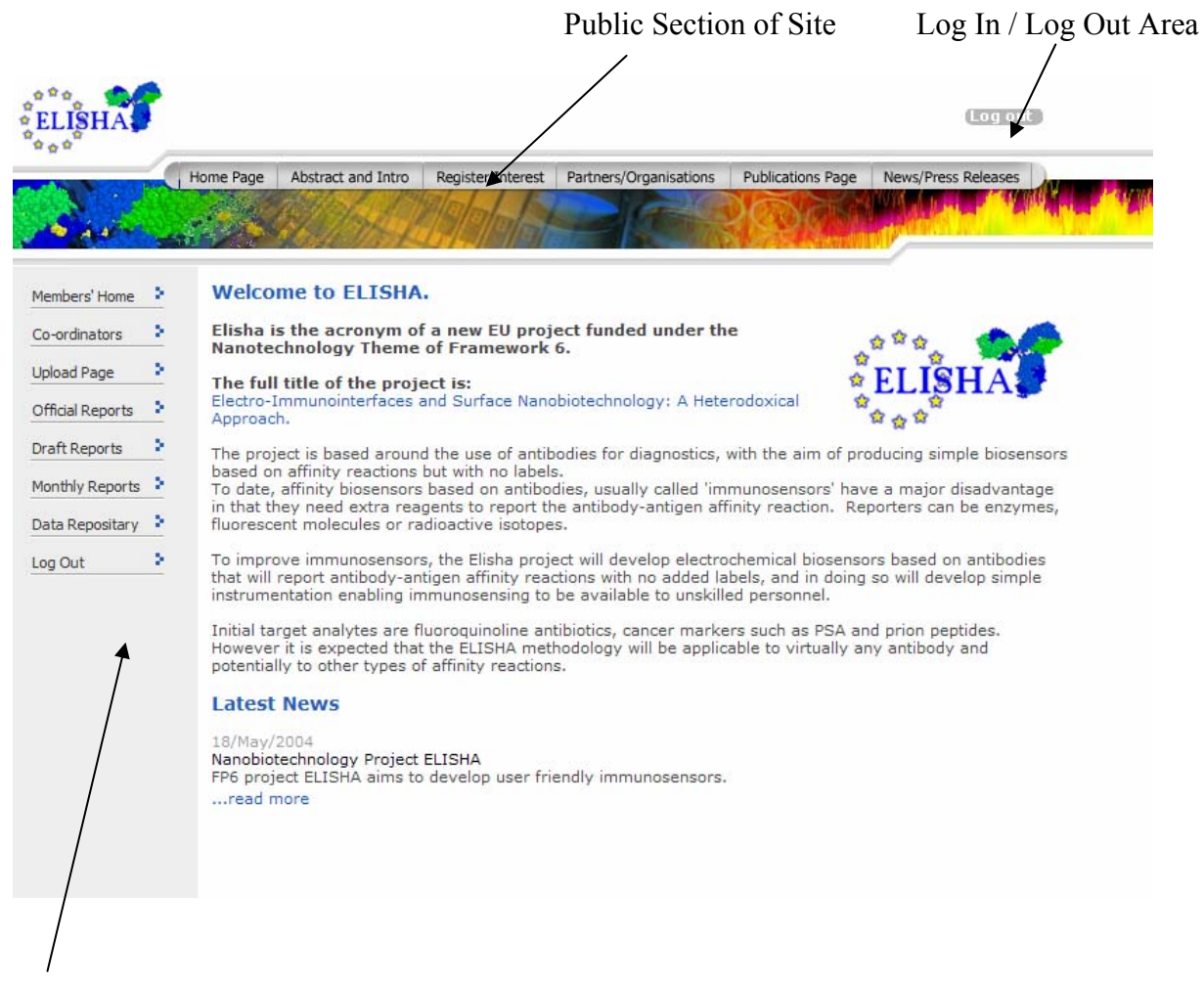
The consortium management has been relatively problem free, with the project manager taking most of the day to day responsibility in communication between partners, organisation of meetings and follow-up for requested information. The consortium itself is made up of partner organisations that function reasonably well together and have been communicating freely over the first period of the project.

The Logo (figure 237) for the project was designed within 3 attempts and indicates the nanoscale molecular structure of a whole IgG antibody linked to the commission stars as a stylised transducer surface. To others the logo looks similar to a key in shape, unlocking the secrets of immunosensors no doubt.

Figure 237. ELISHA Logo



A major achievement is the development of the web site, which is fully operational and contains embedded software that enables instant on-line updates by all the registered users. There are two areas to the site, the public area and a password protected secure area for partners and the scientific officer at the commission. A view of the front page is overleaf (figure 238).



Password Protected Area of Site

Figure 238. Front page of ELISHA website – member log in.

Training in the use of the web site has been carried out at the project meetings. A detailed session took place at the 12 month meeting and partner use is accelerating as the project continues.

It is planned to include data files in the repository, particularly to enable different partners to access them to carry out data processing and sensor comparisons. This section of the site has not been used in great depth for sensor data, however as the common antibodies become available this is expected to change.

The main barrier to depositing data onto a web site seems to be more psychological for the older, more established scientists and changing the thinking to do this as a part of the reporting and communication procedure is proving a challenge.

However it is evident that continued encouragement by the coordinator and project manager is having a positive effect in that the web site traffic by partners is improving and uploads are increasing in number.

Changes to original consortium.

Since the project start there have been minor changes in partner names and groups.

Partner 1 University of Leeds has renamed the group to the 'Biosensors and Biocatalysis Group' or BBG.

Partner 5 has restructured and renamed the whole institute to 'The Tyndall National Institute'

Project timetable / status Gannt chart.

The project timetable is shown overleaf.

The only remaining deviation to the project timescales are in workpackage 1. The complexity of producing the rabbit primers for the respective production of rabbit recombinant antibodies delayed the start of recombinant antibodies as deliverables by up to 3 months at the mid-term point. This has not delayed the sensor development as existing antibodies (see below) have been used to demonstrate new immobilisation and sensor interrogation techniques. The delay was not a major difficulty as the immunosensor fabrication and characterisation (W4), immobilisation schemes (W5) and signal generation / non-specific binding (W7) do not depend on the supply of recombinant antibodies. The other antibodies that are now available will provide the electrochemistry partners with a rich source of materials to continue the detailed work on the specific targets listed in the project annex 1.

The first histidine tagged recombinant Fab fragments were delivered to partner 1 and used in the evaluation of SAM anti-atrazine immunosensors, so timescales are largely recovering to plan. This could be classed as an example of alternative matrices, bringing this part of W5 up to date.

The PSA target was initially shown to give a calibration curve, figure 52, page 47. Further investigation into the PSA immunosensor has revealed that the z' faradaic component are responsible for the signal generation in this type of sensor, page 89. The reminder of the results used model antibodies to enable protocols and immobilisation methods to be explored.

A further example of the system working is in the another target protein biomarker for stroke and trauma, S-100. This was not in the original specification of the project, but since antibodies to S-100 were available and the Fab fragments were delayed, this was tested. The results are clear that S-100 gives a similar calibration curve to PSA, indicating the genericity of the ELISHA immunosensor interrogation protocols for protein biomarkers, figures 54 and 55, pages 48 - 49.

The successful results using the test bed electronics for pulse interrogation of immunosensors is a major breakthrough for the project. Anti-haemoglobin was another readily available antibody in partner 1's laboratory and was tested for the same reasons as above. When the first Fab fragments were supplied just after the work on anti-haemoglobin the system was then tested on these, with much more impressive results, figures 85 - 87, pages 64-66.

All other workpackages are on-time and in line with the estimated timescales shown in the project barchart on page 102.

Table 5. Project Barchart and Status

Puniost Mastings	Viole .		61	Mon			Repo			Report Mid Town					Report					20 Month					Report Final				
Project Meetings	Kick (6 Month				12 Month					Mid-Term					24 Month				30 Month					rmai			
													Year 2									Year 3							٦
Acronym: ELISHA					Year														Ī										
Project Contract No. NMP2-CT-2003-505485																													
Project Totals	,	1 2	ω 4	w	9 1	· ∞	6	9 ;	11	13	14	15	16	18	19	20	22	23	24	25	26	28	29	30	31	33	34	35	36
Workpackage 1. Antibodies																													
Task 1.1 Purified Abs / Haptens																													
Task 1.2 Recombinants / Fab's																													
Workpackage 2. Transducers																													
Task 2.1 Standard Transducers				_		_		_ _		_	_	_		_		_	_				_	_	_						
Task 2.2 Designed Transducers																													
Workpackage 3. Matrix Precursors																													
Workpackage 4. Sensor Fabrication																													
Workpackage 5. Ab Immobilisation																													
Task 5.1 Entrapment Strategies																													7
Task 5.2 Co-Valent Strategies										_								_									_		
Task 5.3 Alternative Matrices																													
Workpackage 6. Sensor Electronics				-		_	_	_ -												_	- -	-	-	_		_	-		
Task 6.1 Test Beds																													
Task 6.2 Prototype																													
Workpackage 7. Signal Generation						-	_													_	_ _	-	-	_		_	_		
Workpackage 8. Evaluation/Processing																													
Task 8.1 Signal Processing																													
Task 8.2 Sample Analysis													_ _	_									_						
Workpackage 9. Laboratory Prototype		17									T			1															
Project Co-ordination																													

Short comments on:

Coordination activities.

The coordination of the project has been relatively straightforward to date. The partners respond quite well to e-mail prompts and are all behaving according to the rules agreed at the Kick-off meeting. The consortium agreement is complete and all partners have signed.

Communication between partners.

Partner communication was a bit slow at the start, however now there seems to be good communication overall. Many partners have visited others to progress the different workpackages and this is continuing as the project progresses.

The collaboration between partners has been much more evident between mid-term and the 24 month point. Groups have met and worked together to produce the results shown in WP's 4, 5, 6 and 7, which indicates a good synergy between partners and a working environment that is very productive. This is expected to continue and develop throughout the project lifetime and it is likely that the relationships will continue beyond this point.

One area that could still improve is communication via the web portal (www.immunosensors.com) and this will be an area of project management that will be continually encouraged throughout the project. More information has been uploaded onto the portal, however it is clear that this is not a first port of call for most partners and telephone or e-mail communication is generally preferred.

Project meetings.

Project meetings have been generally well attended, with members of all partners being present at all three. Each partner was planned to host a meeting, and wherever possible this plan will be kept.

The mid-term project meeting was held in Coimbra, Portugal on the 24th June 2005, as a major bioelectrochemistry meeting will be held at this time and some of the ELISHA results are being presented here. The meeting was a success and the project was found to be on-track and delivering according to the workplans. Significant breakthroughs were found to have occurred and these are continuing.

The 24 month meeting was at Cork, Ireland and hosted by partner 5. The results disseminated here are remarkable and form the basis of the new information contained in this report. As expected the electrochemistry and signal generation, plus new immobilisation strategies are now beginning to dominate. This is entirely to plan and should develop the exploitation routes as time progresses.

Cooperation with other projects.

No direct co-operation has been carried out to date.

The draft plan for using and dissemination of the knowledge was given in the Annex of the 12 month report. This is still developing and an interim eTIP has been submitted as required by the mid-term guidelines.

Interim eTIP

A completed print version included in appendix 4.

ANNEX

Exploitation and Dissemination

Exploitation and Dissemination

The route for exploitation of the results from the ELISHA project involves several aspects and is dependant on successful completion of the individual deliverables listed in the workplan and any other inventions / discoveries that occur as the project proceeds.

IP that will be generated from the project will include:

- i) novel electronic address systems;
- ii) novel methods of fabrication immunosensors
- iii) novel post data acquisition processing software to enable detailed interpretation of results form affinity sensor surfaces.

To date there are 2 major areas that could form the basis of new patent applications:

- 1) The fabrication method that involves blocking thr gold transducer surface with long chain thiols after the electropolymerisation has been carried out an unexpected stability effect on the matrix is observed. This was discovered by Partner 1.
- 2) The development and formation of a rabbit primer library for the production of recombinant antibodies from rabbit cell lines. This is potentially very important and was done by Partner 4.

Also the actual deliverables in the project allow a number of potential routes for exploitation which could include the following specific technical areas:

- A) Availability of specific antibodies as a direct commodity this is a distinct possibility and will be explored in deail with the partners before the mid-term meeting to establish viability and desire.
- B) Fabrication methodology for immunosensor manufacture as detailed above this is already being proven and will increase as the project progresses. The methodology will remain in house
- C) Post data acquisition signal processing software not yet in existence but the outputs will generate new algoritms.
- D) Dedicated immunosensor instrumentation, which incorporates application specific electronic hardware, firmware, data acquisition and control software, and fabricated immunosensors.

The main practical aspects of exploitation of the deliverables will be by:

- 1) Direct dissemination of successful immunosensor results at conferences, exhibitions, workshops and brokerage meetings in addition to direct marketing tools such as the project website. This is already taking place and the mid-term meeting will be after a major bioelectrochemisry conference in Coimbra, Portugal where several of the partners are giving presentations. Several publications are being prepared already.
- 2) Demonstration of the laboratory prototype instrument during the last 2 months of the project. This may come forward in time provided the prototype is performing correctly. Indications are that the est bed performs beyond expectations and as the prototype will be built on this basis the results are expected to be excellent.
- 3) Formation of a new start-up company to manufacture and market the immunosensor platform technology, particularly the sensor fabrication technology with instrumentation from partner 7. There is a new company that has already been set-up to manufacture and market sensors for detection of volatile chemical species. The company profile is as a 'sensor and sensor interrogation' SME and as such may be the vehicle to exploit immunosensors under a division of its activities. This is a point for discussion between the SME partners who have the overall responsibility of developing the industrial and commercial strategy for the project as detailed in the consortium agreement which has been accepted by all partners.

Direct approaches to third party companies having an interest in developing immunosensors may be an option to consider for exploitation. Already the project manager has had an approach from a third party and discussions / negotiations are underway. It is known that a new, well financed biosensor company in the UK is looking for immunosensor platform technology at this time (January 2006) and such it may be prudent to discuss possibilities with them, since they are already a commercial force in the biosensors marketplace. Again this will be a discussion between the SME partners under their role in exploitation.

Basic Points of from the Consortium Agreement.

The consortium agreement was drafted by the SME partners and deals principally with the exploitation of project results and dissemination. The day to day dealings and responsibilities of partners to each other and the commission are clearly stated in the contract and its annexes, especially in the general conditions. The text of the agreement dealing with exploitation and dissemination are reproduced below and the roles of the SME partners and Academic partners are made clear. Annexes have not been reproduced here.

ELISHA Consortium Agreement

ELectro-immuno Interfaces and Surface nanobiotechnology: a Heterodoxical Approach

WHEREAS

- (I) The European Community represented by the Commission of the European Communities ("the Commission") has approved a project called ELectro-immuno Interfaces and Surface nanobiotechnology: a Heterodoxical Approach (ELISHA) under the SIXTH FRAMEWORK PROGRAMME PRIORITY [3] Nano-technologies and nano-sciences, knowledge-based multifunctional materials, and new production processes and devices 'NMP'
- (II) The performance of the ELISHA. Project is governed by Contract Number NMP2-CT-2003-505485 between the Contractors and the Commission ("the Contract").
- (III) The signatories to the Contract wish to agree a basis for the ultimate commercial exploitation of knowledge and results generated in connection with the Contract.

1. **DEFINITIONS**

In this Agreement the following terms shall be defined as follows:

"Contract" the contract between the EU and the University of Leeds number NMP2-CT-2003-505485.

"Annex 1" a copy of the contract NMP2-CT-2003-505485.

"Annex 2"

a copy of *Annex I-Description of Work* of the contract NMP2-CT-2003-505485.

"Annex 3"

a copy of Annex II – General Conditions of the contract NMP2-CT-2003-505485.

"Business Partner"

the two commercial entities who are full partners in the ELISHA project, namely Uniscan Instruments Ltd and Technology Translators Ltd. listed in the contract EU NMP2-CT-2003-505485.

"Commercial Exploitation Entity" any commercial third party created or brought in to assist in exploitation of the IP generated from within the project.

"Academic Partners"

the seven partners of the project who are non-profit making academic institutions, namely University of Leeds, Cranfield University, Ecole Central de Lyon, Technische Universitaet Muenchen, University College Cork (National University of Ireland Cork), Consejo Superior de Investigaciones Cientificas and Universite Joseph Fourier listed in the contract EU NMP2-CT-2003-505485.

"Intellectual Property Rights"

all knowledge and Intellectual Property rights, including but not limited to all letters patent, patent rights, registered designs, design rights and copyright, and other similar proprietary rights, all rights of whatsoever nature in computer programs and other computer software and data, and all intangible rights and privileges of a nature similar to any of the foregoing, and whether or not registered and including all

granted registrations and all applications for registration in respect of any of the same;

"Foreground IPR"

all knowledge and Intellectual Property Rights generated in connection with the Project and funded directly from the project, contract EU NMP2-CT-2003-505485.

"Background IPR"

all knowledge and Intellectual Property Rights, excluding Foreground IPR, owned or controlled by any Party prior to the contract EU NMP2-CT-2003-505485 being signed.

2. IT IS AGREED THAT:

The ELISHA project operates under the articles contained within the contract with the EU. The contact number is NMP2-CT-2003-505485 and a copy of this contract is appended in <u>Annex 1</u> of this consortium agreement.

The partners in the ELISHA project including the official signatories (the European Commission and the University of Leeds) and all other partners listed in the contract who have signed accession to contract documents will operate under the rules and rights of the contract, including all annexes that form an integral part of the contract. The annexes I and II in the 'contact' categorically state the 'description of the work' to be done and the 'general conditions' respectively. These are specifically appended to this consortium agreement as <u>Annex 2 and Annex 3</u>.

The work to be done is the proposed scientific content of the project and an overview of the project content, outcomes, proposed deliverables and milestones, including breakdowns of expected costs and financial usage of each partner. It is also understood that the work content may change as the project progresses and such provisions will be decided by the steering committee, the members of which are listed on page 10 in Annex 2 of this consortium agreement.

The general conditions explicitly state the implementation, deliverables, operational, financial provisions and intellectual property rights wherein the project shall operate (Annex 3 of this agreement).

The operation and outworking of the project consortium will be in accord with the general conditions hereby attached in Annex 3 and duplication of said conditions in the body of the agreement is deemed superfluous.

In consequence, the general conditions will be taken as the basis of this consortium agreement, with the exception of certain issues of intellectual property and exploitation of such IP, wherein the conditions for exploitation are stated below.

Annex 1, Annex 2 and Annex 3 are integral parts of this agreement and constitute the rules by which the partners operate, when taken together with the specific conditions listed in this agreement.

3. SPECIFIC CONDITIONS FOR EXPLOITATION OF KNOWLEDGE

The terms and conditions of the general conditions in Part C – Intellectual Property Rights (page 30 - 33) contained in this agreement in Annex 3, shall generally remain in force regarding:

- 1) the ownership of knowledge
- 2) the protection of knowledge
- 3) the use and dissemination of knowledge from the project
- 4) access rights

However in certain cases the provisions stated below will overrule and supercede the conditions listed in part C of the general conditions, especially in the areas of protection of knowledge and the use and dissemination of knowledge.

In section 3 – the use and dissemination of knowledge from the project it is required to state a detailed route for exploitation and the rights of exploitation of knowledge coming from the project.

The route is stated in detail below and will form the basis of all exploitation of knowledge, IP and results coming from the project.

- 1) All 'Foreground IPR' and 'intellectual property rights' generated in connection with the Project shall be owned by the respective inventors as clearly defined in the general conditions, Annex 2, page 30.
- Protection of knowledge shall be the primary responsibility of the owner, however if the owner does not intend to or cannot protect the knowledge invented they shall inform the Coordinator who will then consult with the 'business partners'. The outcome of such consultation will be either i) to take up the protection of the knowledge in question by the 'business partners' should the knowledge constitute significant IP relating to the exploitation of the project knowledge for the project as a whole or ii) to inform the Commission in accordance with clause II.33.1 of Annex 2, page 31 of the general conditions, in which case the general conditions rules shall apply.
- Direct commercial exploitation of project knowledge shall be performed I the main by the 'business partners' with support from the 'academic partners'. Direct exploitation of 'academic partner' owned knowledge is not excluded, however reciprocal support from the 'business partners' is encouraged.
- Where direct exploitation of knowledge is through the business partners commercial activities using project knowledge and IP, the respective 'academic partners' will receive remuneration on any exploitation of knowledge or IP owned by or generated by them. The terms and level of said remuneration being agreed on a license basis, subject to separate mutually agreed contacts on a case-by-case basis.
- 5) 'Business partners' will receive remuneration directly from the commercial exploitation of their own knowledge and IP.
- 6) 'Background IPR' and 'intellectual property rights' required to allow the commercial exploitation of knowledge generated within the project will be made available by individual owning partners

under specific licenses, subject to separate mutually agreed contacts on a case-by-case basis. Preferential rates to such licenses will be negotiated in good faith between partners to allow greater exploitation potential when combined with knowledge generated within the project.

- 7) If a new 'commercial exploitation entity' is formed for the purpose of commercial exploitation of project deliverables, this will be done under the terms of a separate mutually agreeable contract.
- 8) The 'academic partners' role in any new 'commercial exploitation entity' shall be wholly in the convening of a scientific advisory panel (SAP) that will play a supporting role to the commercial activities of any new entity formed.
- 9) The composition of any board of directors for the 'commercial exploitation entity' shall be primarily determined by the 'business partners'. Comments will be considered from the scientific advisory panel.
- 10) In any area where the 'business partners' do not have expertise in manufacture for commercial exploitation, such manufacture will be sub-contracted, subject to 'business partner' decisions, with the relevant 'academic partners' being offered first refusal of any resulting sub-contract.
- Any new 'commercial exploitation entity' shall be incorporated under the laws of England and Wales.

A second potential route for exploitation of project knowledge is to work with a third party company in a joint venture. Any potential joint venture opportunity would be considered by the steering committee of the project in detail. Where this commercial exploitation route is acceptable and clearly defined, and does not impair or compete with the business partners direct commercial activities, any business deal would be structured to incorporate the best aspects of each participating companies technology and skills, with the knowledge necessary to bring new products to market. Remuneration for project partners will be negotiated on a specific case by case basis.

A third route to exploitation is to license selected areas of the technology to third parties. This area will be carefully evaluated by the steering committee before any license is discussed, and will only be on the basis of application specific fields. Central IP such as generic fabrication technology will not be licensed as a general method.

All partners have accepted the consortium agreement as the way of working through the exploitation and dissemination of results from the project and have signed the consortium agreement.

Appendix 1 Background Characterisation of Existing Antibodies and Comparitive ELISA methods

Background Characterisation of Existing Antibodies - Partner 6.

The objective of the present study was to evaluate the recognition capacity of antisera (As) obtained by heterologous inmunisation as a means of an immunoassay using the model molecule terbutryn.

Some of the haptens used in this study were synthesized previously for development of Irgarol and atrazine assays, (2b,2e & 4a-4d) coupled to horseradish peroxidase (HRP) by active ester method. The heterologous antisera As 80-87 were obtained during development of the Irgarol assay using inmunogen haptens 4c and 4d coupled to keyhole limpet hemocyanin (KLH).

Evaluation of the affinity of As for ETs

The avidity of each antiserum for the different enzyme tracers (ETs) was determined by measuring the binding of serial dilutions of the ETs **2b**, **2e-HRP** and **4a-dHRP** to microtiter plates coated with twelve different dilutions of each serum. Optimal concentrations for ETs and As were chosen that produce absorbance in the range 0.7 to 1 unit of absorbance within 30 min. With these concentrations the ability of the analyte, terbutryn to compete with the ETs for the antibody binding sites was investigated. These experiments were carried out by adding serial dilutions of the analyte and the ETs (appropriately diluted) to the Ab-coated plates.

Optimized competitive ELISAs

Microtiter plates were coated with the antiserum (**As80** or **As 87**) in coating buffer overnight at 4° C. The following day the plates were washed with PBST buffer prior to the addition of a serial dilution of terbutryn and a predetermined dilution of the ET (**2eHRP** or **4aHRP**) and incubated for 30 min at RT. The plates were washed as described before and the substrate solution was added. The enzymatic reaction was stopped after 30 min at RT and read at 450 nm. The standard curve was fitted to a four-parameter logistic equation according to the following formula: $y = A - D/[1 + (x/C)^D] + B$, where A is the maximal absorbance, B the minimum absorbance, C is the concentration producing 50% of the maximal absorbance and D is the slope at the inflexion point of the sigmoid curve.

Cross-reactivity determinations

Stock solutions of different structurally related triazine pesticide were prepared in DMSO and stored at 4° C. Standard curves were prepared in PBST and each IC₅₀ determined in the competitive experiment as described above. The cross-reactivity values were calculated according to the following equation: (IC₅₀ terbutryn/IC₅₀ triazine derivative) x 100.

RESULTS

All evaluated ETs were recognized by all antisera except **2b** for As 87, **2e** for As 86 and **4b** for As 85-87. The ETs which seem to be most recognized are those more similar to the immunogen used and therefore to analyte. Thus, the ETs with a sulfur atom present in the triazine **4a-4d** presented a higher titer than those with chlorine atom such as **2e** and **2b** were hardly recognized by As 86 and 87.

Table 1 shows the characteristics of those assays selected according to their best properties of convenient maximal absorbance versus noise ratio, acceptable slope values (slope>0.7) and good IC_{50} (<0.1 \Box g/L). Particularly good was the combination of **As 87** with tracer **4aHRP**.

Table 1. Characteristics of the best competitive ELISAs

Combination	Abs max	Abs min	IC ₅₀ (μg/L)	slope	Assay #
2b 83	0.762	0.027	0.226	-0.90	1
20 63	0.588	0.025	0.213	-0.89	2
2e 80	0.517	0.014	0.457	-0.95	1
26 80	0.666	0.071	0.421	-0.87	2
4a 87	1.040	0.062	0.056	-1.05	1
4a 07	1.079	0.026	0.059	-1.13	2
4d 84	0.582	0.003	0.138	-0.82	1
4u 04	0.998	0.007	0.213	-0.89	2
4d 87	0.528	-0.003	0.033	-0.76	1
4u 0 /	0.516	-0.001	0.043	-1.33	2

Several triazine pesticides and other cross-reacting compounds were tested to determine the specificity of the immunoassay. The results reported in Table 2 indicate the specifity of the selected immunoassay combination (4aHRP/87). Only the herbicides Irgarol and Terbutylazine exhibit significant interference, which is expected since the immunogen used were the same as that in the development of the Irgarol immunoassay. In the case of Terbutylazine the reason for this recognition could be in the similarity with terbutryn molecule from which only differ in the sulfur atom.

Table 2. Cross-reactivity of some s-triazines and other related compounds for the Terbutryn immunoassay

	2e 80		4a	87
Compound	IC_{50} (nM)	% CR	IC_{50} (nM)	% CR
Terbutryn	1.7	100	0.257	100
Atrazine	> 100	< 0.25	> 100	< 0.25
Irgarol	1.2	141.25	0.48	53.45
Simazine	> 100	< 0.25	> 100	< 0.25
Metsulfuron	> 100	< 0.25	> 100	< 0.25
methyl				
2,4,6-TCP	> 100	< 0.25	> 100	< 0.25
Carbendazime	> 100	< 0.25	> 100	< 0.25
Isoproturon	> 100	< 0.25	> 100	< 0.25
Ametrine	> 100	< 0.25	> 100	< 0.25
Terbutylazine	8.1	14	0.14	70
Chlorpirifos	> 100	< 0.25	> 100	< 0.25

Antisera from heterologous immunizing protocols.

One of the most promising strategies to wide the affinity spectrum of an antiserum towards the goal of antibodies against a family of chemicals (*i.e.* S-triazine herbicides) could be the use of heterologous immunizing protocols. These protocols could be considered as an advance from the simple mix of a collection of structurally related immunogens. We check four heterologous immunizing protocols using two immunogens. For each of the protocols an optimized ELISA immunoassay was developed and the cross reactivity evaluated. In comparison with the cross reactivities observed for the homologous immunization protocols it could be observed that the cross reactivity spectrum is increased for the heterologous antisera.

		Heterologous Immunization						Homologous Immunization				
	AB/	AB	B/A	/B	A/A.	.B/B	B/B	A/A	A/A		B/B	
	4d/	As80	4d/.	As83	4d/.	As84	4d/	\s87	4d//	As15	4d/ <i>i</i>	4s17
Compound	Ec50	% CR	Ec50	% CR	Ec50	% CR	Ec50	% CR	Ec50	% CR	Ec50	% CR
Terbutryn	0.92	100	1	100	0.95	100	0.33	100	0.84	100	0.21	100
Atrazine	>102	<0.9	16.13	6.2	>102	<0.9	10	3.3	>102	<0.8	5.5	3.8
Irgarol	6.57	140	0.72	139	0.79	119	0.6	55	0.57	147.5	0.28	73.5
Ametrine	>100	<0.83	22.7	4.4	>100	<0.9	9.7	3.4	36.5	2.3	7.5	2.8
Terbutilazine	57.5	16	2.85	35	3.12	30	0.51	65	3.6	25	0.27	76
Terbumeton	1.13	81.6	8.33	12.6	12.18	7.8	0.74	45	1.05	80		
Hydroxypropazine	ncr	ncr	ncr	ncr	ncr	ncr	ncr	ncr	ncr	ncr	ncr	ncr

EC50 in nanomolar

These results suggest us that this strategy could be used to prepare antiserum with family affinity but more research is needed in order to get more information to fully control the immunization process.

Comparitive ELISA Assays

The objective for Partner 6 in this work package was the development and evaluation of immunoassays for the new antibodies produced in the project to detect fluoroquinolone and sulphonamide antibiotics in milk.

The key step in the development of ELISA immunoassays is related with the effect of the analytical matrix on the assay. Several parameters must be taken into account such as the impact of the pH, ionic strength, co-solvents, detergents and the matrix by itself.

For fluoroquinolones the two best immunoassays in buffer were studied for matrix effect and performance evaluation. The following figures show how several parameter changet the assay sensitivity and maximum signal.

The final assays in buffer using the optimized parameters showed an improved performance and a better assay stability. Also the assay accuracy and reproducibility were enough good to be used in analytical methods and protocols.

Amax	Amin	IC ₅₀ (nM)	Slope	Linear Range (nM)	LOD (nM)
1.50±0.12	0.10±0.02	3.45±0.54	-0.88 ±0.09	17-0.7	0.27 ±0.1
1.26±0.25	-0.001±0.016	3.65±1.05	-0.64±0.09	30.25-0.41	0.11±0.07

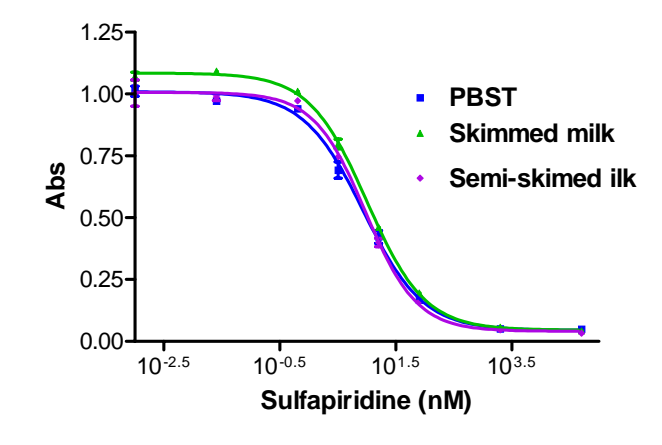
The next step was check the milk matrix effect and how to avoid it using a method as simple as possible.

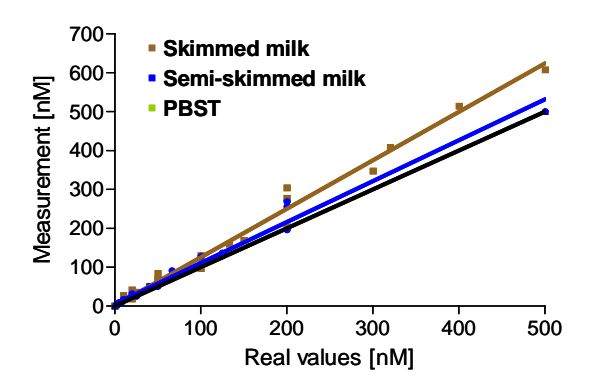
As it could see in the figure matrix effect was function of the milk dilution but in a different way that usual because the signal and the assay characteristics were improved over the assay in buffer and only after a 1:100 dilution the calibration curve is similar to those for buffer. After a careful evaluation of the matrix content and properties and taken into account the fluoroquinolone properties we proposed that it was the content in calcium salts the critical factor to explain the matrix effect. When the reference buffer was supplemented with calcium the two calibration curve (buffer and milk) were very similar. Probably an matrix factor (conceptually similar to the recovery factor in classical chromatography techniques) must be used for every milk type (whole, skimmed, etc) but in any case the assay yield very good results and it could detect several of the fluoroquinolone antibiotics at their MRLs levels using a simple sample dilution procedure.

Analito	LOD (µg/L)	IC ₅₀ (μg/L)	MRLs (Milk) (ppb)	% CR
Ciprofloxacin · HCI	0.025	0.55	100	100
Enrofloxacin	0.048	4.01	100	13
Danofloxacin	0.117	9.47	30	6
Difloxacin · HCI	0.055	2.06	Banned	32
Flumequine	0.442	14.93	50	3
Oxolicínic Ac.	0.454	32.29	Banned	1
Norfloxacin	0.007	0.95		50
Sarafloxacin · HCl	0.021	0.84		75
Ofloxacin	0.392	24.86		2
Marbofloxacin			75	

Amax	Amin	IC ₅₀ (nM)	Slope	Linear Range (nM)	LOD (nM)
1.50±0.12	0.10±0.02	3.45±0.54	-0.88 ±0.09	17-0.7	0.27 ±0.1
1.26±0.25	-0.001±0.016	3.65±1.05	-0.64±0.09	30.25-0.41	0.11±0.07

Following a similar procedure the sulphonamide antibiotics immunoassay was developed and evaluated. This assay showed a lower dependence on the classical parameters and matrix components. Only a sample 1:10 dilution was needed to avoid matrix interference on the assay and the final assay performance was very promising. It could measure the sulfapyridine content in any commercial milk that was assayed and it showed a good the accuracy and reproducibility.

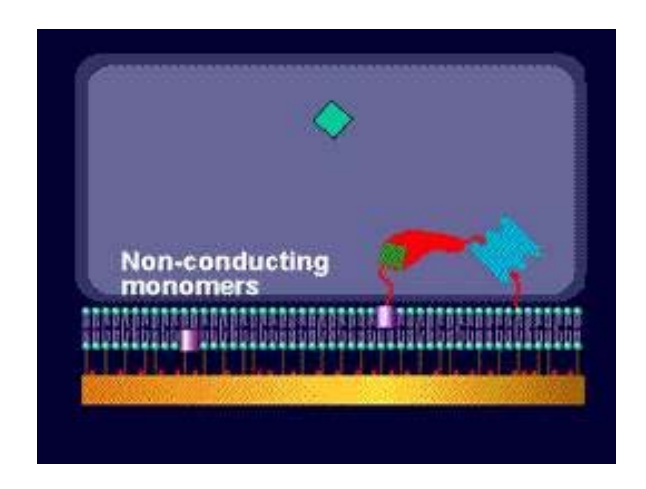


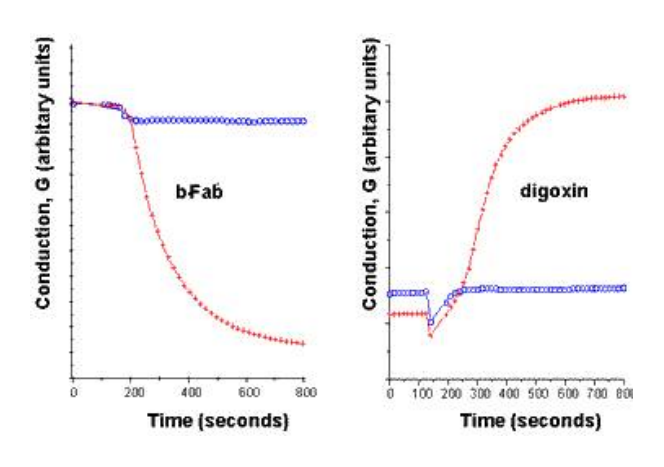


Appendix 2 Existing Immunosensor Formats Potential Competitors

1) Ambri ICSTM Biosensor

In general terms, the biosensor converts a biological binding event into a digital electrical signal. This enables the biosensor to employ computer technology to analyse and define this biological event.





This is an example of a competitive immunoassay turned into an electrochemical immunosensor format. The antibody (red) is attached to a biotin linker (blue) and is complexed with a tethered analyte (green) which in turn immobilises the membrane. Competing analyte (cyan diamond) binds to the antibody which then releases the tether and the membranes align to allow ions to produce an electrochemical signal. Examples are shown for addition of antibody (Fab) followed by addition of analyte (digoxin).

Ambri's first product will be the SensiDxTM System. The System has been designed for point of care diagnostic testing in critical care environments in hospitals. It consists of an instrument, single-use cartridge and quality control materials. A whole blood sample taken from a standard blood collection tube can be analysed utilising the SensiDxTM System; quantitative test results can be provided in just minutes. By delivering precise, quantitative test results in a STAT timeframe, the SensiDxTM System may assist in reducing the time of emergency diagnoses down from hours to minutes. This has a positive impact on both clinical decision-making and treatment costs.

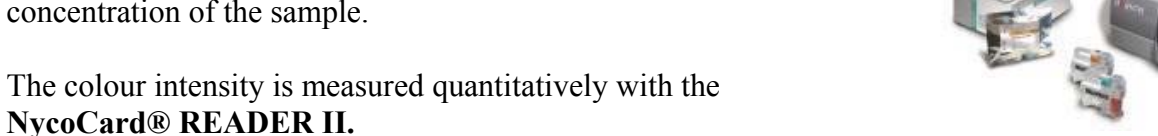
There is a movie of the immunosensor in action on www.ambri.com/Content/display.asp?screen=174

2) Axis-Shield Inc.

NycoCard®CRP Single Test is a solid phase, sandwich-format, immunometric assay. In the test well of the device there is a membrane coated with immobilised CRP specific monoclonal antibodies.

A diluted sample is applied to the test device. When the sample flows through the membrane, the C-reactive proteins are captured by the antibodies. CRP trapped on the membrane will then bind the gold-antibody conjugate added, in a sandwich-type reaction. Unbound conjugate is removed from the

membrane by the washing solution. A paper layer underneath the membrane absorbs excess liquid. In the presence of a pathological level of CRP in the sample, the membrane appears red-brown with colour intensity proportional to the CRP concentration of the sample.



3) Innovative Biosensor Inc.

This company produces a biosensor based on light emission.

The CANARYTM technology is composed of a genetically engineered biosensor that allows for extremely rapid testing of analytes at previously unseen levels of sensitivity and specificity.

The biosensor system uses B-lymphocytes that have been engineered to emit light within seconds of exposure to a specific bacteria, virus or toxin. The genetically engineered B-cell lines are designed to express a calcium sensitive bioluminescent protein in the cytosol. In addition, cells are engineered to express membrane-bound antibodies specific for the antigen of interest

Cross-linking of the antibodies by even minute amounts of the appropriate pathogen elevates intracellular calcium concentrations within seconds causing the bioluminescent molecule to emit light

The light is measured using a portable luminometer and the output result is calculated using a laptop

computer as photon counts per second over time

The data generated in this fashion is semi-quantitative in nature. Alternatively, one can generate a qualitative (yes or no) answer by simply defining a photon counts per second cut-off

The current CANARYTMassay for non-complex liquids and dry samples is a very simple process. Liquid samples require a total of 5 steps and can be performed in less than 3 minutes. For dry samples, the process takes less than 1 minute and involves 4 steps

FIGURE 1. UNIVERSAL EXPRESSION VECTOR FOR MONOCLONAL ANTIBODY SEQUENCE FIGURE 2 Time (sec) FIGURE 3. DETECTION ON E.coli 0157:H7 IN FOOD LIQUID SAMPLE **DRY SAMPLE**

FIGURE 4. ASSAY OPERATION

TOTAL ASSAY TIME ~ 1 MINUTE

4) Texas Instruments Inc.

The product is a miniaturized SPR Device called SPREETA $\underline{www.ti.com/snc/products/sensors/spreeta-highlights.htm}$.

Spreeta is a low-cost SPR based bio-sensing platform enabling real-time, quantitative concentration, affinity and kinetic analysis of biomolecular interactions.

Its unique, patented design makes possible high quality, low-cost SPR instrument configurations from benchtop

analyzers to portable hand-held test devices.



Spreeta's flexible format creates extensive opportunities in many markets like life science R&D, point of care diagnostics, food safety and bio-defense, environmental testing and industrial process control

Spreeta multichannel sensor modules: Tray of 25 costs \$2,250.00 (U.S.), that's \$90 each.

Appendix 3 Biomarkers

New Press Release for Prostate Cancer Diagnosis.

CJD Diagnosis using Prionbiomarkers.

Source: Johns Hopkins Medical Institutions

Date: 2005-05-16

URL: http://www.sciencedaily.com/releases/2005/05/050516080655.htm

New Test For Early Detection Of Prostate Cancer Shows Promise

In the first clinical study of a new blood protein associated with prostate cancer, researchers have found its earliest stages. At the same time, the marker successfully avoids the problem of false positive results that plagues prostate-specific antigen (PSA) testing.

Study results appear in the May 15, 2005, issue of Cancer Research. The lead author is Robert H. Getzenberg, Ph.D., professor of urology and director of research at the James Buchanan Brady Urological Institute at Johns Hopkins.

The traditional two-step approach of PSA testing and digital rectal examination has helped doctors identify prostate tumors early, while the cancers can still be cured. But PSA testing, like many disease-screening procedures, misses some cases of cancer and in other cases erroneously highlights noncancerous conditions.

"This new blood test, when coupled with PSA screening, may help reduce the number of both unnecessary biopsies and undetected prostate tumors," said Getzenberg, In addition to being highly sensitive to prostate cancer, the EPCA test is also very specific to it, meaning that other cancers and benign prostate conditions are not detected, thus boosting doctors' confidence that a positive EPCA test is really a sign of prostate cancer, added Getzenberg.

"Once this test is refined and approved for general use, it will have an impact on the detection and treatment of prostate cancer," said Getzenberg.

For the current study, Getzenberg and colleagues developed a simple test that would detect EPCA in the blood and then measured the EPCA levels in 46 patients, including those with prostate cancer (12 patients), bladder cancer (six patients), colon cancer (two patients), kidney cancer (one patient), spinal cord injury (seven patients) and noncancerous prostate inflammation (two patients), and 16 healthy individuals. The study was conducted at the University of Pittsburgh while Getzenberg was a member of its faculty.

The researchers found that EPCA levels were high in 11 of 12 prostate cancer patients (92 percent) and low in all of the healthy individuals. Only two bladder cancer patients and none of the other patients had elevated EPCA levels, suggesting that for this study, the test was correct 94 percent of the time. For comparison, only one-quarter of patients who undergo biopsies because they have elevated PSA values are actually positive for prostate cancer, while as many as 15 percent of those with low PSA values were found to have prostate cancer as detected by biopsy, according to Getzenberg.

Larger clinical trials are under way to further refine the EPCA test, to make it more sensitive so it can pick up even the smallest traces of the marker, and to verify its usefulness for detecting prostate cancer in a larger sample of patients, said Getzenberg.

Prostate cancer is the most common type of cancer found in American men. The American Cancer Society estimates that there will be approximately 232,090 new cases of prostate cancer in the United States in 2005, and 30,350 men will die of this disease.

Funding for the study was provided by Tessera Inc. Other authors on the report are Barbara Paul, Rajiv Dhir, Douglas Landsittel and Moira Hitchens, all of the University of Pittsburgh.

On the Web: http://cancerres.aacrjournals.org/ http://urology.jhu.edu/robertgetzenberg/index.php

Robert Getzenberg is a paid consultant to and received an unrestricted research grant from Tessera Inc. Under separate agreements between the University of Pittsburgh and Tessera and the Johns Hopkins University and Tessera, Getzenberg is entitled to a share of royalty payments to the universities on sales of licensed products. The EPCA test is the subject of the license agreement between the University of Pittsburgh and Tessera.

This story has been adapted from a news release issued by Johns Hopkins Medical Institutions.

Prions

Biomarkers

A useful clinical diagnostic test for Creutzfeldt-Jacob disease (CJD) is the electro-encephalogram (EEG). An EEG on a patient with CJD shows generalized periodic sharp waves every second. These characteristic changes indicate CJD with a sensivity of 67% and specificity of 86%, if the symptoms have been present for at least 3 months. (1,2).

Several biochemical markers contribute to the differential diagnosis of CJD. These biomarkers include the CSF 14-3-3 protein, the tau protein, metallothioneins and Laminin Receptor Protein (LRP) / Laminin Receptor complex.

In 1967 the 14-3-3 protein was first described by Moore and Perez as an abundant acidic brain protein. The 14-3-3 proteins are a group of multifunctional proteins expressed in all eukaryotic cells. They bind to and modulate the function of cellular proteins including kinases, phosphates and trans-membrane receptors. The 14-3-3 proteins regulate diverse biological processes including neuron development, cell growth and cell cycling. In mammalian tissues there are seven isoforms (beta, gamma, delta, epsilon, eta, sigma, zeta, and tau) that are highly homologous and are encoded by separate genes. Of these isoforms, five are known to be present in neuronal cells; beta, gamma, epsilon, eta, and zeta. The predominant isoform present in sporadic CJD (spCJD) is gamma with smaller amounts of beta, epsilon and zeta (3,4).

At present, The World Health Organization has revised is clinical criteria for the diagnosis of probable spCJD to include a positive 14-3-3 in patients who have progressive dementia of less than 2 years duration. The 14-3-3 protein in cerebral spinal fluid (CSF) of suspected spCJD patients is detected with a sensitivity of 96% and specificity of 92% (3).

A recent study involving a large number of patients with histologically confirmed new variant CJD (vCJD) suggests CSF 14-3-3 has a lower sensitivity for the diagnosis of vCJD than for the diagnosis of spCJD. This study showed CSF 14-3-3 was detected in 50% of the patients with confirmed vCJD and 9% of the control cases (3).

The detection of CSF 14-3-3 in iatrogenic CJD (iCJD) patients is dependent on when the sample is taken. If the CSF sample is taken in the early stages of disease, then only 20% of the patients will have detectable CSF 14-3-3 but the sensitivity rises to 100% in the later of stages of the disease(3).

The sensitivity of CSF 14-3-3 in the detection of familial CJD cases depends on the mutation involved. CSF 14-3-3 is detected in 97% of codon E200K mutation cases, in 100% of V210L mutation cases, in 40% of P102L mutation cases but none in famial fatal insomnia (FFI) (3).

In addition to the problem of false negative results for FFI, there are also a number of reports of CSF 14-3-3 being detected in patients with paraneoplastic syndrome, transverse myelitis, Hashimoto's encephalitis, viral encephalopathies and vascular disorders (3).

A number of approaches are being tried to increase the sensitivity and specifity of CSF 14-3-3. One approach has been the development of isoform specific antisera. To date, most studies have used a polyclonal antiserum that detects all isoforms (3).

Another approach has been the investigation of the tau isoform of the 14-3-3 protein. The Laboratory of Neurobiology at the University of Antwerp has reported the tau 14-3-3 protein has a lower sensitivity (91%) but a higher specificity (97%) (2).

The Department of Neuropathology at Kyushu University, Japan is investigating two isoforms of metallothioneins (MTs). Their findings suggest that the protein expression of MTs is regulated differentially among human prion diseases and modified locally by prions (5).

The Prion Research Group of the Institute of Biochemistry, University of Munich, Germany is investigating the Laminin Receptor Protein (LRP)/Laminin(LN) as a possible biomarker. LRP was first isolated from tumors, plays an essential role in tumorgenesis and has a high affinity to Laminin. Laminin is the first extracellular matrix (ECM) protein detected during embryogenesis. Laminin (LN) is a glycoprotein that mediates cell attachment, communication, differentiation, movement and neurite outgrowth promotion. Studies at the Prion Research Group have found a correlation between LRP/LN levels and PrPSc propagation in certain tissues of mice and hamsters suggesting LRP/LN levels a possible biomarker in a BSE-Test on body fluids of cattle (6).

References and Additional Information for this Section:

- 1.H. C. Hansen, S. Zschocke, H. J. Sturenburg and K. Kunze *Acta Neurologica Scandinavica*. 97: 99-106 (1998) Clinical changes and EEG patterns preceding the onset of periodic sharp wave complexes in Creutzfeldt-Jakob disease
- 2. Biochemical Marker Detection in CSF of CJD disease patients, B. Everbroeck and P.Cras U of Antwerp
- 3. A. Green *Biochemical Society Transaction* (2002) Volume 30, Part 4 Use of 14-3-3 in the diagnosis of CJD disease
- 4. M. Rosenquist, P. Sehnke, r. Ferl, M. Sommarin C. Larsson- *Journal of Molecular Evolution* (2000) 51:446-458 Evolution of the 14-3-3 Protein Family
- 5. http://www.ncbi.nlm.nih.gov/entrez/query.fcgi?CMD=Text&DB=PubMed
- 6. http://www.lmb.uni-muenchen.de/weiss/stefan.htm

Appendix 4 Patents, Publications and Abstracts

Publications to 42 Months:

To date papers have been published with a further in press.

Labeless and reversible immunosensor assay based upon an electrochemical current-transient protocol

Sarah Grant, Frank Davis, Jeanette A. Pritchard, Karen A. Law, Seamus P.J. Higson, Timothy D. Gibson

Analytica Chimica Acta **495** (2003) 21–32

A novel labeless and reversible immunoassay based upon an electrochemical current-transient protocol is reported which offers many advantages in comparison to classical immuno-biochemical analyses in terms of simplicity, speed of response, reusability and possibility of multiple determinations. Conducting polypyrrole films containing antibodies against (1) bovine serum albumin (BSA) and (2) Digoxin were deposited on the surface of platinum electrodes to produce conductive affinity matrices having clearly defined binding characteristics. The deposition process has been investigated using 125I-labelled anti-digoxin to determine optimal fabrication protocols.

Antibody integrity and activity, together with non-specific binding of antigen on the conducting matrix have also been investigated using tritiated digoxin to probe polypyrrole/anti-digoxin films. Amperometric responses to digoxin were recorded in flow conditions using these films, but the technique was limited in use mainly due to baseline instability.

Anti-BSA—polypyrrole matrices were investigated in more detail in both flow and quiescent conditions. No observable response was found in flow conditions, however under quiescent conditions (in non-stirred batch cell), anti-BSA—polypyrrole films have been demonstrated to function as novel quantitative chronoamperometric immuno-biosensors when interrogated using a pulsed potential waveform. The behaviour of the electrodes showed that the antibody—antigen binding and/or interaction process underlying the response observed was reversible in nature, indicating that the electrodes could be used for multiple sensing protocols. Calibration profiles for BSA demonstrated linearity for a concentration range of 0–50 ppm but tended towards a plateau at higher concentrations. Factors relating to replicate sensor production, sample measurement and reproducibility are discussed.

Label-free and reversible immunosensor based upon an ac impedance interrogation protocol Sarah Grant, Frank Davis, Karen A. Law, Andrew C. Barton, Stuart D. Collyer, Seamus P.J. Higson, *, Timothy D. Gibson

Analytica Chimica Acta 537 (2005) 163–168

Abstract

We report the fabrication of a label-free and reagentless immunosensor based on the direct incorporation of antibodies into conducting polymer films along with a subsequent ac impedimetric electrochemical interrogation. Model sensors of this type were prepared by electrochemically polymerising conducting polypyrrole films containing anti-BSA at the surface of screen-printed carbon electrodes. Films containing chloride or anti-human IgG as counter-ions were used as controls. An ac measurement protocol was used to determine the impedance of the electrodes when immersed in water or analyte solutions. A selective and reversible binding of analyte to the electrode could be monitored electrochemically and studies are reported in detail relating analyte concentrations to bulk impedimetric measurements, the real component, the imaginary component and the phase angle of the responses. The results of this study showed detectable and reversible antibody—antigen interactions could be measured and mainly affected the Faradaic behaviour of the electrode. BSA could be detected with a linear response from 0 to 75 ppm.

Immunochemical Determination of Industrial Emerging Pollutants

M.-Carmen Estévez · Héctor Font · Mikaela Nichkova · J.-Pablo Salvador ·Begoña Varela · Francisco Sánchez-Baeza · M.-Pilar Marco (.)

The Handbook of Environmental Chemistry Vol. 5, Part O (2005): 119–180

Abstract A significant number of immunochemical methods have been described for the determination of the most important emerging pollutants. The present chapter is a compilation of the information available today regarding immunochemical determination of industrial residues with a high potential risk of causing negative effects in the environment, wildlife, and public health. Homogeneous immunoassays, ELISAs, FIIAs, immunosensors, and selective immunoaffinity sample treatment methods have been reported for the analysis of an important number of these substances. The bases of these methods are briefly presented. Immunochemical methods for anionic (LAS), nonionic (APEs and APs), and cationic surfactants (BDD12AC and DDAC) are extensively reviewed and the features of these assays discussed, particularly if examples of their application to environmental samples have been described. Similarly, a great amount of information has been collected regarding immunochemical determination of organochlorinated substances such as PCBs,PCDDs,PCDFs,and chlorophenols. On the contrary, immunochemical analysis of organobrominated substances, such as the BFR agents, seems to be still a goal. Immunochemical methods have also been reported for bisphenol A and phthalates showing excellent features. The commercial availability of some of these methods is also presented.

Immunochemical Determination of Pharmaceuticals and Personal Care Products as Emerging Pollutants

M.-Carmen Estévez · Héctor Font · Mikaela Nichkova · J.-Pablo Salvador · Begoña Varela · Francisco Sánchez-Baeza · M.-Pilar Marco

The Handbook of Environmental Chemistry Vol. 5, Part O (2005): 181–244

Abstract A review on immunochemical methods for the analysis of pharmaceuticals is presented. A broad range of pharmaceutical categories and personal care products may reach the aquatic environment after excretion through industrial, domestic, and hospital wastewater. With few exceptions pharmaceuticals for human medicine are not high-production chemicals and the expected environmental concentrations should be low. However, the use of some of these chemicals in veterinary medicine increases the probability that the concentration values in the aquatic environment might reach higher levels. On the other hand certain drugs with limited use are of concern because of their high pharmacological potency, which creates a risk even at trace levels. Attending to these considerations and to the potential human risks, this review focuses on antibiotics, hormones, analgesics, nonsteroidal anti-inflammatory drugs, and cytostatic agents. Although these procedures have only been applied to the analysis of environmental samples on a few occasions, immunochemical methods for several of these substances exist and some of them are commercially available due to their use in clinical laboratories and forensic medicine.

Development and evaluation of C18 and immunosorbant solid-phase extraction methods prior immunochemical analysis of chlorophenols in human urine

Mikaela Nichkova, M.-Pilar Marco*

Analytica Chimica Acta **533** (2005) 67–82

Abstract

Two solid-phase extraction (SPE) methods, based on hydrophobic and selective (antibody–antigen) interactions, have been established and evaluated as clean-up methods prior the immunochemical analysis of 2,4,6-trichlorophenol (2,4,6-TCP) in urine samples. Without a clean-up method the extent of interferences caused by the urine matrix in the ELISA [R. Galve, M. Nichkova, F. Camps, F. Sanchez-Baeza, M.-P. Marco, Anal. Chem. 74 (2002) 468] varies depending on individual urine samples and accurate measurements are only possible when 2,4,6-TCP concentration levels are higher than 40 gL-1. Both sample preparation methods improve detectability of the immunochemical method getting rid of the variability due to the intrinsic individual differences within the urine samples. Even though, the immunosorbent (IS)-SPE method developed has proven to be a superior sample preparation method eliminating completely matrix effects caused by both, non-hydrolyzed (NH) and hydrolyzed urine samples. The LOD reached by the C18-SPE-ELISA method (~4 gL-1 for free and total chlorophenols) is sufficient for exposure assessment of the occupationally exposed population. However, the detectability (0.66 and 0.83 gL-1 in NH and hydrolyzed urine samples, respectively) accomplished by the IS-SPE-ELISA allows also biomonitoring potential exposure of non-occupationally exposed groups. Moreover, the specificity of the IS-SPE procedure can be modulated to provide a group-specific (9 chlorophenols and 2 bromophenols are extracted with an efficacy superior to 85%) or a more selective protocol (only 2,3,4,6-TtCP, 2,4,6-TCP are extracted with a recovery superior to 80% and 2,4,6-tribromophenol with a 70% recovery). On the other hand, the IS-SPE extracts produce cleaner chromatograms allowing quantitation by GC-ECD (or GC-MS) after toluene extraction and derivatization with a LOD near 0.1 gL-1 in NH and hydrolyzed urine samples. The IS-SPE-ELISA method has been validated with GC-ECD using spiked and real urine samples. This study also provides evidences of the general exposure of the population to organochlorinated and organobrominated substances. Measurable levels of 2,4,6-TCP, 2,4,5-TCP, 2,3,4,6-TtCP, 2,4,6-TBP and 2,4-DBP have been detected in some of the samples used in this study.

Electrogeneration of poly(pyrrole)-NTA Chelator film for a reversible oriented immobilisation of histidine-tagged proteins

Naoufel Haddour, Serge Cosnier, Chantal Gondran, Journal of American Chemical Society, 2005, 127, 5752-5753

Quantitative detection of doping substances by a localised surface plasmon sensor Mark P. Kreuzer a,*, Romain Quidant b, Gonc, al Badenes b, M.-Pilar Marcoa

Biosensors and Bioelectronics (in press)

Abstract

Within this communication, consistent evidence of a quantitative biosensing principle for steroidal residue analysis is presented. Our approach uses a simple method for the quantitative determination of an anabolic agent called stanozolol (Sz). Sz (Mw 328) is widely used in sports, horse racing and as a growth promoter in animals for human consumption. Through the use of localised surface plasmons

(LSPs), sustained by three-dimensional noble metal nano-structures, we have developed a highly specific, label-less immunosensor for the detection of this small organic molecule to low levels (nM range). A main practical advantage over conventional flat extended film surface plasmon resonance (SPR) systems is the simplicity of the optical configuration, since there is no need for cumbersome total internal reflection illumination, thus making integration easier. In addition, the active area of the LSP-based sensor is smaller, decreasing the minimum detectable number of molecules involved in the binding event. Assay times are short and the set-up is comprised of relatively cheap instrumentation. Detection levels found here are comparable with SPR, even at this early stage of development and with further modifications, we envisage sensing down to pM (10-12) levels.

Gregoire Herzog, Karine Gorgy, Tioga Gulon and Serge Cosnier. Electrochemistry Communications 7 (2005) 808–814

Electrochemical characterization of photoactivable polypyrrole films and their application for enzyme grafting.

Abstract

New benzophenone derivatives functionalized by electropolymerizable pyrrole, vinylaniline and indole groups have been synthesized and electrochemically characterized. Upon electrochemical polymerization in acetonitrile, only two photoactivable polypyrrole films were prepared. Although the latter differed in the length of the spacer bridging benzophenone and pyrrole groups, similar photografting properties were obtained under irradiation leading to the anchoring of an alkaline phosphatase monolayer. A mean surface coverage of enzyme, 622 ngcm 2, was reached for the poly(pyrrole–benzophenone) films. The enzyme maintained 63% of its initial activity after 30 days indicating a good stability of the photografted molecule.

Serge Cosnier « Electroanalysis 17, 2005, No. 19, 1701 – 1715

Affinity biosensors based on electropolymerised films

Abstract

This review gives an overview on different types of affinity biosensors based on electropolymerized polymer films that are becoming an important class of analytical tools. These affinity biosensors may be classified according to the strategy used for their fabrication, namely entrapment within polymers during their electrochemical growth, simple adsorption onto electropolymerized films, chemical coupling or affinity interactions between bioreceptors and electropolymerized films or direct electrochemical polymerization of the bioreceptor itself. Recently opened perspectives and potential research directions are also discussed.

R. E. Ionescu, S. Cosnier, G. Herzog, K. Gorgy, B. Leshem, S. Herrmann et R. S.Marks, manuscript submitted at Enzyme and Microbial Technology

Amperometric immunosensor for the detection of anti-West Nile virus IgG using a photoactive copolymer.

C. TLILI, H. KORRI-YOUSSOUFI, L. PONSONNET, C. MARTELET, N. JAFFREZICRENAULT *Electrochemical impedance probing of DNA hybridisation on oligonucleotide-functionalised poly pyrrole*

Talanta 68 (2005) 131-137

S. HELALI, C. MARTELET, A. ABDELGHANI, M. A. MAAREF, N. JAFFREZICRENAULT A disposable immunomagnetic electrochemical sensor based on functionalised magnetic beads on gold surface for the detection of atrazine

Electrochimica Acta 51 (2006) 5182–5186

V. IJERI, F. VOCANSON, C. MARTELET, N. JAFFREZIC-RENAULT Capacitive Sensing of Amino Acids Using Caliraxene-Coated Silicon Transducers

W. M. HASSEN, C. MARTELET, F. DAVIS, S. P.J. HIGSON, A. ABDELGHANI, S. HELALI, N. JAFFREZIC-RENAULT

Calix[4]arene based molecules for amino-acid detection

Sensors and Actuators B 124 (2007) 38–45

R. E. IONESCU, N. JAFFREZIC-RENAULT, L.BOUFFIER, T. HEALY, D. G. PINACHO, M.- PILAR MARCO, F. J. SÁNCHEZ-BAEZA, S. COSNIER, C. MARTELET

Impedimetric immunosensor for the reagentless and labeless detection of ciprofloxacin antibiotic Biosensors Bioelectronics (in press)

R. E. IONESCU, N. JAFFREZIC-RENAULT, L.BOUFFIER, T. HEALY, K. KRAMER, S. COSNIER, C. MARTELET

Impedimetric immunosensor for atrazine detection (patent to be pended)

Book chapter:

C. MARTELET, N. JAFFREZIC-RENAULT

"Self Assembled Monolayers for Biosensors" in Biosensors: Methods Express Ed. Paul Millner, Scion Publishing Ltd Juin 2006 ISBN: 1904842127

Photoelectrochemical immunosensor for label-free detection and quantification of anti-cholera toxin antibody.

NAOUFEL HADDOUR, JEROME CHAUVIN, CHANTAL GONDRAN, SERGE COSNIER Journal of the American Chemical Society (2006), 128(30)

Amperometric immunosensor for the detection of anti-West Nile virus IgG using a photoactive copolymer.

R. E. IONESCU, S. COSNIER, G. HERZOG, K. GORGY, B. LESHEM, S. HERRMANN, R.S. MARKS Enzyme and Microbial Technology, 40(3) (2007) 403

New metallic oxide electrodes for the deposition of functionalised polymers.

G. Herzog, N. Haddour, V. Stambouli, P. Chaudouët, C. Gondran, K. Gorgy, S. Cosnier, M. Labeau Sensors and Transducers, **64** (2006) 490-499

Impedimetric immunosensor for the specific label free detection of ciprofloxacin antibiotic

Rodica E. Ionescu, Nicole Jaffrezic-Renault, Laurent Bouffier, Chantal Gondran, Serge Cosnier, Daniel G. Pinacho, M.-Pilar Marco, Francisco J. Sánchez-Baeza, Thomas Healy, Claude Martelet Biosensors & Bioelectronics, submitted

Design of carbon nanotube-polymer network by electropolymerization of SWNT-pyrrole derivative *S. Cosnier and M. Holzinger.*

Electrochimica Acta, in preparation

Amperometric immunosensor for the detection of anti-West Nile virus IgG,

Rodica E. Ionescu, Serge Cosnier, Sebastien Herrmann and Robert S. Marks, Anal. Chem. submitted

Labeless Immunosensor Assay for Fluoroquinolone Antibiotics based upon an AC Impedance Protocol

G.Garifallou, G. Tsekenis, F. Davis, P. A. Millner D. G. Pinacho, F. Sanchez-Baeza, M.-Pilar Marco, T. D. Gibson and S. P. J. Higson, *Anal. Lett.*, in press.

The following abstracts have been presented at International conferences around the world.

Label-less AC Imedimetric antibody based micro-electrode array based sensors for point of care biomedical applictions

Andrew Barton, Stuart Collier, Frank Davis, Georgios Tsekenis, Goulielmos-zois Garifallou, William Roberts and Seamus Higson

9th World Congress on Biosensors 2006. 10 – 12th May 2006. Toronto, Canada.

New Commercial Immunosensors: Exploitation of ELISHA Technology

<u>Tim Gibson</u>, Paul Millner, Seamus Higson, Graham Johnson, John Griffiths, Daniel Lonsdale, Denise Gibson.

9th World Congress on Biosensors 2006. 10 – 12th May 2006. Toronto, Canada.

Designed Affinity Surfaces for Biomolecule Immobilisation and Biosensor Construction.

P.A.Millner, A.Vakurov, H.C.W.Hays, S.A.Weiss, M.Billah and N.A.Pchelintsev. International Workshop on Biosensors for Environmental Analysis. $21^{st} - 23^{rd}$ Feb 2006, Goa, India. Invited Lecture.

Electrostatic Immobilisation Strategies for Attachment of Enzymes and Antibodies to Biosensor Surfaces.

Alex Vakurov, Tim Gibson and Paul A Millner 2nd International Workshop on Surface Modification for Chemical and Biochemical Sensing(SMCBS2005),6th – 10th November 2005, Kazimierz, Poland

Designed Affinity Surfaces for Biomolecule Immobilisation and Biosensor Construction.

Paul A.Millner, AlexVakurov, Henry Hays, Sophie Weiss, Morsaline Billah and Tim Gibson 2nd International Workshop on Surface Modification for Chemical and Biochemical Sensing(SMCBS2005),6th – 10th November 2005, Kazimierz, Poland

SFC-Eurochem

28 août-1^{er} septembre 2005, Nancy (France)

Serge Cosnier, keynote lecture

Biosensors at the convergence of electrochemistry, organic chemistry and biology.

The Tenth International Seminar on Electroanalytical Chemistry (10th ISEC) & The Third Sino-France Workshop on Surface Electrochemistry of Molecules of Biological Interest and Biosensor Application (3rd S-FWSE),

16-19 Octobre 2005, Changchun (China)

Serge Cosnier, lecture

Recent advances in affinity biosensors

1st International Conference on POLLUTION CONTROL AND RESOURCE REUSE FOR A BETTER TOMORROW AND SUSTAINABLE ECONOMY

18-21 octobre 2005, Shanghai (China)

Serge Cosnier, lecture

Optical and amperometric biosensors based on electrogenerated polymers

Second International Workshop on "Biosensors for Food Safety and Environmental Monitoring"

10-12 novembre 2005, Agadir (Maroc)

Serge Cosnier, lecture

Optical and amperometric immunosensors based on electrogenerated polymers

International Conference on enzyme technology « Relatenz 2005 »

 $20\mbox{-}23$ September 2005 , Varadero Beach, Matanzas, CUBA

Serge Cosnier Plenary lecture

« Enzyme sensors based on electrogenerated polymers and clay materials »

Journées d'électrochimie

5-8 Juillet 2005, Saint Malo, FRANCE Naoufel Haddour, Chantal Gondran, Serge Cosnier *Film polymère affin photoélectrosensible pour une détection directe d'immunoréaction*Journées d'électrochimie

5-8 Juillet 2005, Saint Malo, FRANCE

Grégoire Herzog, Karine Gorgy, Serge Cosnier, Tania Konry ,Serge Cosnier and Robert Mark Electropolymérisation de fims photoliants pour l'élaboration d'immunocapteurs et de biopuces

XVIII International Symposium on Bioelectrochemistry and Bioenergetics/3rd ISE Spring Meeting 19 – 24 June Coimbra – PORTUGAL –

G. Herzog, N Haddour, C. Gondran, K. Gorgy S. Cosnier, V. Stambouli, M. Labeau, p Chaudouet. *New semiconductor electrodes for the deposition of functionalised polymers.*

XVIII International Symposium on Bioelectrochemistry and Bioenergetics/3rd ISE Spring Meeting 19 – 24 June Coimbra – PORTUGAL –

Serge Cosnier, Naoufel Haddour, Chantal Gondran, Hubert Perrot, Mathieu Lazerges.

The use of supramolecular architectures for enhancing the sensitivity of piezoelectric biosensors.

International Conference on enzyme technology « Relatenz 2005 » 20-23 September 2005 , Varadero Beach, Matanzas, CUBA R.E. Ionescu, G. Herzog, K. Gorgy, B. Leshem, S. Hermann, S. Cosnier, R.S. Marks Amperometric immunosensor for the detection of anti-West Nile Virus IgG

Ogurtsov V.I, Vakurov A., Sheehan M. M., Millner P.A., Gibson T.D. *Impedance study of a polypyrrole-gold silicon sensor*. BES-ISE 2005 XVIII International Symposium on Bioelectrochemistry and Bioenergetics/3rd ISE Spring Meeting, Coimbra, Portugal, 19–24 June, 2005

Vakurov A., Ogurtsov V. I., Millner P.A., Gibson T.D., Sheehan M. M. *Stabilizing of gold-polypyrrole layer on silicon sensor electrodes by treatment with thiol compounds*. BES-ISE 2005 XVIII International Symposium on Bioelectrochemistry and Bioenergetics/3rd ISE Spring Meeting, Coimbra, Portugal, 19–24 June, 2005

C. TLILI, H. KORRI-YOUSSOUFI, L. PONSONNET, C. MARTELET, J. P MAHY, N.JAFFREZIC-RENAULT "Label free detection of DNA hybridization with EIS measurements" TRANSDUCERS'05 13th International Conference On Solid State Sensors,, Actuators and Microsystems 5-9 Juin 2005, Séoul, Corée

C. TLILI, H. KORRI-YOUSSOUFI, L. PONSONNET, C. MARTELET, N.JAFFREZIC-RENAULT "Electropolymerized polypyrrole with immobilized redox probes for optimisation of direct impedimetric immunosensors" Joint Meeting Bioelectrochemistry 2005, Coimbra 19-24 Juin 2005, Portugal

C. TLILI, H. KORRI-YOUSSOUFI, L. PONSONNET, C. MARTELET, N.JAFFREZICRENAULT "Electrochimie d'impédance: une méthode directe pour la détection d'ADN à base de poly pyrroles fonctionnalisés"

Journées d'Electrochimie 2005, 5-8 Juillet 2005, Saint Malo

C. MARTELET

"Impedance based immunosensors"

IMA Conference Instrumental Methods of Analysis 2-6 Octobre 2005 The Conference Center of the Aldemar Knossos Royal Village Hotel Crète, Grèce (Plenary lecture)

V. S. IJERI, F. VOCANSON, C. MARTELET, N. JAFFREZIC-RENAULT

"Capacitive sensors based on spin coated macrocyclic compounds for determination of aminoacids"

2nd ECHEMS Meeting June 22-25, 2006: Electrochemistry in Surface Functionalization La Palma, The Canary Islands, Spain

R. E. IONESCU, N. JAFFREZIC-RENAULT, C. MARTELET, S. COSNIER

Immunosensor based on impedance spectroscopy for the rapid detection of ciprofloxacin Colloque Jacques Cartier, 4-5 décembre 2006 Grenoble

The Eighth World Congress on Biosensors 24-26 May 2004 Granada, Spain

Serge Cosnier Design of electrochemical and optical enzyme sensors and immunosensors based on electrogenerated polymers

The Eighth World Congress on Biosensors 24-26 May 2004 Granada, Spain Serge Cosnier, Naoufel Haddour, Chantal Gondran

Photoelectrochemical immunosensor for the detection cholera antitoxin antibodies

Capteur biomimétique pour la détection de l'atrazine par Spectroscopie d'impédance

Chantal Gondran, Karine Gorgy, Arielle Le Pellec, Serge Cosnier, Julia Wiebe, Carolin Kraft, Karl Kramer, Javier Ramón, Francisco Sánchez-Baeza and M.-Pilar Marco

Oral communication Xème colloque du groupe français de bioélectrochimie, Céret 5-7 Avril 2006.

Oligosaccharides électropolymérisables pour le dosage spécifique de lectines par SPR

M.P Dubois, C. Gondran, S. Szunerits, S. Fort, S. Cosnier

Oral communication

Xème colloque du groupe français de bioélectrochimie, Céret 5-7 Avril 2006.

Electropolymers for new design of biosensors and microarrays

S. Cosnier, B. Tillier

communication

2nd International congress on nanobiotechnology, Grenoble, 14-16 juin 2006

Biological sensors based on electropolymerized films

Serge Cosnier, lecture

209 th Meeting of The Electrochemical Society, Denver (USA), 7-12 mai 2006

Biointerface design by electropolymerized films

Serge COSNIER

Gordon Conference on Bioelectrochemistry, 3-8 septembre 2006, Aussois, France

Electrochemical immunosensors and DNA sensors

Serge COSNIER

The 4th France-China Workshop on "Surface Electrochemistry of Molecules of Biological Interest & Biosensor Applications" Céret, 17-20 octobre, 2006

Capteurs à protéines et ADN basés sur des concepts non conventionnels

Serge COSNIER

5^{èmes} Journées Maghreb-Europe : Madica 2006 : les matériaux et leurs applications aux dispositifs et capteurs, Mahdia (Tunisie), 30,31 octobre- 1^{er} novembre 2006.

Nanostructured bioassemblies on functionalized polymers and their application to biosensing S. COSNIER

Nanotechnology applications in Bio-Sensors and Detection Systems: International Workshop, Ispra (Italie) 6-7 Decembre 2006.

Fluoroquinolone Detection by a conception of an immunosensor

Daniel G. Pinacho, Karine Gorgy, Serge Cosnier, Francisco Sanchez-Baeza and M.-Pilar Marco XIXth International symposium on BIOELECTROCHEMISTRY and BIOENERGETICS of the international Society of Bioelectrochemistry, Toulouse, 1-4 avril 2007

Immunocapteurs pour le contrôle environnemental et médical

Karine GORGY, Chantal GONDRAN, Arielle LEPELLEC, Serge COSNIER, Daniel G. PINACHO, Javier RAMON, Francisco SANCHEZ-BAEZA, M.-Pilar MARCO, Julia WIEBE, Carolin KRAFT, Karl KRAMER Journées d'électrochimie, 3-6 juillet 2007, Lyon, France, oral communication

Original concepts of biological sensors based on an electro-enzymatic transduction S. COSNIER

International conference on enzyme technology « Relatenz 2007 », 20-23 June 2007, Varadero Beach, Matanzas, Cuba

A study of stabilisation of conductive polymer-gold silicon biosensors by mercaptohexadecanoic acid treatment using electrochemical impedance spectroscopy and equivalent circuit approach modelling. Ogurtsov V. I., Vakurov A., Millner P.A., Gibson T.D., Healy T.

International Congress on Analytical Sciences, ICAS-2006, 25-30 June, Moscow, Russia, pp.638-639.

Electrostatic immobilisation strategies for attachment of enzymes and antibodies to biosensor.

Vakurov A., Ogurtsov V. I., Millner P.A., Gibson T.D., Healy T.

International Congress on Analytical Sciences, ICAS-2006, 25-30 June, Moscow, Russia, p.649

Appendix 5 Print Version Final Interim eTIP prepared Mid-Term And Accepted by the Commission 30th June 2005.

TECHNOLOGICAL IMPLEMENTATION PLAN

Description of project

EC PROGRAMME:	FP6-NMP
PROJECT TITLE:	Electronic Immuno-Interfaces and Surface
	Nanobiotechnology: A Heterodoxical Approach.
ACRONYM:	ELISHA
PROGRAMME TYPE:	6th FWP (Sixth Framework Programme)
CONTRACT NUMBER:	NMP2-CT-2003-505485
PROJECT WEB SITE (if any):	www.immunosensors.com
START DATE:	01 Jan 2004
END DATE:	31 Dec 2006
COORDINATOR DETAILS:	Name: Paul Millner Organisation: University of Leeds Address: Woodhouse Lane, LS2 9JT Leeds, UK Telephone: +44-113-343-3149 E-mail: p.a.millner@leeds.ac.uk

PARTNERS NAME:

Cranfield University at Silsoe, Seamus Higson Ecole Centrale de Lyon, Claude Martelet Technisch Universität München, Berthold Hock Tyndall Research Institute, Michelle Sheehan Applied Molecular Receptors Group, Pilar Marco Uniscan Instruments Ltd, Graham Johnson

Institut de Chimie Moléculaire de Grenoble FR CNRS 2607, Serge Cosnier

Technology Translators Ltd., Denise Gibson

Commission Officer Name:	Michael Browne

Executive summary

Original research objectives

Project Objectives The main aim of the ELISHA project is: • To produce a nanostructured immunosensor format that in practice works as simply the most successful commercial biosensors and which can be manufactured at high quality and low cost. To do this effectively the project has three main objectives: 1) To provide detailed knowledge and understanding of a novel signal transduction mechanism observed in nanostructured affinity-reagent based biosensors. 2) To produce electronic, label free, immunosensor model prototypes that can then be further developed into simple, novel, low-cost and reliable affinity sensors for important clinical, environmental and related analytes. 3) The development of dedicated electronics. The project objectives are designed towards a successful commercial outcome and exploitation of the results of the project was always

anticipated. The combination of the whole of the technical objectives will form the basis of the development of a medical device, able to be used in the same way as the currently available biosensors for diabetes monitoring to give accurate and diagnostic information for disease states such as cancers. Other applications may be in environmental, food and veterinary fields.

Expected deliverables

The expected deliverables of the ELISHA project are listed below. D1: Supply of existing antibodies; D2.: Supply of hapten derivatives; D3: Supply of purified antibodies; D4: Supply of recombinant antibodies and fragments; D5: Characterisation of antibodies and recombinants and fragments; D6: Initial supply of standard metal (gold) on silicon transducers; D7: Stocks of designed metal transducers on silicon substrates; D8: Micro-electrode transducers; D9: Transducers having alternative geometries; D10: Supply of existing monomers; D11: Designed monomers for specific binding; D12: Alternative immobilisation materials; D13: Results to indicate the relationships between polymer formation, antibody type and deposition process for immunosensor fabrication; D14: Detailed protocols for immunosensor fabrication; D15: Nanostructures and Nanoelectronics of different immunosensor types; D16: Monomers, materials and methods for nanostructured immobilisation; D17: Knowledge-based protocols for reproducible immunosensor fabrication and operation; D18: Specialised test bed electronics for sensor interrogation; D19: Electronics for laboratory prototype; D20: Knowledge database and understanding of the signal generation processes in the different nanostructured immunosensor produced; D21: Immunosensors exhibiting reduced non-specific binding; D22: Evaluation reports of affinity sensor systems; D23: Working laboratory prototype sensor system.

Project's actual outcome

Mid-Term the projects actual outcome is as follows: The deliverables listed as measurable outcomes in annex 1 of the contract have been essentially fulfilled, these are listed below together with the notes reported in the mid-term report. Antibodies: 1 pesticide and 1 PSA, 1 hapten reagent [Some Haptens and Purified Antibodies still to come]; 3 types of transducers Au on Si. (1000 total). 100 micro transducers; 2 types of precursors (hydrophilic and biotin labelled) [More precursors to come]; 2 types of immunosensors fabricated /part characterised; Report listing initial immobilized nano – interfaces; 12 Month Report [Completed Mid-February 2005]; 1 fluoroquinoline antibody; 500 designed Pt transducers; 1 Photoactivated precursor; 1 type of immunosensor fabricated / tested (immobilized methods); 1 programmable pulsed waveform test rig; 1 set of design specifications for sensor test rigs / DC test rig; 1 non-specific binding method evaluated Signal generation results from 1 type of entrapped antibody sensor; Mid-Term Report [Target Date June 2005]; The outcomes are essentially on-time and the project is producing the expected deliverables.

Broad dissemination and use intentions for the expected outputs

There are several areas of dissemination of the results of the ELISHA project, not least of which is the academic output in terms of papers and peer reviewed publications (7 in number with 13 conference presentations). The commercial dissemination and subsequent uses of the immunosensors designed and fabricated in the project will be a focus of exploitation. The desingned electronics will enable the manufacture of a laboratory prototype that will be able to be develoed still further into a medical device platform. Changing the immunosensor used will change the specificity of the device. PSA immunosensors will allow the rapid detection of prostate cancer risk. Adapting the ELISHA format to different molecular biomarkers will also enable rapid diagnosis of other diseases as the biomarkers become known. This area is developing and several are already known such as Her-2 (Breast Cancer), CA-125 (Ovarian Cancer), BRCA-1 and 2 (both Breast and Ovarian Cancer) and a new urine biomarker for prostate cancer (EPRA). Environmental testing could benefit from ELISHA format immunosensors for Endocrine Disruptors (estrone, estradiol, estratriol, etc) that are thought to come from contraceptive pill breakdown. Detection of the fluoroquinoline antibiotics is new and antibodies to these are also new. The application areas are in food quality and veterinary areas.

Overview of all your main project results

No.	Self-descriptive title of the result	Category A, B or C*	Partner(s) owning the result(s) (referring in particular to specific patents, copyrights, etc.) & involved in their further use
1	Prostatic Specific Antigen Immunosensor	В	University of Leeds
2	Advanced ac and pulsed waveform sensor interrogation system	В	Uniscan Instruments Ltd

3	Chemical Monomers for Immunosensor Development	В	Institut de Chimie Moléculaire de Grenoble FR CNRS 2607
	Fluoroquinolone Antibiotics Haptens, Conjugates, Antibodies and Immunoassays Kits	В	Applied Molecular Receptors Group
5	Rabbit antibody libraries for fluoroquinolines	В	Technisch Universität München
6	Processes of immobilization of affinity molecules	В	Ecole Centrale de Lyon

^{*}A: results usable outside the consortium / B: results usable within the consortium / C: non usable results

Quantified Data on the dissemination and use of the project results

Items about the dissemination and use of the project results (consolidated numbers)	Currently achieved quantity	Estimated future* quantity
Product innovations	1	5
Process innovations	1	3
New services (commercial)	0	2
New services (public)	0	0
New methods	2	5
Scientific breakthrought	1	3
Technical standards to which this project has contributed	0	0
EU regulations/directives to which this project has contributed	2	4
International regulations to which this project has contributed	0	0
PhDs generated by the project	0	5
Grantees/trainees including transnational exchange of personnel	0	1

^{* &}quot;Future" means expectations within the next 3 years following the end of the project

Comment on European Interest

Community added value and contribution to EU policies

European dimension of the problem

The project is on target to produce new testing instrumentation that will assist in the implementation of healthcare screening for certain cancers and possibly CJD. Alternative application in environmental screening are also being addressed. Screening programs for widespread diseases such as breast and prostate cancer are usually not routine, since the cost outweighs the benefits. The ELISHA platform may contribute towards this to make such screening possible by dramatically lowering costs and simplifying the test in practical terms to one similar to glucose testing.

Contribution to developing S&T co-operation at international level. European added value The contribution to S&T development in the EU is high. This will continue as the project develops. The ELISHA project has drawn upon many different expertises and the availablity of antibody producers in Spain and Germany, who link into the immunosensor expertise in France and the UK to produce the actual immunosensors themselves indicates the true nature of the S&T cooperation. Europe wide funding to support the development phases of the project outputs after the R&D funding finishes will be needed to make commercial production an actuality.

Contribution to policy design or implementation

The e-health policy will be contributed to by the project outcomes since the target analytes are much more orientated towards biomarkers for disease. Cancer screening in particular looks an interesting and necessary market area. The third action plan to combat cancer (1996-2000) Decision No 646/96/EC of the European Parliament and of the Council of 29 March 1996 (OJ No L 95, 16.4.1996, p. 9) had objectives dealing with the prevention of premature deaths due to cancer and ensuring a high level of health protection. Specifically, action 16 called for support for European feasibility studies on mass screening for other cancers (of the ovary, prostate, skin, colon/rectum and mouth), taking particular account of the medical, psychological, social and economic aspects. Taking the ELISHA project outcomes to development phase and production for clinical trials will

Contribution to Community social objectives

Improving the quality of life in the Community:

Quality of life in the Community as a whole should be improved by the simple ability to measure and detect diseases earlier and cheaper using ELISHA immunosensors. As a specific example: There are, at present, no widespread screening programmes in Europe, but it is very likely that the situation will to change in the near future in response to public pressure for more readily available PSA testing, as a result of heightened awareness of PSA and prostate cancer. Health insurance schemes are now including PSA testing in their annual health checks and doctors are beginning to offer the test as a standard part of their health assessment programmes. Screening of cancers and other life threatening diseases is often not done for the simple reason that it is too expensive or it is too complicated to implement at a national or regional level. The ELISHA immunosensor devices are aiming to change this to make it simple and cheap to deploy, thereby improving life quality Europewide

Provision of appropriate incentives for monitoring and creating jobs in the Community (including use and development of skills):

The project could create jobs in the community based on the fact that screening services need staff to operate them and the development of a new business area in the manufacture and testing of immunosensors will also require dedicated skilled staff. The actual provisions for doing this has not yet been worked out at the interim stage and the necessary fuding required to create the manufacturing posts and associated business venture needs to be sourced.

Supporting sustainable development, preserving and/or enhancing the environment (including use/conservation of resources):

Environmental targets are extremely likely and early antibody supply was for pesticides. These types of immunosensors have never been produced in detail since the PSA route gave such good results initially. Environmental immunosensors have to perform in a similar manner to the healthcare ones, so as the flouroquinoline antibodies are tested in the system as the model hapten device, so other availbale antibodies will be tested. The immunosensors for environmental analytes will be a potential route for simple and cheap water monitoring. One large EU wide problem that is continuing to cause concern is the presence of ever increasing concentrations of female steroid hormones and their breakdown products in water, the so-called endocrine disruptors. The water industries are very interested in rapid, sensitive and accurate analytical tools for such materials and the ELISHA sensor types could be developed for such analytes. Again the funding will have to be sourced outside the project.

Expected project impact (to be filled in by the project coordinator)

	_	II other		
	SCALE OF EXPECTED			
EU Policy Goals	IMPACT OVER THE NEXT 10 YEARS -1 0 1 2 3	Not applicable to project	Project Impacttoo difficult to estimate	
1. Improved sustainable economic development and growth, competitiveness	2			
2. Improved employment	1			
3. Improved quality of life and health and safety	3			
4. Improved education	0	✓		
5. Improved preservation and enhancement of the environment	3			
6. Improved scientific and technological quality	2			

7. Regulatory and legislative environment	1	
8. Other	2	

1. Economic development and growth,	Scale of Expected Impacts over the next 10 years (2)	
competitiveness	By Project End -1 0 1 2 3	After Project End -1 0 1 2 3
a) Increased Turnover for project participants - national markets	1	2
b) Increased Turnover for project participants- international markets	1	2
c) Increased Productivity for project participants	0	0
d) Reduced costs for project participants	0	0
e) Improved output quality/high technology content	1	2

2 Employment	Scale of Expected Impacts over the next 10 years (2)	
2. Employment		After Project End -1 0 1 2 3
a) Safeguarding of jobs	1	1
b) Net employment growth in projects participants staff	1	2
c) Net employment growth in customer and supply chains	0	0
d) Net employment growth in the European economy at large	0	0

2 Quality of Life and health and cafety	Scale of Expected Impacts over the next 10 years (2)	
3. Quality of Life and health and safety	By Project End -1 0 1 2 3	After Project End -1 0 1 2 3
a) Improved health care	1	3
b) Improved food, nutrition	0	0
c) Improved safety (incl. consumers and workers safety)	1	2
d) Improved quality of life for the elderly and disabled	0	1
e) Improved life expectancy	0	0
f) Improved working conditions	0	0
g) Improved child care	0	0
h) Improved mobility of persons	0	0

4. Improved education	Scale of Expected Impacts over the next 10 years (2)	
4. Improved education	By Project End -1 0 1 2 3	After Project End -1 0 1 2 3
a) Improved learning processes including lifelong learning		
b) Development of new university curricula		

E. Drocowation and onbancoment of the environment	Scale of Expected Impacts over the next 10 years (2)	
5. Preservation and enhancement of the environment	_	After Project End -1 0 1 2 3
a) Improved prevention of emissions	0	0
b) Improved treatment of emissions	0	0
c) Improved preservation of natural resources and cultural heritage	1	3
d) Reduced energy consumption	0	0

6 SQT quality	Scale of Expected Impacts over the next 10 years (2)	
6. S&T quality	By Project End -1 0 1 2 3	After Project End -1 0 1 2 3
a) Production of new knowledge	2	2
b) Safeguarding or development of expertise in a research area	1	2
c) Acceleration of RTD, transfer or uptake	1	2
d) Enhance skills of RTD staff	1	2
e) Transfer expertise/know-how/technology	1	3
f) Improved access to knowledge-based networks	0	0
g) Identifying appropriate partners and expertise	0	0
h) Develop international S&T co-operation	1	3
i) Increased gender equality	0	0

7 Dogulatow, and logiclative environment	Scale of Expected Impacts over the next 10 years (2)	
7. Regulatory and legislative environment	By Project End -1 0 1 2 3	After Project End -1 0 1 2 3
a) Contribution to EU policy formulation	0	1
Contribution to EU policy implementation	0	1

9. Other (please specify)	Scale of Expected Impacts over the next 10 years (2)	
8. Other (please specify)	By Project End -1 0 1 2 3	After Project End -1 0 1 2 3
	0	2

Description of Results

No.	Title
1	Prostatic Specific Antigen Immunosensor

CONTACT PERSON FOR THIS RESULT

Name	Paul Millner
Position	Professor of Bioelectrochemistry
Organisation	University of Leeds
Address	Woodhouse Lane LS2 9JT, Leeds UK
Telephone	+44-113-343-3149
Fax	+44-113-343-3167
E-mail	p.a.millner@leeds.ac.uk
URL	
Specific Result URL	

SUMMARY

The demonstration of an immunosensor for the detection of PSA at clinically relevant levels is a step forward for medical diagnosis. A labeless immunosensor using anti-PSA and with a simple sample addition to obtain the result is a step towards a new type of immunosensor device. The results obtained are still very preliminary and cannot be used outside of the consortium at this time, however this is expected to change as the project fully delivers.

SUBJECT DESCRIPTORS CODES	
80 BIOSENSORS	
159 DIAGNOSTICS, DIAGNOSIS	
415 NANOBIOTECHNOLOGY	

DOCUMENTATION AND INFORMATION ON THE RESULT

Documentation	Details (Title, ref. number, general description,	Status:
type	language)	PU=Public
		CO=Confidential

INTELLECTUAL PROPERTY RIGHTS

Type of IPR	KNOWLEDGE: Tick a box and give the corresponding details(reference numbers, etc) if appropriate					Pre-existing know-how Tick a box and give the corresponding details(reference numbers, etc) if appropriate	
			(Current	Foreseen	Tick	Details
	Tick	NoP1)	NoI ²⁾	Details	Tick		
Patent applied for							
Patent granted							
Patent search carried out							
Registered design							
Trademark applications							
Copyrights							
Secret know-how	√	√ immunosensor fabrication √					
Other - please specify:							

- 1) Number of **P**riority (national) applications/patents
- 2) Number of Internationally extended applications/patents

MARKET APPLICATION SECTORS

Market application sectors

- 15 Manufacture of food products and beverages
- 33 Manufacture of medical, precision and optical instruments...
- 41 Collection, purification and distribution of water
- 73 Research and development

CURRENT STAGE OF DEVELOPMENT

Current stage of development	Experimental development stage (laboratory prototype)		
Other:			

Quantified data about the result

Items (about the results)	Actual current quantity	Estimated (or future) quantity
Time to application / market (in months from the end of the research project)		
Number of (public or private) entities potentially involved in the implementation of the result:	2	
of which: number of SMEs:	2	
of which: number of entities in third countries (outside EU):		
Targeted user audience: of reachable people		
S&T publications (referenced publications only)		
publications addressing general public (e.g. CD-ROMs, WEB sites)		
publications addressing decision takers / public authorities / etc.		
Visibility for the general public	NO	

Further collaboration, dissemination and use of the result

COLLABORATIONS SOUGHT

R&D	Further research or development	✓	FIN	FIN Financial support	
LIC	Licence agreement		VC	Venture capital/spin-off funding	
MAN	Manufacturing agreement		PPP Private-public partnership		
MKT	Marketing agreement		INFO	Information exchange/training	
JV	Establish a joint enterprise or partnership		CONS	Available for consultancy	
Other	(please specify)	√			
Details:	the results. This particular result is develop this to a fully operational of have two commercial vehicles (sen	the formal commonsor d	first opera nercial dev evelopme	start to look for extra financing to exact the start to look for extra financing to exact the start and the start and device development) in place at developmental funding will be required.	d to dy to

POTENTIAL OFFERED FOR FURTHER DISSEMINATION AND USE

To be discussed at this time.

PROFILE OF ADDITIONAL PARTNER(S) FOR FURTHER DISSEMINATION AND USE

To be discussed at this time.

No.	Title
2	Advanced ac and pulsed waveform sensor interrogation system

CONTACT PERSON FOR THIS RESULT

Name	Graham Johnson
Position	Managing Director
Organisation	Uniscan Instruments Ltd
Address	Sigma House, Burlow Rd, Derbyshire SK17 9JB, Buxton UK
Telephone	+44-1298-70981
Fax	+44-1298-77868
E-mail	graham.johnson@uniscan.co.uk
URL	
Specific Result URL	

SUMMARY

The bespoke ELISHA connector for use with the electrodes that will be used in the ELISHA project has been completed. Dual microcontroller circuitry, with advanced waveform, ultra-low voltage/current analogue, and digital control systems have been integrated into a test rig for the advanced ac and pulsed techniques for sensor interrogation. The pulsed techniques comprise PWS, PPS voltammetry and PAD have been implemented with the ability to specify pulse-widths between tens of microseconds and seconds. The experiments available to users allow for variable amplitude and duration with pulse amplitudes ranging from 1mV to 2volts. Similarly, data acquisition is currently possible at 16bit resolution and 80 KHz, with the number of points limited to 128K samples. Finally, the system incorporates the FFT technique to complete the requirements of the PWS technique. Windows based software for control and analysis has been written. All specified design criteria items have been addressed giving the user control over the experiments, configurations, execution, data display and export.

SUBJECT DESCRIPTORS CODES 28 ANALYTICAL CHEMISTRY 80 BIOSENSORS 666 WATER RESOURCE MANAGEMENT/ENGINEERING

DOCUMENTATION AND INFORMATION ON THE RESULT

Documentation	Details (Title, ref. number, general description,	Status:
type	language)	PU=Public
		CO=Confidential

INTELLECTUAL PROPERTY RIGHTS

Type of IPR	Tick		and g	live the corresponding e numbers, etc) if appi	Pre-existing know-how Tick a box and give the corresponding details(reference numbers, etc) if appropriate		
			C	Current	Foreseen	Tick	Details
	Tick	NoP1)	NoI ²⁾	Details	Tick		
Patent applied for							
Patent granted							
Patent search carried out							

Registered design	√		√	
Trademark applications				
Copyrights	√		√	
Secret know-how	✓		√	
Other - please specify:				

- 1) Number of Priority (national) applications/patents
- 2) Number of Internationally extended applications/patents

MARKET APPLICATION SECTORS

Market application sectors

- 33 Manufacture of medical, precision and optical instruments...
- 73 Research and development

CURRENT STAGE OF DEVELOPMENT

Current stage of development	Experimental development stage (laboratory prototype)
Other:	

Quantified data about the result

Items (about the results)	Actual current quantity	Estimated (or future) quantity
Time to application / market (in months from the end of the research project)	12	
Number of (public or private) entities potentially involved in the implementation of the result:		
of which: number of SMEs:		
of which: number of entities in third countries (outside EU):		
Targeted user audience: of reachable people		
S&T publications (referenced publications only)		
publications addressing general public (e.g. CD-ROMs, WEB sites)		
publications addressing decision takers / public authorities / etc.		
Visibility for the general public	NO	

Further collaboration, dissemination and use of the result

COLLABORATIONS SOUGHT

R&D	Further research or development	FIN	Financial support	
LIC	Licence agreement	VC	Venture capital/spin-off funding	
MAN	Manufacturing agreement	PPP	Private-public partnership	
MKT	Marketing agreement	INFO	Information exchange/training	
JV	Establish a joint enterprise or partnership	CONS	Available for consultancy	
Other	(please specify)			
Details :				

POTENTIAL OFFERED FOR FURTHER DISSEMINATION AND USE

PROFILE OF ADDITIONAL PARTNER(S) FOR FURTHER DISSEMINATION AND USE

No.	Title
3	Chemical Monomers for Immunosensor Development

CONTACT PERSON FOR THIS RESULT

Name	Serge Cosnier
Position	Head of Group
Organisation	Institut de Chimie Moléculaire de Grenoble FR CNRS 2607
Address	Laboratoire d'Electrochimie Organique, Université Joseph Fourier Grenoble, 1301 rue de la Chimie, BP, 5338041Cedex 9, Grenoble FRANCE
Telephone	+33 4 76 51 49 98
Fax	+33 4 76 51 42 67
E-mail	serge.cosnier@ujf-grenoble.fr
URL	
Specific Result URL	

SUMMARY

A total of 9 chemical monomers have been synthesised for use in immunosensor fabrication. Other areas of use will be in electrochemical biosensor production and derivatisation of surfaces. Specific molecular affinity centres have been included in the monomer synthesised including biotin, nitriloacetic acid and benzoquinone.

SUBJECT DESCRIPTORS CODES		
28 ANALYTICAL CHEMISTRY		
80 BIOSENSORS		
597 SYNTHESIS AND NEW MOLECULES		

DOCUMENTATION AND INFORMATION ON THE RESULT

Documentation	Details (Title, ref. number, general description,	Status:
type	language)	PU=Public
		CO=Confidential

INTELLECTUAL PROPERTY RIGHTS

Type of IPR						Pre-existing know-how Tick a box and give the corresponding details(reference numbers, etc) if appropriate	
		Current Forese			Foreseen	Tick	Details
	Tick	NoP1)	NoI ²⁾	Details	Tick		
Patent applied for	✓	1		Biotin loaded surfaces			
Patent granted							
Patent search carried out							
Registered design							
Trademark applications							
Copyrights							

Secret know-how	√		√	
Other - please specify:				

- Number of Priority (national) applications/patents
 Number of Internationally extended applications/patents

MARKET APPLICATION SECTORS

Market application sectors	
73 Research and development	

CURRENT STAGE OF DEVELOPMENT

Current stage of development	Experimental development stage (laboratory prototype)
Other:	

Quantified data about the result

Items (about the results)	Actual current quantity	Estimated (or future) quantity
Time to application / market (in months from the end of the research project)		
Number of (public or private) entities potentially involved in the implementation of the result:		
of which: number of SMEs:		
of which: number of entities in third countries (outside EU):		
Targeted user audience: of reachable people		
S&T publications (referenced publications only)		1
publications addressing general public (e.g. CD-ROMs, WEB sites)		
publications addressing decision takers / public authorities / etc.		
Visibility for the general public	NO	

Further collaboration, dissemination and use of the result

COLLABORATIONS SOUGHT

R&D	Further research or development	FIN	Financial support	
LIC	Licence agreement VC Venture capital/spin-off fund		Venture capital/spin-off funding	
MAN	Manufacturing agreement	PPP	Private-public partnership	
MKT	Marketing agreement	INFO	Information exchange/training	
JV	Establish a joint enterprise or partnership	cons	Available for consultancy	
Other	(please specify)			
Details	:	-		

POTENTIAL OFFERED FOR FURTHER DISSEMINATION AND USE

PROFILE OF ADDITIONAL PARTNER(S) FOR FURTHER DISSEMINATION AND USE

No.	Title
4	Fluoroquinolone Antibiotics Haptens, Conjugates, Antibodies and Immunoassays Kits

CONTACT PERSON FOR THIS RESULT

Name	Pilar Marco
Position	Head of Group
Organisation	Applied Molecular Receptors Group
Address	Department of Biological Organic Chemistry, IIQAB-CSIC, Jorge Girona, 18-26 08034, Barcelona Spain
Telephone	+34-93-400-6171
Fax	+34-93-204-5904
E-mail	mpmqob@iiqab.csic.es
URL	
Specific Result URL	

SUMMARY

The previous knowledge in AMRg-CSIC group about immunization procedures and immunoassays, for non-immunogenic antigens, let to design a set of new chemical compounds structurally related to fluoroquinolone antibiotics that can be used as haptens to be linked over wide class of soluble or solid supports (ie. proteins, polysaccharides, plastics as polystyrene, silicon and metal oxides, etc). The sophisticated chemistry contained within the CSIC in Barcelona has enabled the synthesis of several haptens and their protein conjugates, leading to the raising of polyclonal antibodies to selected fluoroquinolone antibiotics. Based on the synthetic technology, the individual components of assay kits for fluoroquinolone antibiotics will be available. The fully developed assay kits have a significant added value than just reagents alone and will be a potential target for exploitation of the expertise of the CSIC. Future routes to exploitation will include discussions with diagnostics companies and kit suppliers. Future routes to exploitation will include discussions with diagnostics companies and kit suppliers.

SUBJECT DESCRIPTORS CODES
28 ANALYTICAL CHEMISTRY
311 IMMUNOLOGY, IMMUNOTHERAPY, IMMUNOASSAYS

DOCUMENTATION AND INFORMATION ON THE RESULT

	Documentation	Details (Title, ref. number, general description,	Status:
t	type	language)	PU=Public
			CO=Confidential

INTELLECTUAL PROPERTY RIGHTS

<u>Type of IPR</u>				Pre-existing know-how Tick a box and give the corresponding details(reference numbers, etc) if appropriate			
				Foreseen	Tick	Details	
	Tick	NoP1)	NoI ²⁾	Details	Tick		
Patent applied for							
Patent granted							
Patent search carried out							
Registered design							
Trademark							

applications				
Copyrights				
Secret know-how	>		√	
Other - please specify:	√	Stocks of individual reagents for assay kit development		

- 1) Number of **P**riority (national) applications/patents
- 2) Number of Internationally extended applications/patents

MARKET APPLICATION SECTORS

Market application sectors	
73 Research and development	

CURRENT STAGE OF DEVELOPMENT

Current stage of development	
Other:	

Quantified data about the result

Items (about the results)	Actual current quantity	Estimated (or future) quantity	
Time to application / market (in months from the end of the research project)			
Number of (public or private) entities potentially involved in the implementation of the result:			
of which: number of SMEs:			
of which: number of entities in third countries (outside EU):			
Targeted user audience: of reachable people			
S&T publications (referenced publications only)			
publications addressing general public (e.g. CD-ROMs, WEB sites)			
publications addressing decision takers / public authorities / etc.			
Visibility for the general public	NO		

Further collaboration, dissemination and use of the result

COLLABORATIONS SOUGHT

R&D	Further research or development	FIN	Financial support	
LIC	Licence agreement	VC	Venture capital/spin-off funding	
MAN	Manufacturing agreement	PPP	Private-public partnership	
MKT	Marketing agreement	INFO	Information exchange/training	
JV	Establish a joint enterprise or partnership	CONS	Available for consultancy	
Other	(please specify)			
Details	:			

POTENTIAL OFFERED FOR FURTHER DISSEMINATION AND USE

PROFILE OF ADDITIONAL PARTNER(S) FOR FURTHER DISSEMINATION AND USE

No.	Title
5	Rabbit antibody libraries for fluoroquinolines

CONTACT PERSON FOR THIS RESULT

Name	Berthold Hock			
Position	Dean of Faculty			
Organisation	Technisch Universität München			
Address	Center of Life Sciences Weihenstephan, Chair of Cell Biology, Alte Akademie 12 D-85350, Freising Germany			
Telephone	+49-8161-713396			
Fax	+49 8161 - 71 4403			
E-mail	hock@wzw.tum.de			
URL				
Specific Result URL				

SUMMARY

The work within the ELISHA project has enabled a new production route of monoclonals from rabbit. In particular, recombinant rabbit antibody libraries have been developed, which comprise Fab fragments for the detection of fluoroquinolines. The libraries are subsequently applied for the isolation of recombinant Fab fragments. Library development included design of species-selective primer sets, optimized vector systems for phage display and large-scale expression and cloning of Fab genes from rabbits. The results obtained are still preliminary and cannot be used outside of the consortium. The library will exclusively be applied within the consortium during the project. In future, this may be a significant step towards production of many different monoclonal antibodies for selected targets and could be of commercial viability to a number of kit manufacturers.

SUBJECT DESCRIPTORS CODES
28 ANALYTICAL CHEMISTRY
311 IMMUNOLOGY, IMMUNOTHERAPY, IMMUNOASSAYS

DOCUMENTATION AND INFORMATION ON THE RESULT

Documentation	Details (Title, ref. number, general description,	Status:
type	language)	PU=Public
		CO=Confidential

INTELLECTUAL PROPERTY RIGHTS

Type of IPR	Tick		and g	ive the corresponding e numbers, etc) if app		Pre-existing know-how Tick a box and give the corresponding details(reference numbers, etc) if appropriate		
		Current Foreseer					Details	
	Tick	NoP1)	NoI ²⁾	Details	Tick			
Patent applied for								
Patent granted								
Patent search carried out								
Registered design								
Trademark applications								

Copyrights				
Secret know-how	>			
Other - please specify:	√	Rabbit Primer Library Constructed 'in house'	√	

- 1) Number of **P**riority (national) applications/patents
- 2) Number of Internationally extended applications/patents

MARKET APPLICATION SECTORS

Market application sectors

- 15 Manufacture of food products and beverages
- 73 Research and development

CURRENT STAGE OF DEVELOPMENT

Current stage of development	Scientific and/or Technical knowledge (Basic research)
Other:	

Quantified data about the result

Items (about the results)	Actual current quantity	Estimated (or future) quantity
Time to application / market (in months from the end of the research project)	12	
Number of (public or private) entities potentially involved in the implementation of the result:		
of which: number of SMEs:		
of which: number of entities in third countries (outside EU):		
Targeted user audience: of reachable people		
S&T publications (referenced publications only)		
publications addressing general public (e.g. CD-ROMs, WEB sites)		
publications addressing decision takers / public authorities / etc.		
Visibility for the general public	NO	

Further collaboration, dissemination and use of the result

COLLABORATIONS SOUGHT

R&D	Further research or development	FI	N	Financial support	
LIC	Licence agreement	VC		Venture capital/spin-off funding	
MAN	Manufacturing agreement	PP	P	Private-public partnership	
MKT	Marketing agreement	IN	IFO .	Information exchange/training	
JV	Establish a joint enterprise or partnership	СО	ONS	Available for consultancy	
Other	(please specify)				
Details:					

POTENTIAL OFFERED FOR FURTHER DISSEMINATION AND USE

PROFILE OF ADDITIONAL PARTNER(S) FOR FURTHER DISSEMINATION AND USE

No.	Title

6	Processes of immobilization of affinity molecules

CONTACT PERSON FOR THIS RESULT

Name	Claude Martelet
Position	Head of Group
Organisation	Ecole Centrale de Lyon
Address	Laboratoire d'Ingénierie et Fonctionnalisation des Surfaces UMR CNRS 5621 B.P 163F69131, Lyon France
Telephone	+33 (0)4 72 18 62 48
Fax	+33-(0)4 78 33 11 40
E-mail	Claude.Martelet@ec-lyon.fr
URL	
Specific Result URL	

SUMMARY

Immobilization of antibodies, oligonucleotides...onto metallic electrodes using three strategies for the fixation of the affinity molecule: - Grafting on the activated ester of an electropolymerised functionalised polypyrrole - Grafting on the activated ester of an electropolymerised functionalised polypyrrole associated with a redox probe (ferrocenyl group) - Grafting on a SAMs functionalised with an activated ester

80 BIOSENSORS 75 BIOMOLECULES, BIOPLASTICS, BIOPOLYMERS 159 DIAGNOSTICS, DIAGNOSIS 311 IMMUNOLOGY, IMMUNOTHERAPY, IMMUNOASSAYS

DOCUMENTATION AND INFORMATION ON THE RESULT

Documentation	Details (Title, ref. number, general description,	Status:
type	language)	PU=Public
		CO=Confidential

INTELLECTUAL PROPERTY RIGHTS

Type of IPR	Tick		and g	ive the correspondir e numbers, etc) if ap	Pre-existing know-he the corresponding numbers, etc) if appropriate corresponding details(reference numbers, etc) if appropriate				
			C	urrent	Foreseen	Tick	Details		
	Tick	NoP1)	NoI ²⁾	Details	Tick				
Patent applied for									
Patent granted									
Patent search carried out									
Registered design									
Trademark applications									
Copyrights							_		
Secret know-how	✓				√				

Other - please specify:				√	Novel materials
1) Number of P rior	itv (n	ational) appli	cations/patents		

- 2) Number of Internationally extended applications/patents

MARKET APPLICATION SECTORS

Market application sectors
73 Research and development

CURRENT STAGE OF DEVELOPMENT

Current stage of development	
Other:	

Quantified data about the result

Items (about the results)	Actual current quantity	Estimated (or future) quantity
Time to application / market (in months from the end of the research project)	9)
Number of (public or private) entities potentially involved in the implementation of the result:		
of which: number of SMEs:		
of which: number of entities in third countries (outside EU):		
Targeted user audience: of reachable people		
S&T publications (referenced publications only)		
publications addressing general public (e.g. CD-ROMs, WEB sites)		
publications addressing decision takers / public authorities / etc.		
Visibility for the general public	NO	

Further collaboration, dissemination and use of the result

COLLABORATIONS SOUGHT

R&D	Further research or development	FI	N	Financial support	
LIC	Licence agreement	VC		Venture capital/spin-off funding	
MAN	Manufacturing agreement	PP	P	Private-public partnership	
MKT	Marketing agreement	IN	FO	Information exchange/training	
JV	Establish a joint enterprise or partnership	СО	NS	Available for consultancy	
Other	(please specify)				
Details:					

POTENTIAL OFFERED FOR FURTHER DISSEMINATION AND USE

PROFILE OF ADDITIONAL PARTNER(S) FOR FURTHER DISSEMINATION AND USE

Exploitation plans

CONFIDENTIAL

I am the Co-ordinator of the above project, and confirm on behalf of the contracted Partners the information contained in this Technological Implementation Plan, and I authorise its public dissemination.					
Signature:	Name:				
Date:	Organisation:				